AD-A062 912 TRANSPORTATION SYSTEMS CENTER CAMBRIDGE MASS F/G 1/2
BEACON COLLISION AVOIDANCE SYSTEM (BCAS) ALTERNATIVE CONCEPTS F--ETC(U)
SEP 78 J G RAUDSEPS, M D MENN, J VILCANS

UNCLASSIFIED TSC-FAA-78-19 FAA/RD-78/34 NL

1 OF 3
AD
AO 62912

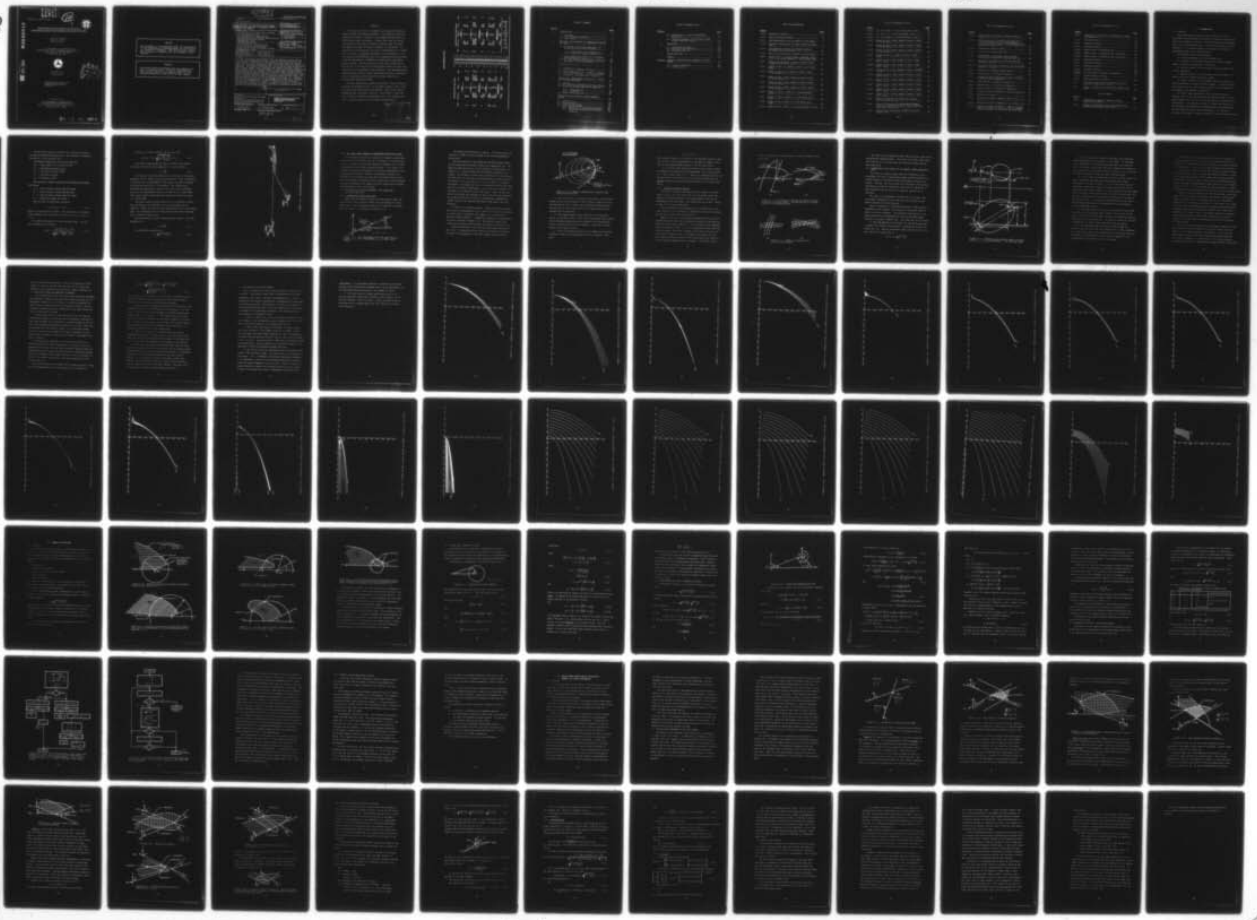

REPORT NO. FAA-RD-78-34

BEACON COLLISION AVOIDANCE SYSTEM (BCAS) ALTERNATIVE CONCEPTS FOR DETERMINING TARGET POSITIONS

Juris G. Raudseps
Michael D. Menn
Janis Vilcans

U.S. DEPARTMENT OF TRANSPORTATION
RESEARCH AND SPECIAL PROGRAMS ADMINISTRATION
TRANSPORTATION SYSTEMS CENTER
Cambridge MA 02142

SEPTEMBER 1978

INTERIM REPORT

Prepared for

U.S. DEPARTMENT OF TRANSPORTATION
FEDERAL AVIATION ADMINISTRATION
Systems Research and Development Service
Washington DC 20590

NOTICE

This document is disseminated under the sponsorship of the Department of Transportation in the interest of information exchange. The United States Government assumes no liability for its contents or use thereof.

NOTICE

The United States Government does not endorse products or manufacturers. Trade or manufacturers' names appear herein solely because they are considered essential to the object of this report.

(12) 208 p.

Technical Report Documentation Page

1. Report No.	2. Government Accession No.	3. Recipient's Catalog No.
FAA-RD-78-34 ✓		

4. Title and Subtitle
(6) BEACON COLLISION AVOIDANCE SYSTEM (BCAS) ALTERNATIVE CONCEPTS FOR DETERMINING TARGET POSITIONS

5. Report Date
(11) September 1978

6. Performing Organization Code

7. Author's
J.G. Raudseps, M.D. Menn, and J. Vilcans

8. Performing Organization Report No.
(14) DOT-TSC-FAA-78-19

9. Performing Organization Name and Address
U.S. Department of Transportation
Research and Special Programs Administration
Transportation Systems Center
Cambridge MA 02142

10. Work Unit No. (TRAIS)
FA8391/R8111

11. Contract or Grant No.

12. Sponsoring Agency Name and Address
U.S. Department of Transportation
Federal Aviation Administration
Systems Research and Development Service
Washington DC 20590

13. Type of Report and Period Covered
(9) Interim Report,
May 1975 - May 1978

14. Sponsoring Agency Code

15. Supplementary Notes
(18) FAA/RD (19) 78/34

16. Abstract

The (Litchford) Beacon-based Collision Avoidance System concept requires the computation of target range and bearing relative to the BCAS aircraft. Techniques for determining target range and bearing under four different assumptions about the ground radar environment are reported. The systems considered are a fully passive BCAS system when there are two ground radars equipped with azimuth reference signals and a single target, two ground radars of which only one has azimuth reference signals and two targets, and two ground radars without ground reference signals and two targets, as well as a BCAS system using both active range measurements and signals from a single ground radar. The report includes the derivations of computational algorithms applicable to the different cases and the results of simulations. It is found that the error sensitivity of the solutions is a function of the geometry of the configuration. Multiple solutions are possible with systems involving only one target. A family of curves is derived and illustrated by examples to permit qualitative evaluation of the solution in any given configuration.

(10) Juris G. /Raudseps, Michael D. /Menn
Janis /Vilcans

17. Key Words	18. Distribution Statement
Beacon-based Collision Avoidance System Passive/Active/Semi-Active CAS Target Position Determination Error Sensitivity	DOCUMENT IS AVAILABLE TO THE U.S. PUBLIC THROUGH THE NATIONAL TECHNICAL INFORMATION SERVICE, SPRINGFIELD, VIRGINIA 22161

19. Security Classif. (of this report)	20. Security Classif. (of this page)	21. No. of Pages	22. Price
Unclassified	Unclassified	208	

Form DOT F 1700.7 (8-72) Reproduction of completed page authorized

PREFACE

This report describes the computation of range and bearing to target aircraft from BCAS measurements. Four different cases are treated which differ in respect to the assumptions made about the ATCRBS ground radar environment. In each case, only the minimal configuration, involving the smallest possible number of radars and targets necessary to obtain a solution, is considered. All computations are performed on the basis of measurements at a single point and assume no a priori knowledge of the configuration. All the algorithms described and used in the simulations were developed at TSC and implemented in FORTRAN on the DEC PDP-10 time-shared computer system. The only exception is the search algorithm for the solution of the single-site configuration, whose key steps were implemented on a programmable hand calculator. The simulations were conducted using simulated random measurement variations consistent with the measurement errors observed in flight tests of the Litchford BCAS feasibility model.

The work reported was sponsored by Richard F. Bock of ARD-250. The draft was reviewed by Robert W. Wisleder, DTS-531, and by Owen E. McIntire and John Brennan, both ARD-251. Much of the computer programming was performed by Henrick O. Lind, Barry I. Fink, and Ronit Procaccia of Kentron International, Ltd. The typing of the draft, although complex, was well done by Barbara Davis.

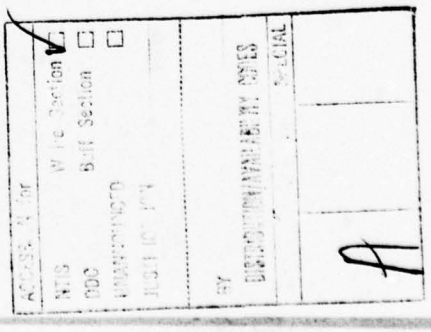

METRIC CONVERSION FACTORS

Approximate Conversions to Metric Measures

Symbol	When You Know	Multiply by	To Find	Symbol
	LENGTH			
in	inches	2.5	centimeters	cm
ft	feet	30	centimeters	cm
yd	yards	0.9	meters	m
mi	miles	1.6	kilometers	km
	AREA			
in^2	square inches	6.5	square centimeters	cm^2
ft^2	square feet	0.09	square meters	m^2
yd^2	square yards	0.8	square meters	m^2
mi^2	square miles	2.6	square kilometers	km^2
	acres	0.4	hectares	ha
	MASS (weight)			
oz	ounces	28	grams	g
lb	pounds	0.45	kilograms	kg
	short tons (2000 lb)	0.9	tonnes	t
	VOLUME			
tsp	teaspoons	5	milliliters	ml
Tbsp	tablespoons	15	milliliters	ml
fl oz	fluid ounces	30	milliliters	ml
c	cups	0.24	liters	l
pt	pints	0.47	liters	l
qt	quarts	0.95	liters	l
gal	gallons	3.8	liters	l
ft^3	cubic feet	0.03	cubic meters	m^3
yd^3	cubic yards	0.76	cubic meters	m^3
	TEMPERATURE (exact)			
°F	Fahrenheit temperature	5/9 (after subtracting 32)	Celsius temperature	°C

Approximate Conversions from Metric Measures

Symbol	When You Know	Multiply by	To Find	Symbol
	LENGTH			
mm	millimeters	0.04	inches	in
cm	centimeters	0.4	inches	in
m	meters	3.3	feet	ft
m	meters	1.1	yards	yd
km	kilometers	0.6	miles	mi
	AREA			
cm^2	square centimeters	0.16	square inches	in^2
m^2	square meters	1.2	square yards	yd^2
km^2	square kilometers	0.4	square miles	mi^2
ha	hectares (10,000 m^2)	2.5	acres	
	MASS (weight)			
g	grams	0.035	ounces	oz
kg	kilograms	2.2	pounds	lb
t	tonnes (1000 kg)	1.1	short tons	
	VOLUME			
ml	milliliters	0.03	fluid ounces	fl oz
l	liters	2.1	pints	pt
l	liters	1.06	quarts	qt
l	liters	0.26	gallons	gal
m^3	cubic meters	35	cubic feet	ft^3
m^3	cubic meters	1.3	cubic yards	yd^3
	TEMPERATURE (exact)			
°C	Celsius temperature	9/5 (then add 32)	Fahrenheit temperature	°F

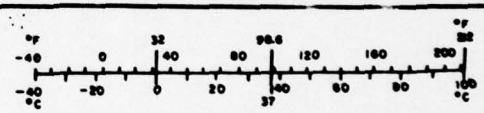

TABLE OF CONTENTS

TABLE OF CONTENTS (Cont.)

LIST OF ILLUSTRATIONS

LIST OF ILLUSTRATION (Cont.)

LIST OF ILLUSTRATIONS (Cont.)

LIST OF ILLUSTRATIONS (Cont.)

LIST OF TABLES

1. INTRODUCTION

1.1 OVERVIEW

This report presents analyses and a design of a set of algorithms for determining the positions of intruder aircraft and ground interrogators relative to the BCAS system from the measurements that the BCAS system makes. Only the static cases are considered, i.e., the determination of positions on the basis of measurements made at the current position.

Five distinct cases are considered:

1) Active interrogations of the intruder only.

2) Location of an intruder when there is only one ground radar, but active interrogation is permitted.

3) Passive location of the intruder, given two radars with azimuth references.

4) Passive location of the intruder, given two radars, of which only one has azimuth reference signals.

5) Passive location of the intruder, given two radars, of which neither has an azimuth reference signal. (In both this and the previous case (4), two intruder aircraft must be replying to both radars or no solution is possible.)

For each of these situations, only the simplest case is treated, that is, the case involving the smallest number of aircraft necessary to solve for the unknown quantities describing the configuration. For instance, in case (2), where the position of the intruder is determined by combining passive mode measurements from one radar with active mode measurements, the solution consists of the range to radar and bearing to only a single intruder.

If several targets are present, improved results can be expected because the system of equations to be solved then becomes over-determined. (Clearly, each single-intruder solution gives a separate value for the distance to the radar.) The computed results can then be expected to be more accurate because, in effect, the measurement errors are reduced by averaging.

Similar improvements in the effective accuracy of computing intruder positions are to be expected when aircraft positions are determined at a succession of points and the tracks are smoothed since, again, the errors are reduced by averaging over time. The consideration of these more complex cases is outside the scope of the present report.

1.2 THE FUNDAMENTAL EQUATIONS

The basic measurements performed by passive BCAS are of (1) the differential time of arrival (TOA), i.e., the time difference between the reception of an SSR interrogation and the reception of its elicited target reply, and of (2) the differential azimuth (DAZ), i.e., the angle at the interrogator between the protected aircraft and the target. Also, for SSR sites that have been suitably modified, own azimuth (OAZ), i.e., the magnetic bearing of own from the radar site, can be determined. The quantities measured are indicated in Figure 1.2-1.

The purely active BCAS measures the TOA of replies to its own interrogations. This is the round-trip travel time of the signals between the BCAS aircraft and the intruder; in effect it amounts to a direct measurement of slant range.

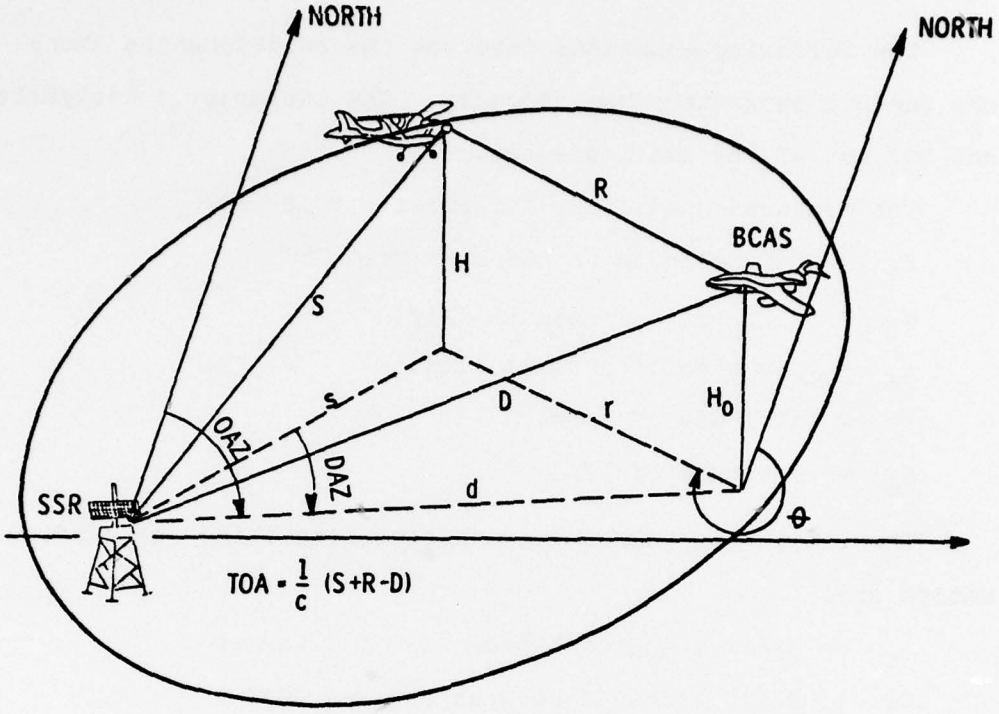

FIGURE 1.2-1. SINGLE-SITE GEOMETRY.

Both the active and passive BCAS obtain own altitude from the on-board encoding altimeter and the intruder altitude by decoding the mode C replies received.

Geometrically, the measurements from one SSR relate the position of the target aircraft to that of the BCAS in the following way:

For a given separation d between the radar and the BCAS, the TOA determines an ellipsoid of revolution on which the target must lie. The radar and the BCAS are at the foci of this ellipsoid. The differential azimuth determines a vertical plane passing through the radar and the target. The target altitude determines its horizontal plane.

The following equations describe the relationships among the various parameters analytically. The subscript i designates one SSR out of the available set.

The measured quantities for passive BCAS are:

β_i = OAZ, azimuth of the BCAS from SSR

α_i = differential azimuth (DAZ)

t_i = the time of arrival (TOA)

H = altitude of target

H_o = altitude of BCAS

The (initially unknown) quantities describing the configuration are:

S_i = slant distance between SSR and target

D_i = slant distance between SSR and BCAS

R = slant distance between BCAS and target

Θ = bearing of target from BCAS

Then the TOA, by definition, satisfies

$$t_i = \frac{1}{c} (S_i + R - D_i) \qquad 1.2.1$$

where c is the velocity of light. For convenience, all expressions hereafter will be written in terms of $T_i = c\, t_i = S_i + R - D_i$.

All angles are measured in the horizontal plane. By the law of cosines, DAZ satisfies

$$\cos\alpha_i = \frac{S_i^2 + D_i^2 - R^2 - 2HH_o}{2\sqrt{(S_i^2 - H^2)(D_i^2 - H_o^2)}} \qquad 1.2.2$$

Finally, it follows from the law of sines that

$$\sin(\beta_i - \theta) = \sqrt{\frac{S_i^2 - H^2}{R^2 - (H-H_o)^2}} \sin \alpha_i \qquad 1.2.3$$

When active measurements are made, the TOA of the replies elicited by the active interrogations is t_o and satisfies

$$t_o = \frac{2R}{c} . \qquad 1.2.4$$

The sections that follow describe the solution of these basic equations for the various cases described above. Each is different in that the set of measurements - and, hence, the set of unknowns for which one must solve - is different. The solutions are described qualitatively in terms of the locus curves determined by the set of measurements based on the replies to a given radar. Then actual solution algorithms and simulation results are given.

1.3 ACTIVE BCAS

The case of purely active BCAS will not be treated in detail. Only the range to the intruder, but not the bearing, can be obtained. Flight test data show the measurements to be consistently good. An illustrative plot of range measured by active interrogation is shown in Figure 1.3-1.

The calculations of static separation are trivial. The slant separation is

$$R = \frac{c\, t_o}{2} \qquad 1.3.1$$

The horizontal separation is

$$r = \sqrt{R^2 - (H-H_o)^2} \qquad 1.3.2$$

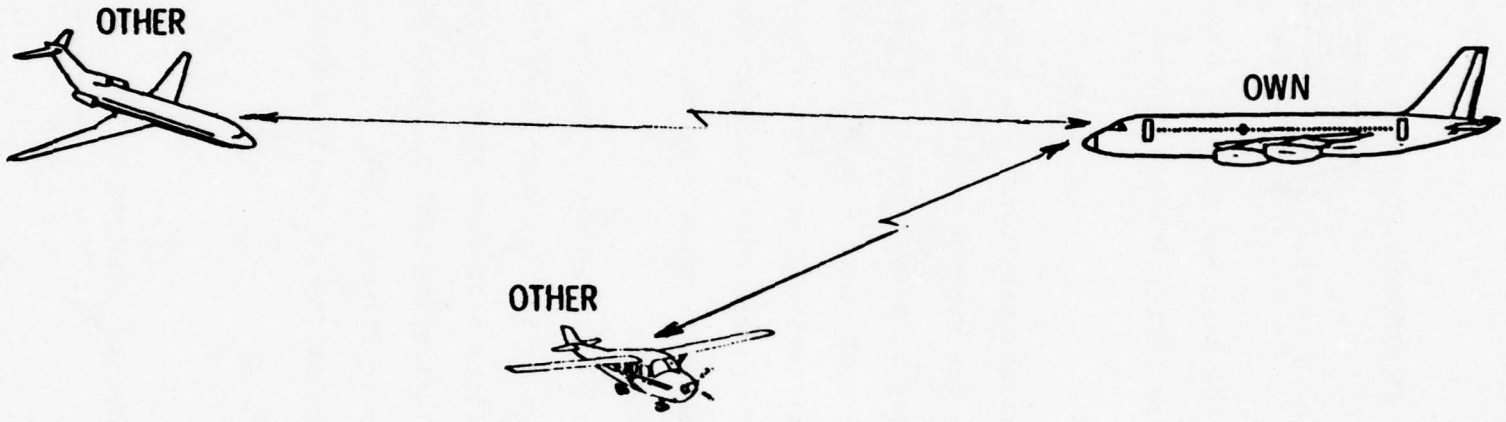

FIGURE 1.3-1. BCAS CONCEPT-ACTIVE BCAS.

2. THE LOCUS CURVE APPROACH TO DETERMINING POSITION OF OTHER

The following discussion is intended to describe qualitatively the nature of the solutions that may be obtained to the BCAS equations. A sequence of essentially geometric arguments will be used to construct the solutions by graphical means. In no sense is it proposed that graphic techniques of solution are appropriate for an operational BCAS system. However, the graphical solutions do illustrate the circumstances under which different kinds of solutions are obtained, indicate the error sensitivity of the solutions in various geometries, and suggest practical algorithms that might be implemented to find the solutions.

2.1 TWO RADARS WITH AZIMUTH REFERENCE, THE PLANAR CASE LOCUS CURVE SOLUTION

2.1.1 Construction of the Locus Curve

Assume that the radars and both the BCAS aircraft (OWN) and the potential threat aircraft (OTHER) are constrained to a horizontal plane. The measurements based on one radar and the target yield β, α, and T, as indicated in Figure 2.1-1.

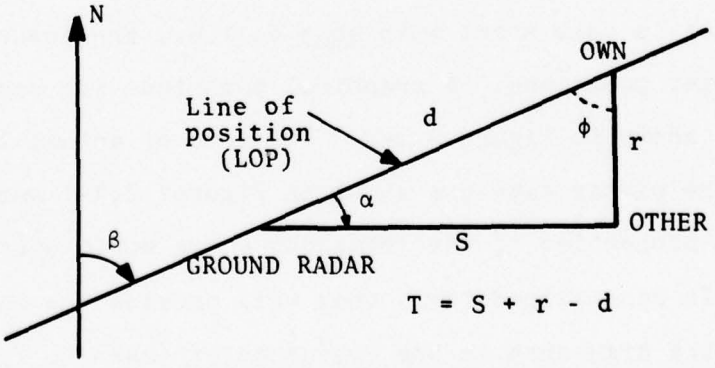

FIGURE 2.1-1. BCAS MEASUREMENTS FROM ONE RADAR FOR ONE TARGET. β, α, AND T ARE MEASURED, r, ϕ, d AND s ARE UNKNOWN

The radar-to-OWN distance is unknown. If it were known, the position of OTHER could be obtained by the following geometric construction:

With the position of the radar and the OWN aircraft fixed, the TOA determines an ellipse on which the target must lie. The radar and OWN are the foci of this ellipse; its major axis is of length T + d. [This follows from the familiar property of an ellipse: an ellipse is a curve such that the sum of the distances from any point on the curve to two given points, called the foci, is constant - i.e., such that s + r = T + d, with T + d given]. Furthermore, the target must lie in a direction from the SSR determined by its azimuth measurement, i.e., on the line eminating from the radar in the direction ($\beta+\alpha$) from north. Thus, one may construct the ellipse and intersect it with a line of known direction. The target must lie at the point of intersection, assuming the correct value of the radar-to-own distance was used in the construction.

In fact, d is initially unknown. Thus all that can be determined from the measurements of T, α, and β is the set of positions for other that is consistent with <u>some</u> d, i.e., the locus of possible target positions. A graphical technique for constructing the locus is shown in Figure 2.1-2. Two sets of actual locus curves for the planar case are shown in Figures 2.4-1 and 2.4-16.

Several properties of the locus curve are worth observing at this time. In generalized form, they will provide the motivation for many of the arguments in the more complex cases to follow.

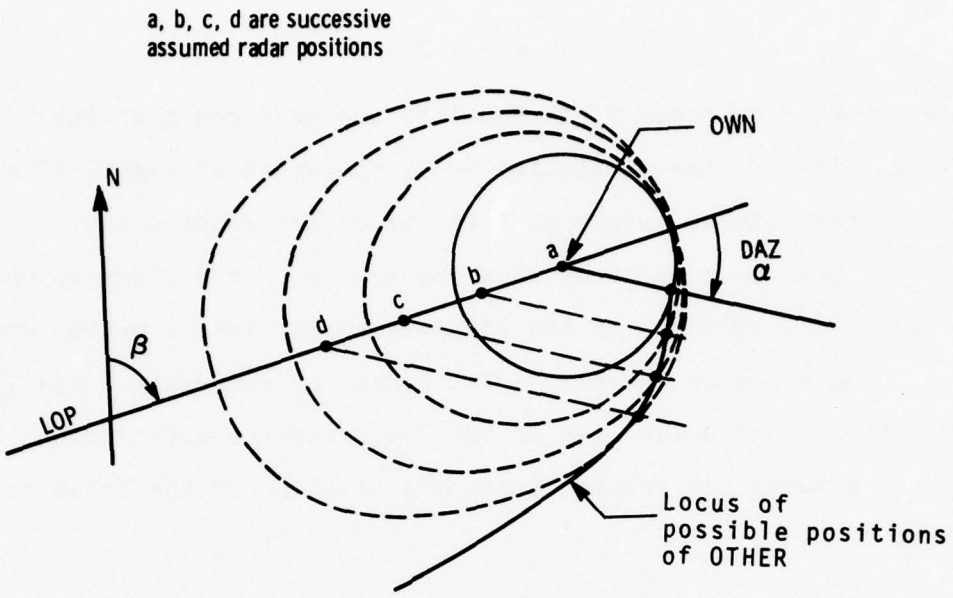

FIGURE 2.1-2. GEOMETRIC CONSTRUCTION OF TARGET LOCUS CURVE FOR PLANAR CASE.

1) The locus curve is confined to that sector of the plane bounded by the line of position (LOP) of OWN to radar and a line intersecting the LOP at OWN at the differential azimuth angle α. Any point not in this sector can not be a target position consistent with the given DAZ.

2) Given <u>any</u> presumed target position in the permitted sector, on the locus curve or not, the corresponding radar position can be determined geometrically by drawing a line through that point to intersect the LOP at the angle α. The point of intersection is the radar position.

3) Given the assumed positions of the target and the radar relative to OWN, the corresponding TOA can be computed. This gives

$$T_c = S + R - D .$$

This computed quantity T_c is equal to the measured quantity T (the TOA in units of time multiplied by c, the speed of light) if and only if the assumed target position is on the locus curve.

4) The locus curve divides the sector of the plane to which the target is confined by the DAZ measurement into a region where $T_c > T$ and a region where $T_c < T$. Hence, by comparing T and T_c one can determine on which side of the locus curve a given point is without knowing the precise shape and location of the locus curve itself.

2.1.2 Finding the Target Position

When OWN is observing two radars and the replies of a given target to both, then two locus curves for the target can be constructed (as described above), one corresponding to the set of measurements from each radar. The target must lie on both. Hence, it must lie at their intersection.

Since the solution is determined by the intersection of two locus curves, it is of interest to examine the nature of the curves and the ways in which they may intersect.

Figure 2.1-3a and 2.1-3b indicate schematically two kinds of intersections that may occur, varying with respect to the angle at which the locus curves intersect. It is evident from the diagrams that the solution is more sensitive to measurement errors when the curves intersect like those in Figure 2.1-3b than in the case for the curves in Figure 2.1-3a. Any change in the values of α, β, and T used in constructing one of the locus curves will result in a curve shifted somewhat from the original. The effect of such

shifts is different in the two cases, as shown in Figure 2.1-4a and 2.1-4b.

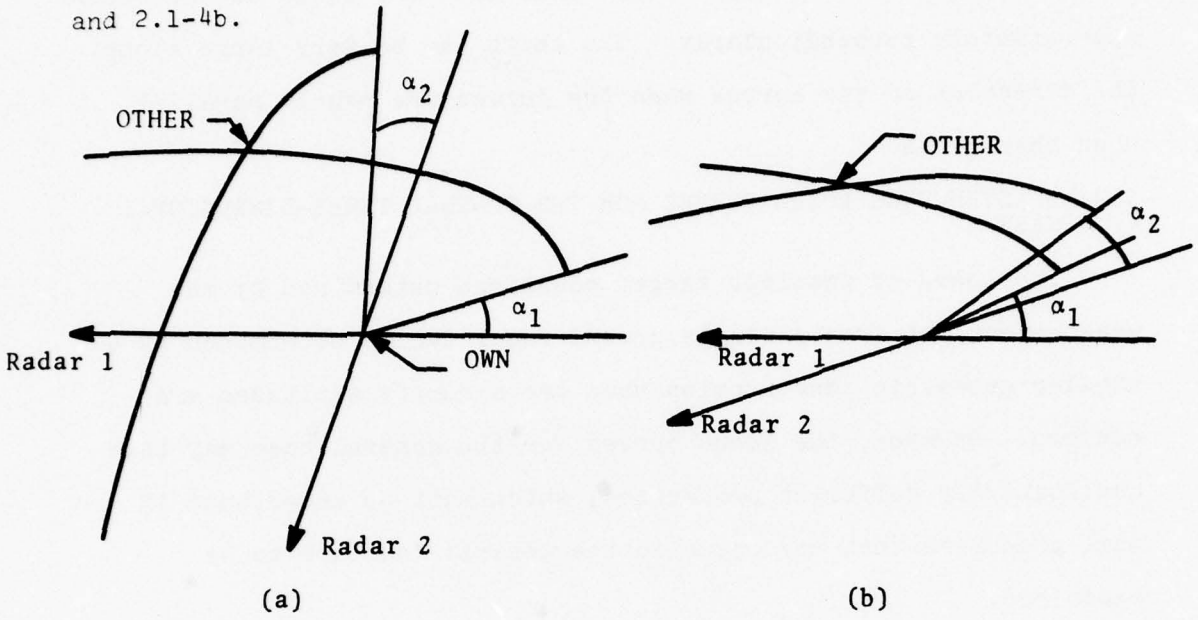

FIGURE 2.1-3. TWO GRAPHICAL SOLUTIONS FOR TARGET POSITION, DETERMINED FROM LOCUS CURVES. THE SOLUTION IN (a) IS LESS SENSITIVE TO MEASUREMENT ERROR.

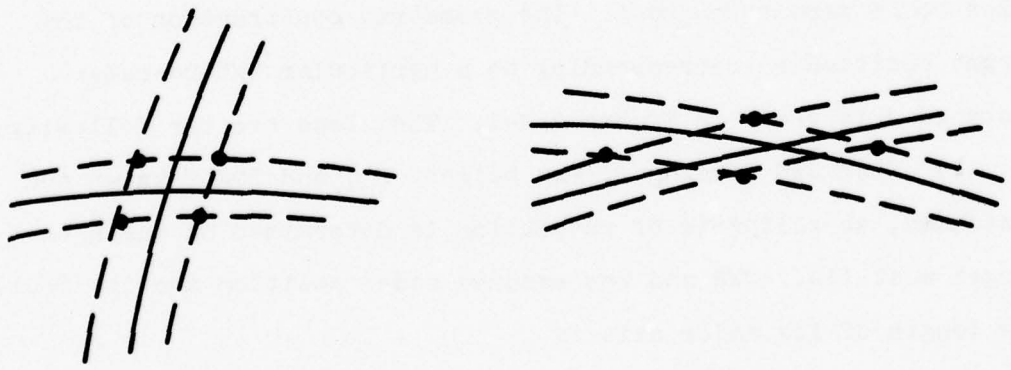

FIGURE 2.1-4. SHIFTS IN SOLUTION DUE TO SHIFTS IN LOCUS CURVES.

The shift will be relatively small when the locus curves cross approximately perpendicularly. The shift can be very large along the direction of the curves when the curves are nearly parallel when they cross.

2.2 CONSTRUCTING LOCUS CURVES FOR THE GENERAL THREE-DIMENSIONAL CASE

The locus of possible target positions determined by the measurement set from a single ground radar can be determined by a similar geometric construction when the aircraft altitudes are nonzero. However, the locus curves for the general case may have qualitatively different properties, which must be understood if some phenomena that may occur in the general case are to be explained.

The steps in the geometric construction of the locus curve for a given combination of TOA, OAZ, DAZ, own altitude H_o and target altitude H are the following:

Again a succession of horizontal distances of OWN-to-radar, designated d, are assumed. The altitude of the ground radar is taken to be zero throughout. The geometric construction of the target position(s) corresponding to a particular OWN-to-radar distance d is shown in Figure 2.2-1. The steps are the following:

1) With OWN Bearing β, own height H_o, and TOA T known and d assumed, an ellipsoid of revolution is determined on which the target must lie. OWN and the assumed radar position are its foci. The length of its major axis is

$$T + D = T + \sqrt{d^2 + H_o^2} .$$

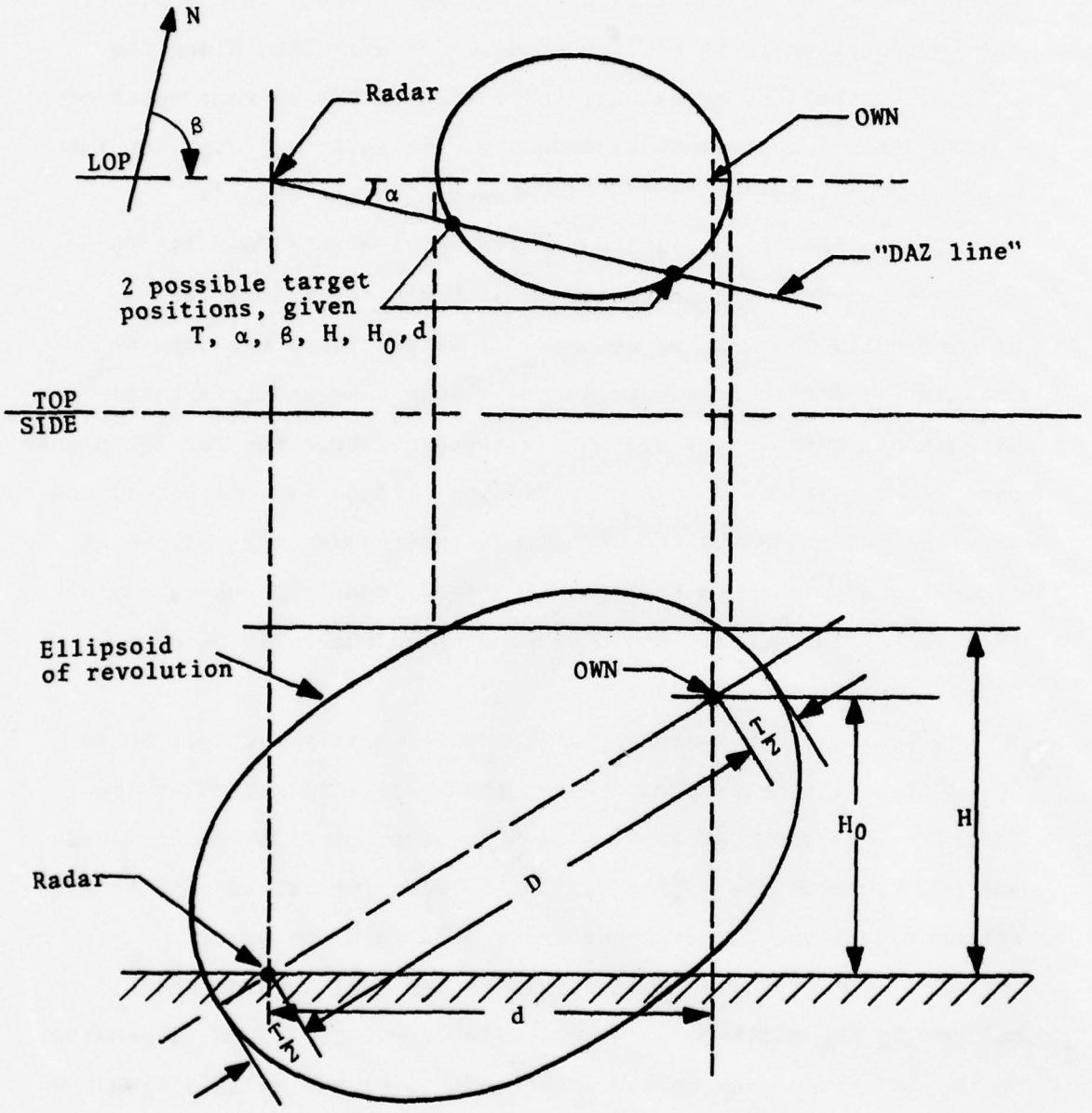

FIGURE 2.2-1. CONSTRUCTION OF POSSIBLE TARGET LOCATIONS, GIVEN T, α, β, H, H_0 AND ASSUMED d. TOP AND SIDE VIEWS.

2) This ellipsoid is assumed to intersect the horizontal plane determined by the altitude H of the target. In the plane, the intersection is an ellipse whose major axis lies along the LOP. (It should be noted that there will always be some value of $H > H_o$ for which the intersection will not exist - i.e., such that the whole ellipsoid is below the target altitude plane.)

3) In the target altitude plane, a line (the "DAZ line") now can be drawn from the projected radar position at an angle determined by the DAZ, as before. It is at this stage that the qualitative differences between the planar case and this three-dimensional case become evident. In the construction for the planar case, the radar position was inside the ellipse (at one focus) and the line determined by the DAZ always intersected the ellipse at exactly one point. In the general three-dimensional case, any of the following cases may occur, depending on the relationships among the parameter values:

(a) The radar position projected vertically may fall inside the ellipse in the altitude plane (though it will not be at its focus). Then the "DAZ line" will intersect the ellipse at exactly one point, as in the planar case. At least for values of d in that neighborhood, the target locus curve will have one branch.

(b) The projected radar position may fall outside the ellipse in the altitude plane (cf. Figure 2.2-1). Then, depending on the DAZ, there may be two intersections of the ellipse with the "DAZ Line", one intersection (at the point of tangency), or no intersection at all (when the DAZ is too large).

The locus curves for the general case are the sequences of points generated for each value of d, as d varies from zero to infinity. The nature of the curves depends on the relative values of the parameters. Figure 2.2-2 shows the cases that may occur.

The curve in Figure 2.2-2a is most nearly like that obtained with all altitudes zero. The only qualitative difference is that the locus curves obtained in the planar case are always concave toward OWN. Here the curve is shown with an inflection away from own in the region corresponding to small values of d (cf. Figures 2.4-1 to 2.4-24). It will be seen that this may result in double solutions for some geometries, which can not occur in the planar case.

The locus curve in Figure 2.2-2b has two branches, which come about due to the radar being outside the ellipse in the altitude plane (cf. Figure 2.2-1). The inner branch, i.e., the branch nearer the LOP, eventually joins the LOP. This occurs for a value of d such that the ellipsoid becomes so steeply inclined that the projected radar position touches the ellipse in the target altitude plane (cf. Figure 2.2-1). For smaller values of d, the projected radar position is inside this ellipse, and the "outer" branch of the locus curve is qualitatively like the locus curve in Figure 2.2-2a.

It is shown in the Appendix that a necessary condition for the locus curves to have the character of those in Figure 2.2-2b is that $T < H$, the target altitude. Furthermore, it is shown that both branches of the locus curve become asymptotically parallel to the LOP. Further, it is shown that, if T, H and H_o are held constant and the DAZ α is increased, the "inner" branch of the locus

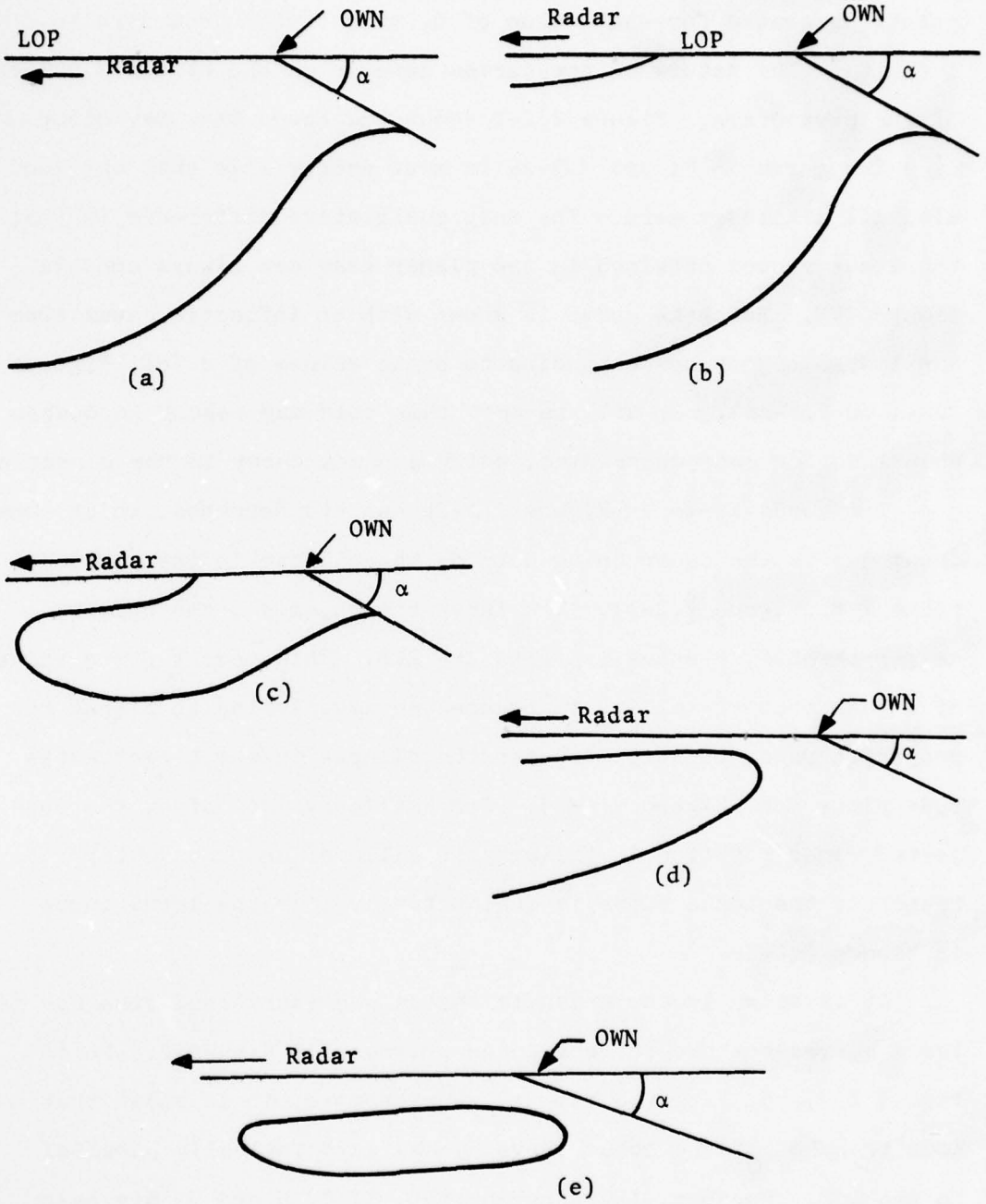

FIGURE 2.2-2. TYPES OF LOCUS CURVES. a-d ARE POSSIBLE CASES. e APPARENTLY DOES NOT OCCUR.

curve moves away from the LOP and the "outer" branch approaches the LOP.

If α becomes sufficiently large, the two branches of the locus curve do not go to infinity, but instead merge, as in Figure 2.2-2c (cf. Figure 2.4-14). It is shown in the Appendix that a sufficient condition for this to occur is that $T < H \sin \alpha$.

Figure 2.2-2d shows a case when the two branches of the locus curve exist separately far from OWN, but which then join, instead of terminating separately. In terms of the geometrical process for constructing locus curves described previously, such a locus can come about when the following happens: Assume that the target altitude is above that of OWN by so much that when the radar is assumed directly under OWN, the ellipsoid does not reach the target altitude plane. This will occur if and only if

$$T < 2 (H-H_o) .$$

It is shown in the Appendix that for any $T > 0$, as the radar moves away from OWN, i.e., as d increases, the ellipsoid eventually will touch the target altitude plane at a point over the LOP and the intersection will expand into an ellipse as d increases further. For sufficiently small α, this ellipse will be cut by the line from the radar at the angle determined by the DAZ. As d increases, this leads to the same asymptotic behavior as previously.

Geometric intuition implies that a locus curve in the form of a closed contour can not occur. If α is so large that no solution exists for $d \to \infty$, then there will not be a combination of circumstances such that the ellipse that forms in the altitude plane

with the radar position outside it can first expand with d fast enough to be cut by the DAZ line and then fail to expand fast enough, so that ultimately the DAZ line no longer intersects it.

2.3 THE LOCUS CURVES AS BOUNDARIES OF REGIONS

In the discussion so far, the locus curves have been described as geometrical constructions which can be drawn for given sets of measurement values T, α, β, H and H_o. It will be convenient in what follows to regard them from an alternative point of view as boundaries separating distinct subregions of the region where the other aircraft may be located.

If own azimuth (that is, the direction of the LOP) and the differential azimuth α are given, then the potential locations of the target aircraft are constrained to a region bounded by the LOP and a line eminating from OWN at an angle α to the LOP. This will be referred to as the solution region. It is the region swept out by the line from the radar at the angle determined by (OAZ + DAZ) as the (horizontal) distance of the radar to OWN ranges from zero to infinity.

The target may be assumed to be at any point within this region defined by its polar coordinates (r,ϕ) where ϕ is in the appropriate interval. Then the radar location consistent with the assumed target position and the given DAZ can be constructed geometrically by drawing a line through the point (r,ϕ) at an angle α to the LOP. The radar position will be at the intersection of this line and the LOP.

Given the position of the target and the radar relative to OWN, the TOA corresponding to the configuration can be computed as

$$T_c(r,\phi) = \sqrt{\frac{\sin^2\phi}{\sin^2\alpha}\, r^2 + H^2} + \sqrt{r^2 + (H-H_o)^2}$$

$$- \sqrt{\frac{\sin^2(\phi+\alpha)}{\sin^2\alpha}\, r^2 + H_o^2} \qquad 2.3.1$$

This is seen to be a function of r and ϕ that is defined and continuous everywhere, and in particular in the solution region, within which it has physical and intuitive meaning.

At every point on a target locus curve, T_c is equal to T, the observed TOA; $T_c > T$ on one side of the curve and $T_c < T$ on the other. Thus the locus curves separate the solution region into regions where $T_c > T$ and $T_c < T$. This implies that the curves must either end on a boundary of the solution region or at infinity - otherwise there would be a path within the solution region such that along the path the continuous finite function $T_c - T$ changed sign without ever going through zero.

In terms of the process for constructing locus curves described previously, it is seen that $T_c < T$ on the side of the locus line lying on the inside of the constant - TOA ellipse and $T_c > T$ on the side corresponding to the outside of the ellipse.

The greatest significance of the observation that the locus curves are boundaries lies is its potential use for finding target aircraft positions by search in the solution region. An algorithm applicable to the single-site geometry is described fully in Section 3.4. An algorithm similar in principle, though more complex, could be constructed for the case of passive operation with two radars with azimuth reference signals. The cases to be considered are identified and described in Section 4.

2.4 THE NATURE OF THE LOCUS CURVES

Plots of families of locus curves are shown in Figures 2.4-1 to 2.4-24. The shape of each curve is determined by the three variables α, H/T, H_o/T. The scale is determined by T. Only a sampling of the possible combinations of parameters have been used in plotting the curves. The families of curves to be plotted on any one graph were selected to show the sensitivity of the curves to changes in the individual parameters. The following conclusions appear to be generally valid:

1) For $T > H$ and $T > H_o$, the curves change relatively little with changes in the differential azimuth (Figures 2-4.1 to 2.4-5). Hence, they are insensitive to DAZ measurement errors.

2) Over a very wide range of altitudes, the curves change very little (except in the quadrant opposite the radar) if both own and target altitudes change together, or, what is equivalent, the radar altitude deviates from its nominal (zero) value (Figures 2.4-6 to 2.4-12). The sensitivity is least when the target and OWN are at coaltitude. Hence, knowledge of true radar altitude is not important to BCAS for determining target positions.

3) The curves do not vary drastically when the relative altitudes of OWN and other change. The curves tend to come closer to the origin - i.e., to OWN when the altitude separation increases. It is important to note that this happens whether OWN is above or below the target (Figures 2.4-13 to 2.4-22). Hence, it does not appear feasible to deduce the altitudes relative to own of other aircraft not equipped with mode C transponders from other BCAS

measurements. It does appear feasible to estimate the range and bearing of such aircraft by assuming them to be at coaltitude, but the horizontal range estimates will be somewhat too high.

4) The locus curves do change quite drastically as the various parameters change when the TOA is small relative to the altitude (Figures 2.4-23 to 2.4-24). Hence, solutions based on measurement sets including small TOA's are likely to be highly error-sensitive.

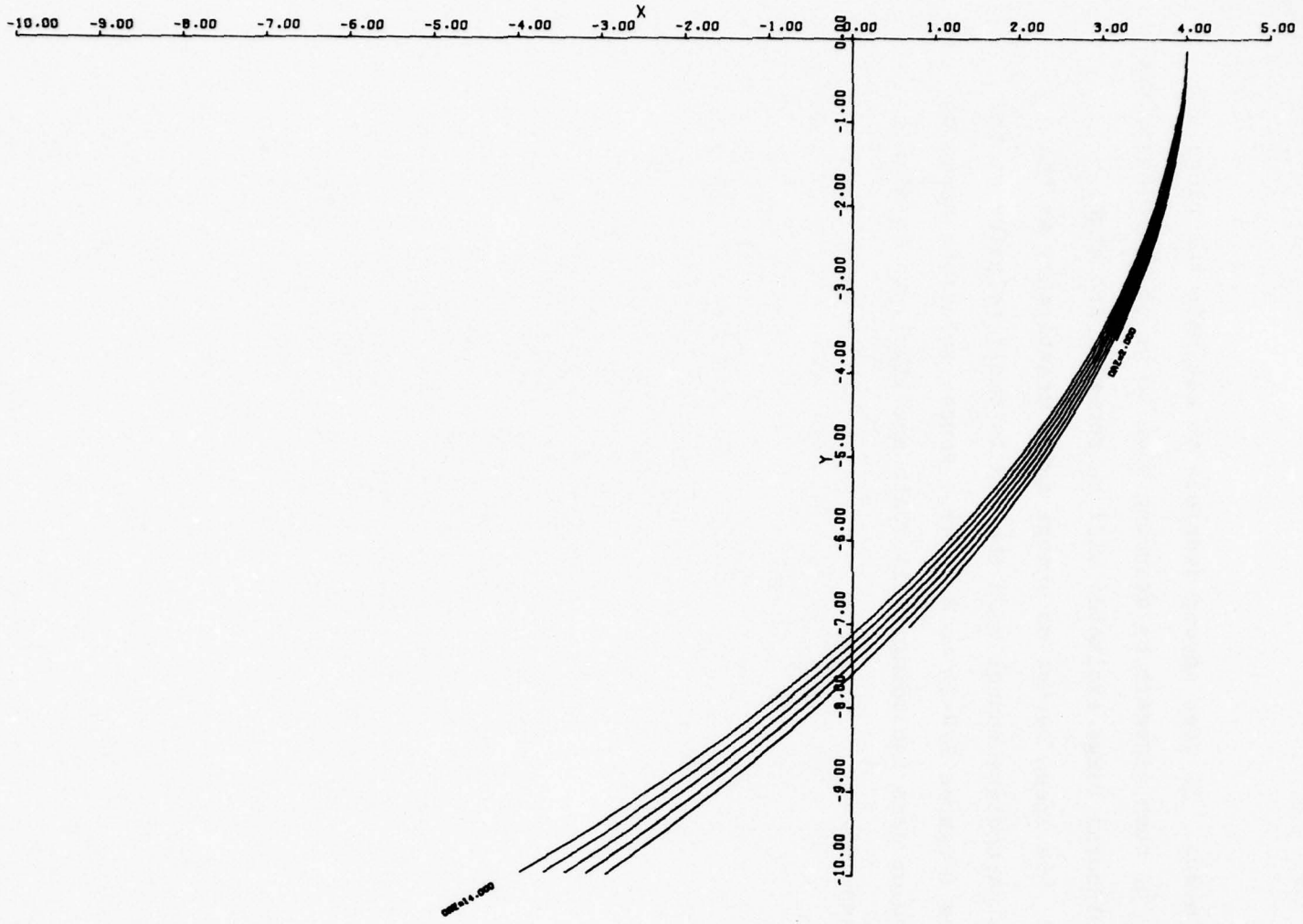

FIGURE 2.4-1. HEIGHT OF OWN = 0, HEIGHT OF OTHER = 0,T = 8.000 MILES.

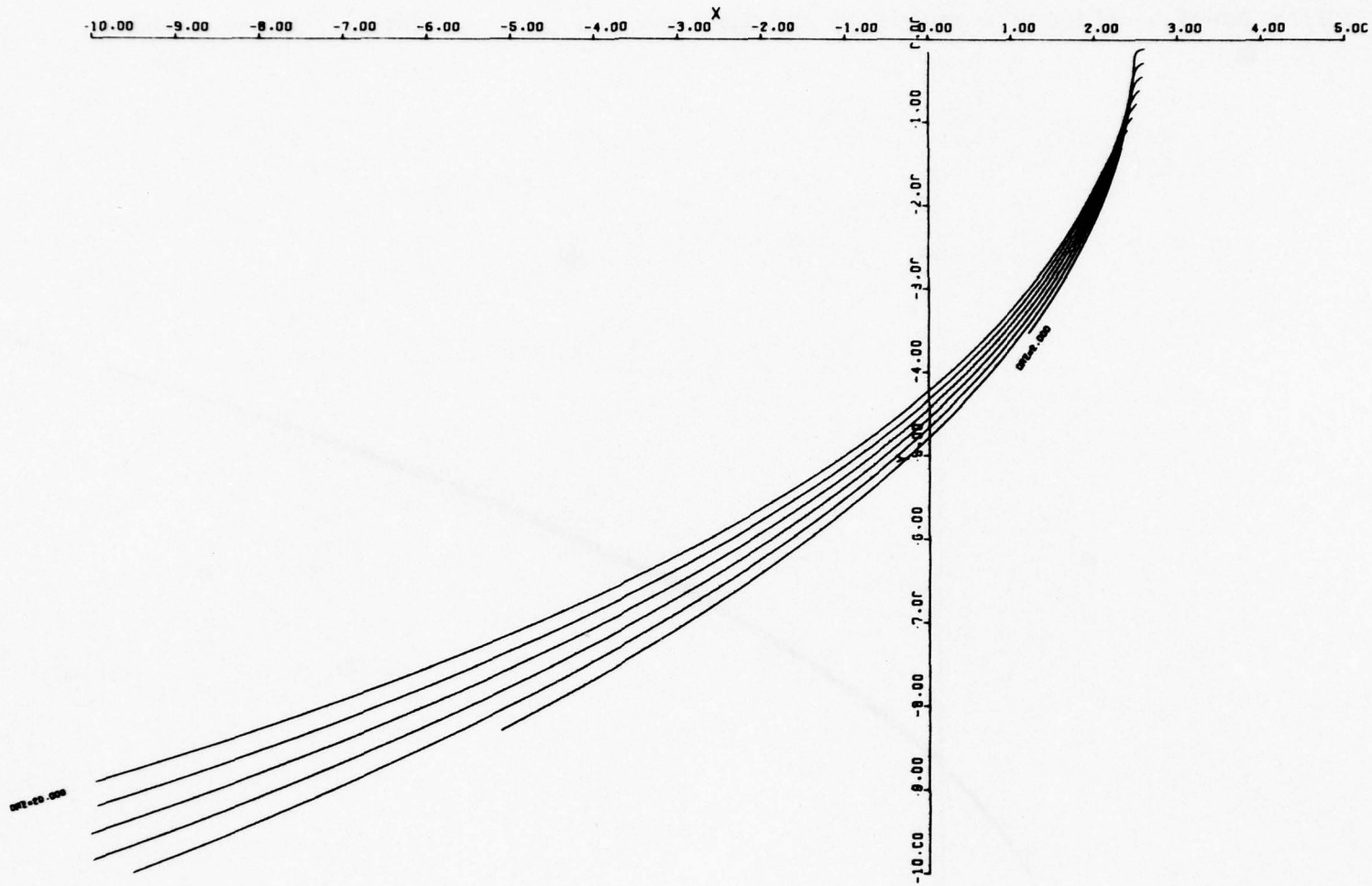

FIGURE 2.4-2. HEIGHT OF OWN = 5000, HEIGHT OF OTHER = 7000,T = 5.000 MILES.

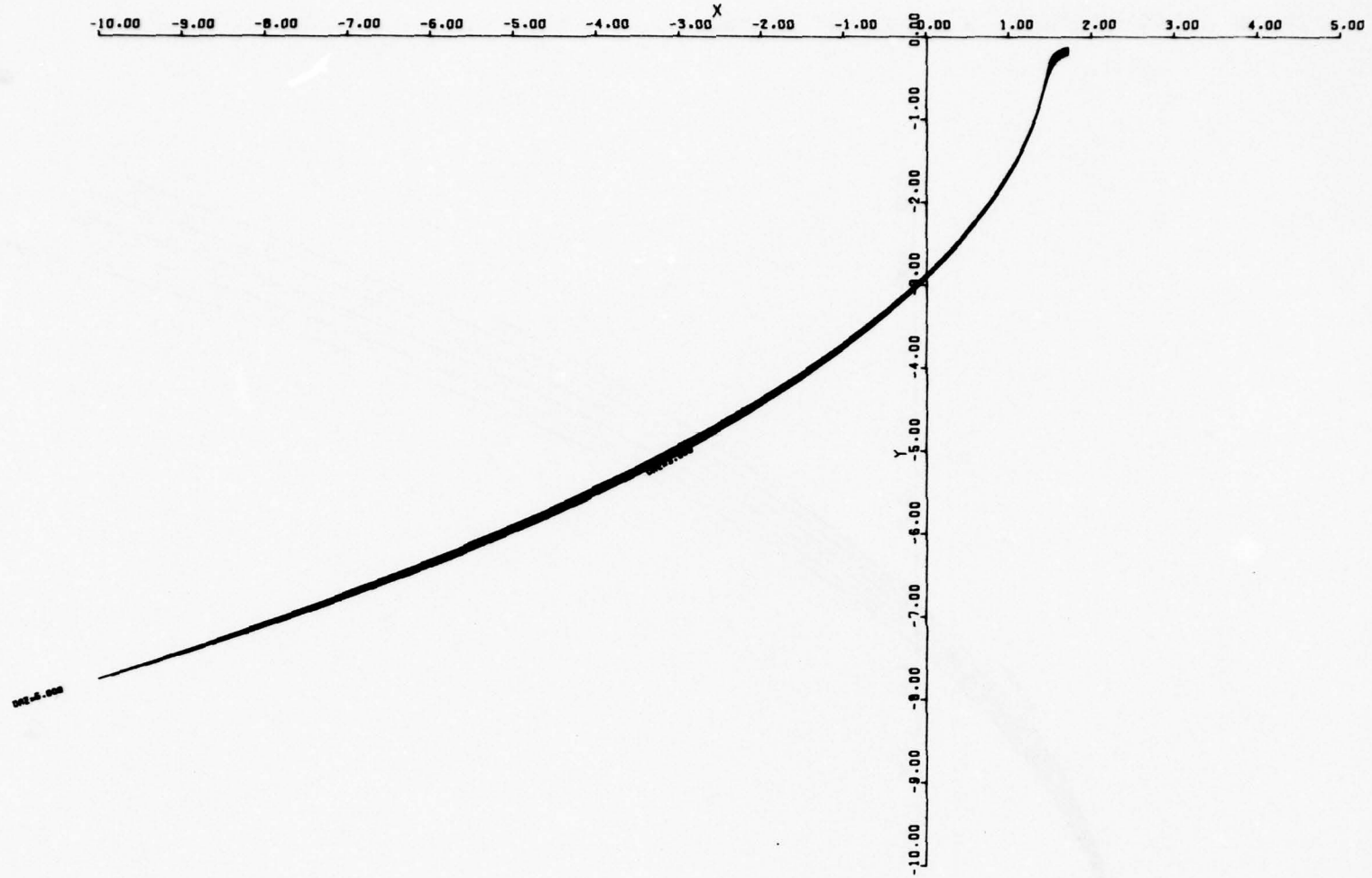

FIGURE 2.4-3. HEIGHT OF OWN = 10000, HEIGHT OF OTHER = 11000,T = 3.000 MILES.

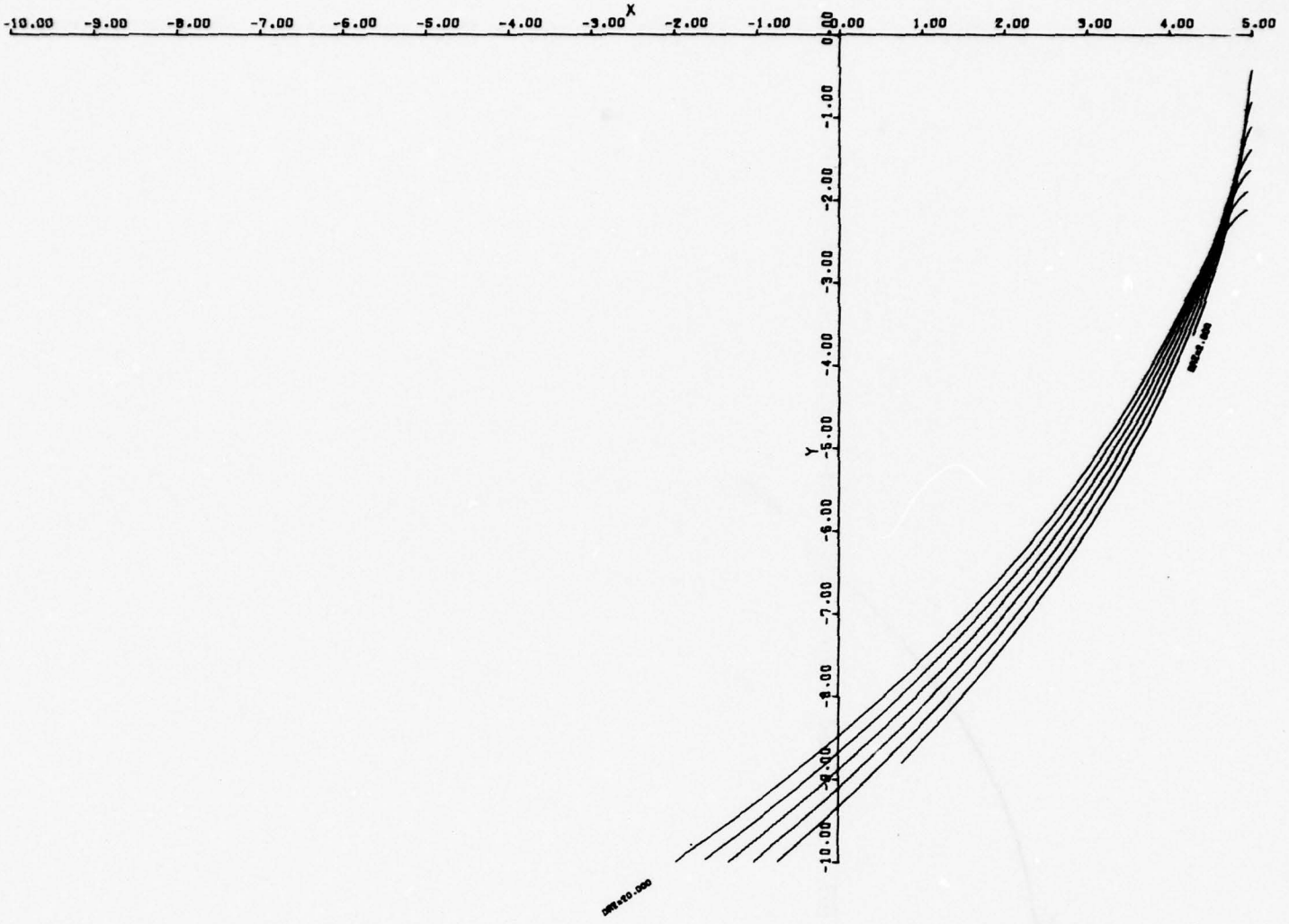

FIGURE 2.4-4. HEIGHT OF OWN = 10000, HEIGHT OF OTHER =12000,T = 10.000 MILES.

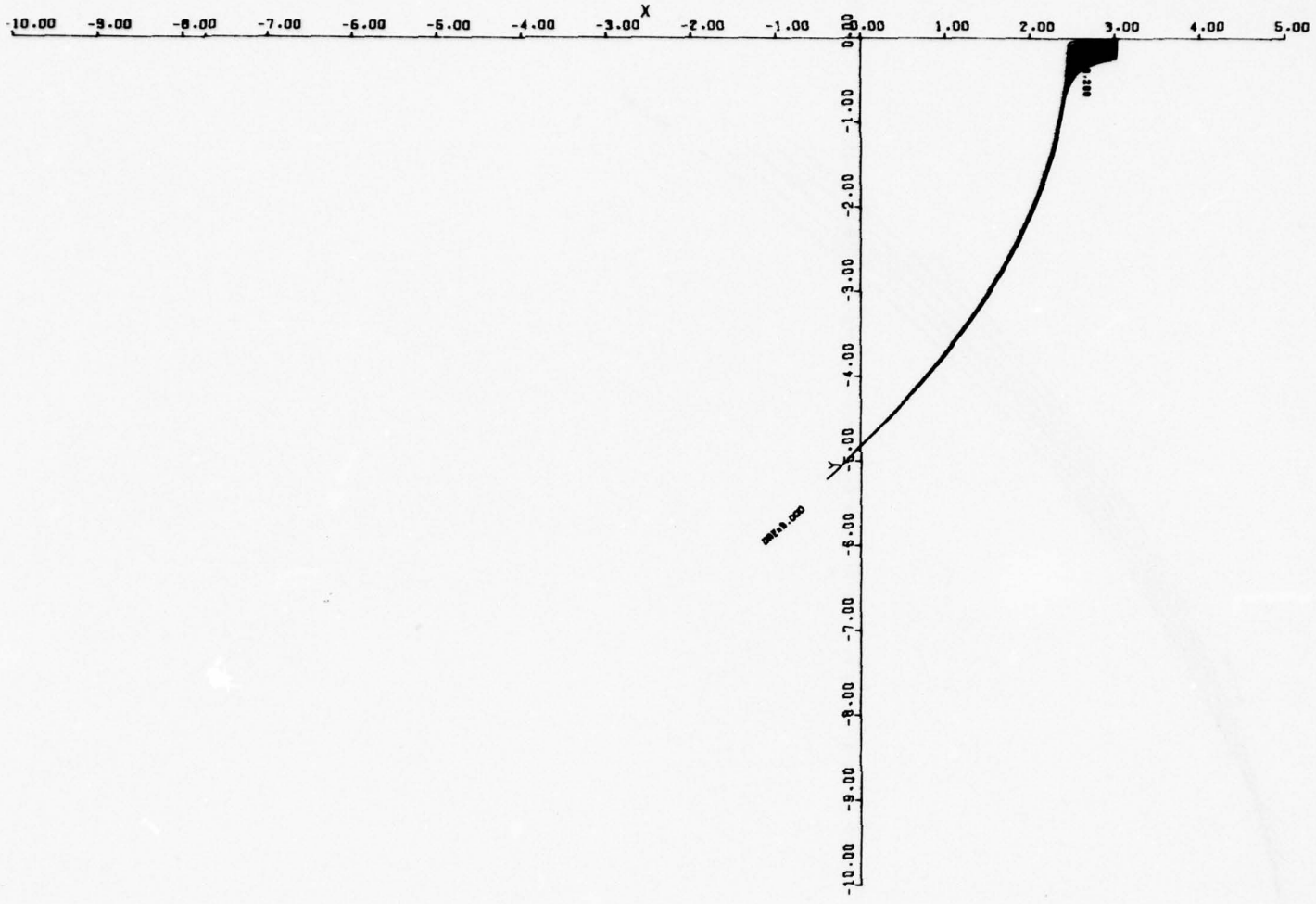

FIGURE 2.4-5. HEIGHT OF OWN - 28000, HEIGHT OF OTHER = 31000,T = 5.000 MILES.

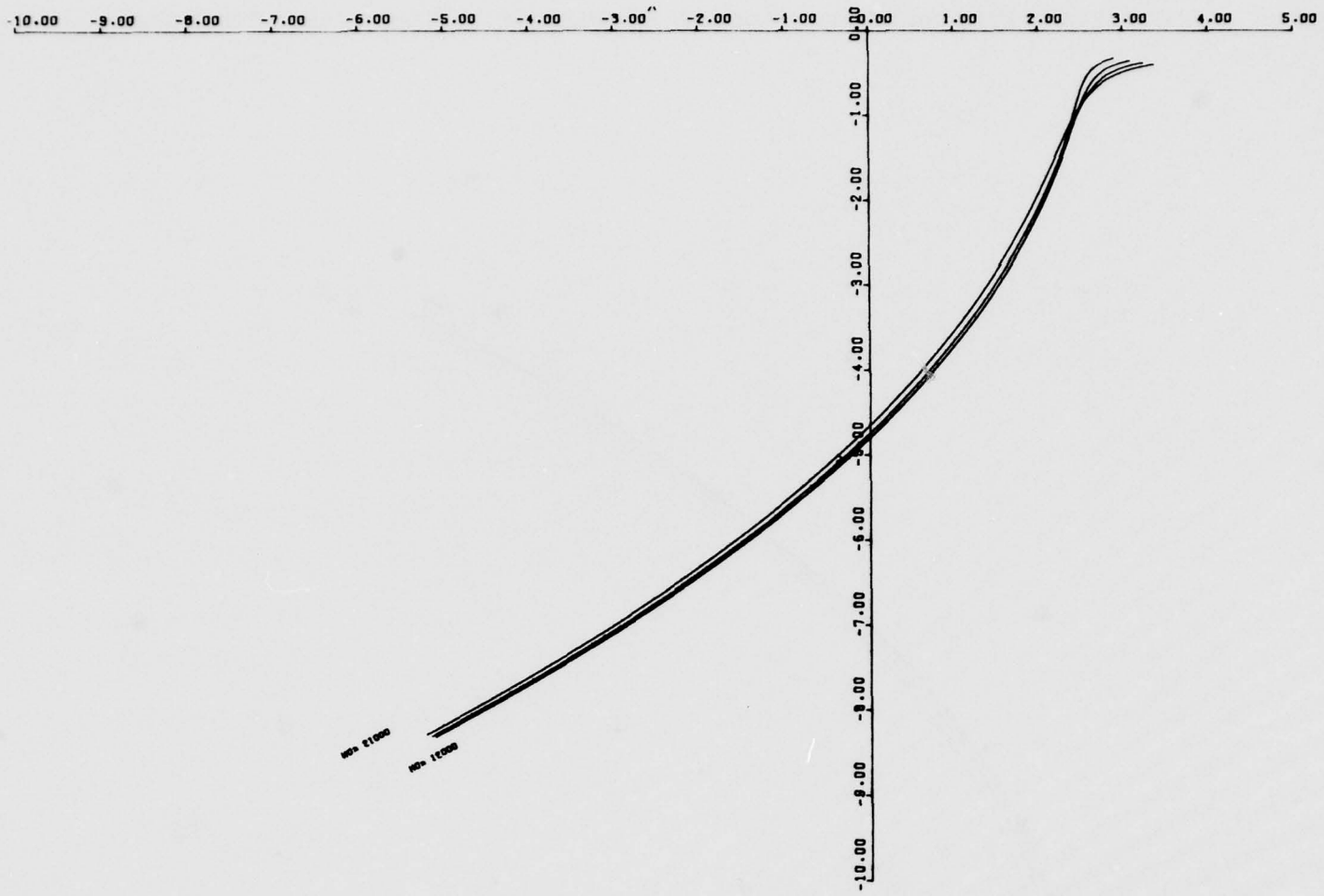

FIGURE 2.4-6. HEIGHT OF OTHER = 12000, T = 5.000 MILES, DAZ = 5.000

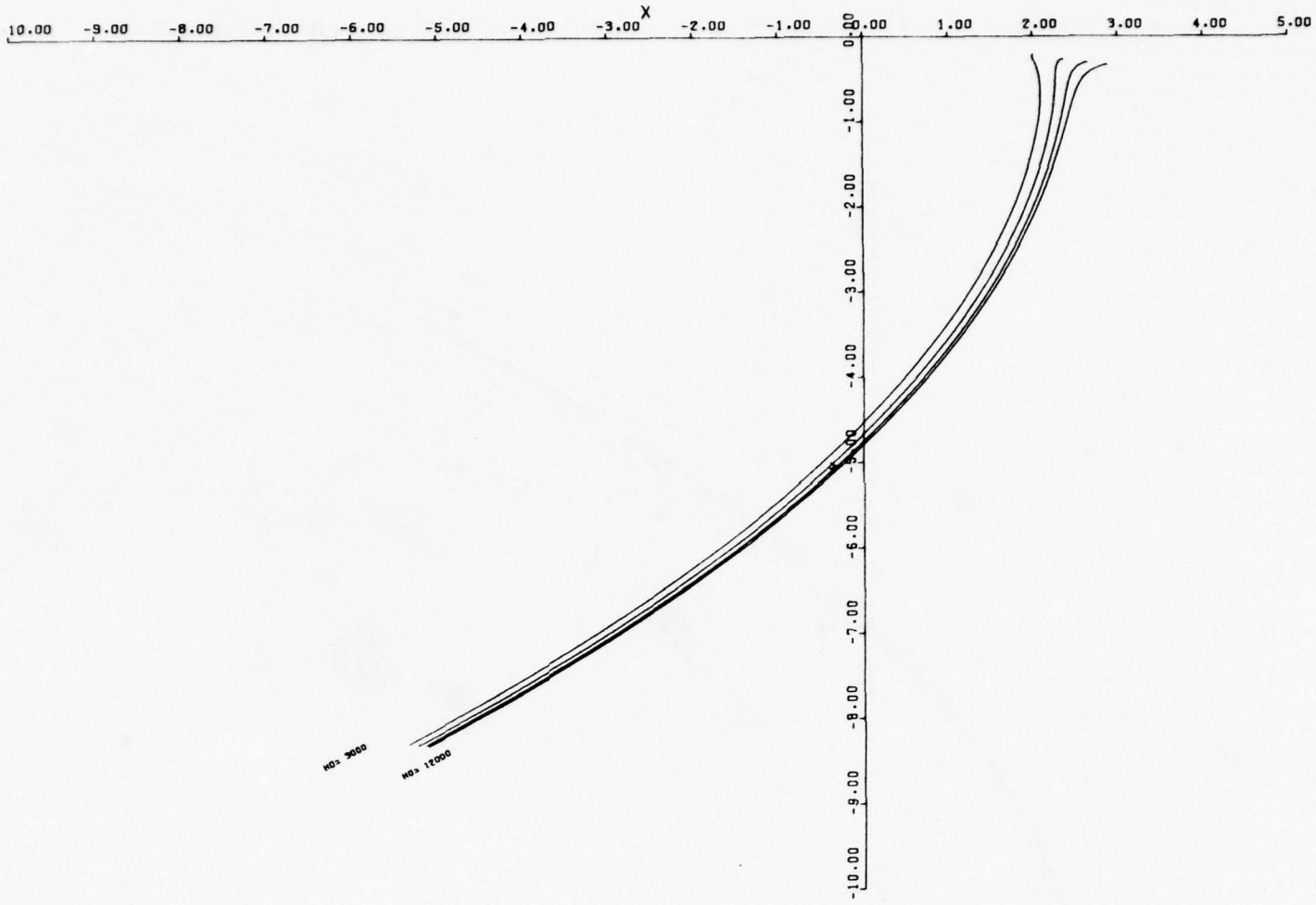

FIGURE 2.4-7. HEIGHT OF OTHER = 12000, T = 5.000 MILES, DAZ = 5.000

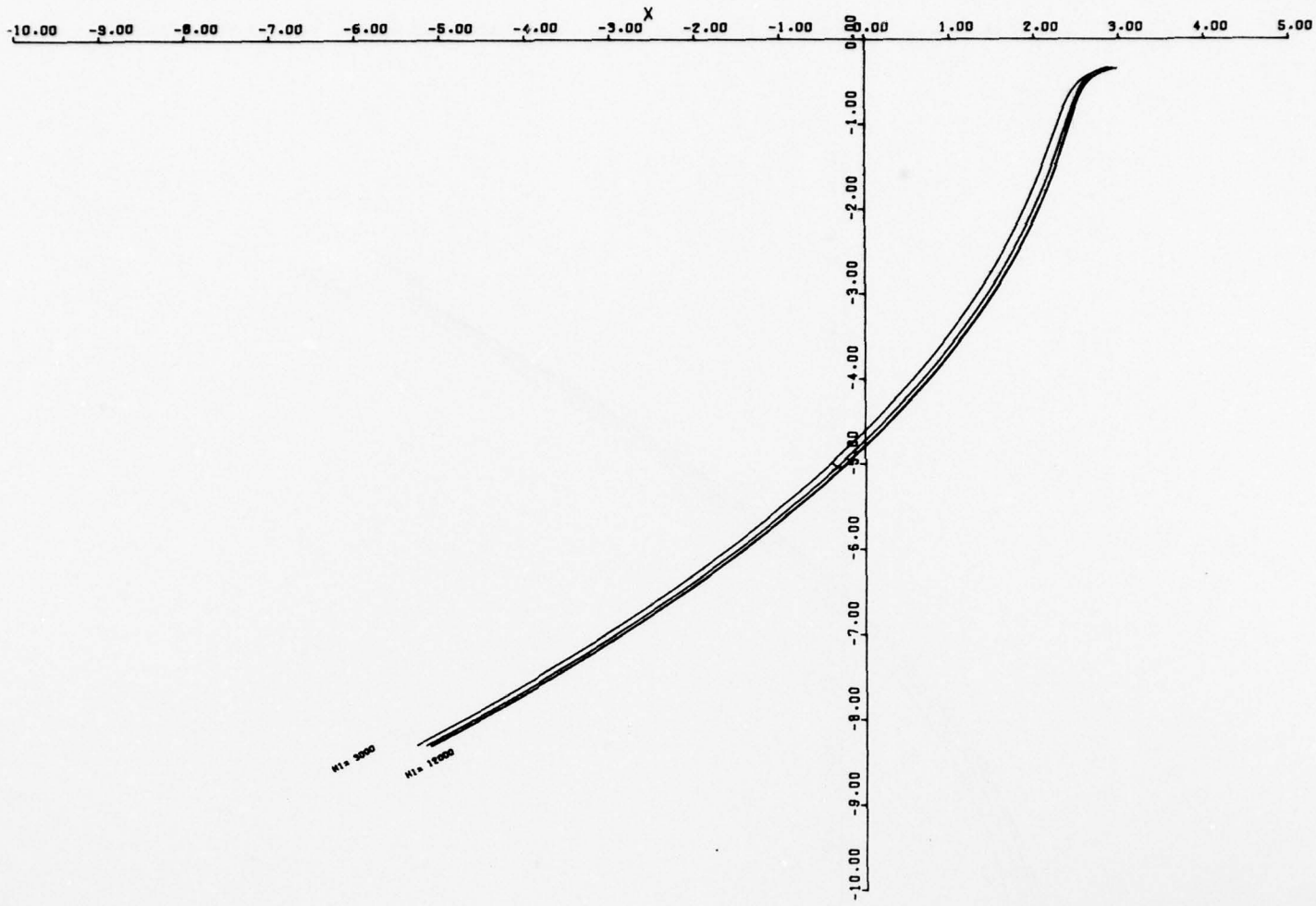

FIGURE 2.4-8. HEIGHT OF OWN = 12000, T = 5.000 MILES, DAZ = 5.000

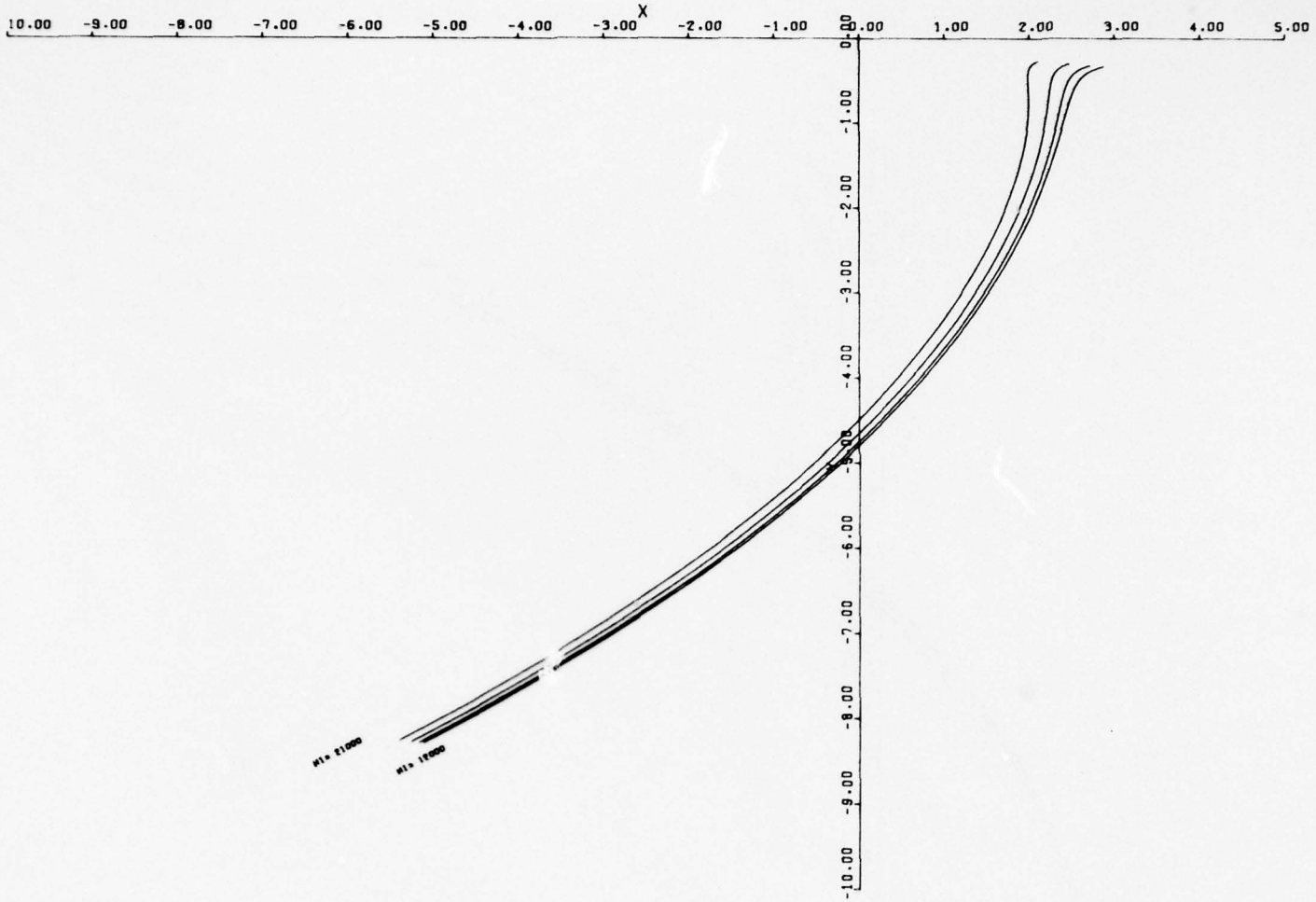

FIGURE 2.4-9. HEIGHT OF OWN = 12000, T = 5.000 MILES,DAZ = 5.000

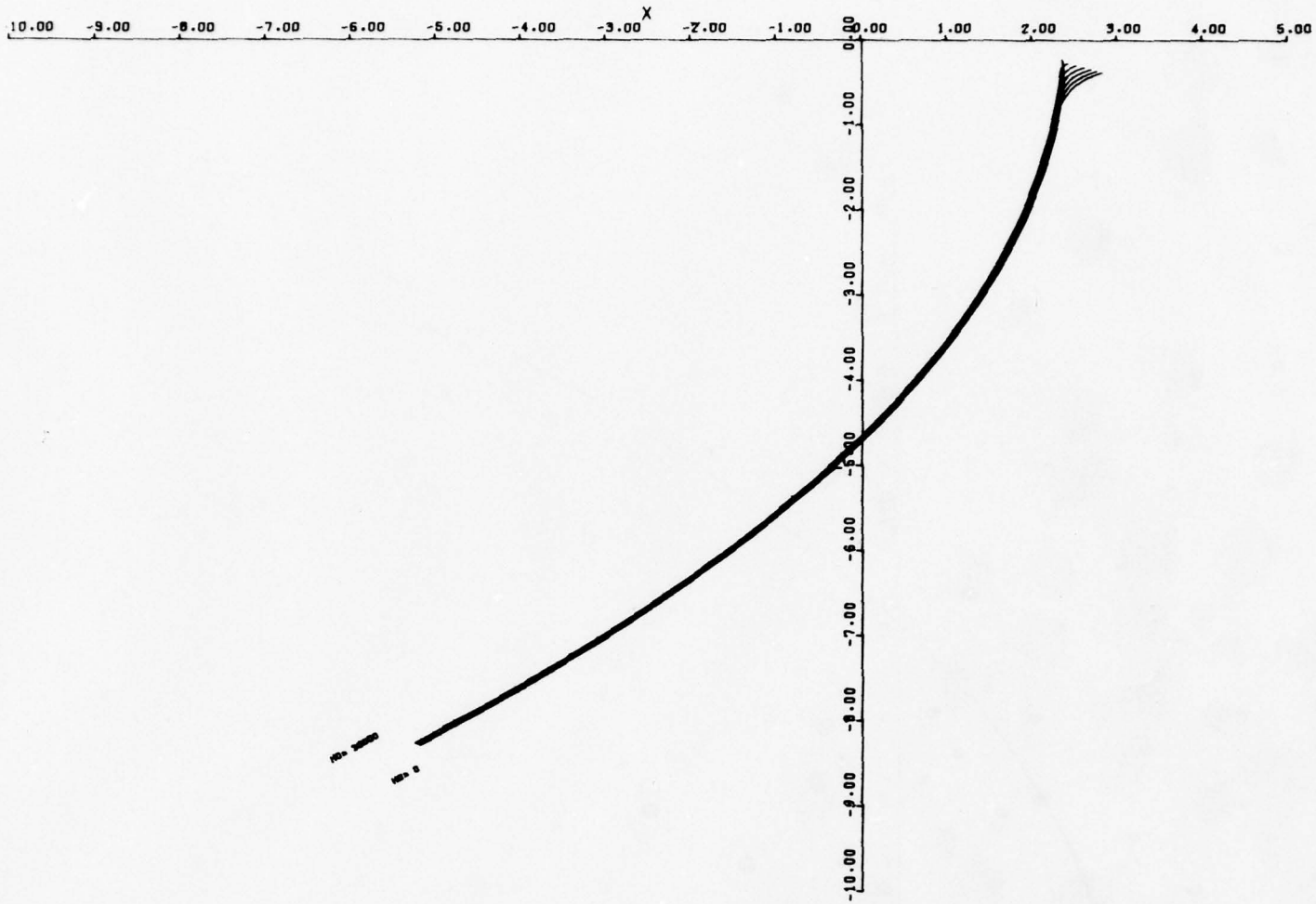

FIGURE 2.4-10. H1 - H0 = 5000, T = 5.000 MILES,DAZ = 5.000.

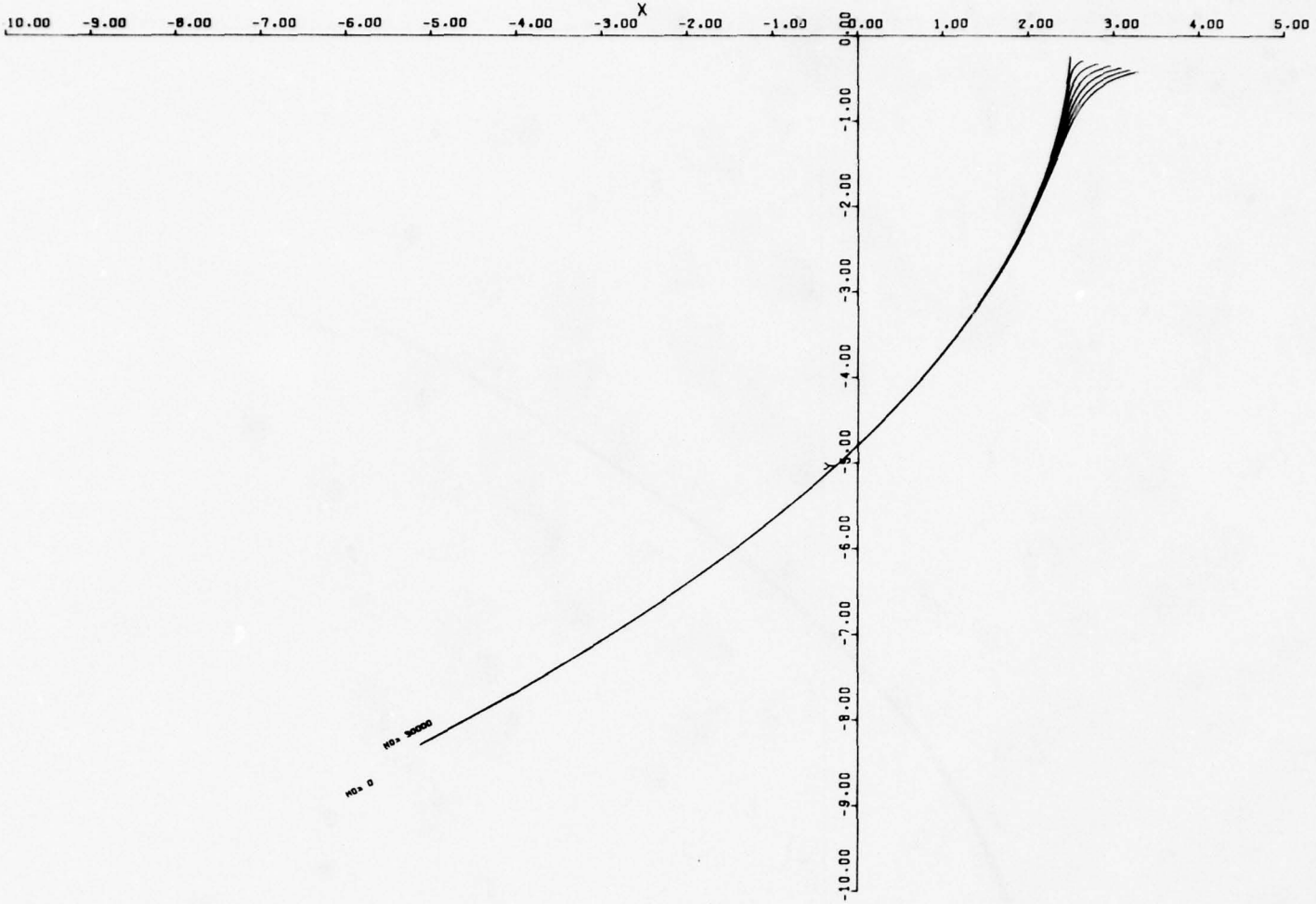

FIGURE 2.4-11. H1 - H0 = 0, T = 5.000 MILES,DAZ = 5.000

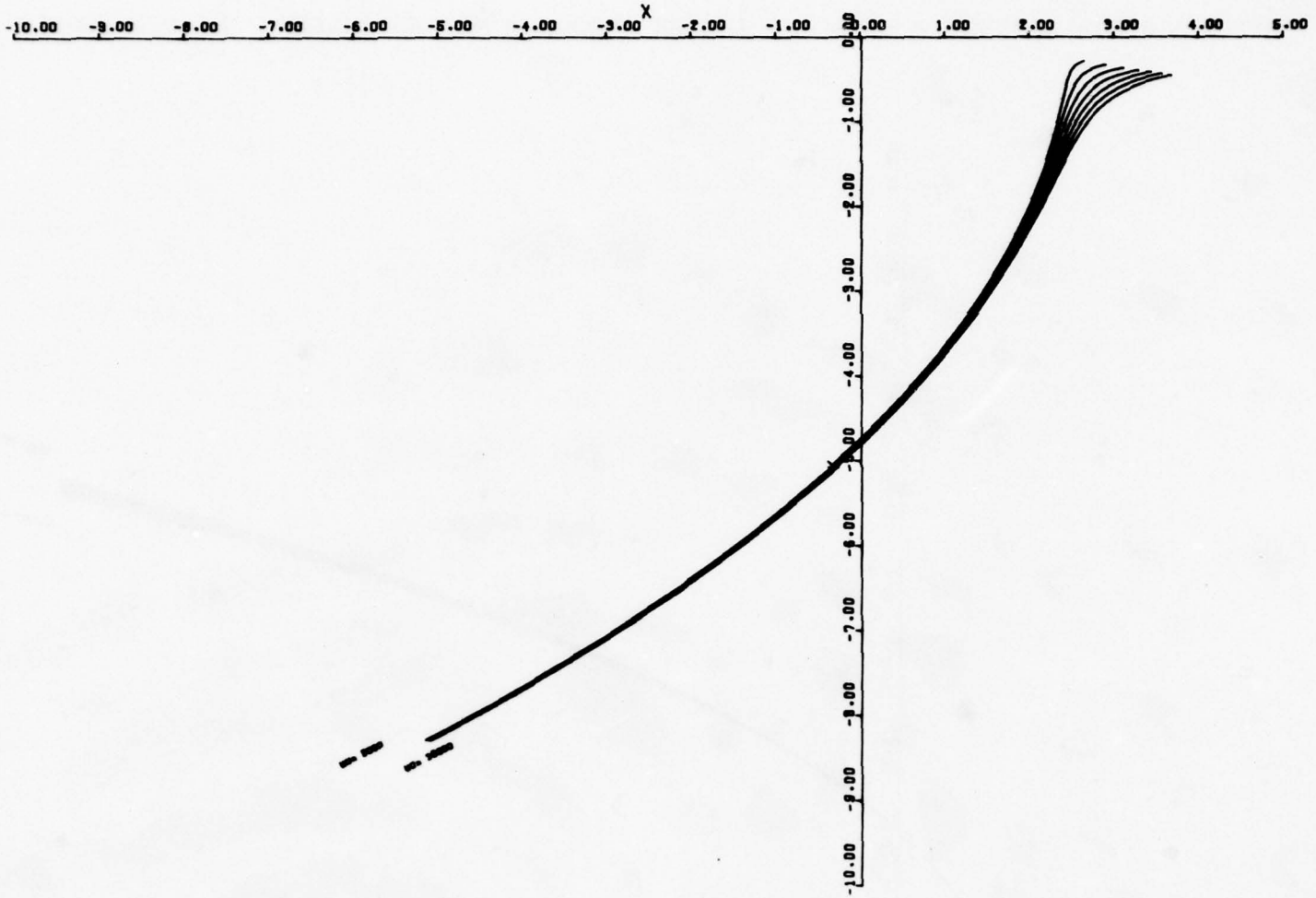

FIGURE 2.4-12. H1 - H0 = -5000, T = 5.000 MILES,DAZ = 5.000.

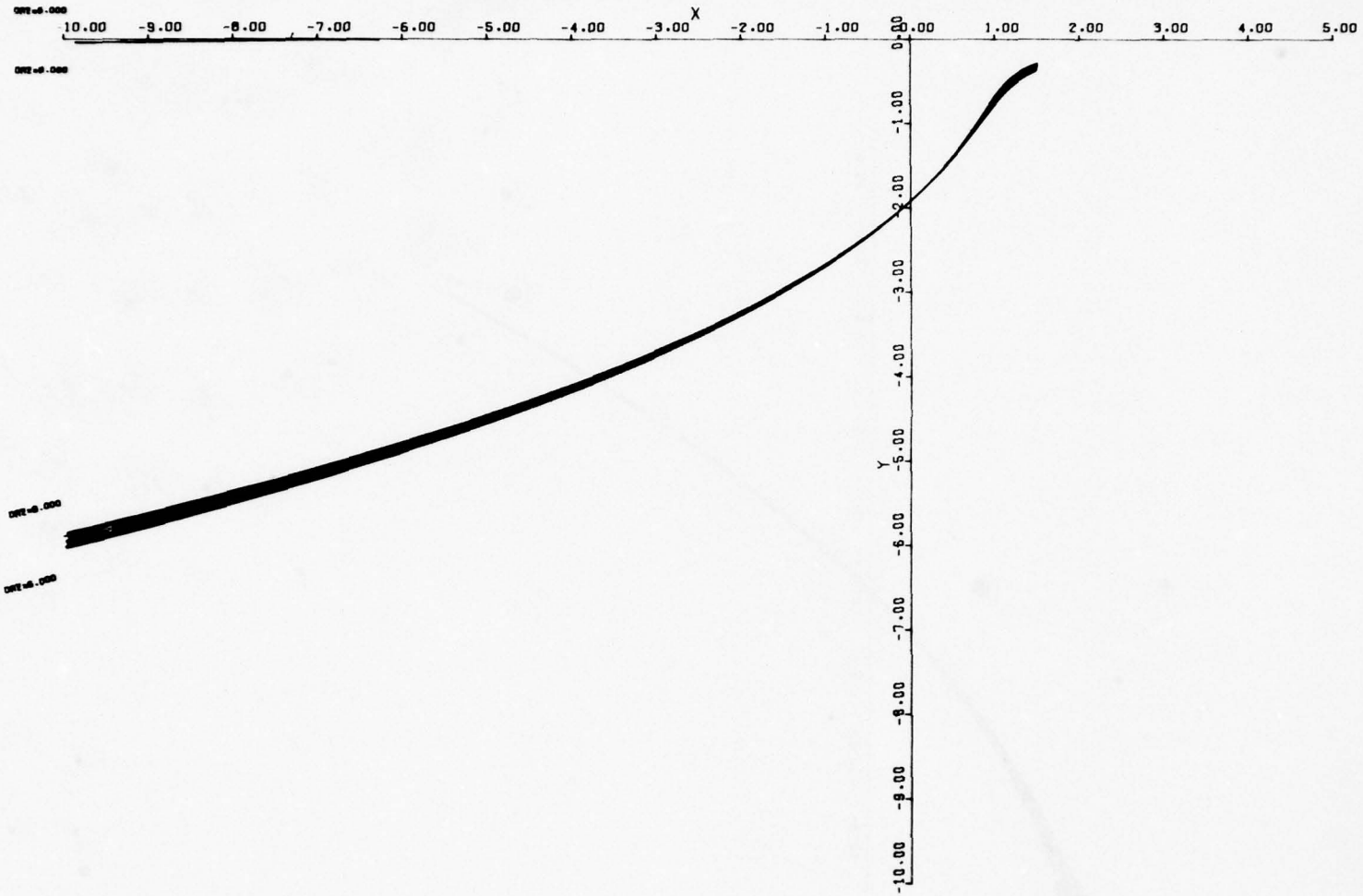

FIGURE 2.4-13. HEIGHT OF OWN = 20000, HEIGHT OF OTHER = 17000,T = 2.000 MILES.

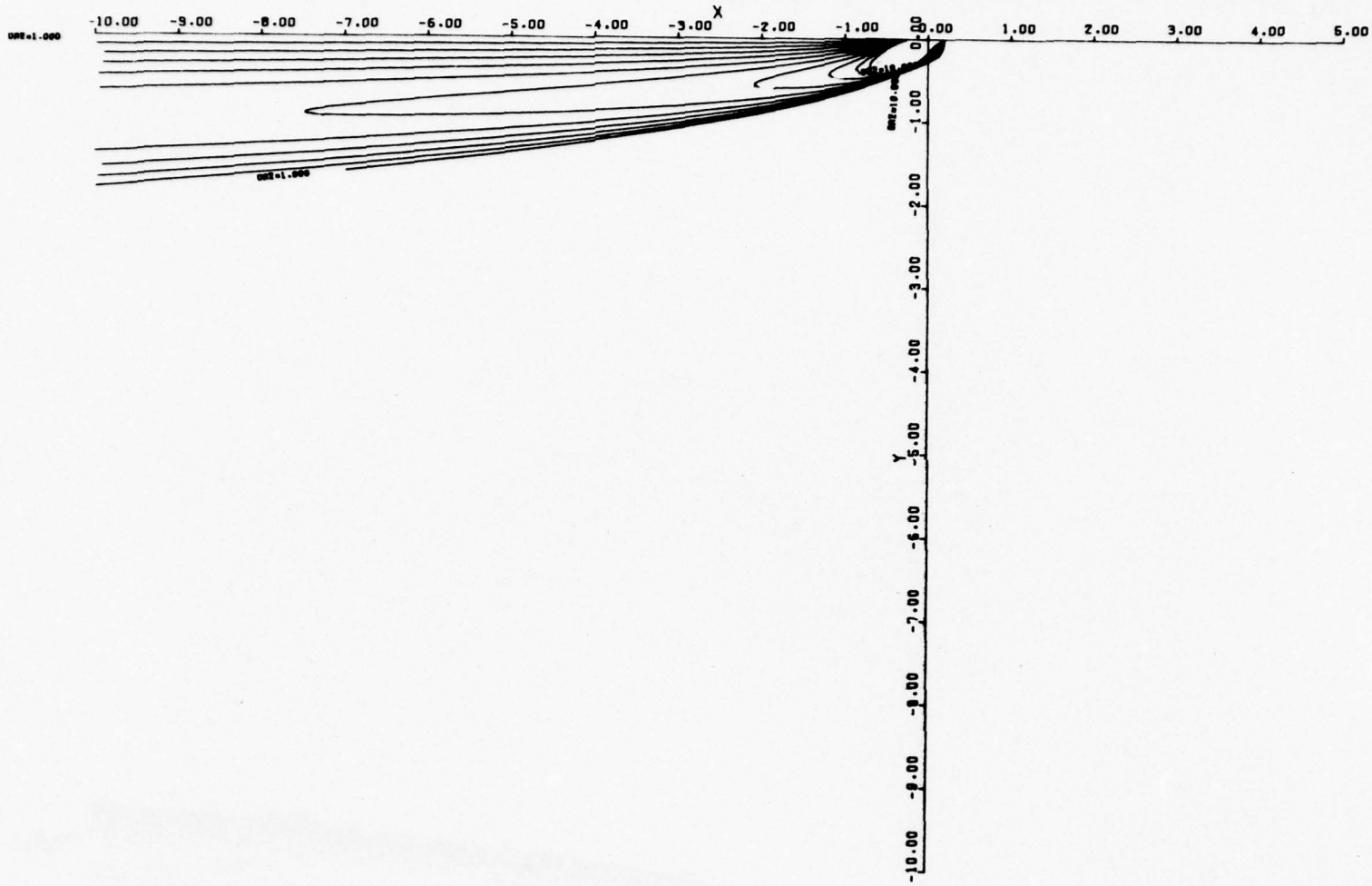

FIGURE 2.4-14. HEIGHT OF OWN = 14000, HEIGHT OF OTHER = 13000,T = 0.200 MILES.

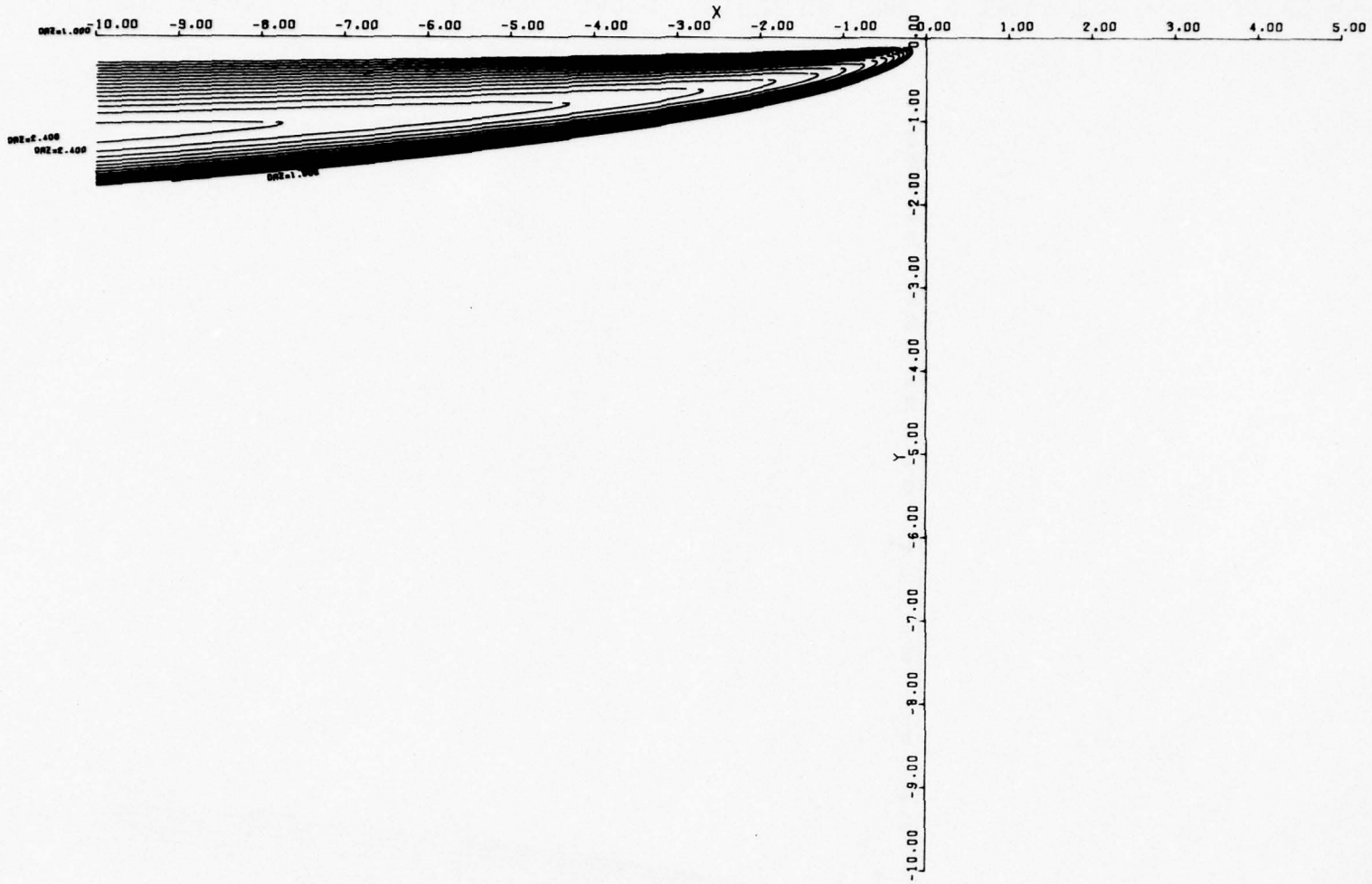

FIGURE 2.4-15. HEIGHT OF OWN = 25000, HEIGHT OF OTHER = 26000, T = 0.200 MILES.

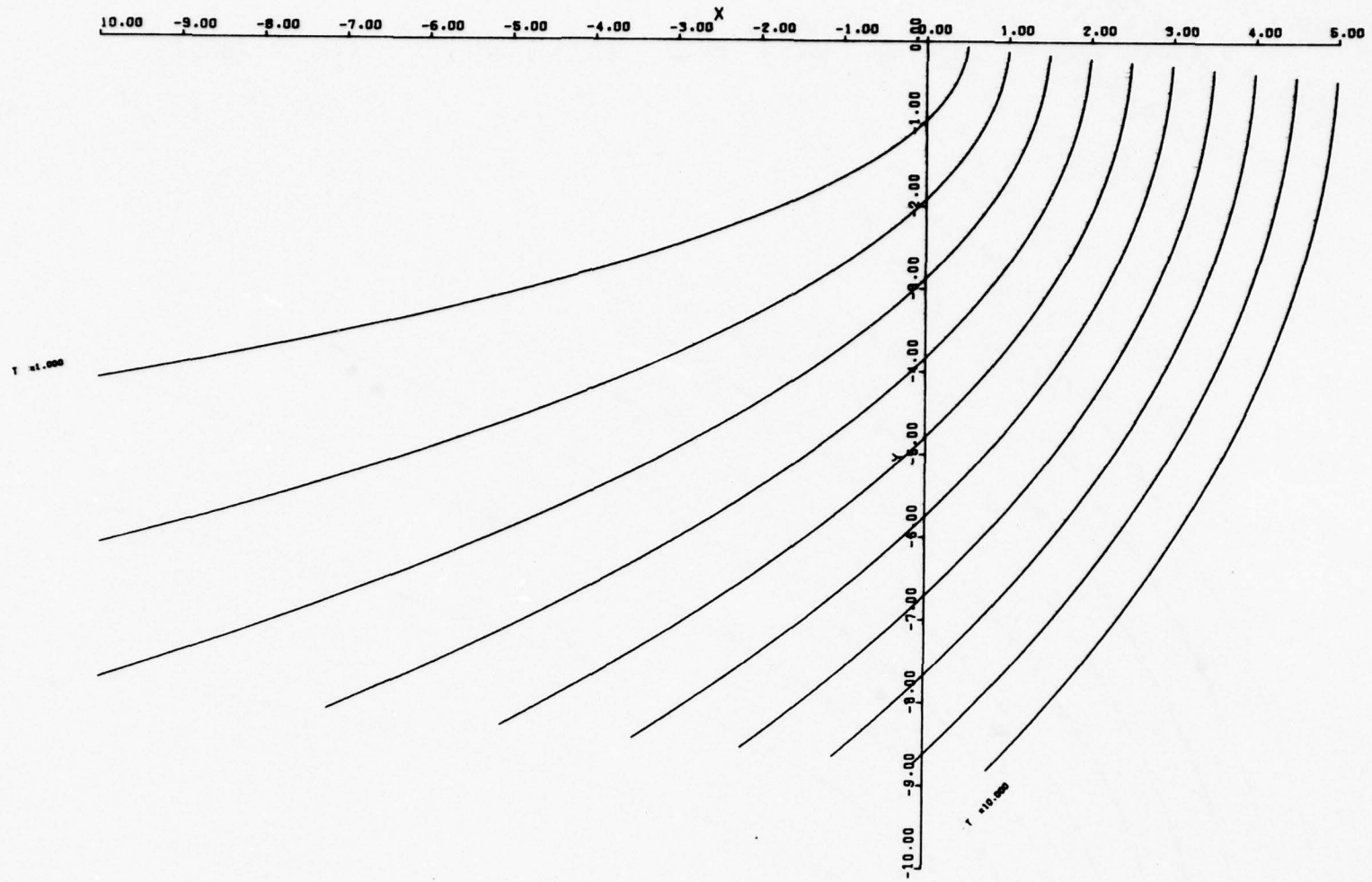

FIGIRE 2.4-16. HEIGHT OF OWN = 0, HEIGHT OF OTHER = 0, DAZ = 5.000.

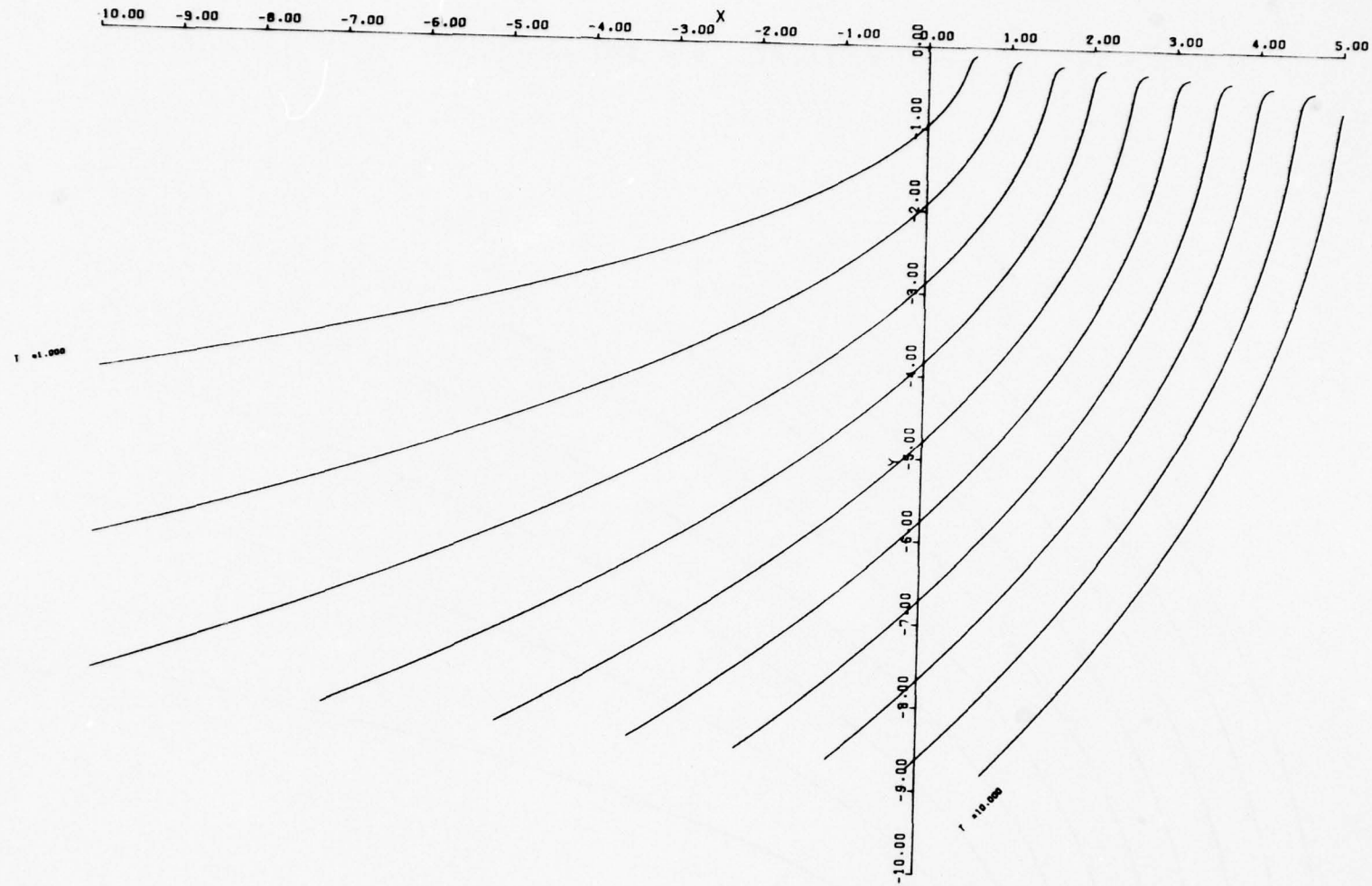

FIGURE 2.4-17. HEIGHT OF OWN = 5000, HEIGHT OF OTHER = 5000, DAZ = 5.000.

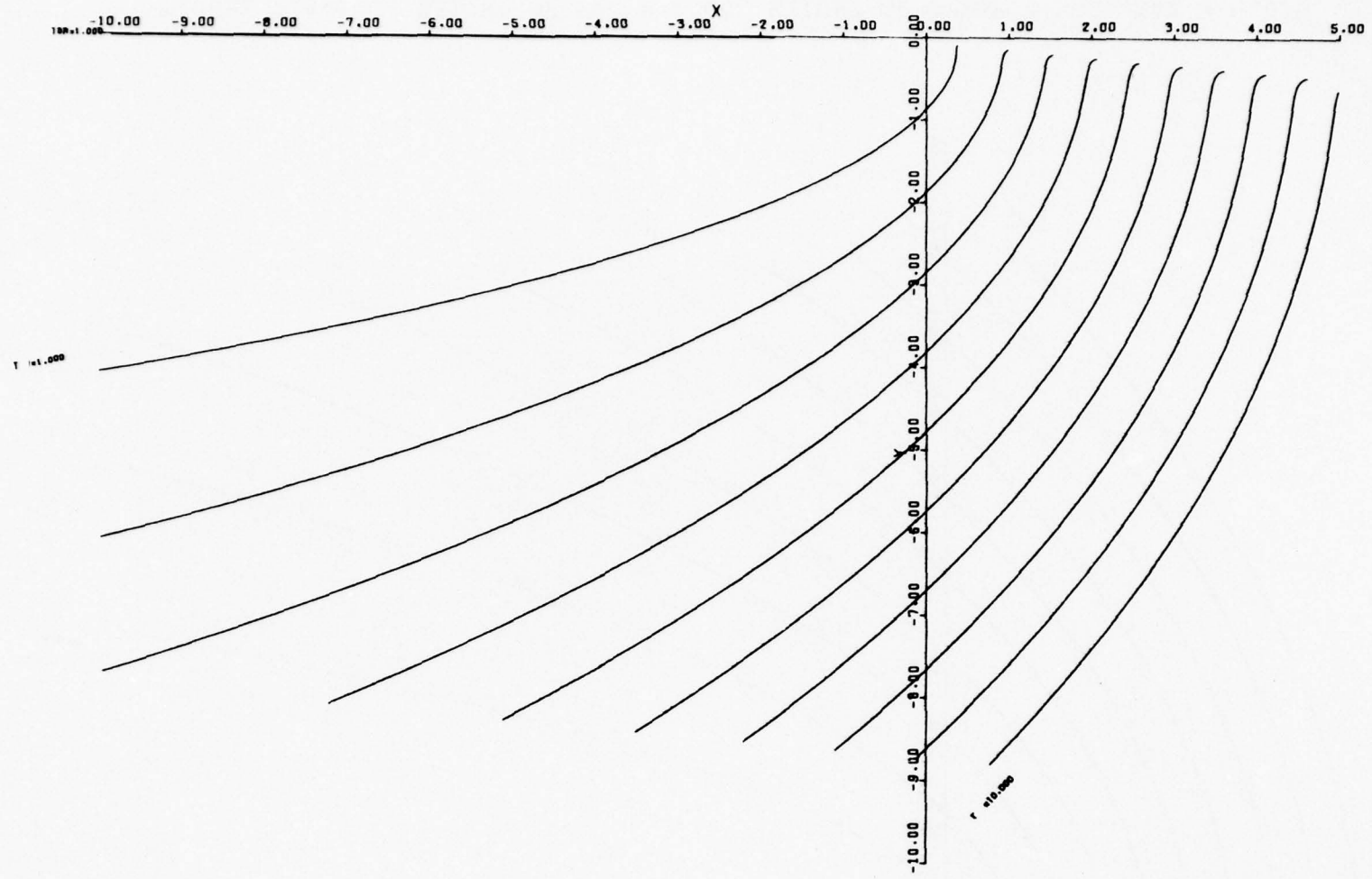

FIGURE 2.4-18. HEIGHT OF OWN = 5000, HEIGHT OF OTHER = 7000,DAZ = 5.000.

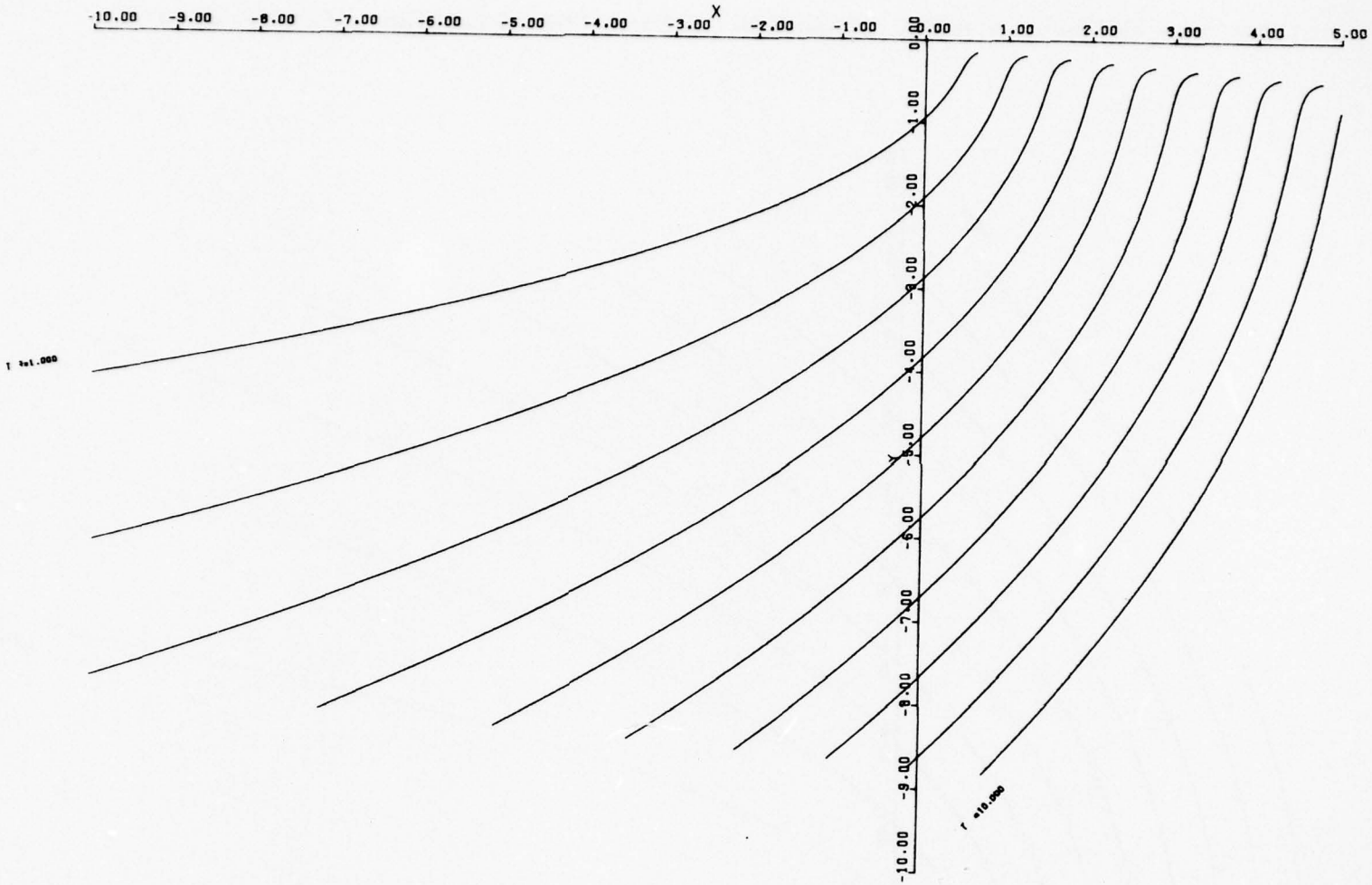

FIGURE 2.4-19. HEIGHT OF OWN = 7000, HEIGHT OF OTHER = 5000,DAZ = 5.000

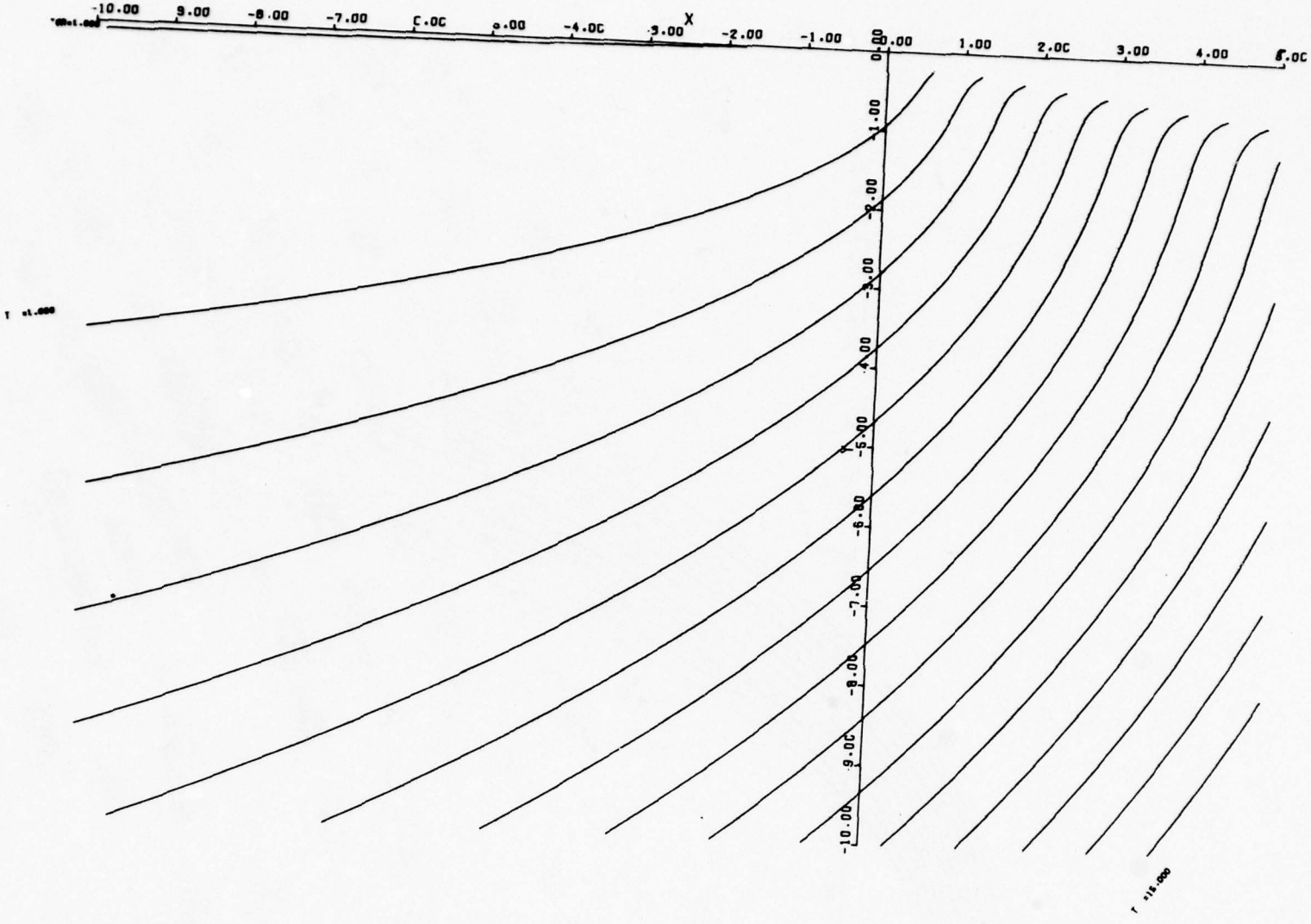

FIGURE 2.4-20. HEIGHT OF OWN = 10000, HEIGHT OF OTHER = 10000,DAZ = 8.000.

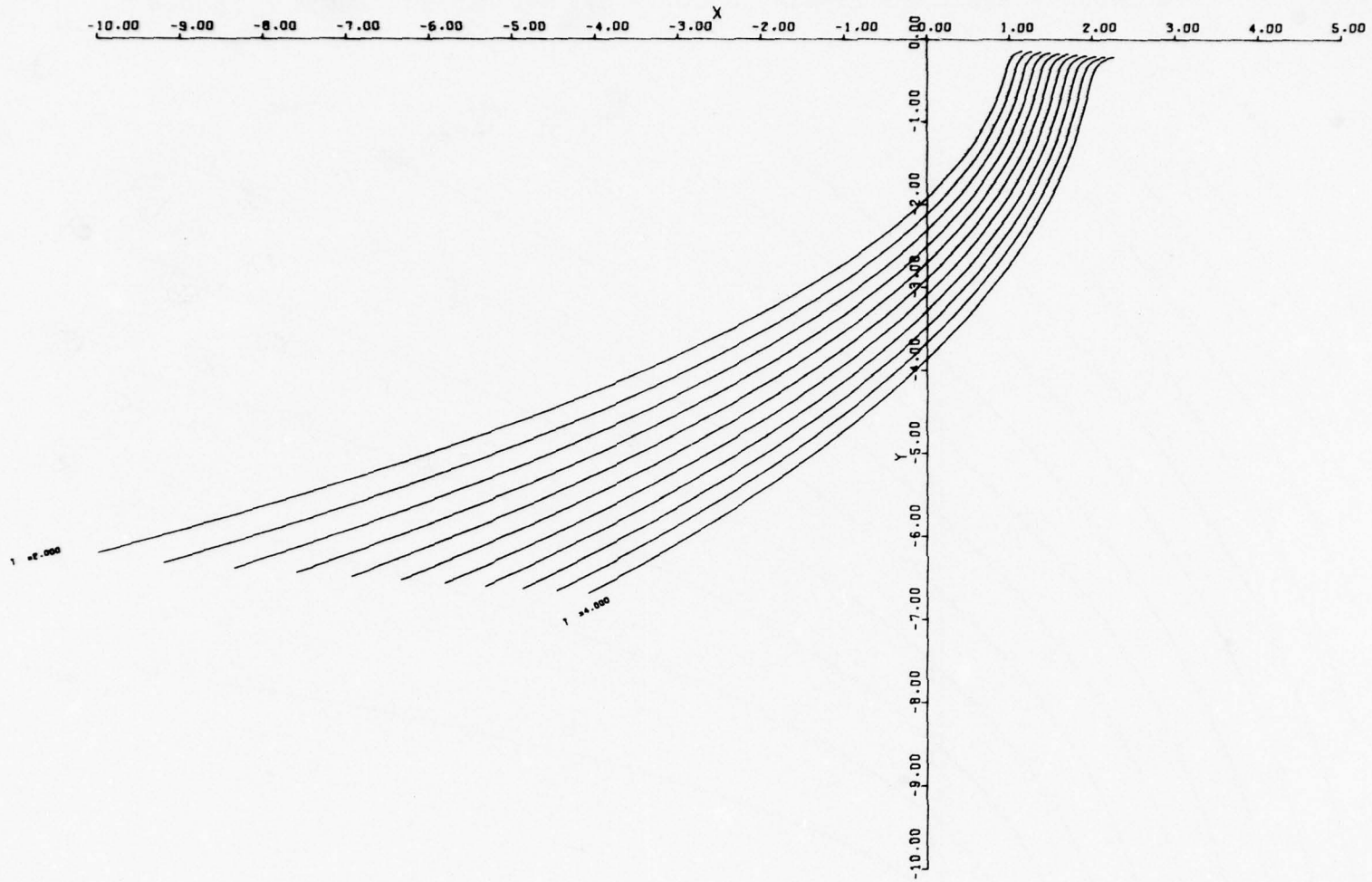

FIGURE 2.4-21. HEIGHT OF OWN = 10000, HEIGHT OF OTHER = 11000,DAZ = 4.000.

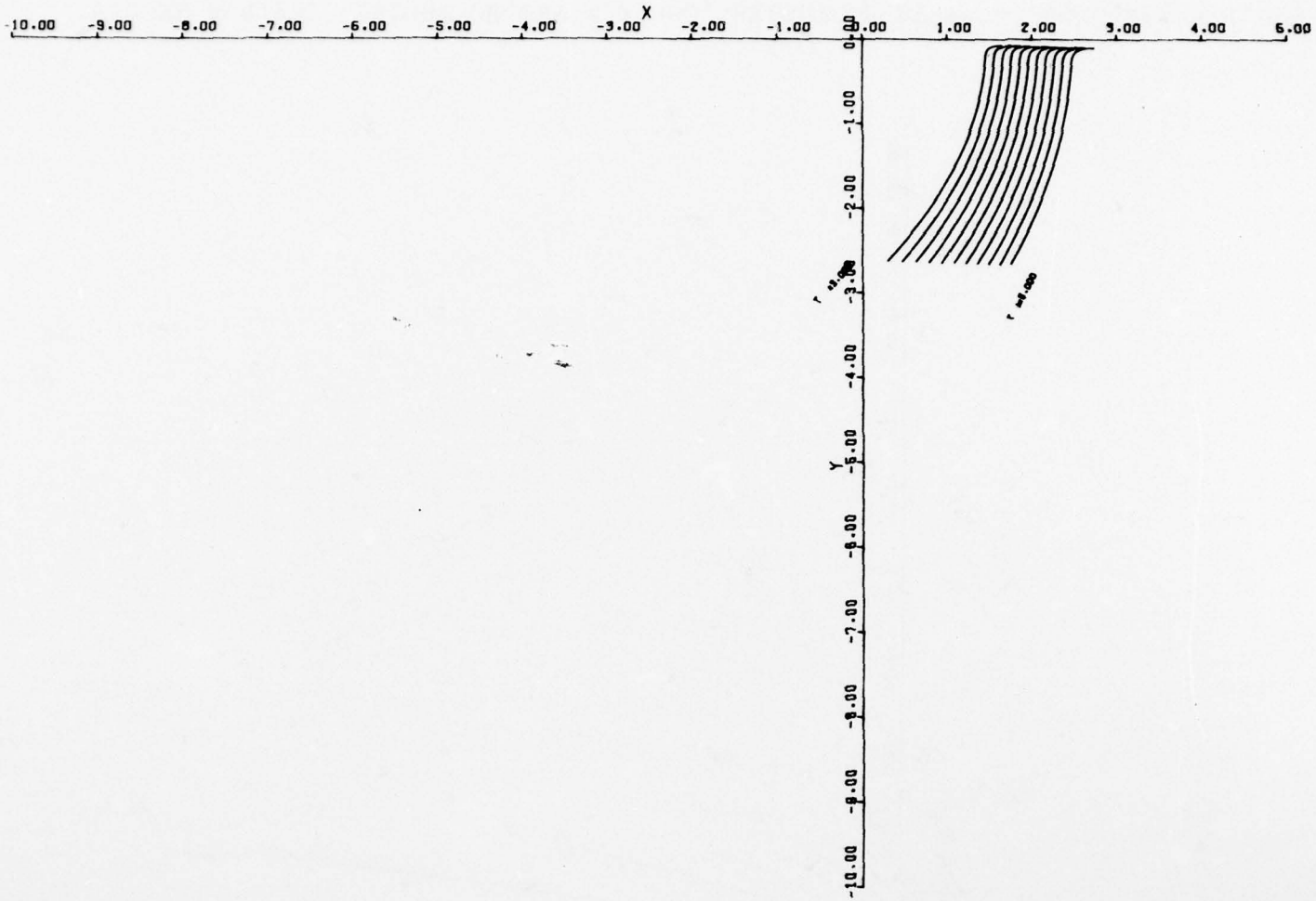

FIGURE 2.4-22. HEIGHT OF OWN = 10000, HEIGHT OF OTHER = 12000,DAZ = 1.500.

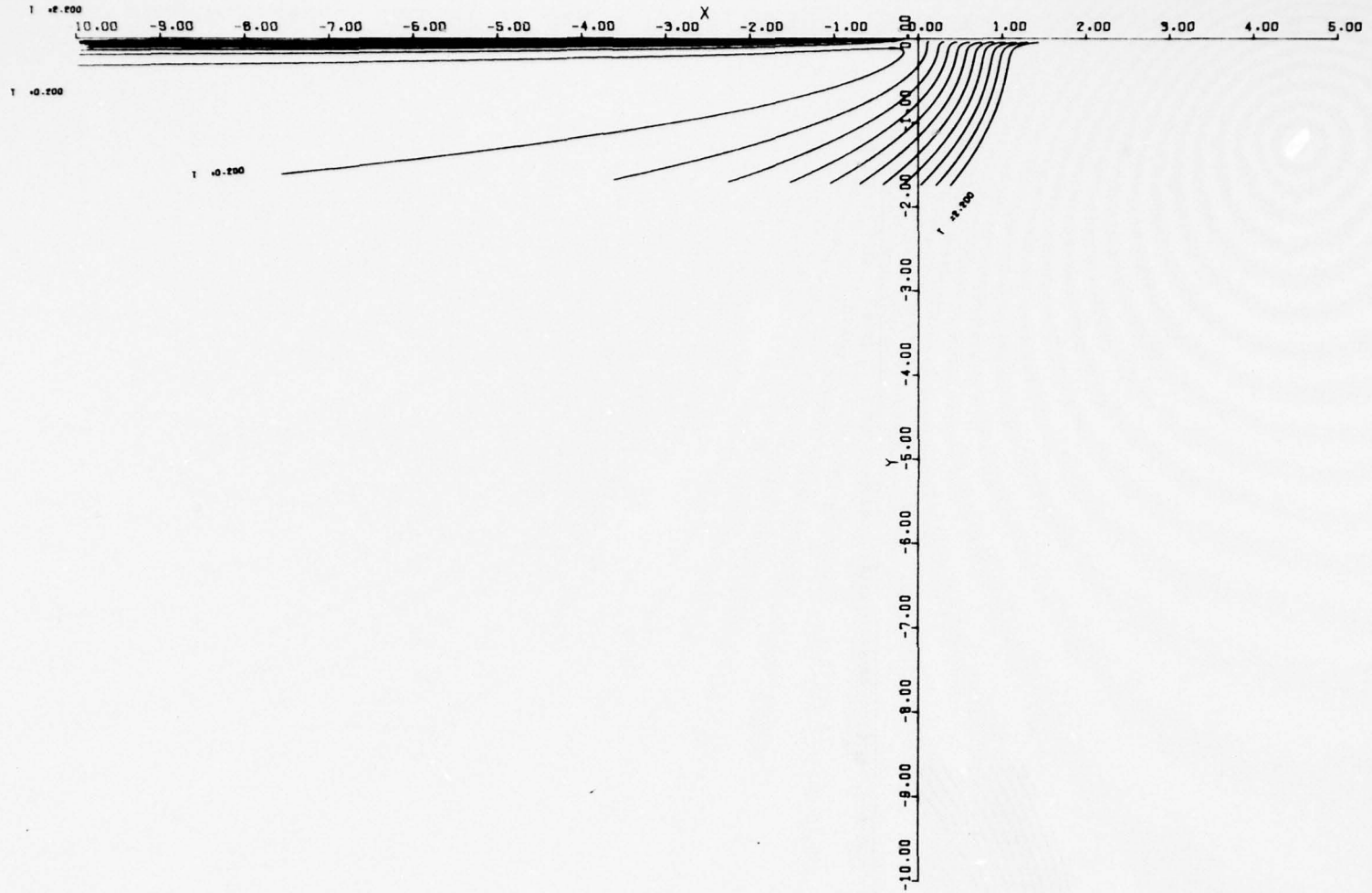

FIGURE 2.4-23. HEIGHT OF OWN = 25000, HEIGHT OF OTHER = 26000,DAZ = 1.000

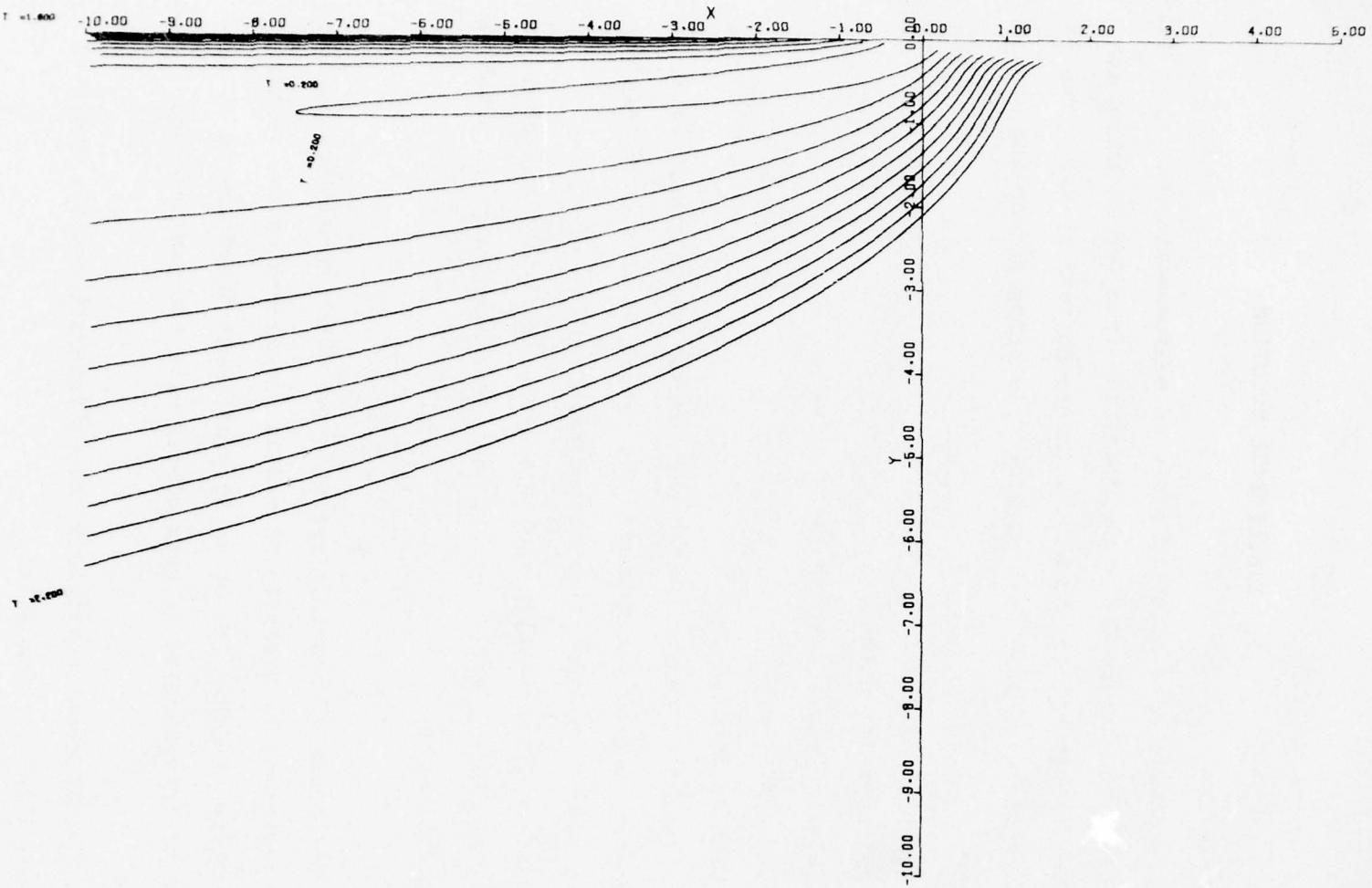

FIGURE 2.4-24. HEIGHT OF OWN = 14000, HEIGHT OF OTHER = 13000,DAZ = 6.000.

3. SINGLE-SITE SOLUTION

3.1 OVERVIEW

The single-site solution rests on measurements made upon the replies to one ground SSR whose direction from OWN is known and upon the target replies to active interrogations by OWN. The measurements available from passive "listening in" on the ground SSR are

Own azimuth β

Differential azimuth α

Passive TOA, where T = TOA·c miles

OWN altitude H_o

OTHER's altitude H

From this set of measurements, the corresponding single radar locus curve can be determined. The nature of this curve can be of any one of the varieties described.

Active interrogation yields a measurement of slant range to OTHER, R. With H and H_o known, the horizontal range to OTHER can be determined as

$$r = \sqrt{R^2 - (H-H_o)^2} \ .$$

Thus the locus of possible positions of OTHER determined by active interrogations is a circle of radius r centered on the vertical projection of OWN. The other aircraft must therefore be at a point of intersection of this circle with the passive radar locus curve.

The different possible kinds of interactions are shown in Figures 3.1-1 through 3.1-5.

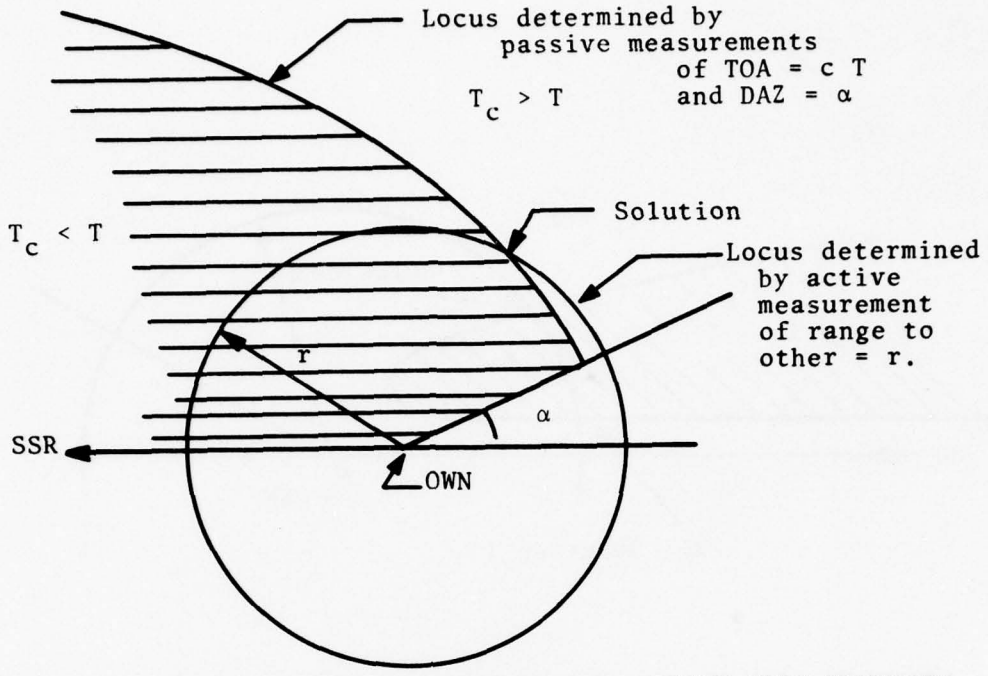

FIGURE 3.1-1. NATURE OF SOLUTION FOR SINGLE-SITE GEOMETRY WHEN ALTITUDES ARE ZERO ($\alpha < 0$).

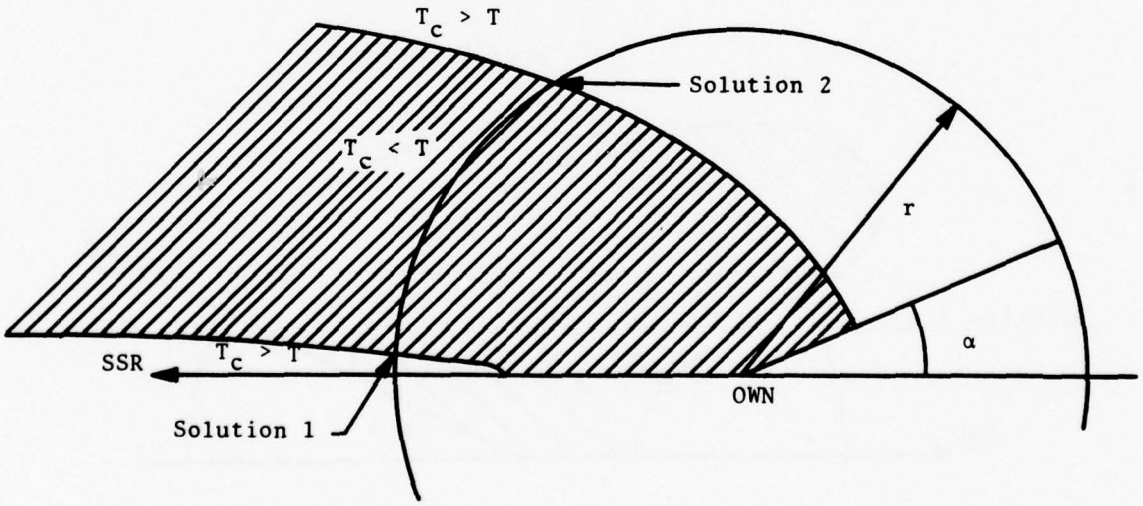

FIGURE 3.1-2. NATURE OF SOLUTIONS FOR SINGLE-SITE GEOMETRY WHEN LOCUS CURVE DETERMINED BY PASSIVE MEASUREMENTS HAS TWO BRANCHES ($\alpha < 0$).

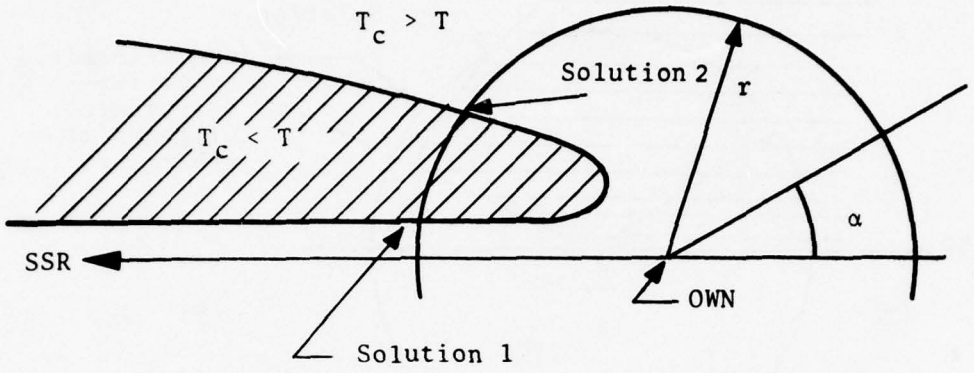

FIGURE 3.1-3. SPECIAL CASE OF SOLUTION, RELATED TO THAT IN FIGURE 3.1-2 (CF. FIGURE 2.4-15).

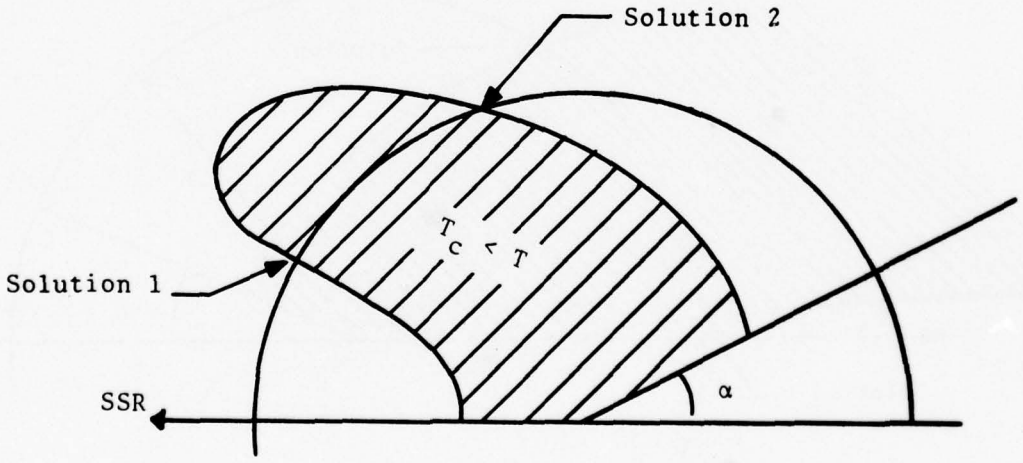

FIGURE 3.1-4. SPECIAL CASE OF SOLUTION, RELATED TO THAT IN FIGURE 3.1-2 (CF. FIGURE 2.4-14).

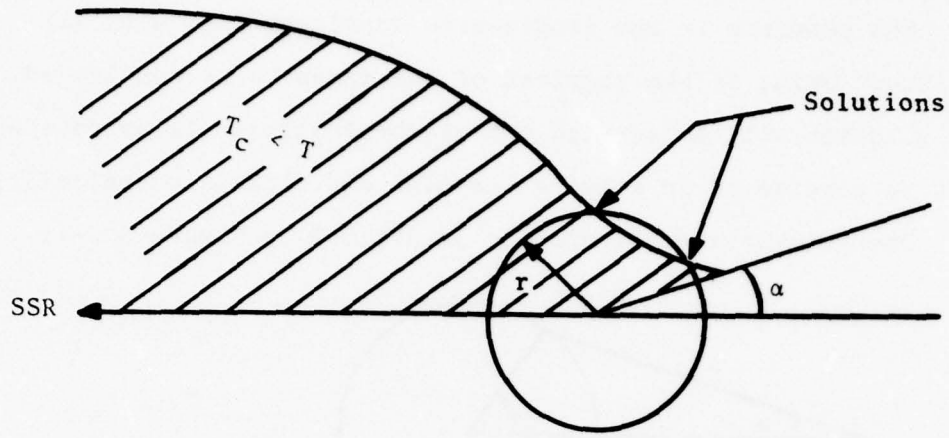

FIGURE 3.1-5. CONDITION WHEN TWO SOLUTIONS CAN EXIST DUE TO CIRCLE DETERMINED BY ACTIVE INTERROGATION INTERSECTING OUTER BRANCH OF PASSIVE MEASUREMENT LOCUS CURVE TWICE ($\alpha < 0$).

Two methods of solution are possible for this configuration. The first is an algebraic method that analytically finds all roots of the equation relating measurements to the target position. The equation is derived in Section 3.2. This algorithm has been implemented as a FORTRAN program written for the PDP-10 time-sharing system at TSC and has been successfully tested.

The second method of solution is essentially a search algorithm based on the properties of the locus curves. The algorithm is outlined in Section 3.4. The search procedure has been implemented on a programmable hand calculator and successfully demonstrated. Due to the constraints of the calculator (100 program steps, 10 memories), only the search procedure, not the logic for determining which case pertains, has been implemented as a program.

3.2 PLANAR CASE, ALGEBRAIC SOLUTION

The geometry in the single-site configuration, with all altitudes zero, is the simplest of the cases to be considered. The solution will be carried out algebraically to illustrate what must be considered in solving the BCAS equations algebraically.

The geometric configuration is defined by Figure 3.2-1.

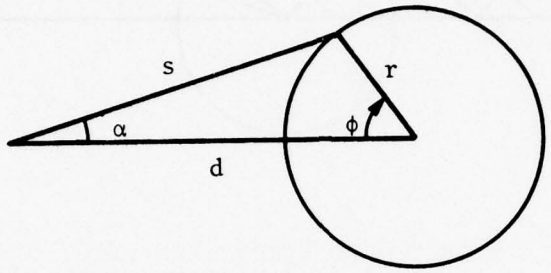

$T = s + r - d$

FIGURE 3.2-1. SINGLE-SITE, PLANAR GEOMETRY

The quantities T, α and r are known, ϕ and d are to be found. One may not assume that d > r. The TOA equation gives

$$T = s + r - d \qquad 3.2.1$$

By the law of sines

$$\frac{s}{\sin \phi} = \frac{r}{\sin \alpha} \qquad 3.2.2$$

and

$$\frac{d}{\sin (180-\alpha-\phi)} = \frac{d}{\sin (\alpha+\phi)} = \frac{r}{\sin \alpha} \qquad 3.2.3$$

Then

$$T = \frac{r}{\sin \alpha} \sin \phi + r - \frac{r}{\sin \alpha} \sin (\phi+\alpha) \qquad 3.2.4$$

or

$$\frac{T-r}{r} \sin \alpha = \sin \phi - \sin (\phi+\alpha) \qquad 3.2.5$$

Now define

$$\gamma = \phi + \frac{\alpha}{2} \qquad 3.2.6$$

Then

$$\frac{T-r}{r} \sin \alpha = \sin \left(\gamma-\frac{\alpha}{2}\right) - \sin \left(\gamma+\frac{\alpha}{2}\right)$$

$$= -2 \cos \gamma \sin \frac{\alpha}{2} \qquad 3.2.7$$

Hence

$$\cos \gamma = \frac{(r-T) \sin \alpha}{2 r \sin \frac{\alpha}{2}}$$

$$= \frac{r-T}{r} \cos \frac{\alpha}{2} \qquad 3.2.8$$

$$\gamma = \pm \cos^{-1} \left(\frac{r-T}{r} \cos \frac{\alpha}{2}\right) \qquad 3.2.9$$

and

$$\phi = -\frac{\alpha}{2} \pm \cos^{-1}\left(\frac{r-T}{r} \cos \frac{\alpha}{2}\right) \qquad 3.2.10$$

Thus it is seen that the equation by which ϕ is determined has two roots. It remains to be established which of these roots is an actual solution of the geometric problem.

Let

$$\phi_1 = -\frac{\alpha}{2} + \cos^{-1} \left(\frac{r-T}{r} \cos \frac{\alpha}{2}\right) \qquad 3.2.11a$$

$$\phi_2 = -\frac{\alpha}{2} - \cos^{-1} \left(\frac{r-T}{r} \cos \frac{\alpha}{2}\right) \qquad 3.2.11b$$

It is apparent that ϕ_2 results in a position for OTHER on the wrong side of the LOP - i.e., inconsistent with the sign of α. Hence only ϕ_1 is a valid solution to the problem posed. Thus this problem is seen to have a unique solution, assuming that a solution exists. It is to be noted that there obviously exist sets of values of r, T, and α such that

$$\left| \frac{r-T}{r} \cos \frac{\alpha}{2} \right| > 1$$

Then there is no value of ϕ that satisfies Equation 3.2.5.

The fact that there may be sets of measured values for which no solution exists is important to recognize. Such a situation could not arise if all measurements were noise-free. However, given that the measurements are corrupted by independent random noise, the possibility of "unrealizable" measurement sets exists and must be considered in designing any algorithm for determining the position of other, lest there be a program "crash" when the situation occurs.

3.3 THREE-DIMENSIONAL CASE - ALGEBRAIC SOLUTION

The algebraic equation to be solved is derived as follows: Given

$$R = \sqrt{r^2 + (H-H_o)^2} \qquad 3.3.1$$

the time-of-arrival equation expressed in range dimensions can be written

$$T - R + \sqrt{d^2 + H_o^2} = \sqrt{s^2 + H^2} \qquad 3.3.2$$

which squares to

$$(T-R)^2 + d^2 + H_o^2 + 2(T-R)\sqrt{d^2 + H_o^2} = s^2 + H^2 \qquad 3.3.3$$

so that

$$(T-R)^2 + d^2 - s^2 + H_o^2 - H^2 = -2(T-R)\sqrt{d^2 + H_o^2} \qquad 3.3.4$$

By the law of sines (cf. Figure 3.3-1)

$$d = \frac{r \sin(\theta-\beta-\alpha)}{\sin \alpha} \qquad 3.3.5$$

and

$$s = \frac{r \sin(\theta-\beta)}{\sin \alpha} \qquad 3.3.6$$

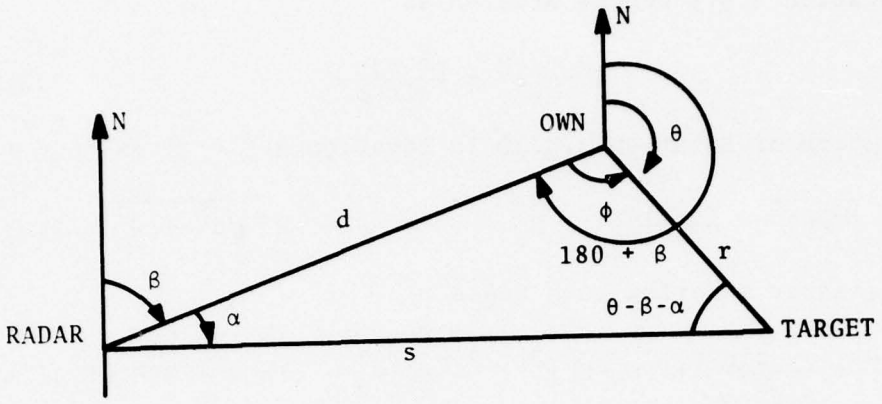

FIGURE 3.3-1. SINGLE-SITE GEOMETRY/PLAN VIEW.

Subtraction of 3.3.6 from 3.3.5 and trigonometric manipulation yields

$$d - s = \frac{r}{\sin \alpha} \left[\sin(\theta-\beta-\alpha) - \sin(\theta-\beta)\right]$$

$$= - \frac{2r}{\sin \alpha} \cos(\theta-\beta-\frac{\alpha}{2}) \sin \frac{\alpha}{2} \quad . \qquad 3.3.7$$

Similarly

$$d + s = \frac{2r}{\sin \alpha} \sin(\theta-\beta-\frac{\alpha}{2}) \cos(\frac{\alpha}{2}) \qquad 3.3.8$$

Multiplication of 3.3.7 and 3.3.8 yields

$$d^2 - s^2 = - \frac{4r^2 \sin(\theta-\beta-\alpha/2) \cos(\theta-\beta-\alpha/2) \sin(\alpha/2) \cos(\alpha/2)}{\sin^2 \alpha} \qquad 3.3.9$$

Let $\gamma = 2\beta - 2\theta + \alpha$

Then Equation 3.3.9 can be written as

$$d^2 - s^2 = \frac{r^2 \sin \gamma}{\sin \alpha} \qquad 3.3.10$$

Substitution of Equation 3.3.10 in Equation 3.3.4 gives

$$(T-R)^2 + \frac{r^2 \sin \gamma}{\sin \alpha} + H_o^2 - H^2 = -2(T-R)\sqrt{d^2 + H_o^2} \qquad 3.3.11$$

so that, after squaring both sides

$$(T-R)^4 + \frac{r^4 \sin^2 \gamma}{\sin^2 \alpha} + (H_o^2-H^2)^2 + \frac{2\, r^2 (T-C)^2}{\sin \alpha} \sin \gamma + 2(H_o^2-H^2)(T-R)^2$$

$$+ 2(H_o^2-H^2)\, r^2 \frac{\sin \gamma}{\sin \alpha} = 4(T-R)^2 \left(\frac{r^2 \sin^2(\theta-\beta-\alpha)}{\sin^2 \alpha} + H_o^2 \right) \qquad 3.3.12$$

Now

$$\sin^2 (\theta-\beta-\alpha) = \frac{1 - \cos\left(2(\theta-\beta-\alpha)\right)}{2}$$

$$= \frac{1 - \cos \left(-2(\theta-\beta-\alpha)\right)}{2}$$

$$= \frac{1 - \cos (\gamma+\alpha)}{2} \qquad 3.3.13$$

$$= \frac{1 - \cos \gamma \cos \alpha + \sin \gamma \sin \alpha}{2}$$

Substitution of 3.3.13 in 3.3.12, rearrangement and multiplication by $\sin^2 \alpha$ gives

$$\sin^2\gamma\, r^4 + \sin\gamma \left\{ 2r^2 (H_o^2-H^2) \sin\alpha \right\} + \cos\gamma \left\{ 2(T-R)^2\, r^2 \cos\alpha \right\}$$

$$+ \left\{ (T-R)^4 \sin^2\alpha + (H_o^2-H^2)^2 \sin^2\alpha + 2(H_o^2-H^2)(T-R)^2 \right.$$

$$\left. - 4(T-R)^2 H_o^2 \sin^2\alpha - 2(T-R)^2 r^2 \right\} = 0 \qquad 3.3.14$$

This is of the form

$$a_1 \sin^2\gamma + a_2 \sin\gamma + a_3 \cos\gamma + a_4 = 0 \qquad 3.3.15$$

Transpose $a_3 \cos\gamma$, square and substitute $1 - \sin^2\gamma$ for $\cos^2\gamma$.

The result is

$$b_4 \sin^4\gamma + b_3 \sin^3\gamma + b_2 \sin^2\gamma + b_1 \sin\gamma + b_o = 0 \qquad 3.3.16$$

where

$$b_4 = r^8$$

$$b_3 = 4r^6 (H_o^2 - H^2) \sin\alpha$$

$$b_2 = 2r^4 \left\{3(H_o^2-H^2)^2 \sin^2\alpha + 2(T-R)^4 \cos^2\alpha + (T-R)^4 \sin^2\alpha + 2(T-R)^2\left(H_o^2-H^2-2H_o^2 \sin^2\alpha - r^2\right)\right\}$$

$$b_1 = 4r^2(H_o^2-H^2) \sin\alpha\left\{(T-R)^4 \sin^2\alpha + (H_o^2-H^2)^2 \sin^2\alpha + 2(T-R)^2\left(H_o^2-H^2-2H_o^2 \sin^2\alpha - r^2\right)\right\}$$

$$b_o = \left\{(T-R)^4 \sin^2\alpha + (H_o^2-H^2)^2 \sin^2\alpha + 2(T-R)^2\left(H_o^2-H^2-2H_o^2 \sin^2\alpha - r^2\right)\right\}^2 - 4r^4 (T-R)^4 \cos^2\alpha$$

Equation 3.3.16 is a quartic equation which may be solved closed form for sin γ.

There may be up to four real roots of 3.3.16 (i.e., up to four possible values of sin γ) between -1 and 1. There is at most one value of θ corresponding to each possible value of sin γ. Each root is treated as follows:

Equation 3.3.15 is used to compute cos γ. Since sin γ and cos γ are now known, γ may be computed uniquely.

$$\gamma = 2\beta - 2\theta + \alpha \quad \text{so}$$

$$\theta = \frac{1}{2}(2\beta+\alpha-\gamma) \qquad 3.3.17$$

The difficulty now arises that 3.3.17 only determines ϕ up to $\pm\pi$. (An angle has two half-angles.) However, there is only one solution θ consistent with the requirement that θ lie in the interval

determined by β and α (cf. Section 2.1 and Figure 2.1-1). For $|\phi-\beta| < 180°$, sgn $(\phi-\beta)$ = sgn α. Thus the bearing angle θ corresponding to every real root of Equation 3.3.15 in the interval (-1,1) can be determined uniquely. Then Equation 3.3.5 is used to solve for d and 3.3.6 for s.

Equations 3.3.2 and 3.3.11 are squared en route to producing 3.3.15. It is, then, possible to introduce extraneous roots of 3.3.16 by these steps. If the signs of the left and right hand sides of 3.3.2 or 3.3.3 disagree, the root is discarded.

The fourth-order polynomial equation 3.3.15 has a single root of multiplicity four when T = R. The root, obtained by factoring, is

$$\sin \gamma = \frac{H^2 - H_o^2}{r^2} \sin \alpha \qquad 3.3.18$$

Numerical techniques of solving the equation will encounter difficulties (due to numerical roundoff effects) when this condition occurs or nearly occurs, i.e., when $T \approx R$.

The algorithm as coded tests for this condition, and when it occurs, uses the expression in 3.3.18 as an initialization to solve by Newton's method the nonlinear equation obtained by substituting in 3.3.2 the expressions for s and d in 3.3.6 and 3.3.7.

Alternatively, the search algorithm described in the next section could be used.

3.4 SINGLE-SITE GEOMETRY - SOLUTION BY SEARCH

The position of the target aircraft and the distance to the ground SSR's can be determined by a one-dimensional search, based on the known properties that the solution may have.

The cases are distinguished by the behavior of the quantity T_c along the boundaries of the solution region. In particular, T_c has to be evaluated at two points to distinguish the differences among the cases that require different search algorithms. These points are at

$$r = \sqrt{R^2 - (H-H_o)^2} \qquad 3.4.1$$

and at $\phi = 0$ and $\phi = 180 - \alpha$; when ϕ is defined by Figure 3.3-1.

$$T_c(r,0) = T_1 = H + R - \sqrt{r^2 + H_o^2} \qquad 3.4.2$$

and

$$T_c(r,180-\alpha) = T_2 = \sqrt{r^2 + H^2} + R - H_o \qquad 3.4.3$$

The cases of interest are defined in Table 3.4-1

TABLE 3.4-1. DEFINITION OF CASES FOR SEARCH LOGIC FOR SINGLE-SITE GEOMETRY

T_1	T_2	Case	Corresponding Figures
$< T$	$> T$	I	3.1-1
$> T$	$> T$	II	3.1-2, 3.1-3, 3.1-4
$< T$	$< T$	III	3.1-5
$> T$	$< T$	Not possible	

The condition that $T_1 > T$ and $T_2 < T$ can not occur, since this would require that

$$T_1 > T > T_2 \qquad 3.4.4$$

or

$$H + H_o > \sqrt{r^2 + H^2} + \sqrt{r^2 + H_o^2} \qquad 3.4.5$$

which can not occur for real values of r.

Once the pertinent case has been identified, the solution points can be found by search. The search is based on the observation that T_c is greater than T on one side of the locus line and

less than T on the other. If (T_c-T) is of opposite sign at two points in the solution space, the locus line must lie between them. The search then proceeds very simply. It is known that the solution point(s) must lie on a circle of radius r in a sector

$$0 < \phi < 180° - \alpha \qquad 3.4.6$$

for $\alpha > 0$ and a sector

$$0 > \phi > -180° + \alpha \qquad 3.4.7$$

for $\alpha < 0$.

The search in principle proceeds by evaluating (T_c-T) at a succession of values of ϕ at increments of $\Delta\phi$. When (T_c-T) changes sign, it is known that the solution point is within the last previous increment. Accordingly, the direction of search is reversed, using increments of ϕ half as large as before. As $\Delta\phi$ is successively halved, the successive values of the test points approach the true solution point and

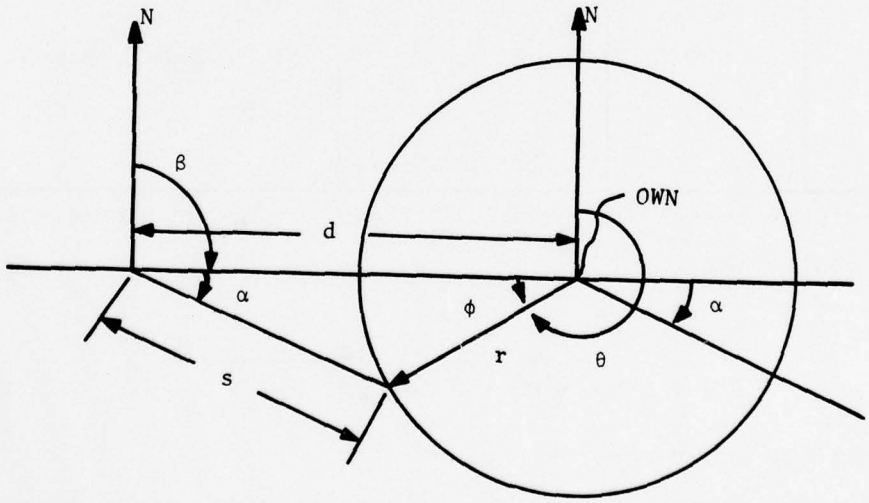

FIGURE 3.4-1. RELATIONSHIP OF VARIABLES USED IN SEARCH ALGORITHM FOR SINGLE-SITE GEOMETRY SOLUTION. CASE WITH α AND ϕ POSITIVE IS SHOWN.

$$| \phi_{true} - \phi_{test} | < |2 \Delta \phi|$$

Thus, the iteration can be terminated whenever $\Delta\phi$ is small enough to guarantee the desired accuracy.

Simplified flow charts for the solution by search are shown in Figures 3.4-2 and 3.4-3. The search algorithm necessarily always converges when there is exactly one solution point in the range being searched and that solution arises because the passive radar locus curve intersects the circle determined by the active radar.

When there is one solution point due to the passive radar locus curve being tangent to the active radar circle, then the algorithm will find the solution only in the unlikely event that one of the test points selected happens to be the exact solution point. Since the difference $(T-T_c)$ does not change sign along the circle on either side of the solution point, there will be no reversal of the search direction as when ϕ goes past the solution. The situation will be similar when a near-tangency condition exists - i.e., when the curves cross twice, but the crossing points are so close together that both lie between successive test values of ϕ. The likelihood of this happening can be reduced by initially choosing the spacing between test points small (i.e., choosing the parameter designated as N in the flow chart in Figure 3.4-2 to be large) at the cost of lengthening the search procedure. In any case, the algorithm must make allowances for not finding a solution, if only to accommodate the case that, due to errors in the measurements, no solution compatible with the measurements exists.

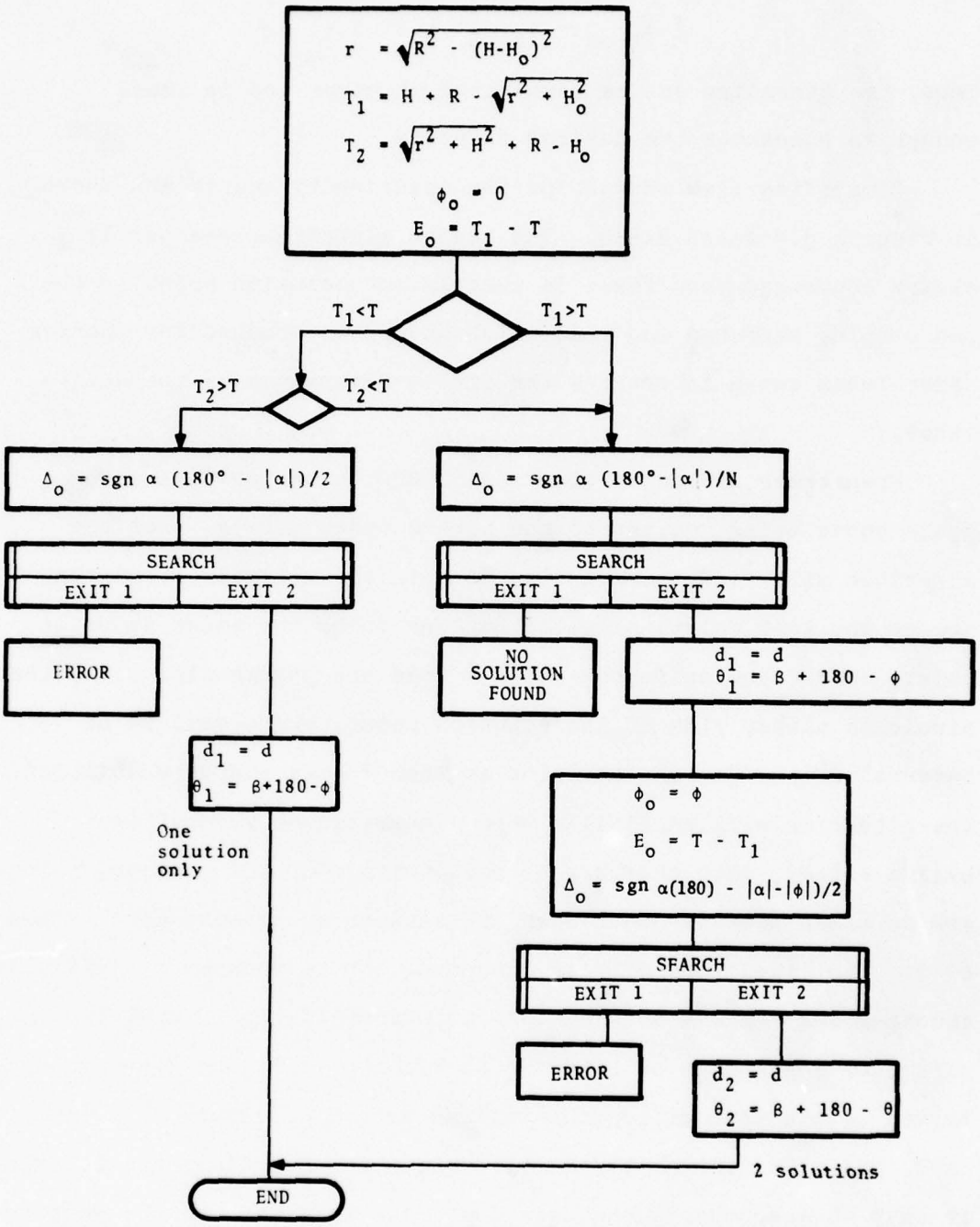

FIGURE 3.4-2. FLOW CHART FOR ALGORITHM TO SOLVE SINGLE-SITE GEOMETRY BY SEARCH. TOA T, DAZ α, OAZ β, SLANT RANGE R, ALTITUDES H AND H_o ARE GIVEN MEASUREMENTS. SEARCH IS SUBROUTINE (FIGURE 3.4-3). N AND M (FOR SEARCH) ARE CHOSEN VALUES.

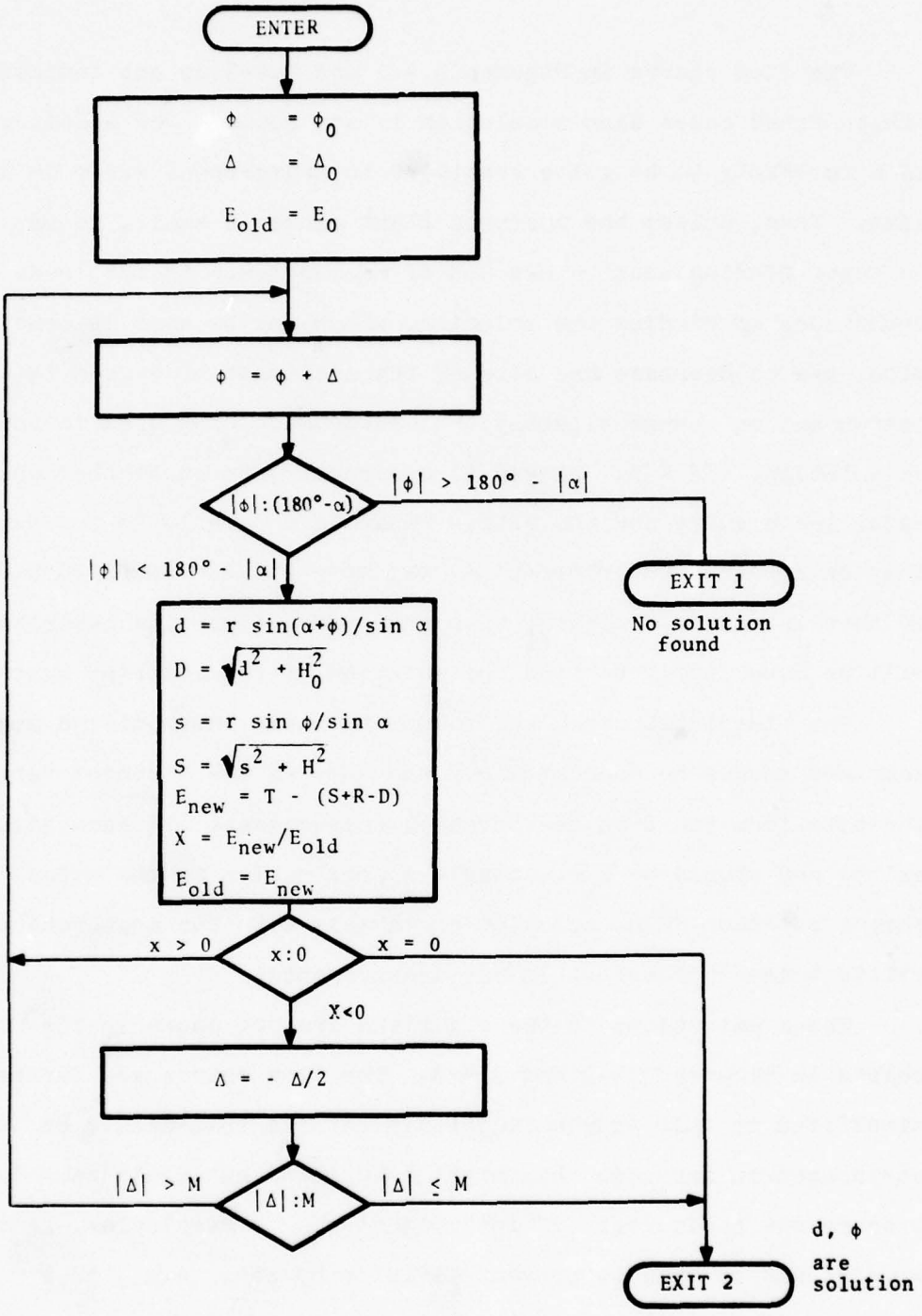

FIGURE 3.4-3. FLOW CHART FOR SEARCH SUBROUTINE USED IN SOLVING SINGLE-SITE PROBLEM. T, R, r, α, H, H_0, ϕ_0, Δ_0, E_0, AND M ARE INPUT PARAMETERS.

The flow charts in Figures 3.4-2 and 3.4-3 do not indicate how to treat cases when a solution is not found. The actual solution is likely to be quite sensitive to measurement error in any case. Thus, unless the measured slant range is small, it may not be worth finding until a new set of measurements is obtained. Two techniques of finding the solution, wnich may be used in combination, are to decrease the size of the increment of ϕ used in the search and to change slightly the measurement of R used in the calculation. If R is changed in a direction to cause the passive radar locus curve and the active radar locus circle to intersect if they do not (and to intersect at two more widely separated points if they intersect already), then the search algorithm described will be more likely to find the solution of the modified system.

The midpoint between the solutions using the modified measurement set should be approximately the same as the midpoint between the solutions based on the original measurements (if such solutions exist) and should be a reasonable approximation to the actual target position if no solution compatible with the measurements exists because of errors in the measurements.

These extensions to the algorithm are not shown in the flow charts in Figures 3.4-2 and 3.4-3. The flow charts are further simplified in that they omit certain details that should be incorporated in any code that might be written but would only obscure the basic logic if included here. In particular, provision should be made to prevent division by zero (e.g., if $\alpha = 0$) and to prevent false termination of the search because the test values of ϕ appear beyond the solution region ($|\phi| > 180° - |\alpha|$) due to numerical roundoff errors.

3.5 ACCURACY OF THE SINGLE-SITE SOLUTION

A test was run in which RADAR was located 20 nautical miles due south of OWN, OWN had height 20,000 feet, and OTHER flew a level semi-circle of radius 3 nautical miles centered 1000 feet above OWN.

The bearing of OTHER from OWN was initially taken as 1 degree and was incremented by 2 degrees up to 179 degrees. The computation was performed 10 times at each step with random normally distributed input errors based upon sigmas of .15 microseconds for the two TOA's, $100/\sqrt{12}$ feet for the two altitudes, and .2 degrees for locating the center mark of the main beam passing through a point (either North, OWN, or OTHER).

The algebraic solution was used. Let θ denote the bearing of OTHER from OWN relative to LOP. Two solutions were generally found for $1° \leq \theta \leq 65°$ and $113° \leq \theta \leq 179°$. When $1° \leq \theta \leq 10°$ and when $163° \leq \theta \leq 179°$, sets of perturbed inputs that produce no solutions are not uncommon. It is also not uncommon, especially in the second of these regions, for the perturbed inputs to produce two nearby computed values of ϕ, one on either side of the true value. This suggests near tangency of the circle determined by active interrogation and the locus curve determined from the passive measurements.

The error sensitivity (for the closest computed configurations, assuming there is at least one) varies with θ. In the best range, θ not very far from 90°, the standard deviation in the error for θ is a little over 1/2 degree. For θ in the worst ranges, close to 0 or 180 degrees, the standard deviation is about 2 degrees.

In the best range, the standard deviation of the error in the computed radar distances is between 0.5 and 1 nautical miles. In the bad ranges there are standard deviations of over 5 nautical miles.

There is large inherent error sensitivity when the absolute value of the differential azimuth is small (i.e., when OWN, RADAR and OTHER are nearly colinear). Given such a configuration, it is not uncommon for the algorithm to produce no solutions from perturbed inputs.

The algorithm, as coded, writes out a default solution if either

1) no solution is produced by the general method or
2) the differential azimuth is so small that error sensitivity makes the computed solutions suspect. In this case the computed solutions are also output.

The default solution involves placing OTHER either in between or opposite RADAR from OWN. The choice is made by contrasting the TOA as measured from RADAR with OWN TOA. (If 1/2 OWN TOA is less than TOA, OTHER is opposite.)

If the default solution is used, d is not computed.

4. PASSIVE MODE RANGE-BEARING CALCULATION: RADARS WITH AZIMUTH REFERENCES

4.1 OVERVIEW

It is assumed that for the purpose of facilitating the implementation of BCAS, modifications will be made to either all or a large fraction of the SSR ground sites so that they will emit signals allowing BCAS systems to determine the angular orientation of the SSR antennas at any instant.

This will allow the simplest of the purely passive BCAS operating modes. In areas where there is coverage by two suitably placed radars with azimuth references, BCAS can determine range and bearing to a single target.

There are configurations of two radars and a single intruder for which the solution is extremely sensitive to perturbations of the input variables, i.e., the measurements. In addition, it will be seen that under some circumstances measurements from two radars will give multiple solutions, each of which corresponds to a distinct radar-aircraft configuration, and all of which are completely consistent with all the measurements from the two radars.

In either of these troublesome cases, there is advantage to using other measurements if these are available. One may then obtain a more accurate target position determination by getting a less error-sensitive solution or at least having an average of several error-sensitive solutions. When the measurements from two radars result in multiple solutions, either active interrogation or the measurements from some additional radar will generally be inconsistent with all but one of these solutions, which can then

be taken to correspond to the actual configuration. The data management schemes appropriate to select measurement sets and check solutions for consistency are considered to be beyond the scope of this report.

The particular method of implementing the azimuth reference signals is not important for the analysis that follows. Similarly, the question of whether true north or local magnetic north should serve as the reference direction is not considered. In the simulations, it is assumed that the reference directions for the two sites are the same, and the determination of own azimuth is subject only to random measurement errors.

Since radar altitudes are unknown, the radars are assumed to be at sea level. The nature of the locus curves is such that this assumption should have no significant effect on the results. In general, the influence of small altitude variations on errors in computed positions was found to be small.

4.2 THE SOLUTIONS DESCRIBED BY THE LOCUS CURVES

The nature of the solutions to the problem can be described in terms of the locus curves. In addition, an enumeration of the possible cases also suggests that the solution(s) can be found by a search algorithm. The algorithm would have to be somewhat more complex than that for the single-site geometry described in Section 3.4, in that it would have to perform search in two dimensions, rather than one. The precise choice of the directions for search is unimportant as long as the whole solution region can always be spanned.

The principle of the search algorithm would be similar to that in Section 3.4 - i.e., a locus curve lies between a pair of points such that $T - T_c$ changes sign in going from one to the other. A solution point is at the intersection of two locus curves, or the point where four different regions (characterized by the algebraic signs of $T_1 - T_{1c}$ and $T_2 - T_{2c}$) meet. Thus starting from one of the straight lines bounding a solution region, the search algorithm would find a locus curve by going in some trial directions and then find the intersection by searching in a direction generally along the locus line already found. If all possible cases are properly considered, all solution points can be found to within arbitrary precision. Difficulties will arise if near-tangencies occur between locus lines. The solutions in such cases are bound to be intrinsically inaccurate (measurement error sensitive), but their approximate positions can be determined, as in the single-site case, by modifying the measurement parameters (generally the TOA's) in a direction such as to increase the intersection region that is small.

The solution regions to be considered are classified in Figure 4.2-1. Knowledge of the signs of the differential azimuths by itself restricts the target position to one of the four regions indicated in the figure. The regions are separated from each other by the extended lines of position (LOP's) between OWN and each radar. These are the lines passing through the position of OWN whose direction is determined by the own azimuth (OAZ) measurements.

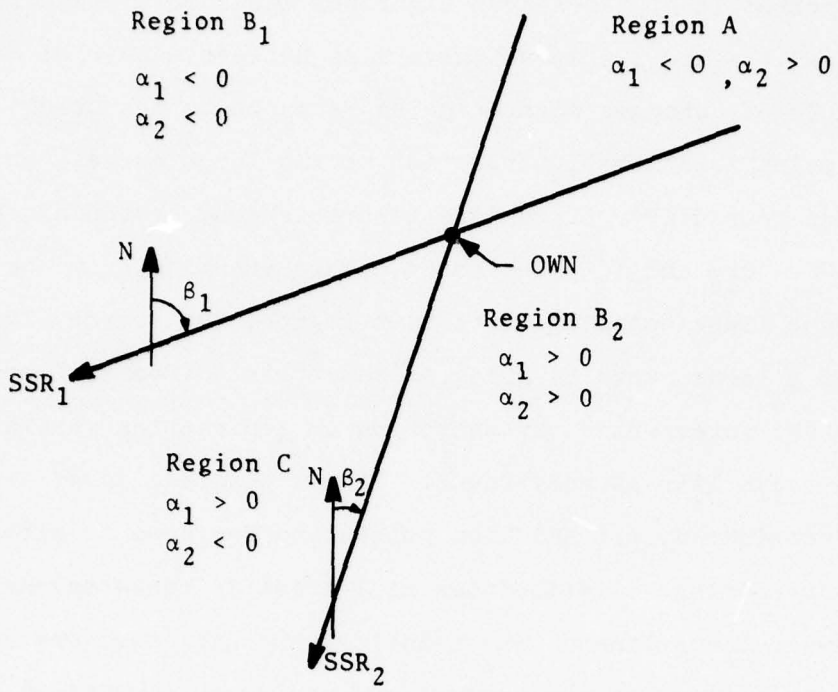

FIGURE 4.2-1. DEFINITION OF SOLUTION REGION TYPES.

The regions A, B1 and B2, and C are qualitatively different, and the nature of the solution in each may be different when the solution is sought in 3 dimensions.

Region A is bounded by the extensions of the LOP's beyond OWN away from the radars. It is characterized by having no radar on its boundaries. Barring exceptionally unfavorable situations (to be discussed below), the locus curves for solutions in this range will be like those in Figure 4.2-2. There will be one solution, constrained to lie in the sector bounded by lines in the directions $\beta_1 + \alpha_1 (\alpha_1 < 0)$, and $\beta_2 + \alpha_2$ $(\alpha_2 > 0)$ from own. The solution point can be determined either by some suitable algorithm based on the analytical properties of the functions involved or

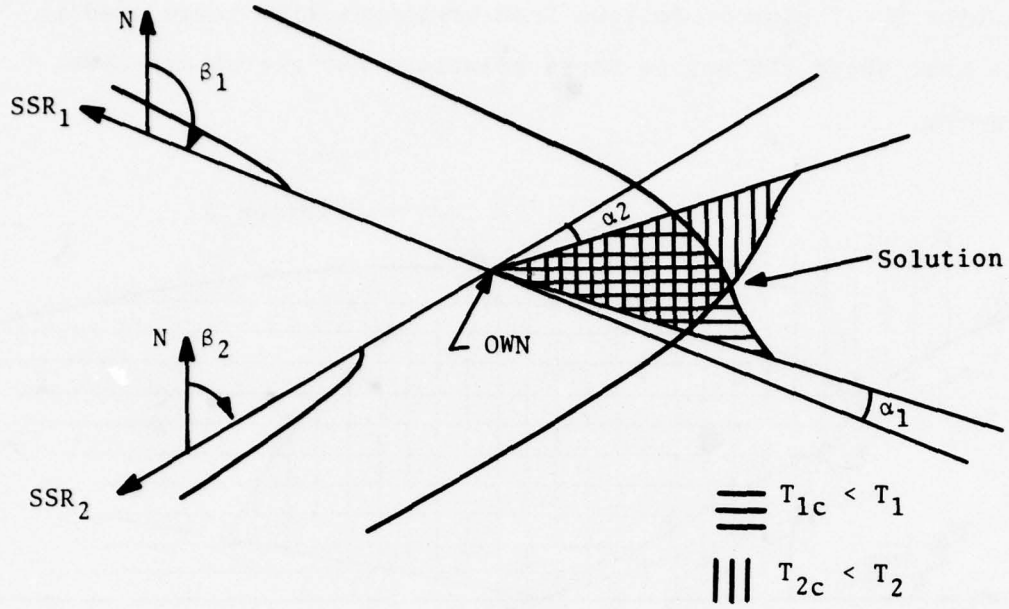

FIGURE 4.2-2. USUAL NATURE OF SOLUTION IN REGION A.

by a search algorithm. Given any initial point in the region of possible solutions, the direction of search for an improved approximation can be determined readily from the sign of (T_1-T_{1c}) and (T_2-T_{2c}).

Figure 4.2-3 shows a potential situation when there might be multiple solutions in region A. This might occur if the radars are almost directly on opposite sides of OWN, one gives rise to locus curves with two branches, and the other has a very small differential azimuth. The case is shown (with all the small angles drawn large, for clarity) for mathematical completeness; it is highly unlikely in practice. Solution 1 is the usual solution in Region A, solution 2 the alternative. For realistic sets of measurement values there can not be two symmetrical solutions like

Solution 2. The proof follows from arguments like those used to show that there can not be three solutions for the single-site geometry.

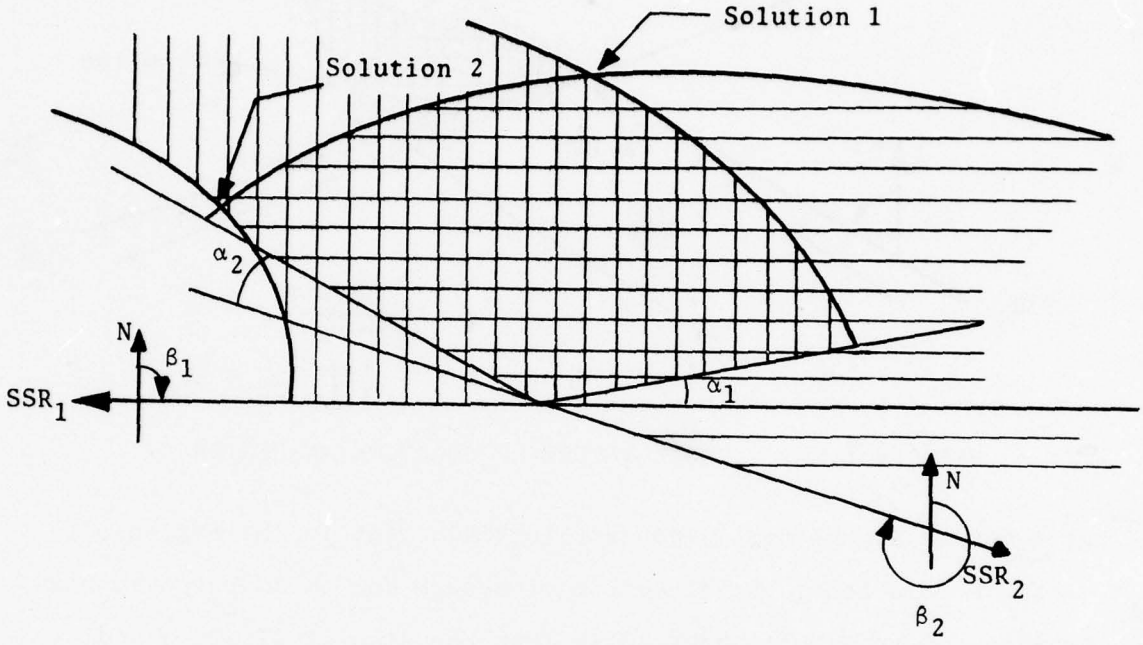

FIGURE 4.2-3. EXCEPTIONAL CASE OF MULTIPLE SOLUTION IN REGION A (ANGLES DRAWN EXAGGERATED).

Region B_1 and B_2 are sectors bounded on one side by the LOP from OWN to a radar and beyond and on the other by the extension of LOP beyond OWN away from the radar. They are characterized by having one radar on their boundaries. Again barring exceptionally unfavorable configurations, the locus curves determine solutions according to the scheme of Figure 4.2-1.

It is seen that solutions in region B_1 are constrained to lie in the sector bounded by lines emanating from own and going in the directions $(\beta_1-\pi)$ and $(\beta_2-\alpha_2)$. Two solutions may occur in

this sector, depending on the exact characteristics of the locus curves. Either solution may be present alone, or both may be present together.

The usual nature of the locus curves in Region B_1 is that shown in Figure 4.2-4.

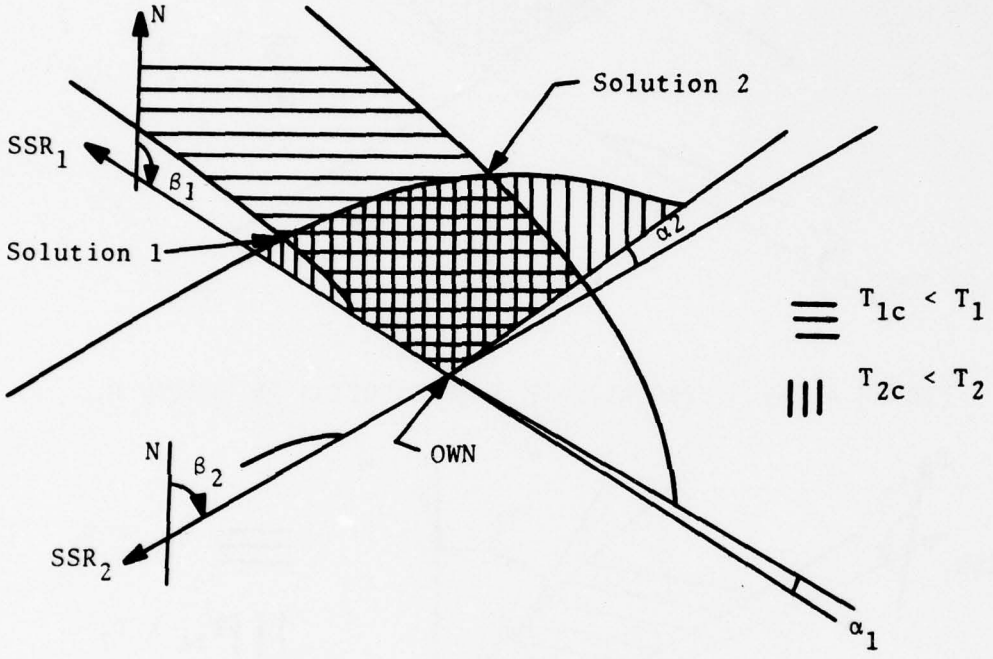

FIGURE 4.2-4. USUAL NATURE OF SOLUTION IN REGION B_1.

The "inner" branch of the locus curve determined by the measurements from radar 1 may or may not be present. Special cases are shown in Figures 4.2-5 and 4.2-6.

The cases shown can be distinguished by evaluation T_{1c} and T_{2c} along the lines bounding the solution region. The solution designated in Solution 1 in Figures 4.2-4 and 4.2-5 will exist only if there is an interval along the LOP from OWN toward radar 1 such that $T_{ic} > T_1$ and $T_{2c} < T_2$, If such an interval does not exist,

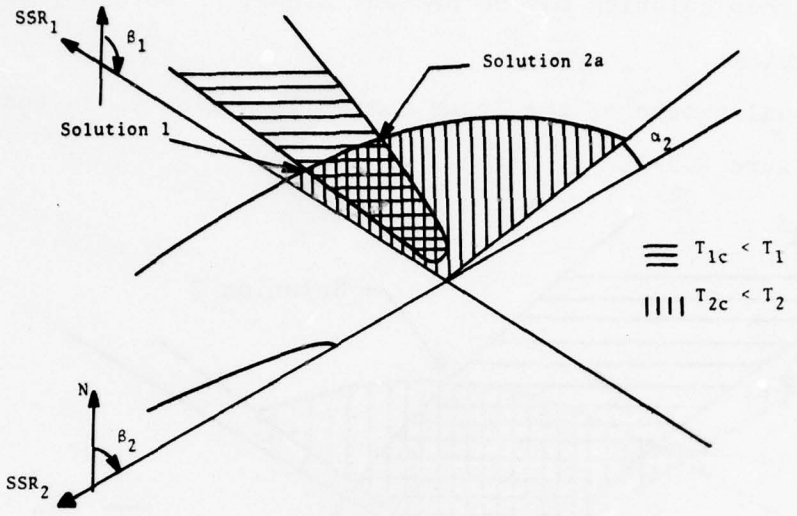

FIGURE 4.2-5. SPECIAL CASE I OF SOLUTION IN REGION B_1.

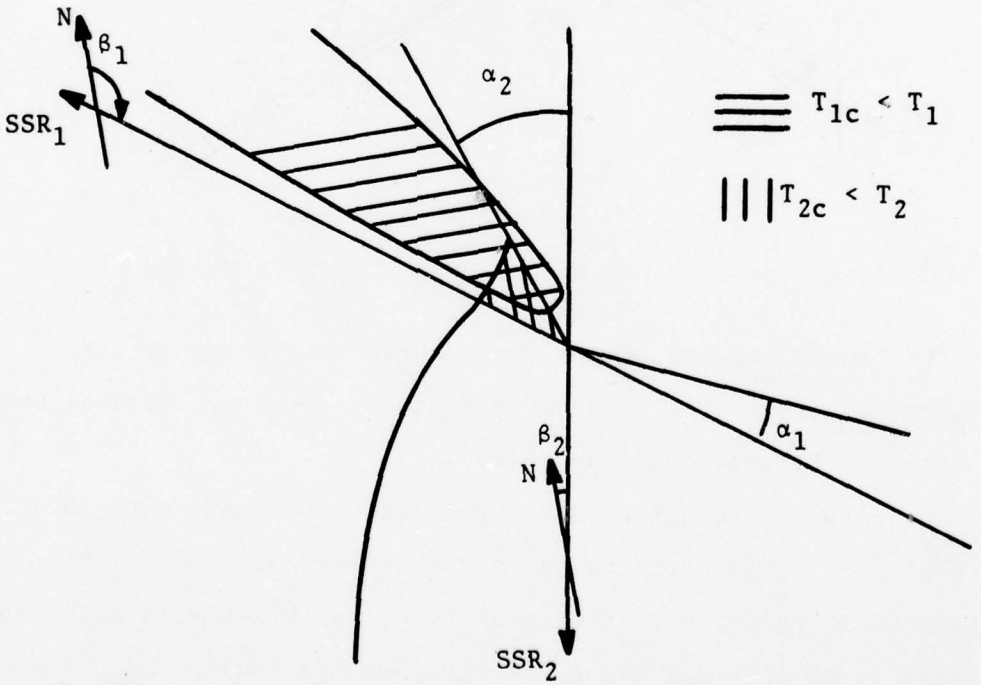

FIGURE 4.2-6. SPECIAL CASE II OF SOLUTION IN REGION B_1.

then either the "inner" branch of the radar 1 locus curve shown in Figure 4.2-4 is not present, or it does not intersect the locus curve due to the measurements from radar 2. If $T_{1c} > T_1$ everywhere along the LOP from own toward radar 1, then the nature of the locus curve determined by the measurements from radar 1 is like that shown in Figures 4.2-5 and 4.2-6. The question of the existence of a second solution in the region can then be determined by evaluating T_{1c} and T_{2c} along the other boundary of the region in which solutions are possible, i.e., the line in (usually) the direction $\beta_2 + \alpha_2$ from OWN.

Figure 4.2-7 shows that the boundary can sometimes be the line from OWN in the direction $\beta_1 + \alpha_1$. If a locus curve is of the form in Figure 2.2-2c rather than of the form 2.2-2b - i.e., not going to infinity, the nature of the solutions that may be obtained should generally not change.

A special case, not illustrated, may occur if both radars are in essentially the same direction from OWN and the locus curves have "inner branches" that intersect. Then there will in theory be three solutions. In practice, all the solutions will arise from the crossings of nearly parallel lines and will be extremely error sensitive. (This is intuitively clear - if there are two radars and a target nearly colinear with OWN, the (small) TOA and DAZ measurements will not permit good determination of range to the target.)

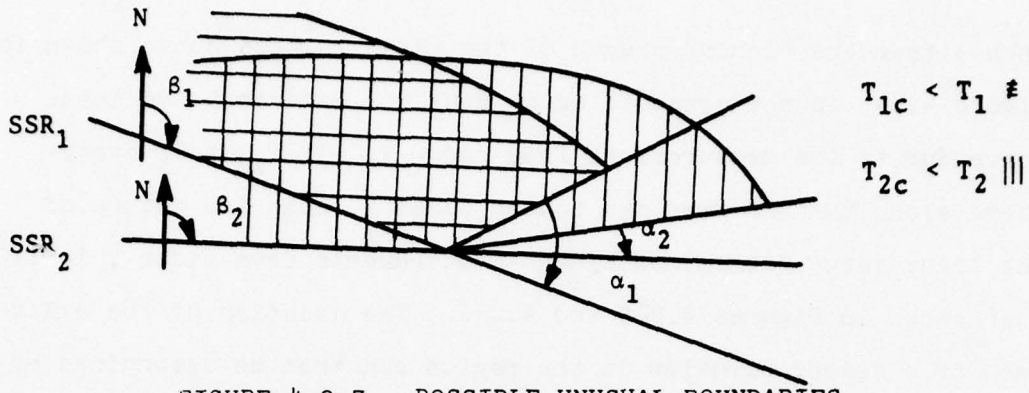

FIGURE 4.2-7. POSSIBLE UNUSUAL BOUNDARIES OF SOLUTION REGION B_1.

Region C is that region bounded by the LOP's - i.e., the sector "between the radars" when viewed from OWN. Given that there is a solution in this region, there may be one, two, or three, depending on which of the "inner loops" of the locus curves exists and intersects the outer loops, as indicated in Figure 4.2-8 (a theoretical worst case is five solutions, if the radar LOP's are so close that the "inner loops" also cross twice. This is of no practical concern). The solution indicated as Solution 1 will always occur, the others may or may not.

Figure 4.2-8 shows another possible configuration of solutions in Region C which may occur if the target altitude is above that of OWN. If the solution exists at all with locus curves of this nature, then either the pairs of solutions 1 and 2 or the pairs 1 and 3 must exist together. Barring tangency conditions, there are either 2 or 4 solutions. Thus, for instance, if Solutions 1 and 2 exist, then either 3 and 4 both exist or neither exists.

Figure 4.2-10 shows the nature of the solution if

$$T_2 > 2\,(H-H_0) > T_1.$$

It is seen that generally Solution 1 and 2 will both exist.

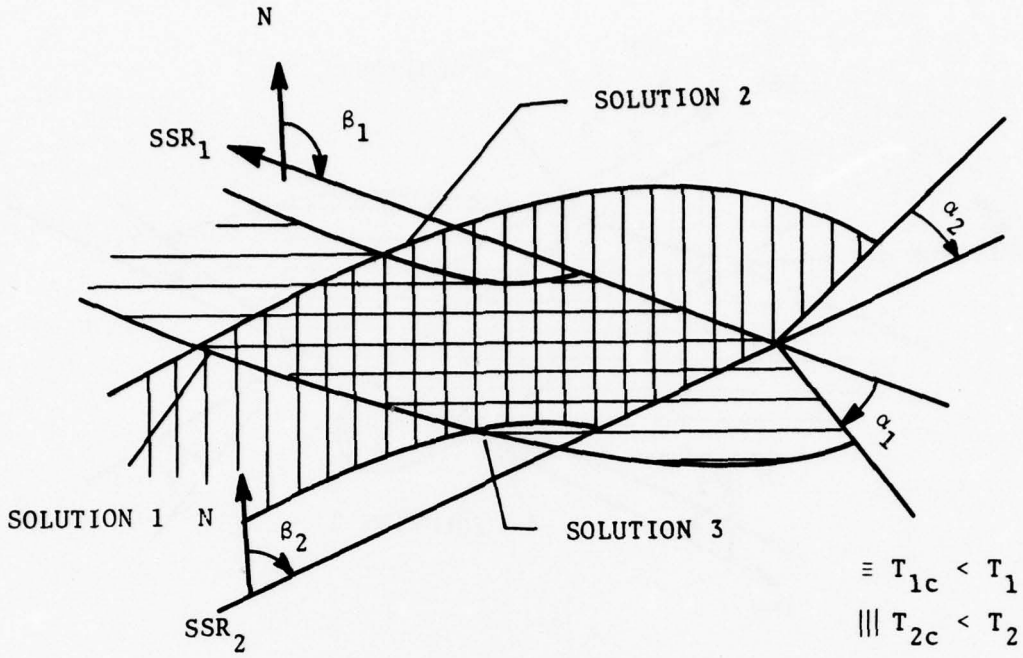

FIGURE 4.2-8. SOLUTIONS IN REGION C.

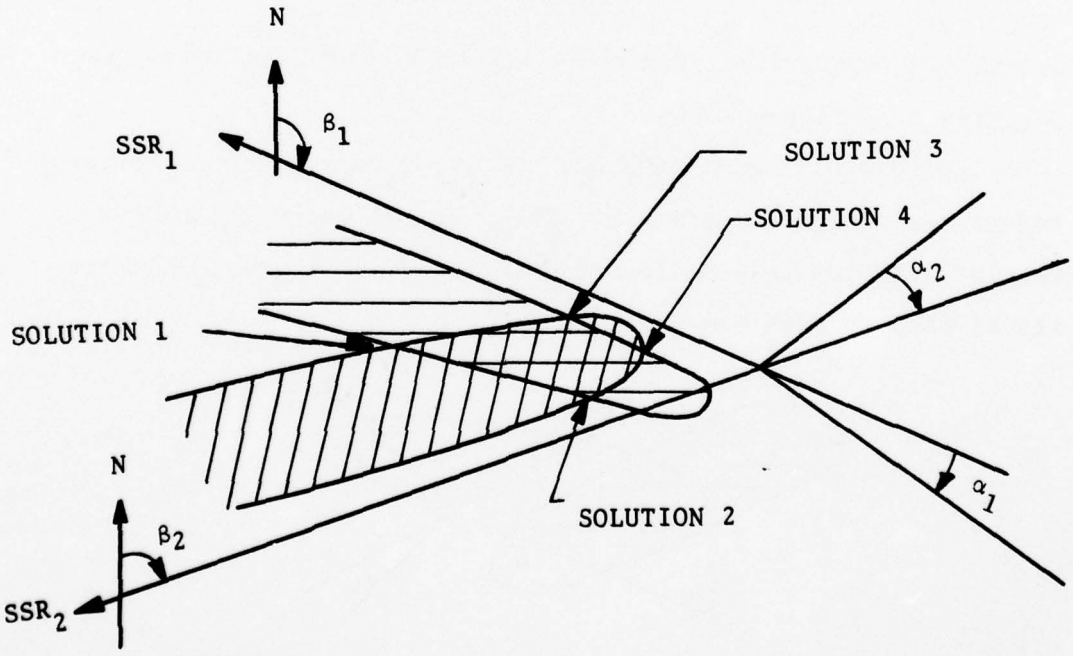

FIGURE 4.2-9. POSSIBLE SOLUTIONS IN REGION C WHEN $2(H-H_o) > T_1, T_2$.

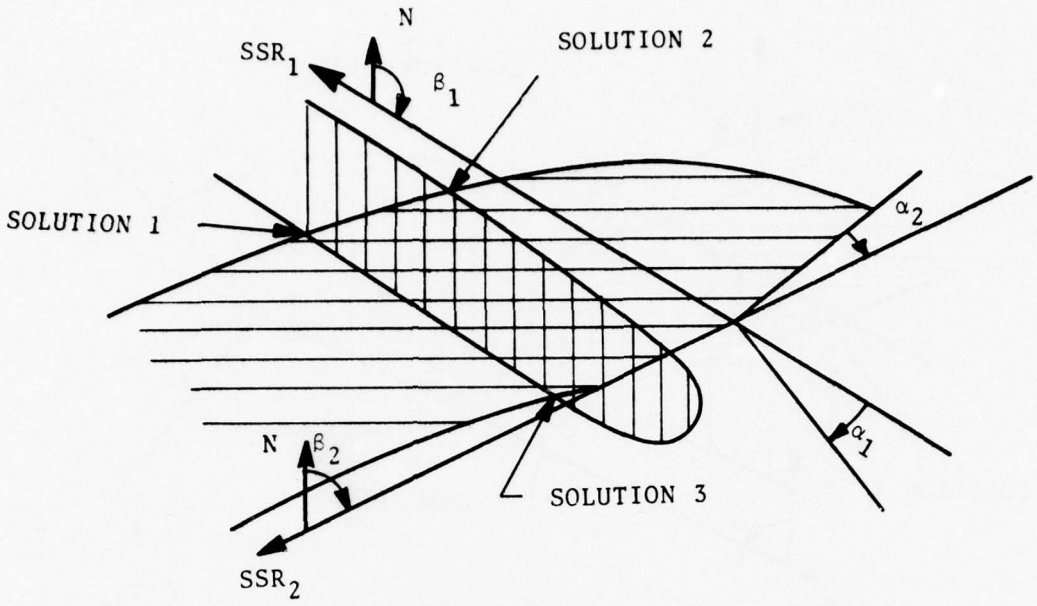

FIGURE 4.2-10. POSSIBLE SOLUTIONS IN REGION C, $T_2 > 2(H-H_o) > T_1$.

Solution 3 is possible, and there may be a fourth solution like Solution 4 in Figure 4.2-9.

The possibility exists that the locus curves for one or both radars may not go to infinity. The possible cases which give results qualitatively different from those shown previously are illustrated in Figure 4-2.11.

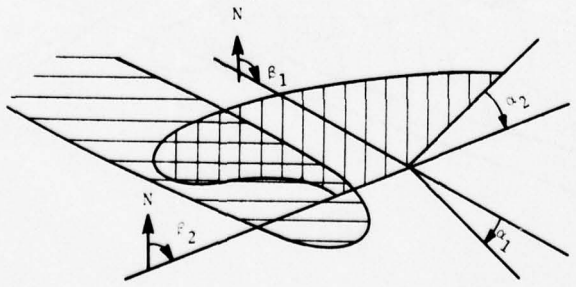

FIGURE 4.2-11. POSSIBLE SOLUTION IN REGION C. RESULT IS QUALITATIVELY THE SAME IF LOCUS CURVE DUE TO MEASUREMENTS FROM RADAR 1 IS OF ANY OF THE OTHER TYPES.

4.3 RANGE AND BEARING COMPUTATION ALGORITHM

This section describes the computer algorithm developed at TSC and implemented as a FORTRAN routine to run on the DEC PDP-10 time-sharing system at TSC. The algorithm converges to a correct solution except in some cases when the solution is extremely sensitive to perturbations in the parameters (i.e., measurement errors). Since the algorithm starts by finding an approximate solution based on the assumption that all altitudes are zero, the solution generally found is that closest to the planar solution. As presently implemented, the algorithm does not attempt to find more than one solution. The algorithm is developed in the following:

Assume that the environment of OWN contains two radars at sea level, equipped with azimuth reference signals, and a target aircraft.

Let r denote the horizontal distance from OWN to the target and let θ be the bearing of the target from OWN, relative to North. For i = 1,2 let d_i denote the horizontal distance from OWN to the i-th radar. The problem is to determine r,θ and the d_i from the input BCAS (given) data.

Let

H_o = height of OWN

H = height of OTHER

and for i = 1,2 let

β_i = bearing of OWN from the i-th radar

α_i = (bearing of OTHER from the i-th radar) - (bearing of OWN from the i-th radar), i.e., the differential azimuth of the target measured from the i-th radar.

For i = 1,2 let s_i be the horizontal distance from radar 1 to the target. Let

$$T_i = \sqrt{s_i^2 + H^2} + \sqrt{r^2 + (H-H_o)^2} - \sqrt{d_i^2 + H_o^2} \qquad 4.3.1$$

$\frac{T_i}{c}$ (where c is the speed of light) is the differential time of arrival (TOA) measured from the i-th radar. The given data consists of H_o, H, β_1, β_2, α_1, α_2, T_1, T_2.

Consider the following diagram, where the points labelled OWN and OTHER are really the horizontal projections of OWN and OTHER.

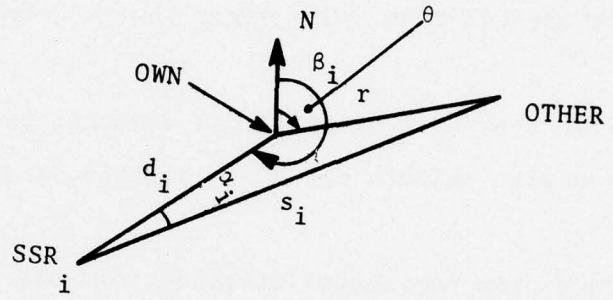

The angle of the triangle whose vortex is at OWN is $\beta_i - \theta$ and the angle whose vortex is at OTHER is $\pi - (\beta_i - \theta + \alpha_i)$.

By the law of sines

$$d_i = \frac{r \sin(\beta_i - \theta + \alpha_i)}{\sin \alpha_i} \qquad 4.3.2$$

s_i may also be computed in terms of α_i, β_i, r and θ from the geometry of the same triangle.

The expressions for d_i and s_i may be substituted in 4.3.1.

The results is of the form

$$T_i = F(r, \theta, \alpha_i, \beta_i, H, H_o) \qquad i = 1,2 \qquad 4.3.3$$

4.3.3 is a system of two equations which must be solved for the unknowns r,θ. Then 4.3.2 computes the d_i.

The method of solution involves an initialization followed by an iteration.

4.3.1 Initialization

The initialization assumes that the radar distances d_i are large compared to r, H and H_o. It then finds a function $f(r,\theta,\alpha_i,\beta_i,H,H_o)$ such that for each i, $f(r,\theta,\alpha_i,\beta_i,H,H_o)$ will approximate $F(r,\theta,\alpha_i,\beta_i,H,H_o)$ and solves the system

$$T_i = f(r,\theta,\beta_i,H,H_o) \qquad 4.3.4$$

Let $d(r,\theta,\alpha,\beta) = \frac{r \sin(\alpha+\beta-\theta)}{\sin \alpha}$ and for each i let $d_i = d(r,\theta,\alpha_i,\beta_1)$. (Note that this definition is consistent with 4.3.2)

The law of cosines and some algebraic manipulation show that

$$T_i = F(r,\theta,\alpha_i,\beta_i,H,H_o) = \frac{r^2 - 2rd_i \cos(\theta-\beta_i) + H^2 - H_o^2}{\sqrt{d_i^2 + r^2 - 2d_i r \cos(\theta-\beta_i) + H^2} + \sqrt{d_i^2 + H_o^2}} + \sqrt{r^2 + (H-H_o)^2} \qquad 4.3.5$$

If it is assumed that $d_i >> r, H, H_o$, then the denominator of the first term of F is close to $2 d_i$, and

$$f(r,\theta,\beta,H,H_o) = - r \cos(\theta-\beta_i) + \sqrt{r^2 + (H-H_o)^2} \qquad 4.3.6$$

is a good approximation of F.

Let

$$A = 1 - \cos(\beta_2-\beta_1) \qquad 4.3.7$$

$$V = \frac{1}{A^2}\left((T_1+T_2)^2 + (4-2A)T_1T_2 - 2A(H-H_o)^2\right) \qquad 4.3.8$$

and

$$W = \frac{2(T_1+T_2)}{A^2}(4-2A)T_1T_2 + (A^2-2A)(H-H_o)^2 \qquad 4.3.9$$

The system of equations 4.3.4 has two solutions (r,θ). The two values of r are given by $V \pm W$.

V+W is chosen if the target lies in the smaller wedge determined by $Radar_1$ - OWN - $Radar_2$. Otherwise, V-W is chosen.

Once r is known, it is not difficult to solve for θ.

The initialization uses the (r,θ) computed above to compute numbers $\hat{T}_i$ in such a way that the correct solution of the system

$$\hat{T}_i = f(r,\theta,\beta_i,H,H_o) \qquad i = 1,2$$

will be a better initialization than the one previously computed. The solution of this system is the initialization.

4.3.2 Iteration

Let $M(r,\theta)$ denote the 2x2 matrix

$$M(r,\theta) = \begin{bmatrix} \frac{\partial F}{\partial r}(r,\theta,\alpha_1,\beta_1,H,H_o) & \frac{\partial F}{\partial \theta}(r,\theta,\alpha_1,\beta_1,H,H_o) \\ \frac{\partial F}{\partial r}(r,\theta,\alpha_2,\beta_2,H,H_o) & \frac{\partial F}{\partial \theta}(r,\theta,\alpha_2,\beta_2,H,H_o) \end{bmatrix} \qquad 4.3.10$$

If, after the $i^{\underline{th}}$ iterative step, the approximate solution is (r_i,θ_i) then (r_{i+1},θ_{i+1}) is defined by the matrix equation

$$\begin{bmatrix} r_{i+1} \\ \theta_{i+1} \end{bmatrix} = \begin{bmatrix} r_i \\ \theta_i \end{bmatrix} + M(r,\theta)^{-1} \begin{bmatrix} T_1-F(r_i,\theta_i,\alpha_1,\beta_1,H,H_o) \\ T_2-F(r_i,\theta_i,\alpha_2,\beta_2,H,H_o) \end{bmatrix} . \qquad 4.3.11$$

The iteration stops if

1) $i = 20$

or

2) $r_{i+1}-r_i$ and $\theta_{i+1}-\theta_i$ are both sufficiently small.

The iteration is along a vector field. If (r,θ) is the solution, then (r,θ) is a sink of this field, but it is not the only sink. In particular, $(-r,\theta)$ (which is geometrically meaningless) and $(r,\pi+\theta)$ are both sinks. If either of these two additional sinks is chosen by the iteration, the computed position of the other will be the reflection about OWN of the true position. Fortunately, it is not difficult to tell, from the input data, if this reflection has been computed. Therefore, the algorithm can correct the "mistake" of finding the wrong sink.

4.4 NATURE OF THE SOLUTION

The algorithm described in the previous section converges to a correct solution except when the aircraft and radars are in certain configurations in which the solution is extremely sensitive to small variations in the measurements. The iteration then may not converge.

The term "correct solution" designates a solution which describes a configuration for which the noise-free TOA, DAZ and OAZ measurements would be precisely those from which the solution was obtained. Generally, only one such solution exists, but under some circumstances there may be several solutions. Such a case is illustrated by the third simulation run described in Section 5 and is discussed below.

It is important to state again that the false solution is not a construct due to some deficiency in the algorithm or to excessive measurement errors.

It is instead one of two configurations of radars and aircraft which result in identical sets of measurements (of TOA, DAZ, OAZ and altitudes) being made by the BCAS. When two distinct configurations are possible sources of the measurements obtained, the nature of the algorithm determines which it will find, but it is essentially a matter of chance whether this is in fact the actual configuration.

Though calculations made at only one instant and based only on the nominal inputs cannot determine whether a particular solution that has been obtained corresponds to the actual configuration, in practice there may often be additional data available that allow the decision to be made. It should be possible to extend the algorithm to determine the alternative solutions when these exist.

A number of checks can be performed on the solution: If the range to one or both of the radars has been calculated in some other context, a rough consistency check can be performed. Active interrogations can be performed to get an independent estimate of the range to the target as a check on the value computed from the passive measurements. Finally, if a time sequence of successive configurations is computed, though the improper solution may be found at each time, these configurations will not be consistent in time. Thus, in the case of the example in the simulated sequence, it may be observed that the calculated distance between the radars is about 38 miles when the improper solution is first found and continuously changes to about 56

miles some 46 seconds later. It must be noted, however, that the calculated distance to the radars is quite sensitive to measurement errors and shows large random variation between successive instants of calculation. Thus inconsistencies in calculated distances to radars can be taken to be reliable indicators of an improper solution only if they are very large or sustained over a period of time.

A more satisfactory answer to the problem of multiple solutions would be an algorithm that determined all solutions wherever several exist. Further software in the system could then resolve the ambiguity, either by calling for active range measurements or by evaluating the track data. It may be anticipated that when several distinct solutions exist which are quite different, it should be easy to determine the actual configurations. When the solutions are distinct but relatively similar, the resolution of the ambiguity may be more difficult.

In addition to configurations for which the BCAS measurements are such that several distinct consistent solutions may be calculated, there exist configurations in which relatively large displacements of the targets or radars lead to small changes in the measurements made by BCAS. Inversely, small changes in the measurements (such as those due to quantization and noise) lead to large changes in the configuration corresponding to the measurement set. This means that the values of range and bearing calculated from noisy measurements will show large deviations from their actual values as a result of the

random errors.

Two problems then arise in these regions: First, the values of range and bearing that may be found when the equations describing the measurements are solved may be quite far from the actual values. Second, the nature of the problem is such that the iterative algorithm described above for solving the system may fail to converge.

The "bad" configurations generally are the following:

1. Both radars in the same direction from the BCAS aircraft (OAZ_1-OAZ_2 less than $\sim 10^o$).
2. The intruder aircraft between the BCAS and one of the ground radars ($|\beta_1-\theta|$ less than $\sim 15^o$).
3. The intruder aircraft in the direction opposite the radar from BCAS ($|\beta_1-\theta- 180^o|$ less than $\sim 3^o$).

The precise extent of the bad ranges depends also on the other aspects of the configuration--altitudes, distances to the radars, distance of the target, and the magnitude of the bearing angle that is not the primary contributor to the problem. In general, the bad ranges tend to be wider when the aircraft are at higher altitudes. In the case of configurations 2 and 3, when the intruder is colinear with the BCAS and the radar, the bad range widens and splits when the aircraft are at high altitudes. The errors in the computed positions are large when the intruder aircraft is on either side of the radar-BCAS line, but moderate when directly on the line.

All of the enumerated effects can be explained qualitatively by the behavior of the locus curves shown in the Figures in Section 2.

AD-A062 912 TRANSPORTATION SYSTEMS CENTER CAMBRIDGE MASS F/G 1/2
BEACON COLLISION AVOIDANCE SYSTEM (BCAS) ALTERNATIVE CONCEPTS F--ETC(U)
SEP 78 J G RAUDSEPS, M D MENN, J VILCANS
UNCLASSIFIED TSC-FAA-78-19 FAA/RD-78/34 NL

2 OF 3
AD
AD 62912

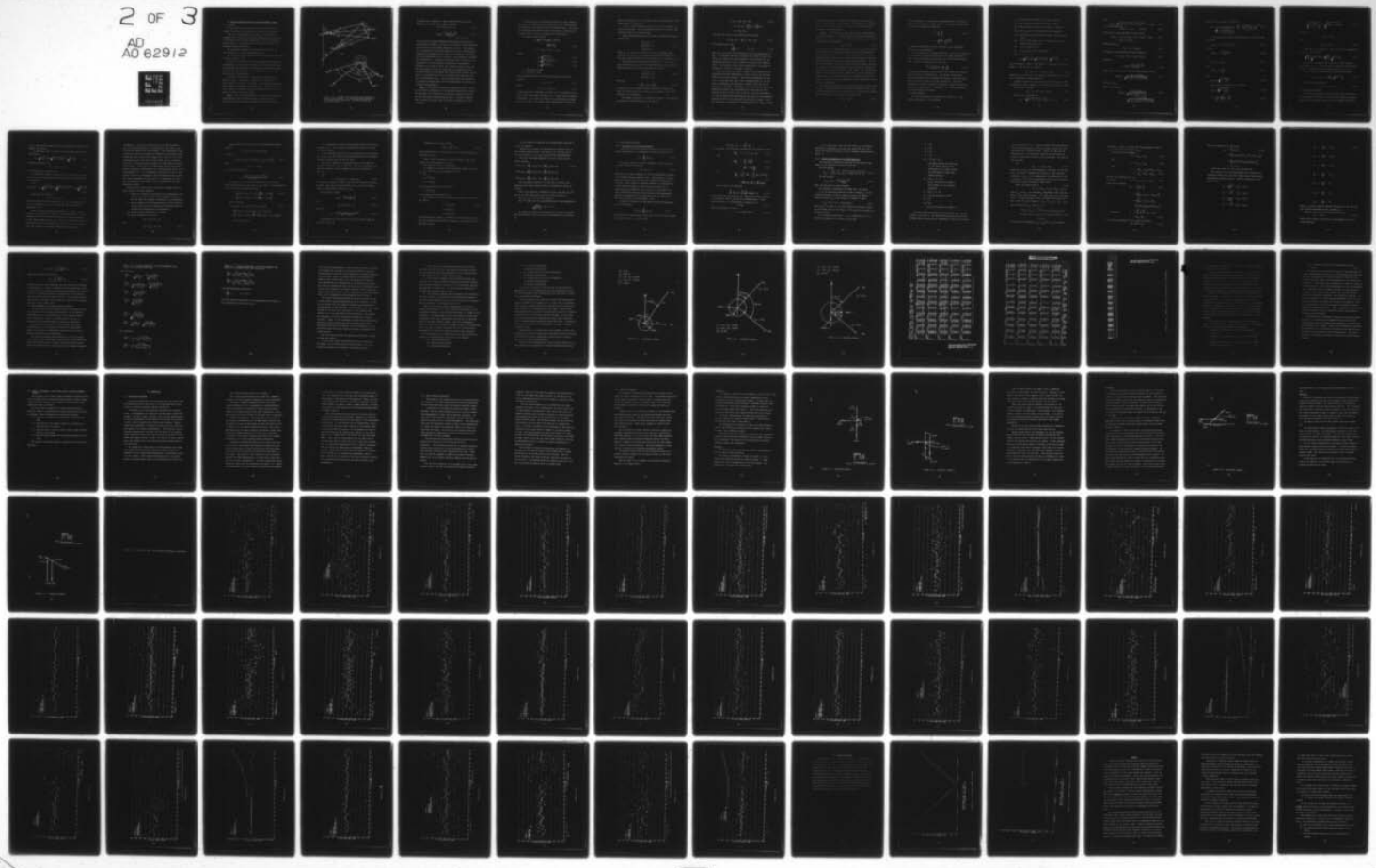

5. PASSIVE MODE BCAS WITHOUT AZIMUTH REFERENCE SIGNALS

5.1 OVERVIEW

A purely passive BCAS system without azimuth reference signals can operate when there are two radars and two targets.

Since all the measurements available to the system are invariant under rotation of the whole configuration, the bearing of one radar may be specified arbitrarily. The three relative bearing angles in the configuration are defined in terms of the arbitrary reference direction.

The quantities measured are four TOA's, four DAZ's, and three altitudes, or eleven measurements in all.

The interrelationship between measured and derived parameters is shown in Figure 5.1-1.

Solutions to be found are for the parameters describing the configuration. These are two distances to the ground interrogators from OWN, two distances to both targets, three bearing angles and three aircraft altitudes, or ten parameters in all. Thus, the problem is overdetermined.

The method of solution is complicated and consists of a number of steps. At the end, a solution is sought which in a useful sense is a best fit to the data. The solution proceeds in three separate essentially independent steps - coarse initialization, iterative refinement, and least-squared-error fitting. In outline the steps are the following.

Step 1: The coarse initialization is based on the simplifying assumptions that the BCAS-to-target distances are much smaller than the BCAS-to-radar distances and that all aircraft

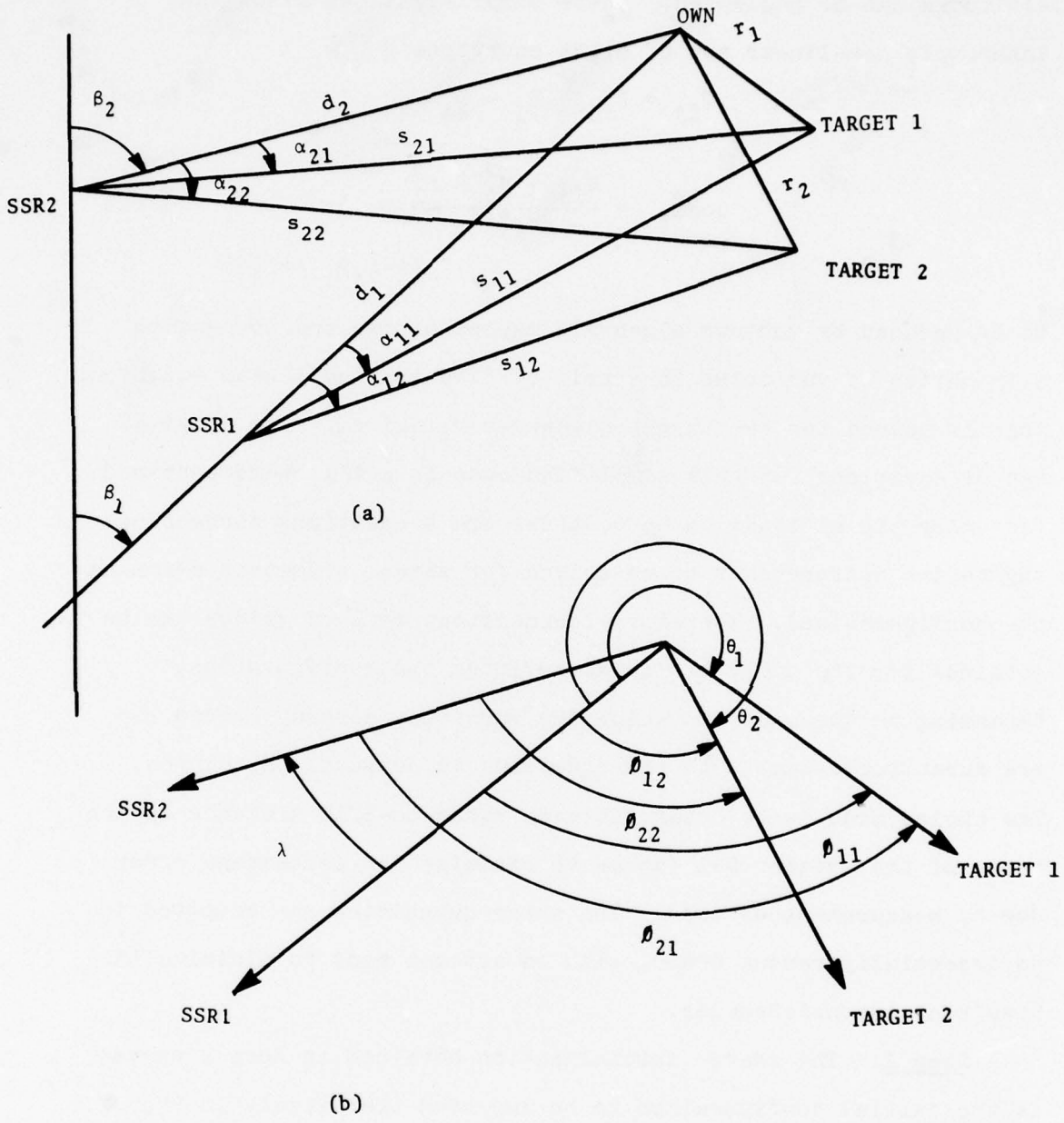

FIGURE 5.1-1. DEFINITION OF VARIABLES IN TWO-RADAR, TWO TARGET CONFIGURATIONS. (a) SHOWS HORIZONTAL DISTANCES, (b) DEFINES ANGLES ABOUT OWN. ALL ANGLES SHOWN ARE POSITIVE IN SIGN.

altitudes can be neglected. These simplifications allow the inherently non-linear set of eight equations

$$T_{ij} = S_{ij} + R_j - D_i \qquad 5.1.1$$

$$\cos\alpha_{ij} = \frac{s_{ij} + d_i^2 - r_1^2}{2s_{ij}\, d_i} \qquad 5.1.2$$

$$(i=1,2;\ j=1,2)$$

to be reduced by various algebraic manipulations and successive elimination of variables to a pair of simultaneous linear equations that is solved for the target distances r_1 and r_2. The original set of equations for this simplified case is still overdetermined (assuming the altitude to be 0, there are 8 equations corresponding to the measurements to be solved for seven parameters defining the configuration). Therefore inconsistent sets of values can be obtained for the other variables defining the configuration, depending on the order in which the variables already solved for are substituted back into the equations to evaluate the others. The choice made is to determine each radar-to-BCAS distance on the basis of the greater DAZ (so as to minimize the percentage error due to measurement errors). The other quantities are computed in an essentially random order, with no attempt made to minimize the resultant inconsistencies.

Step 2: The coarse initialization obtained in Step 1 serves as the initial configuration to be improved iteratively in Step 2. The main goal of the process is to take into proper account the aircraft altitudes, neglected during Step 1. Further, explicit note is taken of the fact that the system of equations is overdetermined.

The calculations are performed iteratively. Thus distances and angles are computed for the projection of the 3-dimensional configuration of the aircraft on the horizontal plane. The effect of the aircraft altitudes is taken into account by modifying the measured values of TOA to compensate for the altitude.

One may note that the TOA

$$T = \sqrt{s^2 + H^2} + \sqrt{r^2 + (H-H_o)^2} - \sqrt{d^2 + H_o^2} \qquad 5.1.3$$

$$= s + \varepsilon_S + r + \varepsilon_R - d - \varepsilon_D$$

where

$$\varepsilon_S = \sqrt{s^2 + H^2} - s \qquad 5.1.4$$

$$\varepsilon_R = \sqrt{r^2 + (H-H_o)^2} - r \qquad 5.1.5$$

$$\varepsilon_D = \sqrt{d^2 + H_o^2} - d \qquad 5.1.6$$

H - altitude of target

H_o - altitude of BCAS

One can therefore write a simplified, apparently linear TOA equation

$$t = s + r - d \qquad 5.1.7$$

where

$$t = T - \varepsilon_S - \varepsilon_R + \varepsilon_D \,. \qquad 5.1.8$$

At each step of the iteration, the value of t is recomputed on the basis of the best current estimates of s, r and d until convergence is achieved - i.e., until the values do not significantly change from step to step. (In certain "bad" configurations the process

does not converge and it is therefore always terminated after some fixed number of iterations.)

A set of three independent equations in the two unknowns d_1 and d_2 is developed. This overdetermined system is solved at each iterative step in the following way:

Three equations developed on the basis of geometric arguments require that:

$$\begin{aligned} F_1(d_1,d_2) &= 0 \\ F_2(d_1,d_2) &= 0 \\ F_3(d_1,d_2) &= 0 \end{aligned} \qquad 5.1.9$$

where F_1, F_2, and F_3 are functions only of the BCAS-to-radar distances (d_1 and d_2), the measured differential azimuths, and (the best current estimates of) the adjusted TOA's (Equation 5.1.3).

These equations are mutually inconsistent - i.e., for any pair of values (d_1,d_2), not all three functions F_1, F_2, F_3 will be identically zero, but rather they will have values

$$\begin{aligned} F_1(d_1,d_2) &= e_1 \\ F_2(d_1,d_2) &= e_2 \\ F_3(d_1,d_2) &= e_3 \end{aligned} \qquad 5.1.10$$

such that

$$E = \left(e_1^2 + e_2^2 + e_3^2\right) \neq 0 \qquad 5.1.11$$

At each step, the iterative algorithm determines changes (Δd_1, Δd_2) to d_1 and d_2 such as to reduce E, the measure of the inconsistency of the equations.

The changes $(\Delta d_1,\Delta d_2)$ are computed as follows: The equations are made into linear equations in Δd_1 and Δd_2.

$$F_i\ (d_1 + \Delta d_1,\ d_2 + \Delta d_2) \qquad 5.1.12$$

$$= F_i\ (d_1, d_2) + \frac{\partial F_i}{\partial d_1} \Delta d_1 + \frac{\partial F_i}{\partial d_2} \Delta d_2$$

$$= e_i\ (\Delta d_1,\ \Delta d_2)$$

One seeks the values of Δd_1 and Δd_2 which minimize

$$E\ (\Delta d_1,\ \Delta d_2) = \sum_i e_i\ (\Delta d_1,\ \Delta d_2)^2 \qquad 5.1.13$$

The minimum occurs when

$$\frac{\partial E}{\partial \Delta d_j} = 0 \qquad (j = 1,2) \qquad 5.1.14$$

This is a set of two linear equations in the two unknown Δd_1 and Δd_2. Its solutions are used to improve the current values of d_1 and d_2, to compute the other parameters that determine the configuration from these, and to update the values of the adjusted TOA's. The iterative step is then repeated until convergence is obtained (or failure to converge is evident).

When this process is used to compute the configuration from simulated noise-free measurements, perfect results are obtained (where the process converges). When noisy measurements are used (i.e., in the practical case), then reasonably good fits to the actual configuration are obtained. However, these are not the best fits to the data. Furthermore, as in the case of Step 1, the parameters defining the configuration are determined by first finding one pair of them - here d_1 and d_2 - and then determining the rest successively by substituting the values of the parameters already solved for into expressions involving the others. Since the overall set of equations is overdetermined, the values obtained

will not in general be consistent. No attempt is made in this step to revolve these inconsistencies. The theoretically optimum solution is obtained by Step 3, for which the results obtained here serve as initial values.

Step 3. The final step is again an iterative squared-error minimization process. The eleven quantities measured by BCAS are expressed as functions of the ten various coordinates defining the radar-aircraft configuration.

$$y_\ell = F_\ell (X) \qquad 5.1.15$$

where y_ℓ is the ℓ-th measurement and $X = (x_1 \ldots x_{10})$ is the vector of coordinate values defining the radar aircraft configurations. The components of X are the two BCAS-to-radar distances, the two BCAS-to-aircraft distances, the three relative angles to aircraft and radar from the BCAS, and the three aircraft heights. The y_ℓ are the following: four TOA's, three reported altitudes, and for each radar the sum and difference of the differential azimuths of the two target aircraft relative to that radar. (The sum and differences of the DAZ's are used, rather than the DAZ's themselves, because there is correlation between the measurement noise components of the DAZ's, but not between the noise components of their sums and differences.)

The actual measurements m_ℓ are noise corrupted, so that there will be a random discrepancy e_ℓ between the predicted value y_ℓ of a given measurement when the configuration is described by a given set of parameters X and the actual measurement m_ℓ.

$$e_\ell = m_\ell - y_\ell(X) \qquad 5.1.16$$

This discrepancy e is ascribed to measurement error. By what is known as the principle of least squares, the assumed configuration best fits the measurement data when

$$E = \sum_{\ell} \frac{e_{\ell}^2}{\sigma_{\ell}^2} \qquad 5.1.17$$

$$= \sum_{\ell} \frac{\left(m_{\ell} - y_{\ell}(X)\right)^2}{\sigma_{\ell}^2}$$

is minimized (where σ_{ℓ}^2's are the variances of the independent errors in the measurements).

The X minimizing E is found iteratively. The set of equations for the errors are first made into a set of linear equations in terms of ΔX, incremental changes about the true minimum configuration. The set of equations is of the form

$$\frac{m_{\ell} - F_{\ell}(X_{opt})}{\sigma_{\ell}} = \sum_{k} \frac{\partial F_{\ell}}{\partial x_k} \qquad 5.1.18$$

The partial derivatives are evaluated at the current best approximation of the true configuration. Temporarily holding these partial derivatives fixed, standard multivariate regression techniques are used to find the ΔX that minimizes E. The set of coordinates X is then corrected by adding the computed ΔX and the process is repeated until it converges - i.e., until successive ΔX's become sufficiently small.

5.2 INITIALIZATION

The case considered is illustrated in Figure 5.1-1. The notation throughout is the following.

r_j = the horizontal distance from OWN to target j

d_i = the horizontal distance from OWN to radar i

s_{ij} = the horizontal distance from radar i to target j

R_j, D_i and S_{ij} are the corresponding slant distances

α_{ij} is the differential azimuth of target j measured from radar i

ϕ_{ij} is the angle between the i-th radar and the j-th target, viewed from OWN

H_o is the height of OWN

H_j is the height of the j-th target

For i = 1,2, j = 1,2

$$T_{ij} = \sqrt{s_{ij}^2 + H_j^2} + \sqrt{r_j^2 + (H_j - H_o)^2} - \sqrt{d_i^2 + H_o^2} \qquad 5.2.1$$

α_{ij} = (bearing of target j from radar i) - (bearing of own from radar i. From the law of consines

$$r_j^2 = s_{ij}^2 + d_i^2 - 2 \cdot d_i \cdot s_{ij} \cos\alpha_{ij} \qquad 5.2.2$$

Equation 5.2.1 is the (i,j) TOA equation and Equation 5.2.2 is the (i,j) differential azimuth equation.

Assume all heights are zero and that the distances r_j (BCAS to target) are small compared to the distances d_i (BCAS to radar).

By the law of cosines

$$s_{ij}^2 = r_j^2 + d_i^2 - 2 r_j d_i \cos\theta_{ij} \qquad 5.2.3$$

Hence, by the TOA equation

$$T_{ij} = \sqrt{r_j^2 + d_i^2 - 2 r_j d_i \cos\theta_{ij}} + r_j - d_i \qquad 5.2.4$$

and

$$T_{ij}/d_i = \sqrt{1-2(r_j/d_i)\cos\theta_{ij} + (r_j/d_i)^2} - 1 + r_j/d_i \qquad 5.2.5$$

By the approximation

$$(1+x)^n \simeq 1 + nx \qquad (|x|<<1) \qquad 5.2.6$$

which will be used repeatedly in what follows

$$T_{ij}/d_i \simeq - r_j/d_i \cos\phi_{ij} + 1/2 (r_j/d_i)^2 + r_j/d_i \qquad 5.2.7$$

$$\simeq r_j/d_i (1-\cos\phi_{ij})$$

Multiplying by d_i

$$T_{ij} = r_j (1-\cos\phi_{ij}) \qquad 5.2.8$$

According to the differential azimuth equation

$$r_i^2 = s_{ij}^2 + d_i^2 - 2 \cdot s_{ij} \cdot d_i \cdot \cos\alpha_{ij} \qquad 5.2.9$$

Therefore

$$\cos\alpha_{ij} = \frac{s_{ij}^2 + d_i^2 - r_j^2}{2\, s_{ij} \cdot d_i} \qquad 5.2.10$$

Substitution of 5.2.1 in 5.2.10 and simplification yields

$$\cos\alpha_{ij} = \frac{d_i - r_j \cos\phi_{ij}}{\sqrt{r_j^2 + d_i^2 - 2 \cdot r_j \cdot d_i \cos\phi_{ij}}} \qquad 5.2.11$$

Let $t_{ij} = r_j/d_i$

Then 5.2.11 becomes

$$\cos\phi_{ij} = \frac{1-t_{ij}\cos\phi_{ij}}{\sqrt{1-2t_{ij}\cos\phi_{ij} + t_{ij}^2}} \qquad 5.2.12$$

$$= \frac{1-t_{ij}\cos\phi_{ij}}{\sqrt{(1-t_{ij}\cos\phi_{ij})^2 + t_{ij}^2 \sin^2\phi_{ij}}}$$

and, since $1-t_{ij}\cos\phi_{ij}$ is positive,

$$\cos\alpha_{ij} = \frac{1}{\sqrt{1 + \frac{t_{ij}^2 \sin^2\phi_{ij}}{(1-t_{ij}\cos\phi_{ij})^2}}} = \left(1 + \frac{t_{ij}^2 \sin^2\phi_{ij}}{(1-t_{ij}\cos\phi_{ij})^2}\right)^{-1/2} \quad 5.2.13$$

To an approximation neglecting all powers of t_{ij} higher than the second

$$\cos\alpha_{ij} \simeq 1 - \frac{1}{2} t_{ij}^2 \sin^2\phi_i, \quad 5.2.14$$

so that

$$\sin^2\phi_{ij} \quad \frac{2\cdot(1-\cos\alpha_{ij})}{t_{ij}^2} \quad 5.2.15$$

Let

$$A_{ij} = 1 - \cos\alpha_{ij}. \quad 5.2.16$$

Then

$$\sin^2\phi_{ij} = \frac{2\,A_{ij}}{t_{ij}^2} \quad 5.2.17$$

and

$$\cos\phi_{ij} = \pm\sqrt{1 - \frac{2\,A_{ij}}{t_{ij}}} \quad 5.2.18$$

Substitution of 5.2.18 in 5.2.8 yields

$$T_{ij} = r_j\sqrt{1 - \frac{2\,A_{ij}}{t_{ij}}} \quad 5.2.19$$

$$1 - \frac{2\,A_{ij}}{t_{ij}^2} = \left(\frac{T_{ij}}{r_i} - 1\right)^2 \quad 5.2.20$$

$$t_{ij} = \sqrt{\frac{2\,A_{ij}}{2\,\frac{T_{ij}}{r_j} - \frac{T_{ij}^2}{r_j^2}}} = r_j \sqrt{\frac{2\,A_{ij}}{T_{ij}} \cdot \frac{1}{r_j - T_{ij}}} \qquad 5.2.21$$

By definition

$$t_{ij} = r_j/d_i$$

Hence

$$t_{i2}/t_{i1} = r_2/r_1 \,. \qquad 5.2.22$$

Divide the (i,2) equation of 5.2.21 by the (i,1) equation and use 5.2.20. The result is

$$\sqrt{\frac{2A_{i2}}{T_{i2}}}\sqrt{2\,r_1 - T_{i1}} = \sqrt{\frac{2A_{i1}}{T_{i1}}}\sqrt{2\,r_2 - T_{i2}} \qquad 5.2.23$$

When 5.2.23 is squared, the result is a linear equation in the variables r_1, r_2. There are two such equations corresponding to i=1,2. These may be solved simultaneously for r_1, r_2.

Given i, choose j such that A_{ij} is maximal and compute

$$d_i = r_i/t_{ij} = \frac{T_{ij}}{2\,A_{ij}}\sqrt{2\,r_i - T_{ij}} \qquad 5.2.24$$

s_{ij} may now be computed by

$$s_{ij} = T_{ij} - r_j + d_i \qquad 5.2.25$$

5.3 ITERATIVE IMPROVEMENT

This section describes an algorithm that takes the output of the initialization algorithm of the previous section and produces a result that is correct (except for the bad ranges described in

(5.6) if the measured quantities (TOA's, differential azimuths and heights) are correct.

An observation that is central to the algorithm is that the TOA equations

$$T_{ij} = \sqrt{s_{ij}^2 + H_j^2} + \sqrt{r_j^2 + (H_j - H_o)^2} - \sqrt{d_i^2 + H_o^2} \qquad 5.3.1$$

simplify considerably to

$$T_{ij} = s_{ij} + r_i - d_i \qquad 5.3.2$$

if the heights are assumed to be 0.

If approximate values are known for s_{ij}, d_i and r_i the error in 5.3.2 can be approximated and absorbed into the left-hand side of the equation.

Let

$$U_{ij} = T_{ij} + s_{ij} - \sqrt{s_{ij}^2 + H_j^2} + r_j - \sqrt{r_j^2 + (H_j - H_o)^2} - d_i + \sqrt{d_i^2 + H_o^2} \qquad 5.3.3$$

Then from 5.3.1 and 5.3.3

$$U_{ij} = s_{ij} + r_j - d_i \qquad 5.3.4$$

Given old values for the variables d_i, r_j, s_{ij} the algorithm uses 5.3.3 to approximate the U_{ij} and then uses the simplified TOA equations 5.3.4.

There is another important observation to be made. Superficially, it seems that the system to be solved consists of eight equations (the four TOA and four differential azimuth equations) in the eight unknowns d_i, r_j, s_{ij}. There is, however, an additional constraint that must be placed on the d_i, r_j, s_{ij} so as to ensure that this variable set actually corresponds to a geometric

configuration. One way of seeing this is to count dimensions. The input measurement space is 11-dimensional (four TOA's, four differential azimuths and three heights). The configuration space locates four points (the radars and targets) on the ground, eight dimensions, and includes three heights for a total of 11, but two configurations are 'the same' if they differ only by a rotation about own. This takes away one degree of freedom from the configuration space. Thus, the set of measurement vectors that correspond to geometric configurations is a 10-dimensional subset of an 11-dimensional set. If a measurement vector does not lie in this subset, there is no configuration that corresponds to that vector. For 'most' measurement vectors, then, it is impossible to solve for a configuration and reality is best represented by an overdetermined system.

There are two obvious ways to modify the original system of eight equations in eight unknowns;

1. Change the variable set describing the configuration from $\{d_i, r_j, s_{ij}, H_j\}$ to a set of ten variables in such a way that each set actually corresponds to a configuration.
2. Add an equation to the original system of eight equations in such a way that if the equation is satisfied then the variable set corresponds to a configuration.

The second of these options will be chosen.

Let U_{ij} be defined as in 5.3.3 so

$$U_{ij} = s_{ij} + r_j - d_i$$

and

$$s_{ij} = U_{ij} - r_j + d_i \qquad 5.3.5$$

Substitution of 5.3.5 into the (i,j) differential azimuth equation

$$r_j^2 = s_{ij}^2 + d_i^2 - 2\, d_i s_{ij} \cos\alpha_{ij}$$

results in

$$0 = A_{ij}d_i^2 - A_{ij}d_i r_j + A_{ij}U_{ij}d_i - U_{ij}r_j + \tfrac{1}{2}\,U_{ij}^2 \qquad 5.3.6$$

where

$$A_{ij} = 1 - \cos\alpha_{ij}$$

5.3.6 may be solved for r_j

$$r_j = \frac{A_{ij}d_i^2 + A_{ij}\,U_{ij}\,d_i + \frac{1}{2}\,U_{ij}^2}{U_{ij} + A_{ij}\;\;d_i} \qquad 5.3.7$$

For fixed j, 5.3.7 gives two expressions (i=1,2) for r_j. These expressions may be set equal to each other. Cross-multiplication of the resulting equation yields

$$\left(A_{1j}d_i^2 + A_{1j}U_{1j}\,d_1 + \tfrac{1}{2}\,U_{1j}^2\right)\left(U_{2j} + A_{2j}d_2\right) \qquad 5.3.8$$
$$= \left(A_{2j}d_2^2 + A_{2j}U_{2j}d_2 + \tfrac{1}{2}\,U_{2j}^2\right)\left(U_{1j} + A_{1j}d_1\right)$$

After regrouping

$$0 = A_{1j}A_{2j}d_1^2\;d_2 - A_{1j}A_{2j}d_1 \cdot d_2^2 + A_{1j}U_{2j} \cdot d_1^2 \qquad 5.3.9$$
$$+ \left(A_{1j}A_{2j}U_{1j} - A_{1j}A_{2j}U_{2j}\right)\,d_i\;d_2 - A_{2j}U_{1j}d_2^2$$
$$+ \left(A_{1j}U_{1j}U_{2j} - \tfrac{1}{2}\,A_{1j}U_{2j}^2\right)d_1 + \left(\tfrac{1}{2}\,A_{2j}U_{1j}^2 - A_{2j}U_{1j}U_{2j}\right)\,d_2$$
$$+ \;\tfrac{1}{2}\,U_{ij}U_{2j}(U_{1j}-U_{2j})$$

5.3.9 represents a system of two equations (j=1,2) in the two unknowns d_1, d_2. Once these two variables are known, it is easy to find the others.

It was mentioned earlier that the computation of the variables d_i, r_j, s_{ij} involves solving an overdetermined system of equations. Therefore, another equation must be found.

Φ_{ij} will be taken to be a positive angle of less than 180 degrees if and only if α_{ij} is positive. With this convention, the angle with vertex 0 that is spanned by d_1 and d_2 is given by $\Phi_{2j} - \Phi_{1j}$.

Thus

$$0 = \sin(\Phi_{22}-\Phi_{12}) - \sin(\Phi_{21}-\Phi_{11}) \qquad 5.3.10$$

5.3.10 can be written in terms of the sines and cosines of the Φ_{ij} and will, then, yield a third question in d_1, d_2 if the $\sin \Phi_{ij}$, $\cos\Phi_{ij}$ are expressed in terms of d_1, d_2.

By the law of cosines

$$\cos\Phi_{ij} = \frac{s_{ij}^2 - d_i^2 - r_j^2}{2\, d_i\, r_j} \qquad 5.3.11$$

Also

$$s_{ij} = U_{ij} + d_i - r_j \qquad 5.3.12$$

and 5.3.7

$$r_j = \frac{A_{ij} \cdot d_i^2 + A_{ij} U_{ij}\, d_i + \frac{1}{2} U_{ij}^2}{U_{ij} + A_{ij}\, d_i} \qquad 5.3.13$$

Substitution of 5.3.12 and 5.3.13 in 5.3.11 gives $\cos\Phi_{ij}$ as a function of d_1, d_2.

Similarly, by the law of sines,

$$\sin\Phi_{ij} = \frac{s_{ij}}{r_j} \sin\alpha_{ij} \qquad 5.3.14$$

and substitution of 5.3.12 and 5.3.13 in 5.3.14 gives $\sin\phi_{ij}$ as a function of d_1, d_2.

When 5.3.10 is expressed in terms of $\sin\phi_{ij}$, $\cos\phi_{ij}$ the result is a third equation in d_1, d_2.

The iteration may now be described.

An iterative step starts with approximate values of the d_i, r_j, s_{ij}. Next the U_{ij} are computed by 5.3.3.

Let

$$0 = F^1(d_1,d_2)$$

$$0 = F^2(d_1,d_2)$$

be the two equations of 5.3.9 and let

$$0 = F^3(d_1,d_2)$$

be the equation derived from 5.3.10

The iteration proceeds by finding an approximate solution to the system

$$0 = F^1(d_1,d_2) \qquad 5.3.15$$

$$0 = F^2(d_1,d_2)$$

$$0 = F^3(d_1,d_2)$$

then computing the r_j and s_{ij} in terms of the d_i and then going to the next iterative step unless the changes in the variables have been small enough.

It only remains to describe how the approximate solution to 5.3.15 is computed.

Suppose d_1, d_2 denote the approximations obtained prior to the current iterative step. The object is to find Δd_1, Δd_2 in such a way that $d_1 + \Delta d_1$, $d_2 + \Delta d_2$ are better approximations.

The best linear approximation to 5.3.15 is given by the matrix equation

$$- F^1(d_1,d_2) = \frac{\partial F^1}{\partial d_1}(d_1,d_2)\,\Delta d_1 + \frac{\partial F^1}{\partial d_2}(d_1,d_2)\,\Delta d_2 \qquad 5.3.16$$

$$- F^2(d_1,d_2) = \frac{\partial F^2}{\partial d_1}(d_1,d_2)\,\Delta d_1 + \frac{\partial F^2}{\partial d_2}(d_1,d_2)\,\Delta d_2$$

$$- F^3(d_1,d_2) = \frac{\partial F^3}{\partial d_1}(d_1,d_2)\,\Delta d_1 + \frac{\partial F^3}{\partial d_2}(d_1,d_2)\,\Delta d_2$$

The approximate solution to 5.3.16 that is found is the weighted least square solution where the weights are chosen as follows:

First, each equation is weighted in such a way that the i^{th} row of the coefficient matrix of 5.3.16 will have norm 1.

For $j = 1, 2,$ let $r_j = \min (U_{1j}, U_{2j})$.

The j^{th} equation of the normalized system is then weighted by

$$\frac{r_j}{\sqrt{r_1^2 + r_2^2}}, \text{ for } j = 1, 2$$

No claims are made for the optimality of this set of weights. They were chosen by trial and error and probably can be improved on.

5.4 LEAST SQUARES FITTING

5.4.1 Derivation of the Normal Equations

Assume that there are defined M functions y_m, which are all linear combinations of N independent variables x_n, where $M \geq N$.

$$y_m = \sum_{n=1}^{N} \beta_{mn} x_n \qquad 5.4.1$$

The β_{mn} are taken to be known constants. The y_m are given as noise-corrupted measurements.

$$y_m' = y_m + n_m \qquad 5.4.2$$

where n_m is the noise component in the m-th measurement, assumed to be random with zero expected value. The problem is to determine the values of the x_n's that best explain the measurements obtained. (This problem is somewhat different in principle from a more familiar problem, in which both the y_m and a set of variables x_{mn} are measured, and the task is to determine a set of β_n defining the functional relationship of the measurements. However, the equations to be solved will have the same form, with the β's and x's in interchanged roles.)

A measure of how well the x_n's explain any given measurement y_m' is the residual

$$r_m = y_m' - \sum_{n=1}^{N} \beta_{mn} x_n \qquad 5.4.3$$

The principle of least squares states that the best overall explanation y_m' is that set of x_n's for which

$$R(x_1, x_2 \ldots x_n) = \sum_{m=1}^{M} r_m^2$$

is a minimum. The conditions satisfied at the minimum are that

$$\frac{\partial R}{\partial x_n} = 0 \quad (n = 1,2 \ldots N) \qquad 5.4.4$$

Now

$$\frac{\partial R}{\partial x_n} = \sum_{m=1}^{M} \frac{\partial r_m^2}{\partial x_n} \qquad 5.4.5$$

$$= \sum_{m=1}^{M} 2 r_m \frac{\partial r_m}{\partial x_n} \qquad 5.4.6$$

or

$$\frac{\partial R}{\partial x_n} = \sum_{m=1}^{M} 2\left(y'_m - \sum_{\ell=1}^{N} \beta_{m\ell} x_\ell\right)(-\beta_{mn}) \qquad 5.4.7$$

$$= -2\sum_{m=1}^{M} \beta_{mn} y'_m + 2\sum_{\ell=1}^{N} x_\ell \left(\sum_{m=1}^{M} \beta_{m\ell}\beta_{mn}\right)$$

Hence, there are N equations

$$\sum_{m=1}^{M} \beta_{mn}\, y'_m = \sum_{\ell=1}^{N}\left(\sum_{m=1}^{M} \beta_{m\ell}\beta_{mn}\right) x_\ell \qquad 5.4.8$$

to be solved for the values of x_ℓ. These are N linear equations in N unknowns, and the solution is straightforward. Using matrix notation, if corresponding to equation 5.4.1

$$Y = BX, \qquad 5.4.9$$

then the solution to 5.4.8 is

$$X = (B\, B^T)^{-1}\, B^T\, Y'. \qquad 5.4.10$$

It is a known result that when the errors n_m are normally distributed, independent, and with zero means and equal variances, the resultant solution is also a maximum likelihood estimate of X.

5.4.2 Linear Approximation of the BCAS Equations

The equations relating the positions of the aircraft and radars to the quantities measured by BCAS are:

The TOA equation

$$T_{i,j} = \sqrt{s_{i,j}^2 + H_j} + \sqrt{r_j^2 + (H_j - H_o)^2} - \sqrt{d_i^2 + H_o^2} \qquad 5.4.11$$

The DAZ equation

$$\alpha_{i,j} = \pm \cos^{-1} \frac{d_i^2 + s_{i,j}^2 - r_j^2}{2 \cdot d_i s_{ij}} \qquad 5.4.12$$

where the sign must be chosen properly.

The subscript i designates the radar and j the target.

r_j is the horizontal distance of OWN to target; d_i is the horizontal distance of OWN to radar; H_o and H_j are OWN and target altitudes; s_{ij} is the distance of target to radar.

$$s_{i,j} = (d_i^2 + r_j^2 - 2 d_i r_j \cos\phi_{i,j}) \qquad 5.4.13$$

where ϕ_{ij} is the angle at the BCAS between the direction toward the i-th radar and the j-th target. (All angles are defined in a horizontal plane.)

The coordinates describing a given configuration will be defined as components of a vector X as follows:

$x_1 = d_1$

$x_2 = d_2$

$x_3 = r_1$

$x_4 = r_2$

$x_5 = \lambda = \beta_2 - \beta_1$

(the angle between the directions to the radars, equal to the difference of the radar azimuths β_i with respect to some arbitrary reference)

$x_6 = \phi_{1,1} = \theta_1 - \beta_1$

(θ_i is the azimuth of target i with respect to the arbitrary reference)

$x_7 = \phi_{2,1} = \theta_2 - \beta_1$

$x_8 = H_o$ (the altitude of OWN)

$x_9 = H_1$

$x_{10} = H_2$

(H_i is the altitude of target i)

The basic BCAS measurements in modified form are the components of a vector Y. The modifications assure that the measurement noise in each term is independent of that in the others

and has variance of one. It may be observed that the differential azimuth measurements of the two target aircraft for the same radar have correlated errors. Hence, the sums and the differences of the differential azimuths are used, since the errors in these will be shown to be uncorrelated. The proof is the following:

Let

$$\alpha_{i,j} = \phi_{i,j} - \phi_{i,o} \qquad 5.4.14$$

where $\phi_{i,j}$ and $\phi_{i,o}$ are the bearings of the target and own aircraft from radar i, measured with respect to some arbitrary reference. $\alpha_{i,j}$ is in fact measured as the difference of two such angles. The error in measurement for each is the error in defining the radar interrogator beam center.

Hence, the measured DAZ is 5.4.15

$$\alpha'_{i,j} = (\phi_{i,j} + n_{i,j}) - (\phi_{i,o} + n_{i,o})$$

where $n_{i,j}$ and $n_{i,o}$ are zero-mean, independent noise terms assumed to have equal variances, $\sigma^2 = \frac{1}{2}\sigma_\alpha^2$, where σ_α^2 is the variance of the DAZ measurement error, estimated from flight test data. Then the noise component of $\alpha_{i,j}$ is $n_{\alpha_{i,j}} = n_{i,j} - n_{i,o}$. The covariance of $n_{\alpha_{i,1}}$ and $n_{\alpha_{i,2}}$ is

$$E(\{n_{\alpha_{i,1}} n_{\alpha_{i,2}}\}) = E(\{(n_{i,1}-n_{i,o})(n_{i,2}-n_{i,o})\})$$

$$= E\{n_{i,1} n_{i,2} - n_{i,o} n_{i,2} - n_{i,o} n_{i1} + n_{i,o}^2\} \qquad 5.4.16$$

$$= \sigma^2 \neq 0$$

since the noise components $n_{i,1}$, $n_{i,2}$ and $n_{i,o}$ are mutually

independent. Hence it is seen that the measurement noise of $\alpha_{i,1}$ is correlated with that of $\alpha_{i,2}$.

Consider now the variables

$$s = \alpha_{i,1} + \alpha_{i,2} \qquad 5.4.17$$

and

$$d = \alpha_{i,1} - \alpha_{i,2} \qquad 5.4.18$$

Then

$$s = (\phi_{i,1} - \phi_{i,o}) + (\phi_{i,2} - \phi_{i,o})$$

$$= \phi_{i,1} + \phi_{i,2} - 2\phi_{i,o} \qquad 5.4.19$$

and the noise component of s is

(3.4.2-10)
$$n_s = n_{i,1} + n_{i,2} - 2n_{i,o} \qquad 5.4.20$$

which has the variance

$$\sigma_s^2 = E\left[n_s^2\right] \qquad 5.4.21$$

$$= E\left[(n_{i,1} + n_{i,2} - 2n_{i,o})^2\right]$$

$$= E\left[n_{i,1}^2 + n_{i,2}^2 + 4n_{i,o}^2 + 2n_{i,1}n_{i,2} - 4n_{i,1}n_{i,o} - 4n_{i,2}n_{i,o}\right]$$

$$= 6\sigma^2 = 3\sigma_\alpha^2$$

Similarly,
$$d = (\phi_{i,1} - \phi_{i,o}) - (\phi_{i,2} - \phi_{i,o})$$

$$= \phi_{i,1} - \phi_{i,2} \qquad 5.4.22$$

and the noise component of d is n_d with a variance

$$\sigma_d^2 = 2\sigma^2 = \sigma_\alpha^2 \qquad 5.4.23$$

Now the covariance of n_s and n_d is

$$C_{s,d} = E\left[n_s n_d \right] \qquad 5.4.24$$

$$= E\left[(n_{i,1}+n_{i,2}-2n_{i,o})(n_{i,1}-n_{i,2}) \right]$$

$$= E\left[n_{i,1}^2 - n_{i,2}^2 - 2n_{i,o}n_{i,1} + 2n_{i,o}n_{i,2} \right]$$

$$= \sigma^2 - \sigma^2 = 0$$

Hence the errors in s and d are uncorrelated.

The errors in the other measurements are inherently uncorrelated (except for a possible common bias in the altitude measurements, which we ignore). Then the components of the vector Y are:

$$y_1 = \frac{1}{\sqrt{3}\sigma_\alpha} \cdot (\alpha_{1,1} + \alpha_{1,2})$$

$$y_2 = \frac{1}{\sigma_\alpha} (\alpha_{1,1} - \alpha_{1,2})$$

$$y_3 = \frac{1}{\sqrt{3}\sigma_\alpha} (\alpha_{2,1} + \alpha_{2,2})$$

$$y_4 = \frac{1}{\sigma_\alpha} (\alpha_{2,1} - \alpha_{2,2})$$

$$y_5 = \frac{1}{\sigma_T} T_{1,1} \qquad 5.4.25$$

$$y_6 = \frac{1}{\sigma_T} T_{1,2}$$

$$y_7 = \frac{1}{\sigma_T} T_{2,1}$$

$$y_8 = \frac{1}{\sigma_T} T_{2,2}$$

$$y_9 = \frac{1}{\sigma_H} H_o$$

$$y_{10} = \frac{1}{\sigma_H} H_1$$

$$y_{11} = \frac{1}{\sigma_H} H_2$$

where σ_α, σ_T and σ_H are the standard deviations of the DAZ, TOA and altitude measurement errors, respectively.

There is, then, a set of non-linear equations

$$y_i = f_i(X) \qquad 5.4.26$$

which in the vicinity of $X = X_o$ may be approximated by a set of linear equations.

$$y_i = f_i(X_o) + \sum_{n=1}^{11} \frac{\partial f_i(X)}{\partial x_n} \Delta x_n \qquad 5.4.27$$

which can be written in the form

$$\Delta y_i = \sum_{n=1}^{11} \frac{\partial f_i(X)}{\partial x_n} \Delta x_n \qquad 5.4.28$$

where Δy and Δx are the deviations from the values at the assumed configuration X_o. The set of equations 5.4.28 corresponds in form to the set 5.4.1 for which the solution was derived in the previous section. The partial derivatives evaluated at a point near the assumed solution play the roles of the β's. The non-zero partial derivatives of TOA, DAZ, and altitude with respect to the coordinates are listed in Table 5.4-1.

5.5 EFFECTIVENESS OF THE INITIALIZATION ALGORITHM

It may be noted that the overall process of finding the solution consists of (1) a coarse initialization, (2) an iterative improvement on the initialization and (3) an iterative squared error minimization. This is a complex process, and one is naturally led to consider whether it can not be simplified.

The function of the steps is the following: the coarse initialization (1) is necessary to establish the approximate region in the space of configuration coordinates for the more refined further steps to be applicable.

The iterative squared error minimization (3) will converge to the same solution independent of the precise initialization as long as the initial point is within a sufficiently small region about the solution point (a local minimum of the summed residuals).

TABLE 5.4-1. PARTIAL DERIVATIVES OF BCAS MEASUREMENTS WITH RESPECT TO COORDINATES ABOUT OWN

TOA Derivatives:

$$\frac{\partial T_{ij}}{\partial d_i} = -\frac{d_i}{\sqrt{d_i^2 + H_o^2}} + \frac{d_i - r_j \cos\phi_{ij}}{\sqrt{s_{ij}^2 + H_o^2}}$$

$$\frac{\partial T_{ij}}{\partial r_j} = \frac{r_j}{\sqrt{r_j^2 + (H_j - H_o)^2}} + \frac{r_j - d_i \cos\phi_{ij}}{\sqrt{s_{ij}^2 + H_j^2}}$$

$$\frac{\partial T_{ij}}{\partial \theta_j} = \frac{d_i\, r_j \sin\phi_{ij}}{\sqrt{s_{ij}^2 + H_j^2}}$$

$$\frac{\partial T_{2j}}{\partial \lambda} = \frac{d_2\, r_j \sin\phi_{2j}}{\sqrt{s_{2j}^2 + H_j^2}}$$

$$\frac{\partial T_{ij}}{\partial H_o} = \frac{H_o - H_j}{\sqrt{r_j^2 + (H_j - H_o)^2}}$$

$$\frac{\partial T_{ij}}{\partial H_j} = \frac{H_j}{\sqrt{s_{ij}^2 + H_j^2}} + \frac{H_j - H_o}{\sqrt{r_j^2 + (H_j - H_o)^2}}$$

DAZ Derivatives:

$$\frac{\partial \alpha_{ij}}{\partial d_i} = -\frac{r_j \sin\phi_{ij}}{d_i^2 - 2d_i r_j \cos\phi_{ij} + r_j^2}$$

$$\frac{\partial \alpha_{ij}}{\partial r_j} = \frac{d_i \sin\phi_{ij}}{d_i^2 - 2d_i r_j \cos\phi_{ij} + r_j^2}$$

TABLE 5.4-1. PARTIAL DERIVATIVES OF BCAS MEASUREMENTS WITH RESPECT TO COORDINATES ABOUT OWN (Continued)

$$\frac{\partial \alpha_{ij}}{\partial \theta_j} = \frac{-d_i\, r_j \cos\phi_{ij} + r_j^2}{d_i^2 - 2d_i\, r_j \cos\phi_{ij} + r_j^2}$$

$$\frac{\partial \alpha_{2j}}{\partial \lambda} = \frac{d_2\, r_j \cos\phi_{2j} - r_j^2}{d_2^2 - 2d_2\, r_j \cos\phi_{2j} + r_j^2}$$

Altitude Measurement Derivatives:

$$\frac{\partial \hat{H}_j}{\partial H_j} = 1 \qquad (j = 0,1,2)$$

All other partial derivatives of the measurements with respect to the coordinates are identically zero.

If the initial approximation is too far from the proper solution, the iteration may converge to an entirely different solution, corresponding to some other local minimum of the summed residuals. The appropriate measure of effectiveness of an initialization scheme in this context then is not the accuracy with which it itself determines the configuration of the aircraft and radars, but rather the probability that the least square minimization which follows will converge to the proper solution. That solution is a maximum likelihood estimate of the configuration, given the measurements, and is independent of the algorithm used to find it.

The coarse initialization step (1) was not expected to lead to particularly accurate approximations of the solution. It was for this reason that the iterative procedure for improving the initialization (2) was developed. This procedure, too, will either converge to its best fit to the data if it is started close enough to it, or to some other solution otherwise. The regions of convergence of the two iterative procedures are, however, different. Again, if this procedure to improve the coarse initialization is used in conjunction with the final squared error minimization procedure, the measure of its effectiveness is the probability that the overall process ultimately converges to the proper solution.

When the three processes are applied successively, a number of things may happen:

a) The first coarse initialization may be so bad that no convergence to the proper solution can take place - i.e., the iterative processes will converge to some other solution.

b) The first coarse initialization may not give a good starting point for the final least-square minimization process, but the subsequent iterative improvement to the initialization (2) may result in such a "good" starting point.

c) The iterative squared error minimization process may converge to the proper solution starting from either the approximate solution produced by process (1) or the presumably improved approximation of process (2). It may take fewer iterations to converge from one than from the other.

d) The iterative squared error minimization may converge to the proper solution if started at the approximation produced by the first coarse iteration (1), but not if started at the approximation produced by the iterative process (2).

Since both the first, coarse initialization (1) and the iterative improvement on it (2) are heuristic algorithms, it was considered necessary to test them experimentally in a range of configurations. The performance of both was compared to what could be achieved if the true configuration were used as the starting point for the next iterative stage. (The true configuration should not itself be the solution produced by any of the algorithms, since it is not in general consistent with the noise-corrupted measurements from which the algorithms derive their solution.)

The following series of computations then were performed for a range of configurations and the results were compared:

A. (1) Coarse Initialization

(2) Improved Initialization

(3) Residual Minimization

B: (1) Coarse Initialization

(3) Residual Minimization

C: (0) Initialization with True Configuration

(3) Residual Minimization

D: (0) Initialization with True Configuration

(2) Improved Initialization

(3) Residual Minimization

It is also of interest to see how well the initialization algorithms (1) and (2) approximate the true configuration, since if their performance were reliably good, the final step (3) might be an unnecessary refinement.

The configurations for which these tests were performed are shown in Figures 5.5-1 through 5.5-3. In each case, the BCAS aircraft and one intruder aircraft were assumed to be at fixed positions relative to a configuration of two radars. Results were then evaluated with a second intruder aircraft placed in a sequence of positions on a circle about the BCAS aircraft. At each position, the calculation was performed ten times, with a different set of simulated random measurement errors each time. A representative set of outputs for one configuration is shown in Figures 5.5-4a to 5.5-4c.

Qualitatively, the results were the following: Im most configurations, the final squared error minimization process converges to the proper solution, independent of what process is used to arrive at the starting approximation.

There are some configurations in which neither sequence A nor the sequence B for obtaining the starting approximations allowed

d_1 = 15 mi.

d_2 = 33.54 mi.

r_1 = 5 mi, H_1 = 22,000'

r_2 = 3 mi, H_2 = 18,000'

H_0 = 20,000'

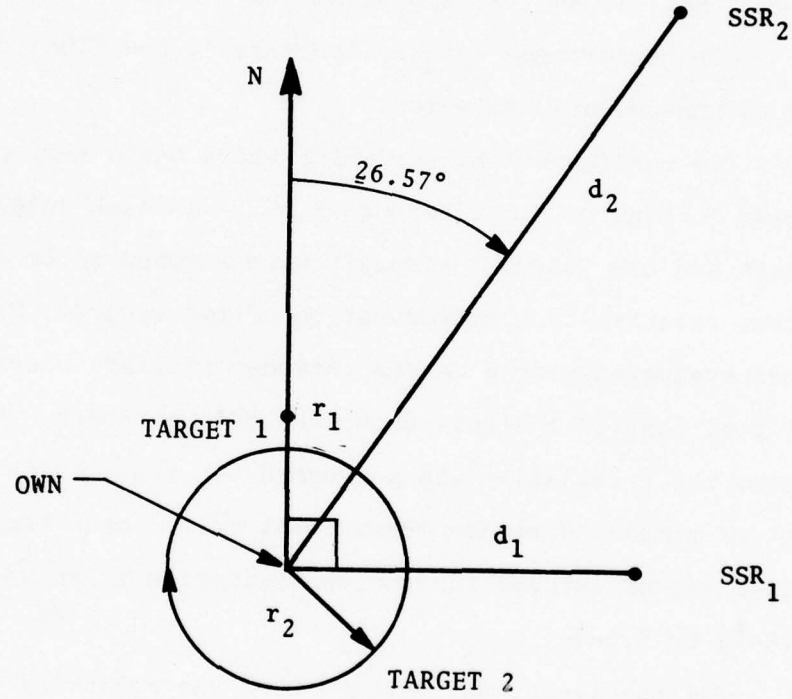

FIGURE 5.5-1. SIMULATED PATTERN 1.

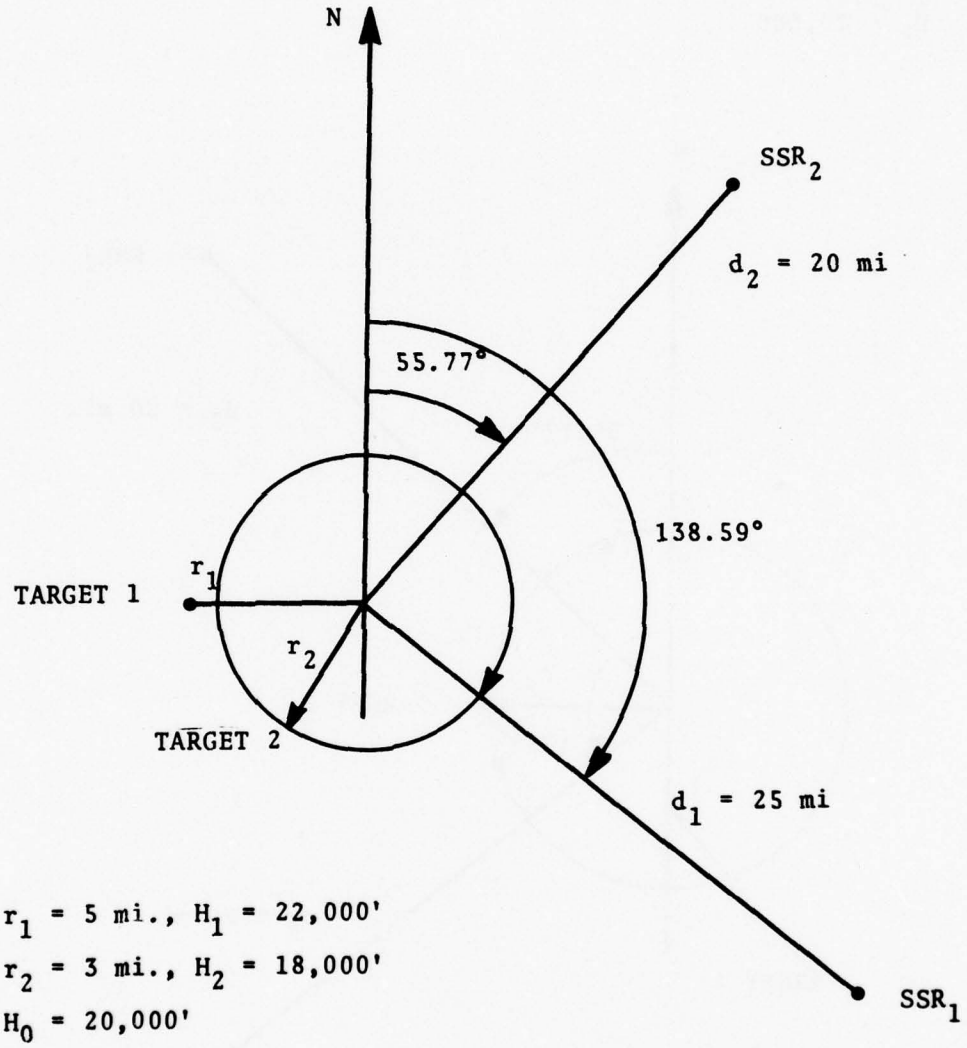

FIGURE 5.5-2. SIMULATED PATTERN 2.

r_1 = 3 mi., H_1 = 22,000'

r_2 = 5 mi., H_2 = 18,000'

H_0 = 20,000'

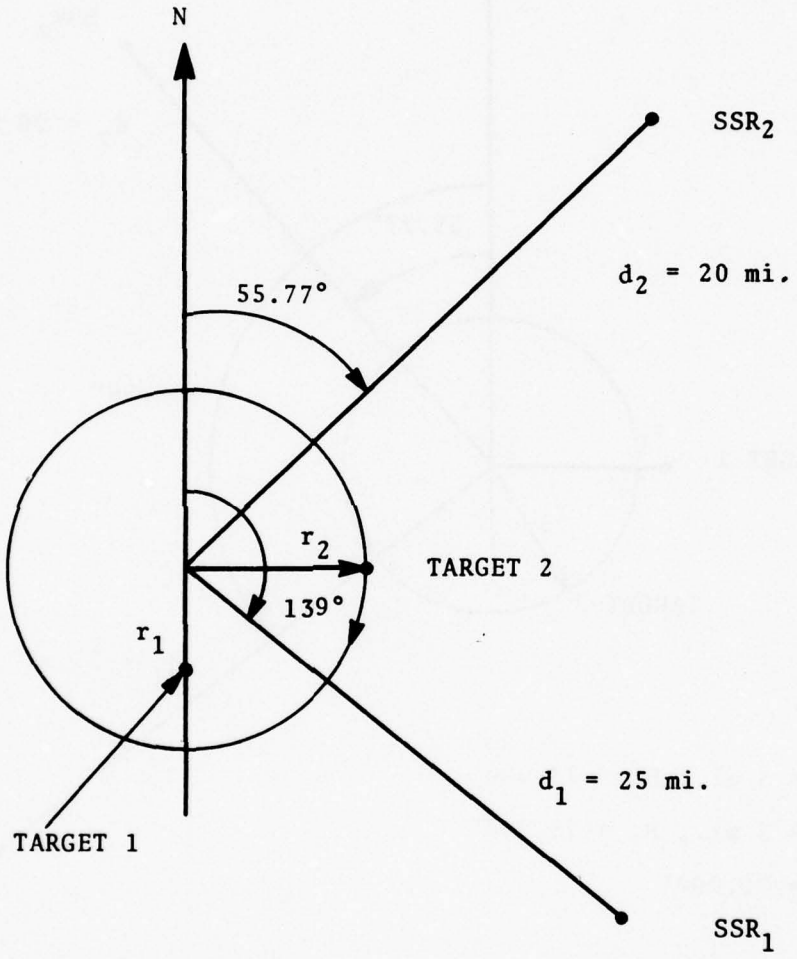

FIGURE 5.5-3. SIMULATED PATTERN 3.

TRUE CONFIGURATION

RADAR 1		RADAR 2		TARGET 1			TARGET 2			OWN
RANGE	BEARING	RANGE	BEARING	RANGE	BEARING	HEIGHT	RANGE	BEARING	HEIGHT	HEIGHT
29.28	138.59	28.28	55.77	3.282	-35.23	22888.	5.888	89.97	18888.	28888.

THERE ARE 12 SETS OF INPUT DATA PER CONFIGURATION

---ERRORS---

MODULES USED	RADAR 1 RANGE	RADAR 1 BEARING	RADAR 2 RANGE	RADAR 2 BEARING	TARGET 1 RANGE	TARGET 1 BEARING	TARGET 1 HEIGHT	TARGET 2 RANGE	TARGET 2 BEARING	TARGET 2 HEIGHT	OWN HEIGHT	# ITER COMPUT	# ITER LSQUAR	RESID
TC	-12566.	A1.82	3278.	-123.21	-311.	-184.56	26.	2229.	84.97	-36.	23.	9	0	0
TCL	-12559.	A1.82	3271.	-123.81	-311.	-184.56	26.	2229.	84.97	-36.	23.	9	1	0
T L	-94.	1.52	-928.	-1.91	14.	-2.17	25.	-1579.	-0.22	-36.	23.	8	4	5.89
IC	-12566.	A1.82	3278.	-123.21	-311.	-184.56	26.	2229.	84.97	-36.	23.	9	0	0
ICL	**********	**********	**********	4.24	**********	**********	185.	**********	**********	-118.	**********	9	28	**********
I	32893.	5.61	7273.	8.34	139.	-8.97	26.	11796.	14.44	-36.	23.	8	8	7523.44
I L	-95.	1.52	-928.	-1.91	14.	-2.17	25.	-1579.	-0.22	-36.	23.	8	7	5.89

---ERRORS---

MODULES USED	RADAR 1 RANGE	RADAR 1 BEARING	RADAR 2 RANGE	RADAR 2 BEARING	TARGET 1 RANGE	TARGET 1 BEARING	TARGET 1 HEIGHT	TARGET 2 RANGE	TARGET 2 BEARING	TARGET 2 HEIGHT	OWN HEIGHT	# ITER COMPUT	# ITER LSQUAR	RESID
TC	-2386.	-2.25	1828.	1.61	122.	1.99	-4.	34.	-1.35	-15.	-36.	5	0	78.41
TCL	-3381.	-1.81	1598.	-1.38	33.	-1.26	-4.	-348.	-8.47	-15.	-36.	5	4	8.18
T L	-3381.	-1.81	1598.	-1.38	33.	-1.26	-4.	-349.	-8.47	-15.	-36.	8	18	8.18
IC	-2386.	-2.25	1828.	1.61	122.	1.99	-4.	34.	-1.35	-15.	-36.	6	0	78.41
ICL	-3382.	-1.81	1598.	-1.38	33.	-1.26	-4.	-349.	-8.47	-15.	-36.	8	8	8.18
I	1346.	-8.52	1673.	8.46	149.	-8.47	-4.	4969.	4.98	-15.	-36.	8	8	692.98
I L	-3381.	-1.81	1598.	-1.38	33.	-1.26	-4.	-348.	-8.47	-15.	-36.	8	4	8.18

---ERRORS---

MODULES USED	RADAR 1 RANGE	RADAR 1 BEARING	RADAR 2 RANGE	RADAR 2 BEARING	TARGET 1 RANGE	TARGET 1 BEARING	TARGET 1 HEIGHT	TARGET 2 RANGE	TARGET 2 BEARING	TARGET 2 HEIGHT	OWN HEIGHT	# ITER COMPUT	# ITER LSQUAR	RESID
TC	-6243.	A8.99	1829.	-124.66	6298.	-185.39	18.	2337.	83.67	8.	43.	6	0	0
TCL	-6243.	88.99	1829.	-124.66	6298.	-185.39	18.	2337.	83.67	8.	43.	6	1	0
T L	-1787.	-2.81	182.	8.25	844.	8.32	18.	585.	-8.86	8.	43.	8	3	1.23
IC	-6243.	88.99	1829.	-124.66	6298.	-185.39	18.	2337.	83.67	8.	43.	6	0	0
ICL	**********	**********	**********	34.23	**********	**********	**********	**********	**********	**********	**********	6	28	**********
I	17391.	1.81	4831.	2.87	99.	1.88	18.	11588.	18.86	8.	43.	8	8	3893.73
I L	-1787.	-8.81	181.	8.25	844.	8.32	18.	584.	-8.86	8.	43.	8	5	1.23

---ERRORS---

MODULES USED	RADAR 1 RANGE	RADAR 1 BEARING	RADAR 2 RANGE	RADAR 2 BEARING	TARGET 1 RANGE	TARGET 1 BEARING	TARGET 1 HEIGHT	TARGET 2 RANGE	TARGET 2 BEARING	TARGET 2 HEIGHT	OWN HEIGHT	# ITER COMPUT	# ITER LSQUAR	RESID
TC	2788.	-1.53	-2636.	6.65	235.	7.89	-57.	-1618.	-3.25	38.	38.	6	0	724.28
TCL	249.	8.66	-1572.	8.11	1.	-8.38	-57.	-281.	8.54	38.	38.	6	5	1.83
T L	248.	8.66	-1571.	8.11	1.	-8.38	-57.	-288.	8.54	38.	38.	8	3	1.83
IC	2788.	-1.53	-2636.	6.65	235.	7.89	-57.	-1618.	-3.25	38.	38.	6	0	724.27
ICL	258.	8.66	-1571.	8.11	1.	-8.38	-57.	-288.	8.54	38.	38.	8	5	1.83
I	1164.	2.59	-3883.	1.89	183.	8.97	-57.	3634.	4.29	38.	38.	8	8	324.78
I L	258.	8.66	-1571.	8.11	1.	-8.38	-57.	-281.	8.54	38.	38.	8	4	1.83

---ERRORS---

MODULES USED	RADAR 1 RANGE	RADAR 1 BEARING	RADAR 2 RANGE	RADAR 2 BEARING	TARGET 1 RANGE	TARGET 1 BEARING	TARGET 1 HEIGHT	TARGET 2 RANGE	TARGET 2 BEARING	TARGET 2 HEIGHT	OWN HEIGHT	# ITER COMPUT	# ITER LSQUAR	RESID
TC	3365.	-3.98	363.	9.13	918.	11.16	-38.	2288.	-1.34	17.	-28.	8	0	493.49
TCL	392.	-1.29	2338.	8.73	49.	1.11	-38.	993.	8.19	17.	-28.	8	5	3.49
T L	391.	-1.29	2338.	8.73	49.	1.11	-38.	993.	8.18	17.	-28.	8	3	3.49
IC	3365.	-3.98	363.	9.13	918.	11.16	-38.	2288.	-1.34	17.	-28.	8	0	493.49
ICL	392.	-1.29	2338.	8.73	49.	1.11	-38.	993.	8.19	17.	-28.	8	5	3.49
I	-6172.	-2.42	-1795.	1.68	101.	1.28	-38.	2742.	8.94	17.	-28.	8	8	68.94
I L	391.	-1.29	2338.	8.73	49.	1.11	-38.	993.	8.15	17.	-28.	8	4	3.49

FIGURE 5.5-4a. SAMPLE OUTPUT OF SIMULATION RUN.

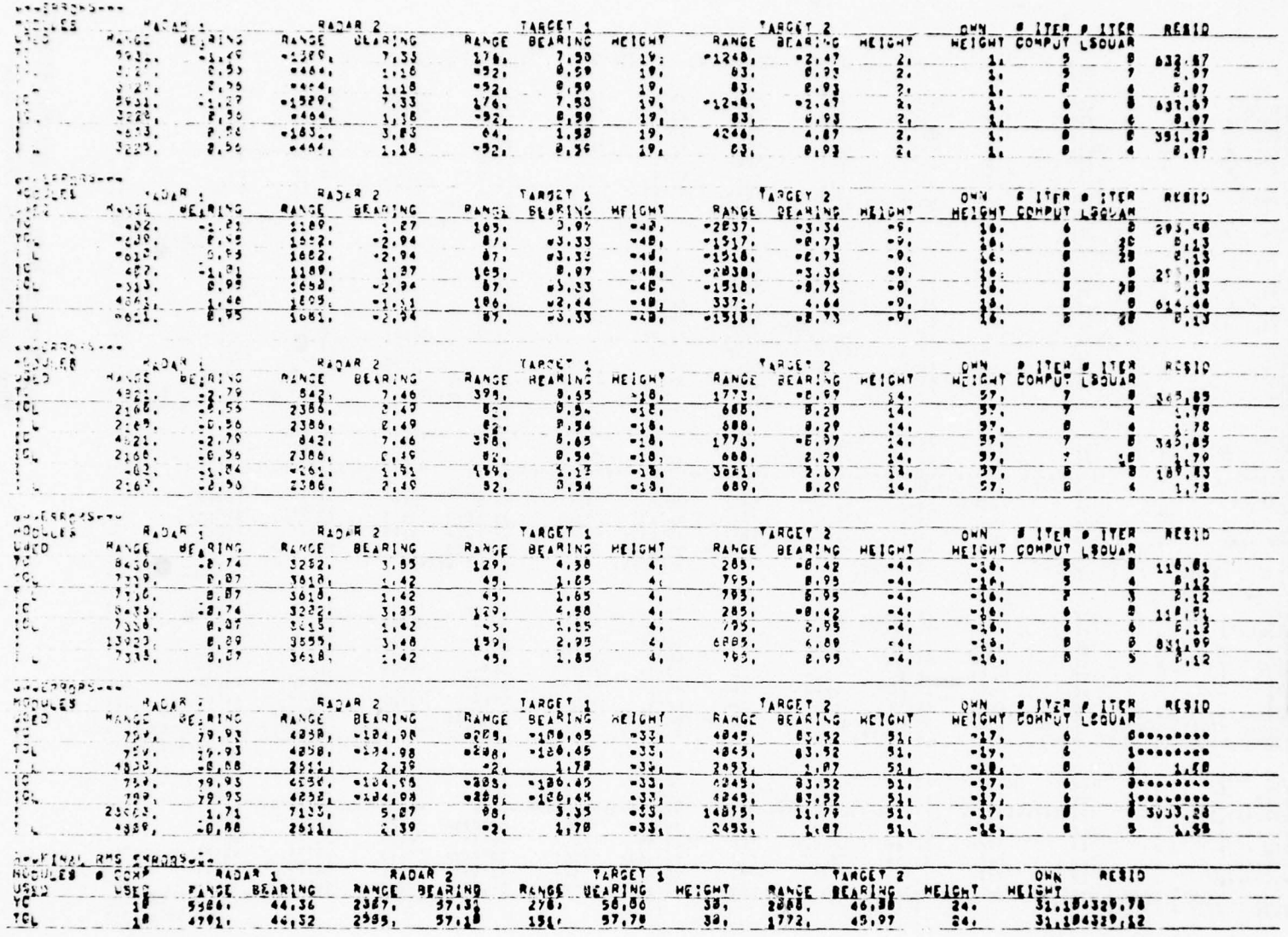

FIGURE 5.5-4b. SAMPLE OUTPUT OF SIMULATION RUN (CONTINUED).

FIGURE 5.5-4c. SAMPLE OUTPUT OF SIMULATION RUN (CONTINUED).

the final process to converge to a practically useful approximation of the actual configuration.

Overall, the final process is most likely to converge when it begins at the approximate solution derived by the initial coarse approximation followed by the iterative improvement (sequence A). However, the situation does occur that the final squared-error minimization procedure converges to the proper solution when starting from the initial "coarse" approximation, but not from the configuration obtained by the iterative "improvement" (sequence B).

Solutions were attempted at 216 different configurations of radars and targets. Ten sets of noisy measurements were simulated at each position. In 106 of these configurations, the final squared error minimization process converged to the proper solution every time, regardless of whether the initial coarse approximation or the iteratively improved approximation were used as starting points. In 159 configurations, the proper solution was obtained every time if the better of the two possible initializations were selected.

If the success rate is calculated over the total number of trials - 216 positions with 10 sets of simulated noisy measurements at each - the following percentages are obtained:

- Successful Convergence with either Initialization (A and B) 68.9%
- Successful Convergence only with First Initialization (B, not A) 5.8%
- Successful Convergence Only with Iteratively Improved Initialization (A, not B) 7.6%

- No Convergence with Either Initialization (Neither A nor B) 17.7%

The squared error minimization process (3) converged when the actual configuration was used as the initialization more than with any other initialization (though this does not imply that the solution found was always a good approximation to the actual configuration). There were also configurations in which the sequences involving step (2), the iterative improvement of the initialization (i.e., sequences A and D) diverged, whereas all other sequences converged. These observations indicate that the heuristically derived initialization algorithms could possibly be improved. On the whole, however, the initialization algorithms tend to fail in what are inherently bad ranges for the system of equations - that is, configurations in which the situation is inherently highly sensitive to measurement errors. Hence, improvement in the initialization procedures would not necessarily lead to significantly improved system performance.

The approximate configurations computed by the initialization schemes on the average are considerably farther from the true configurations than the configurations computed by the final step which minimizes the residual. Hence, the initialization algorithms by themselves do not give results indicative of how well the configuration can be determined from the measurements. The values that they, by themselves, determine should not be used for target tracking.

5.6 OVERALL ASSESSMENT OF THE SYSTEM WITHOUT AZIMUTH REFERENCE SIGNALS

The accuracy of the target range and bearing calculations that can be obtained from the BCAS measurements based on radars without azimuth reference signals can be judged from the results of the simulations shown in Section 6.

As in the case of radars with azimuth reference signals, there are ranges of configurations in which good solutions can not be obtained. These configurations include the following:

(1) when the two radars are colinear when viewed from the BCAS

(2) when either of the target aircraft is in between the BCAS and one of the radars

(3) when the BCAS is directly between either target aircraft and one of the radars

(4) when the BCAS aircraft and both target aircraft are in a line.

The extent of each band range is a function of the total configuration.

6. SIMULATION

6.1 SIMULATION TECHNIQUE

The various algorithms for determining radar and target range and bearing from own on the basis of the BCAS measurements were tested in a series of digital computer simulations.

In principle, all the simulations contained the following steps. A configuration of radars and own and target aircraft was assumed. The TOA's, DAZ's, and OAZ's that the BCAS would measure in such a configuration in the absence of noise and other sources of error (such as quantization effects) were computed. Random numbers were generated to represent the various error sources and were added to the "perfect measurements". The resulting "noise-corrupted measurements" were then used as inputs to the computational algorithms, which used them to derive the positions of the radars and targets relative to OWN. The results of these computations were compared with the originally assumed configuration to find the errors.

The random error terms added to the measurements were drawn from normal distributions with variances chosen to match the variances of the corresponding measurements, as determined during the test flights. Where angular measurements have correlated errors, the random error terms in the simulations reflected this.

The errors introduced were the following:

TOA: Normally distributed error, mean zero, standard deviation 0.15 microseconds, independent for each measurement.

Altitudes: Normally distributed error, mean zero, standard deviation 30 ft., independent for each measurement. (This is probably not a good way to model altitude errors; however, the computed results were quite insensitive to altitude errors, so that the faults of the model are not important.)

Azimuth measurements: The measurement error is due to the incorrect determination of the beam center position from the bursts of pulses received when the beam is pointed at OWN, at OTHER, or in an azimuth reference direction. The errors were modeled as zero-mean, normally distributed, random components with standard deviation of 0.2° in each measurement of direction. This leads to DAZ and OAZ errors with standard deviations of 0.3° and the proper mutual correlation.

Although the simulations were set up in such a way that one or more of the aircraft were placed at consecutive positions of what might be flight trajectories, the calculations at each position were carried out completely independent of each other. The purpose of the simulations was to determine how well the BCAS measurements at a single point could determine the aircraft configuration. An actual operational system should do better since it would smooth the data, i.e., combine the measurements at a given instant with previous measurements

in such a way as to give a better estimate of the true position. The simulation in each case used the minimum number of measurements to determine the configuration. Again, an operational system might frequently do better, using more than the minimum number of radars to track a target aircraft, or basing calculations of radar position on more than the minimum number of tracked targets.

Since the simulations were strictly for static position calculations rather than for dynamic computation of aircraft tracks, one complicating factor with regard to the measurements was neglected. It was assumed that the measurements, subject to the errors discussed, were available at the nominal times. In the actual BCAS environment, the measurements are made at times determined by the asynchronous rotation of the locked radars, i.e., roughly every four seconds for the short-range SSR's. Thus, when the measurements from one radar are received, those from the other may be up to about four seconds old. An operational system would have to include some mechanism for taking the differences in measurement times into account. Experience with test data (see Section 7) indicates that the effect of the asynchronous measurement times is minor. Therefore, the results of the static simulation should not be significantly affected by omitting this factor from consideration.

6.2 THE SITUATIONS SIMULATED

The purpose of the simulations was to test quantitatively the accuracy of the BCAS range-bearing calculating algorithms for the cases with and without SSR azimuth reference signals.

A succession of configurations with two radars, a BCAS aircraft, and two target aircraft were set up and the "noise-free measurements" of TOA, DAZ and OAZ were calculated. To this set of "measurements" appropriate "noise" terms were added to create a set of "noisy measurements". Each algorithm then used the appropriate subset of these "noisy measurements" to compute the range and bearing from OWN of the target aircraft and the radars. The errors of the resulting solutions were computed by comparing the solutions obtained with the configuration initially assumed.

The calculations using azimuth reference pulses from two radars were carried out for each target aircraft separately. The calculations using the "no azimuth reference" solution were carried out for the configuration as a whole. Two different situations were assumed for this case. These were (1) partial equipage of radars with azimuth reference signals and (2) no azimuth reference signals from any ground radars.

For the first situation, it is assumed that in each radar coverage region, one SSR is equipped with azimuth reference

signals. Then, once the BCAS has computed the relative directions of the radars and target aircraft, it can use the directly measured direction to this one radar to properly orient the whole configuration.

For the second situation, it is assumed that the BCAS computes the shape of the configuration, but has no direct way of establishing its orientation. This can be done only in a dynamic situation when the BCAS is flying in a known direction and computing the shape of the configuration at successive points along its path. The distance between the two SSR's and the direction from one SSR to the other do not change with time. In concept, the BCAS can then determine its own position relative to this fixed line at a number of successive points in time. The angle between the fixed line between the radars and the line determined by the successive positions of the BCAS aircraft (which lies along the known flight direction) can then be determined and used to orient the whole configuration of radars and aircraft.

For the first of these two situations, the measures of accuracy for the computed results are the RMS errors in range and bearing to the radars and the other aircraft. For the second situation, the range errors are inherently the same as for the first. The bearing errors are computed relative to the line connecting the radars, which is assumed known.

6.3 SIMULATION RESULTS

The patterns of simulated configurations of radars and aircraft are shown in Figures 6.3-1 to 6.3-4. The aircraft were placed at successive positions of their "tracks" as though they were moving in straight lines at a constant speed. In all but the final pattern, there was a "near miss" between the BCAS and Target 1.

Figures 6.3-5 to 6.3-38 show the errors in the computed range and bearing values, that is, the differences between the computed and true values. All points that would have been outside the limits of the plots (in either direction) are shown below the horizontal axis. These may be regarded as "wild" points in the results.

All the values of a given variable which were computed by different techniques are shown on the same plot, indicated by different symbols. It is to be noted that when radar distances were computed using the azimuth reference signals from both radars, a separate calculation was carried out for each target. The results are shown separately. The radar bearings for this case are then merely the simulated measurement errors.

The bearing errors shown for the computations based on no azimuth reference signals are calculated relative to the line connecting the radars.

When one radar only is assumed to have azimuth reference signals, it is always radar 1.

Pattern 1

For Pattern 1 (Figure 6.3-1 and Figures 6.3-5 to 6.3-12), the initial configurations allow accurate computations of most variables by all the computational schemes. In some cases, the no-azimuth-reference algorithm fails to converge because of bad initialization. This occurs because the BCAS is almost directly between radar 2 and target 1. Where the algorithm overcomes this difficulty, the computed results are very accurate.

The final configurations are generally unfavorable to accurate computation, largely because target 1 comes between the BCAS and both target 2 and radar 2.

The computations of distance to radar 2 are bad throughout because the differential azimuths of both targets with respect to radar 2 are consistently small.

The bearing errors are seen to be large for the no-azimuth-reference system and quite acceptable with two radars with azimuth references. The results for the system with one azimuth reference signal are intermediate.

Pattern 2

For Pattern 2, good solutions are found by all systems in all but three limited conditions.

The initial configuration is such that radar 1 is very close to the BCAS and between the BCAS and target 1. BCAS operation in such a configuration is not anticipated. All systems fail to compute the configuration.

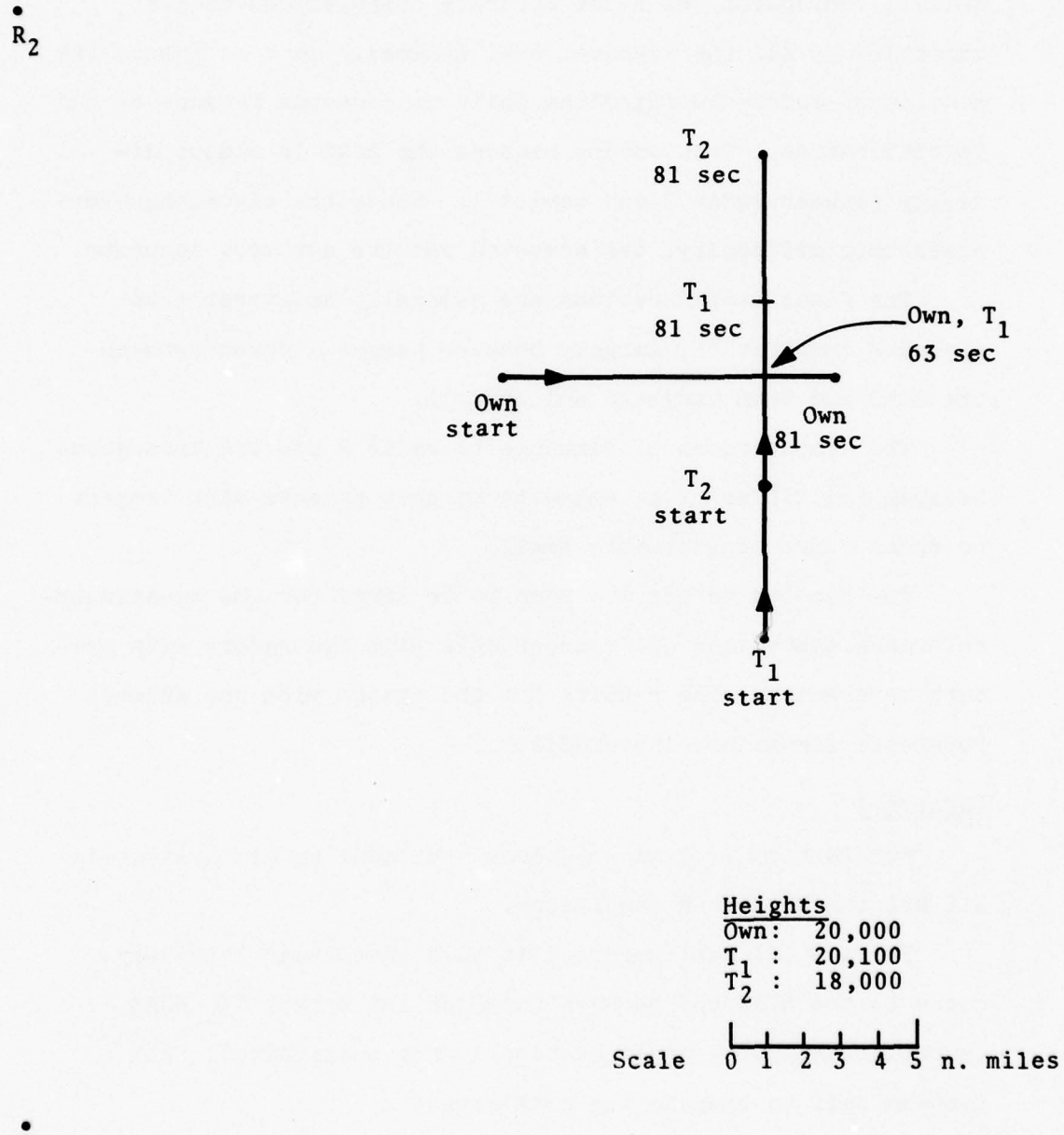

FIGURE 6.3-1. SIMULATED PATTERN 1.

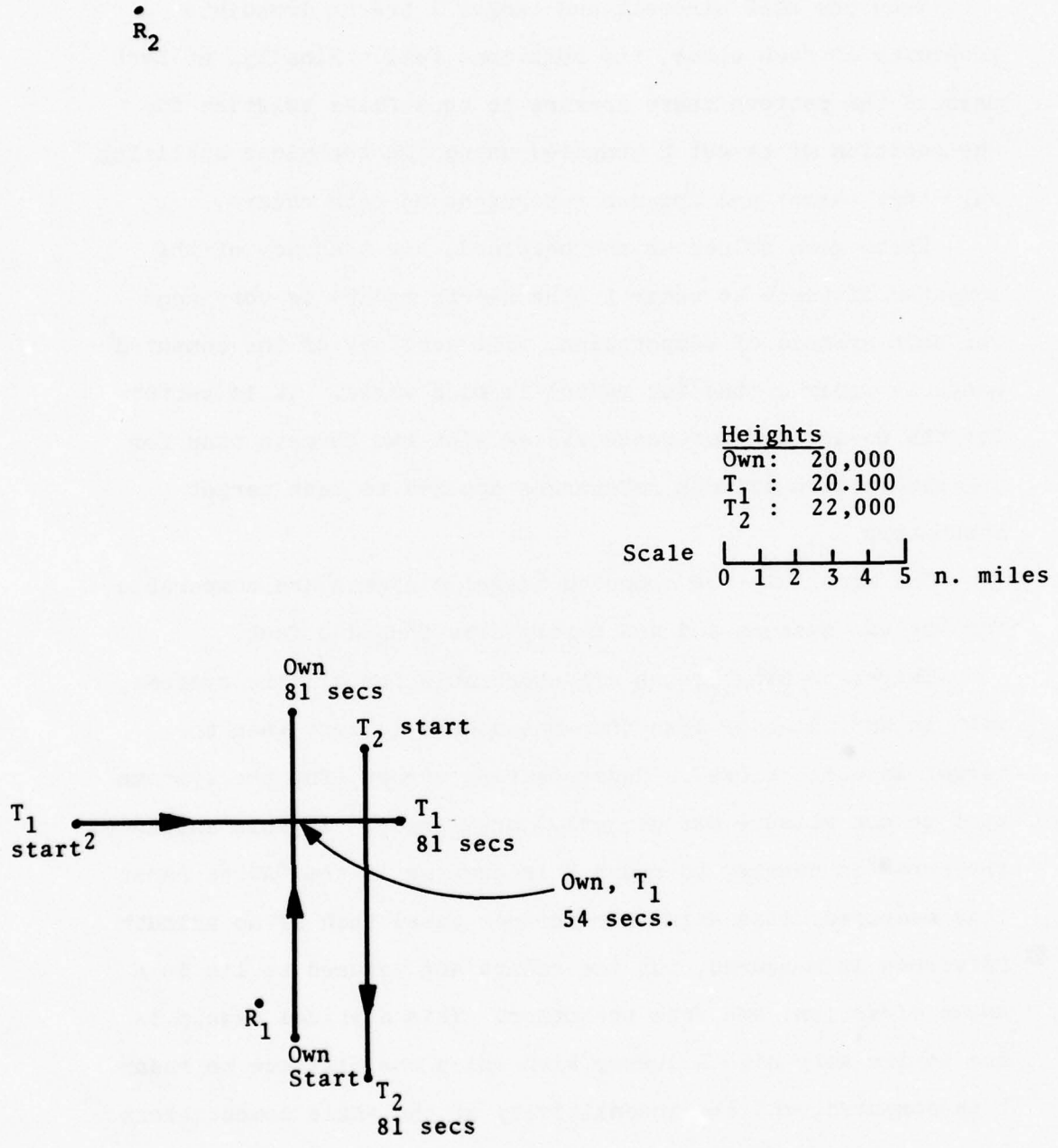

FIGURE 6.3-2. SIMULATED PATTERN 2.

When the BCAS aircraft and target 1 are in immediate proximity of each other, the solutions fail. Finally, at both ends of the pattern there appears to be a false solution for the position of target 2 computed using the technique utilizing only that target and azimuth references on both radars.

Where good solutions are obtained, the accuracy of the computed distance to radar 1 (the nearby radar) is very good for both systems of computation. The accuracy of the computed range to radar 2 (the far radar) is much worse. It is better for the no-azimuth-reference system with two targets than for the system with azimuth references applied to each target separately.

The errors in the computed target distance are comparable for the two systems and are mostly less than 200 feet.

Target-bearing errors are comparable for all the systems, with an RMS value of less than one degree (except when the target is quite close). Radar-bearing errors (for the systems that do not measure OAZ directly) are larger. In this instance, the error in bearing to radar 2 is greater if the OAZ to radar 1 is measured, (one azimuth reference case) than if no azimuth reference is measured, but the radars are assumed to lie in a known direction, one from the other. This atypical result is due to the very high accuracy with which the distance to radar 1 is computed, and the insensitivity of the angle computations to the distance to radar 2.

Pattern 3

For the configurations that constitute pattern 3, the algorithm depending on azimuth reference signals from both radars converges to a satisfactory solution almost everywhere. The exceptions are two individual points near the beginning, when the calculations involving target 1 fail to converge. It must be noted that in these instances BCAS, the target, and radar 1 are at the vertices of an approximately equilateral triangle - a configuration that violates the assumptions about the nature of the solutions that are to be sought.

It may also be noted that at about the point of nearest approach (at the time of the near miss), the computed target bearing and radar distance values have large errors, but the target distance does not.

In contrast, it may be noted that the no-azimuth-reference solutions for the configurations near the beginning of the pattern show large errors in the computed distance to target 1, while the other computed quantities do not have exceptionally large errors. This example illustrates the rather subtle nature of the "bad ranges" that may be encountered in solving for the shape of the configuration in the absence of azimuth reference signals. All the solutions obtained are correct in the sense that the computed residuals show that they fit the measurements quite closely. The great error sensitivity seems to arise from the circumstance that, when viewed from the BCAS, both targets (in direction) lie between the radars, 33° and 46° from the radars. When these angles become slightly larger, the error sensitivity of the solution disappears.

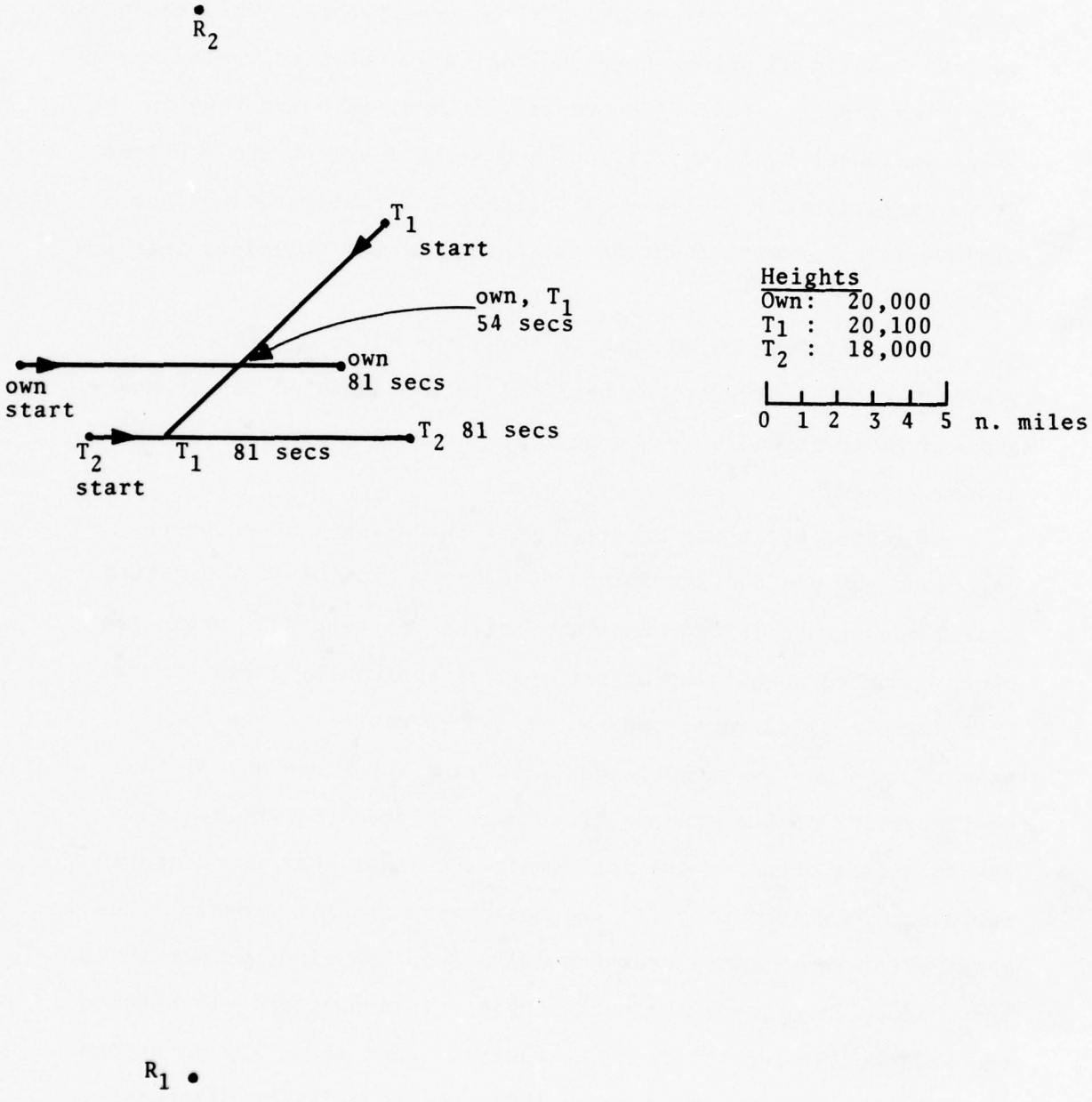

FIGURE 6.3-3. SIMULATED PATTERN 3.

The range errors to both targets become approximately 200 feet RMS.

Pattern 4

Pattern 4 illustrates the case of an alternate solution being found by the technique relying on both radars being equipped with azimuth reference signals. The false solution is consistently found for target 2 from the 34th sampling point on. The smoothness and continuity of the false track is evident in the error plot for the computed distance to radar 1 (Figure 6.3-29), and the distance and bearing to the target on the plots for which the scale has been compressed (Figures 6.3-33 and 6.3-38).

The other effects seen for this pattern that merit comment are:

The differential azimuth measurements relative to radar 2 are small for both targets. Correspondingly, the errors in the computed distance to radar 2 are large. This has the further effect of making the error in the computed bearing of this radar (for the no-azimuth-reference and one-azimuth-reference cases) large.

For the later configurations in the pattern, both targets are approximately between the BCAS and radar 1. In these configurations, the no-azimuth-reference solution has very large errors in computed range. The bearing errors appear to have a somewhat narrower bad range.

In the same set of configurations, the 2-azimuth-reference solution for target 1 is also bad, again because target 1 is between the BCAS and the radar.

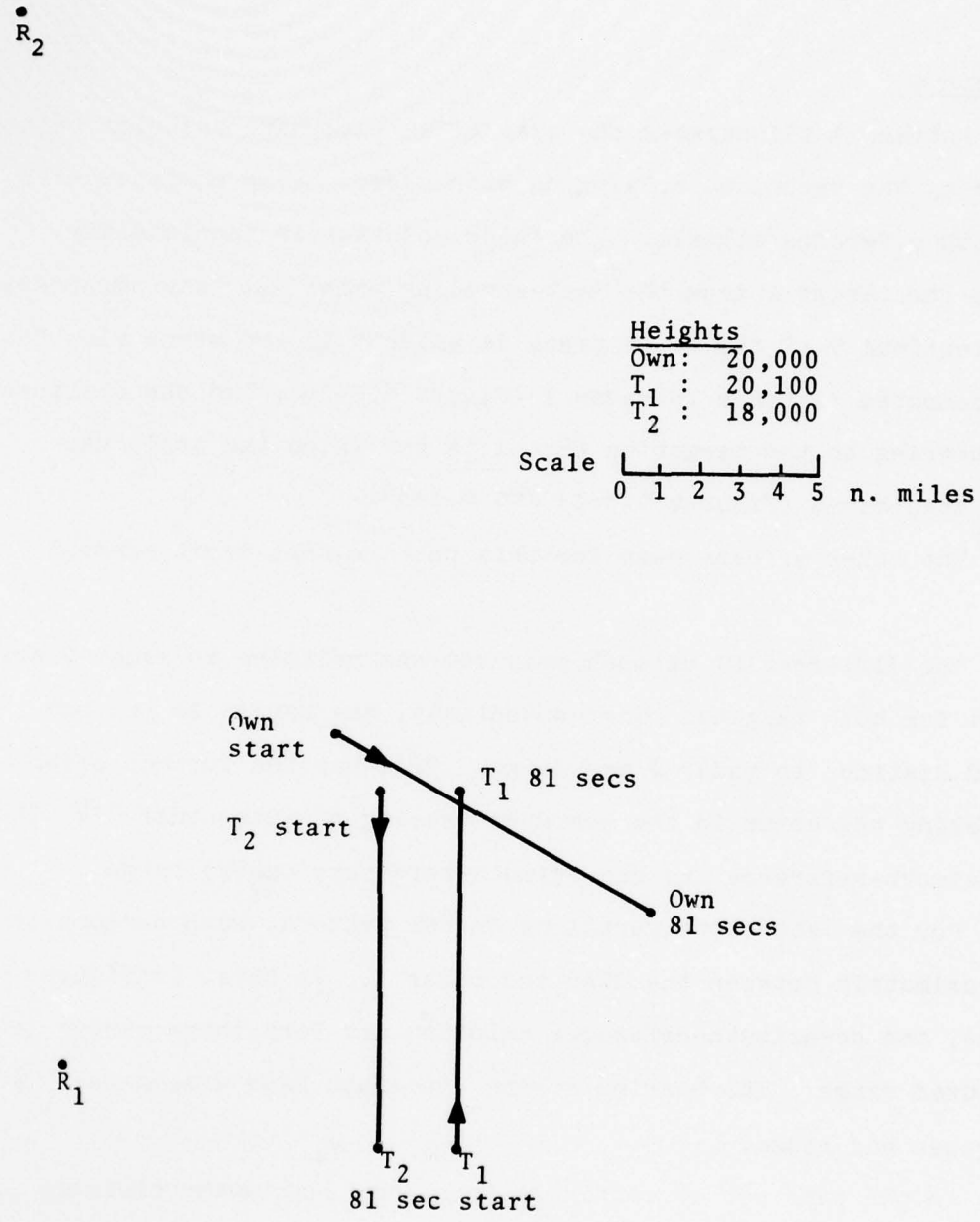

FIGURE 6.3-4. SIMULATED PATTERN 4.

FIGURE 6.3-5 TO FIGURE 6.3-38 POSITION ERRORS COMPUTED IN SIMULATION

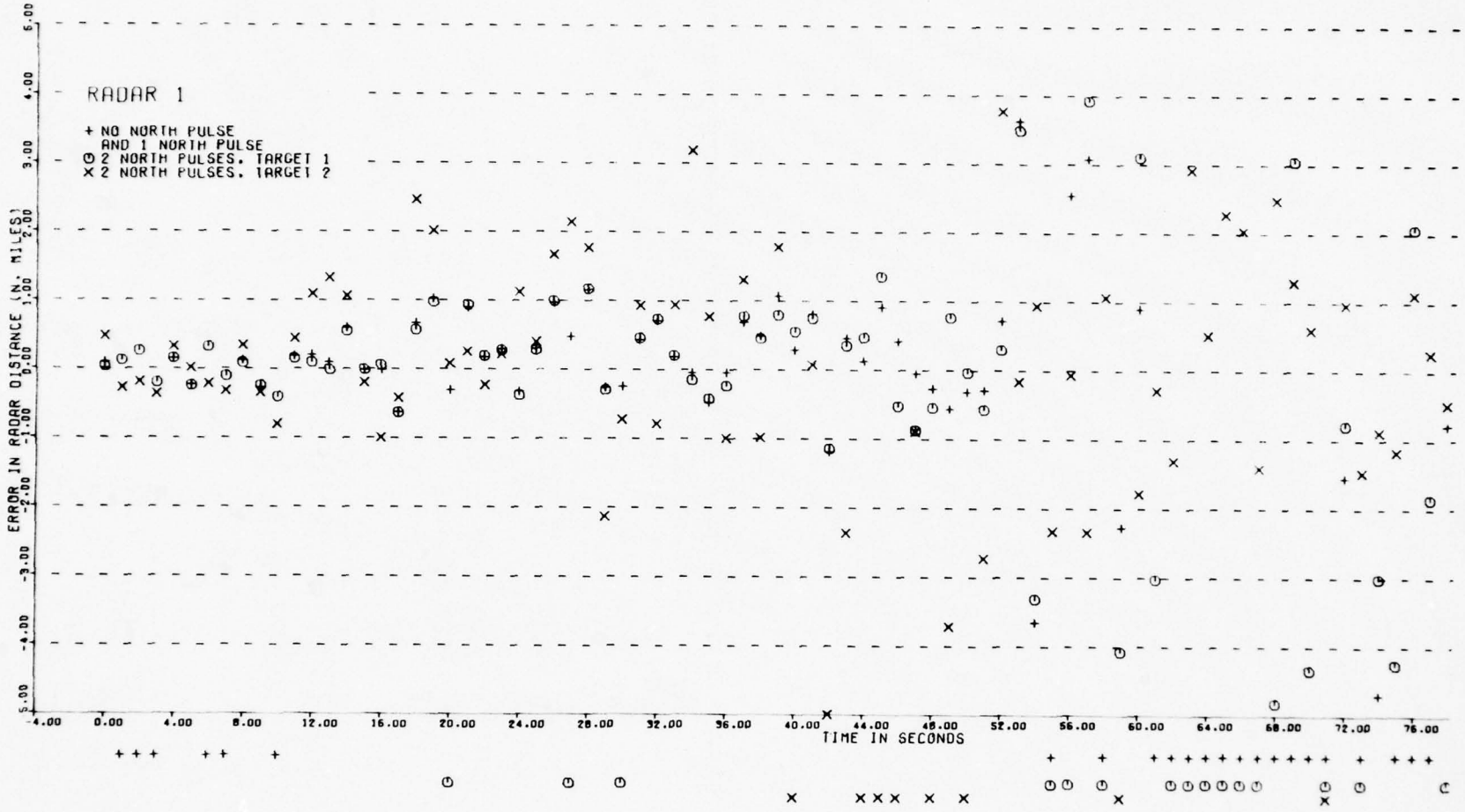
RADAR 1
+ NO NORTH PULSE
AND 1 NORTH PULSE
⊙ 2 NORTH PULSES. TARGET 1
× 2 NORTH PULSES. TARGET 2
ERROR IN RADAR DISTANCE (N. MILES)
6.00
4.00
3.00
2.00
1.00
0.00
-1.00
-2.00
-3.00
-4.00
-5.00
-4.00
0.00
4.00
8.00
12.00
16.00
20.00
24.00
28.00
32.00
36.00
40.00
44.00
48.00
52.00
56.00
60.00
64.00
68.00
72.00
76.00
TIME IN SECONDS

FIGURE 6.3-5.

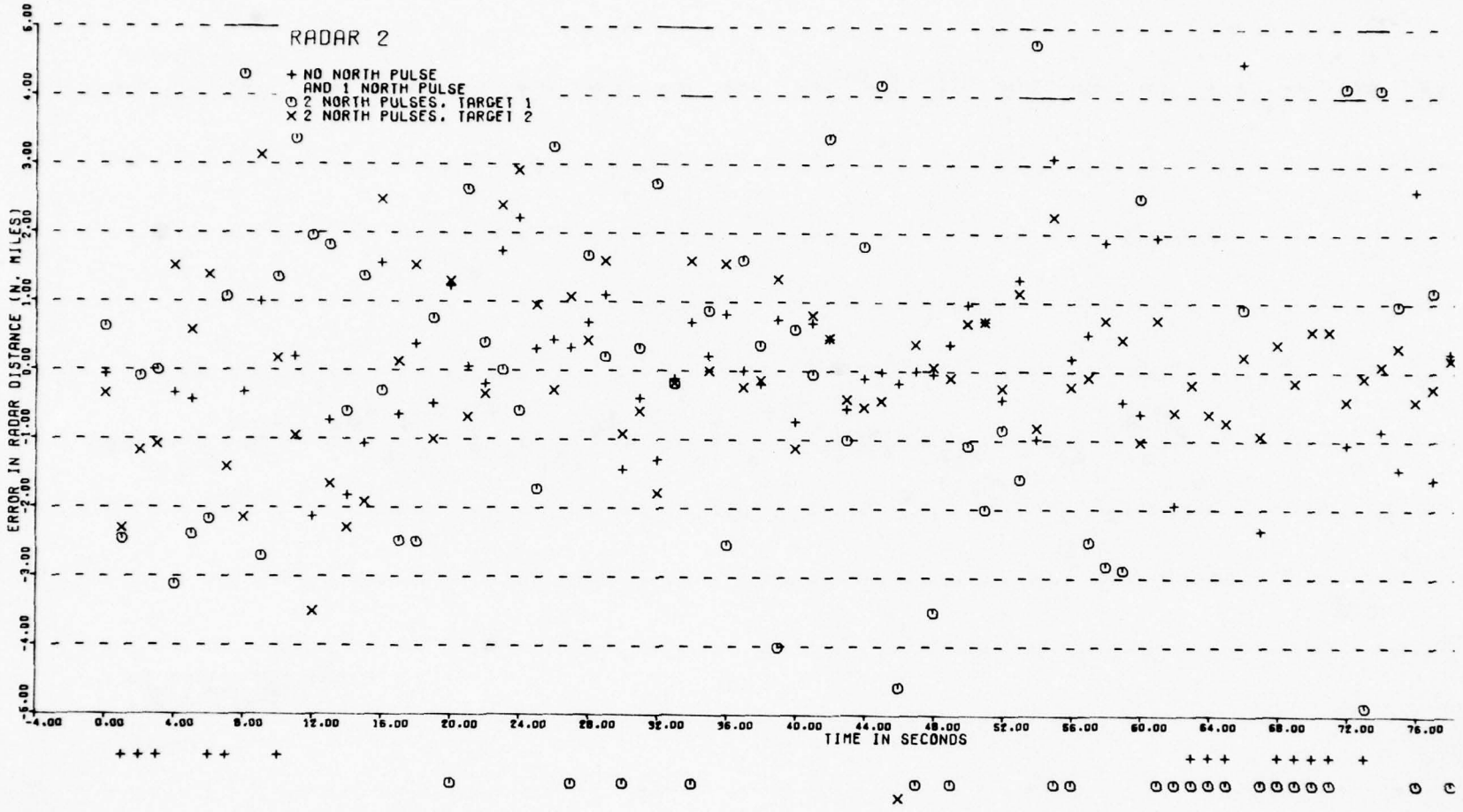
RADAR 2
+ NO NORTH PULSE
AND 1 NORTH PULSE
⊙ 2 NORTH PULSES, TARGET 1
× 2 NORTH PULSES, TARGET 2
ERROR IN RADAR DISTANCE (N. MILES)
6.00
4.00
3.00
2.00
1.00
0.00
-1.00
-2.00
-3.00
-4.00
-5.00
-4.00
0.00
4.00
8.00
12.00
16.00
20.00
24.00
28.00
32.00
36.00
40.00
44.00
48.00
52.00
56.00
60.00
64.00
68.00
72.00
76.00
TIME IN SECONDS

FIGURE 6.3-6.

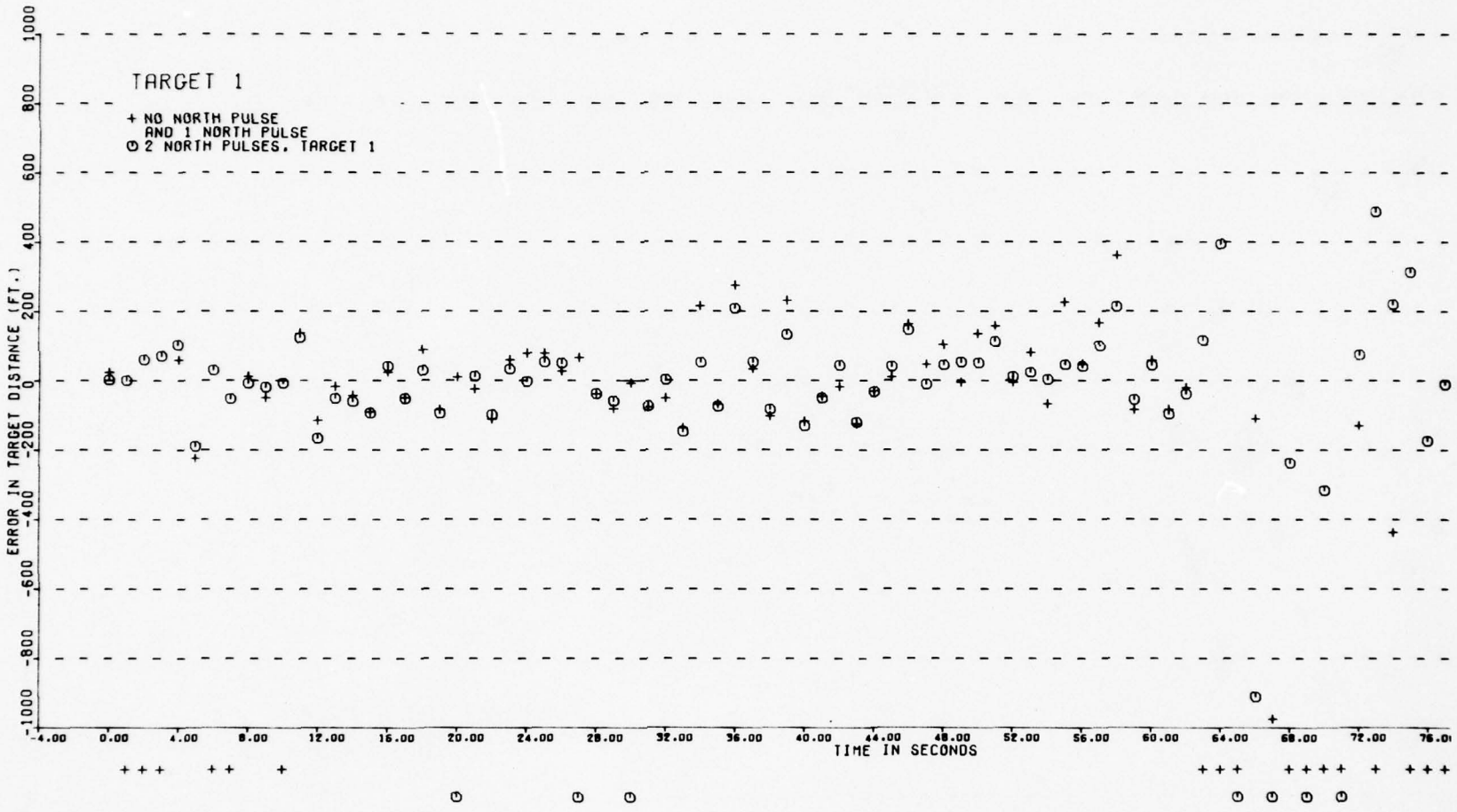
TARGET 1
+ NO NORTH PULSE
AND 1 NORTH PULSE
⊙ 2 NORTH PULSES, TARGET 1
ERROR IN TARGET DISTANCE (FT.)
1000
800
600
400
200
0
-200
-400
-600
-800
-1000
-4.00
0.00
4.00
8.00
12.00
16.00
20.00
24.00
28.00
32.00
36.00
40.00
44.00
48.00
52.00
56.00
60.00
64.00
68.00
72.00
TIME IN SECONDS

FIGURE 6.3-7.

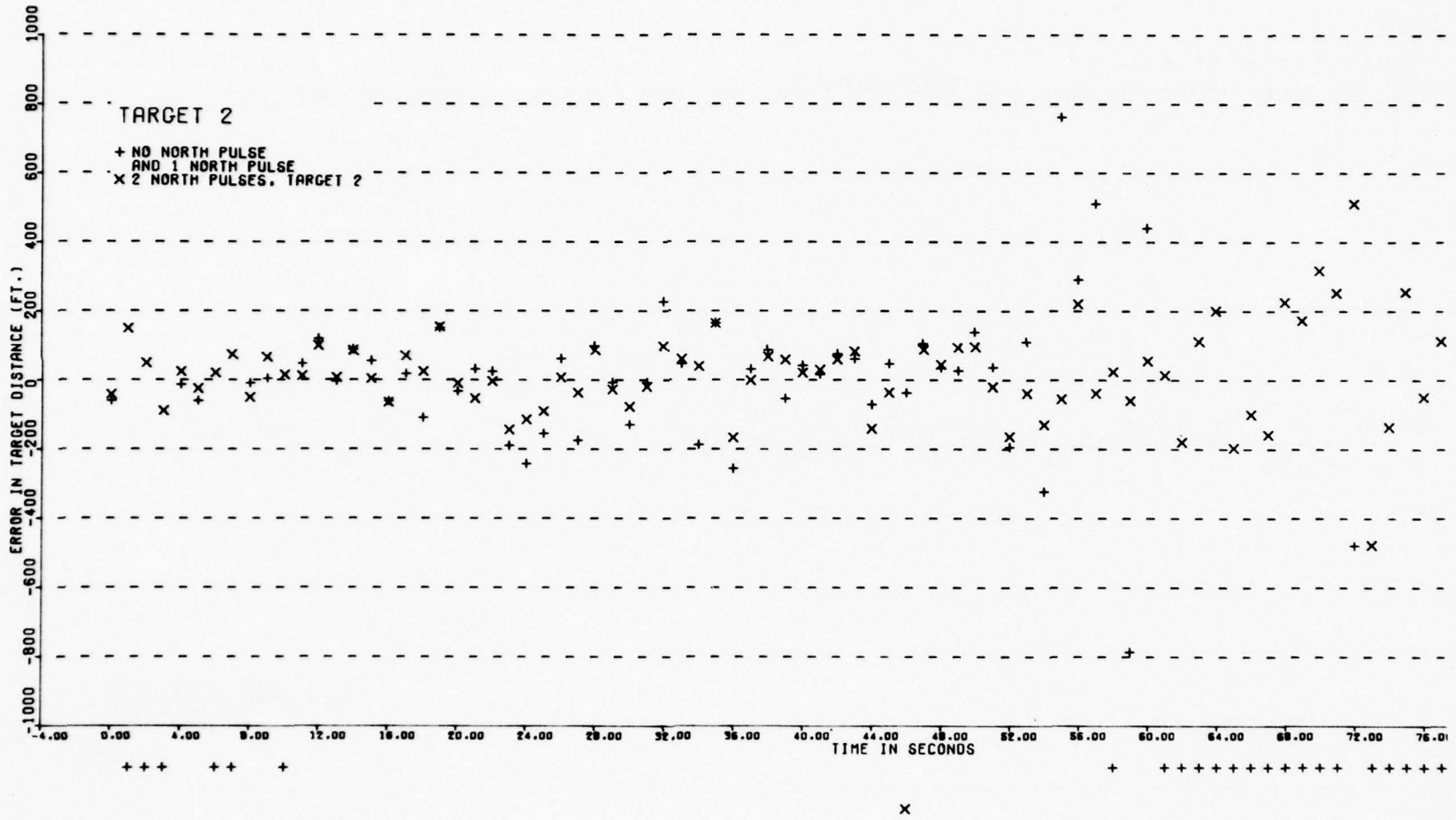
TARGET 2
+ NO NORTH PULSE
AND 1 NORTH PULSE
× 2 NORTH PULSES. TARGET 2
ERROR IN TARGET DISTANCE (FT.)
1000
800
600
400
200
0
-200
-400
-600
-800
-1000
-4.00
0.00
4.00
8.00
12.00
16.00
20.00
24.00
28.00
32.00
36.00
40.00
44.00
48.00
52.00
56.00
60.00
64.00
68.00
72.00
TIME IN SECONDS

FIGURE 6.3-8

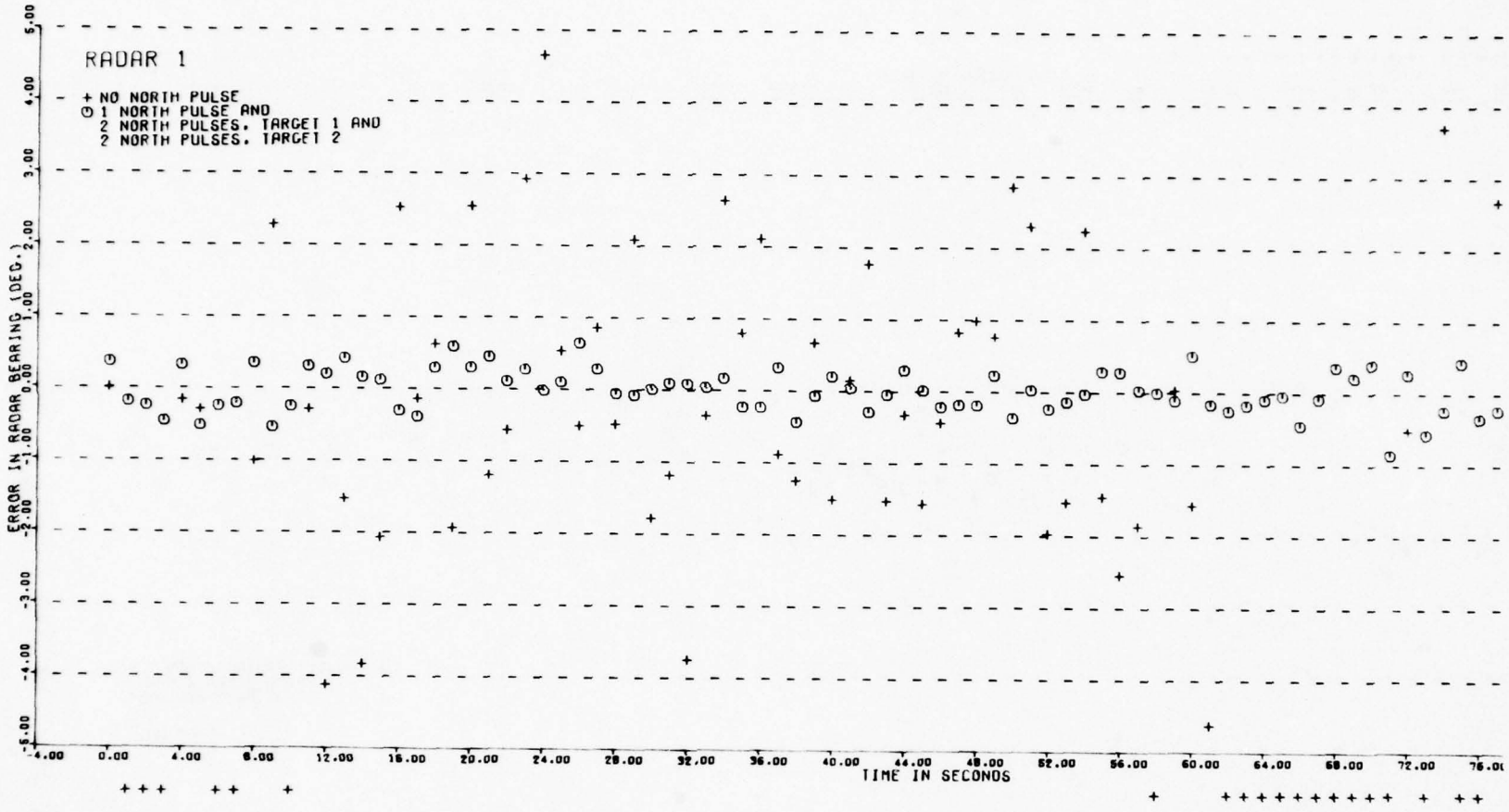
RADAR 1
+ NO NORTH PULSE
⊙ 1 NORTH PULSE AND
2 NORTH PULSES. TARGET 1 AND
2 NORTH PULSES. TARGET 2
ERROR IN RADAR BEARING (DEG.)
5.00
4.00
3.00
2.00
1.00
0.00
-1.00
-2.00
-3.00
-4.00
-5.00
-4.00
0.00
4.00
8.00
12.00
16.00
20.00
24.00
28.00
32.00
36.00
40.00
44.00
48.00
52.00
56.00
60.00
64.00
68.00
72.00
TIME IN SECONDS

FIGURE 6.3-9.

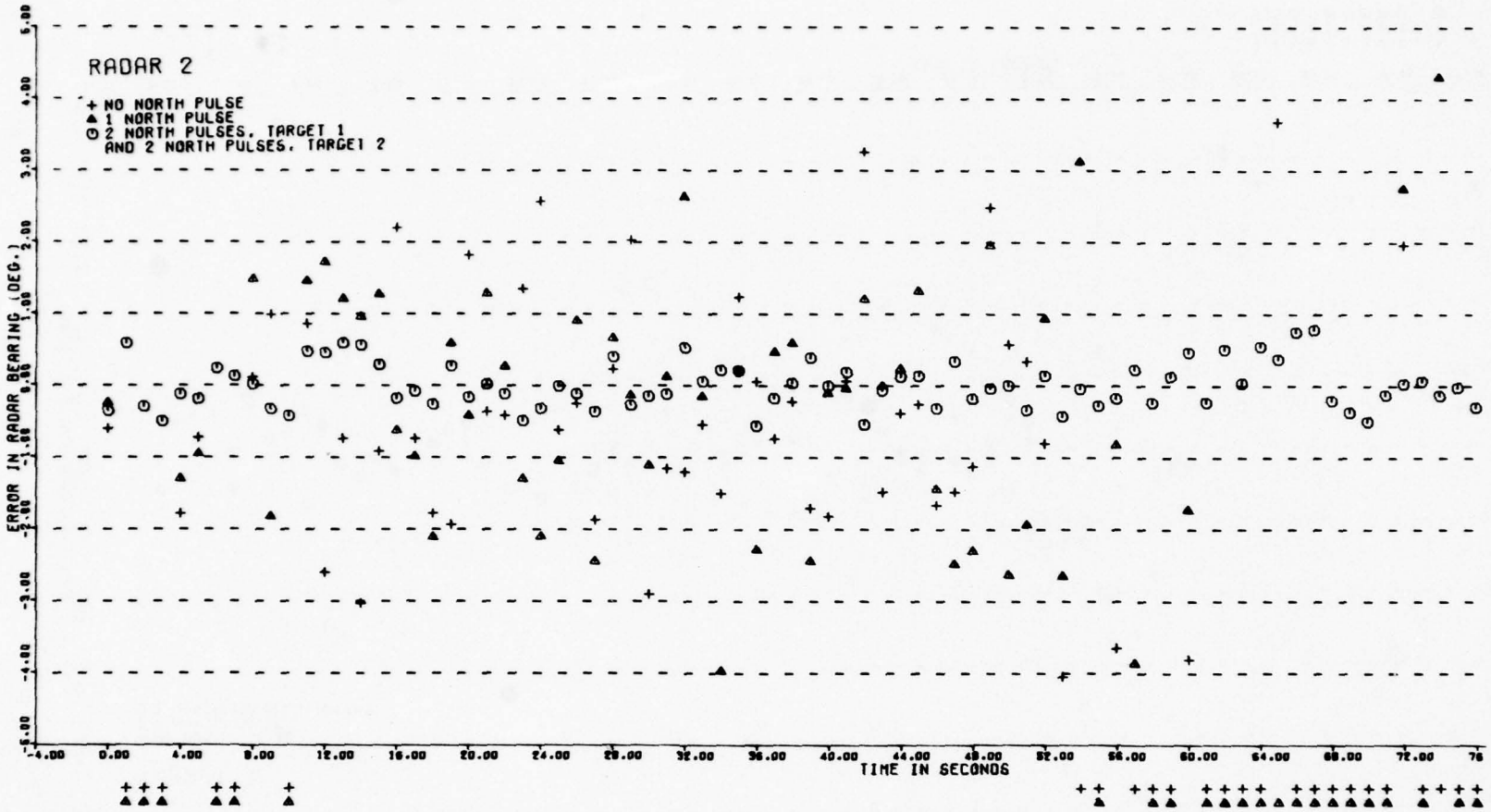
RADAR 2
+ NO NORTH PULSE
▲ 1 NORTH PULSE
Ⓣ 2 NORTH PULSES, TARGET 1
AND 2 NORTH PULSES, TARGET 2
ERROR IN RADAR BEARING (DEG.)
TIME IN SECONDS

FIGURE 6.3-10.

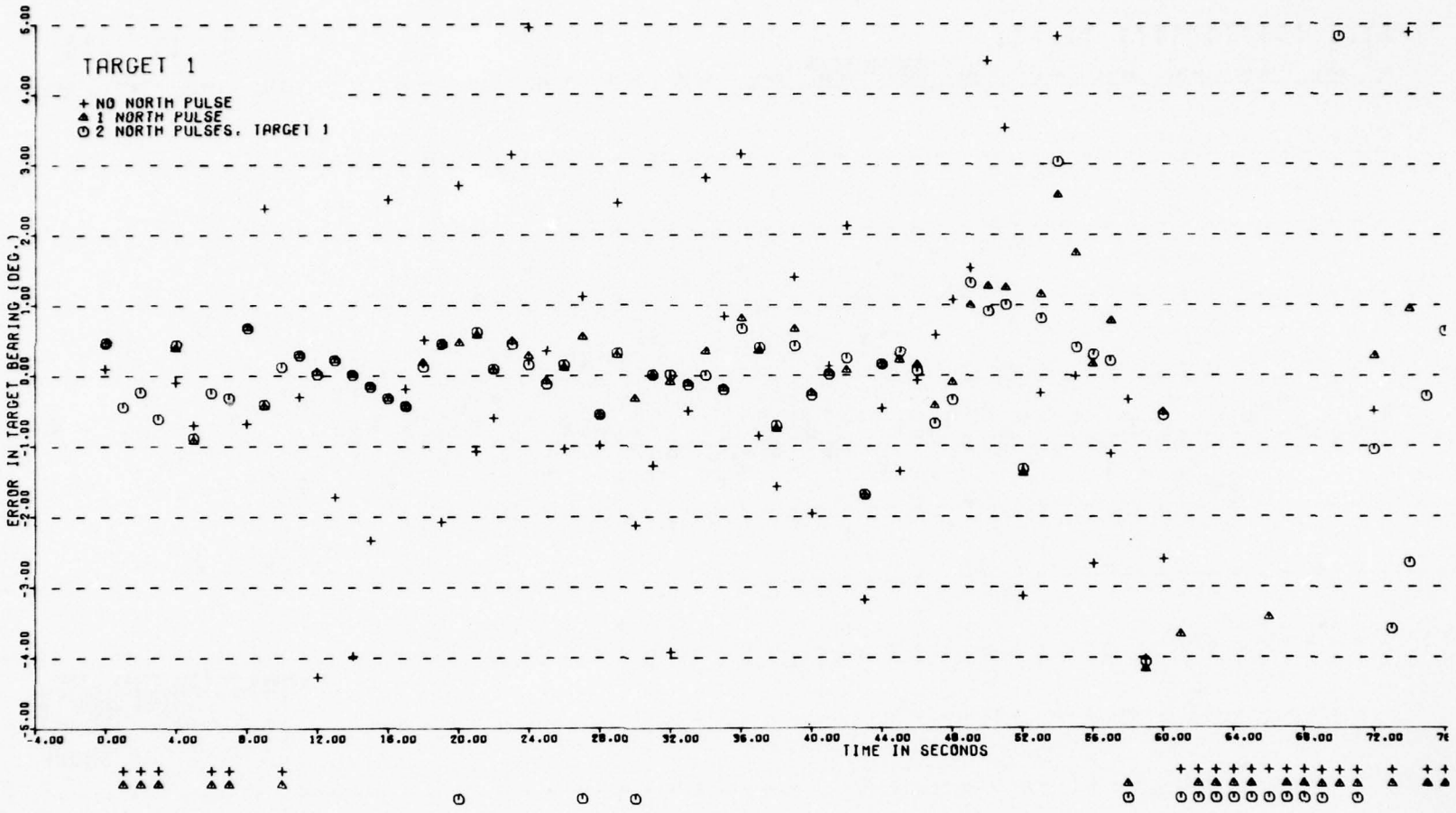
TARGET 1
+ NO NORTH PULSE
▲ 1 NORTH PULSE
⊙ 2 NORTH PULSES, TARGET 1
ERROR IN TARGET BEARING (DEG.)
TIME IN SECONDS

FIGURE 6.3-11.

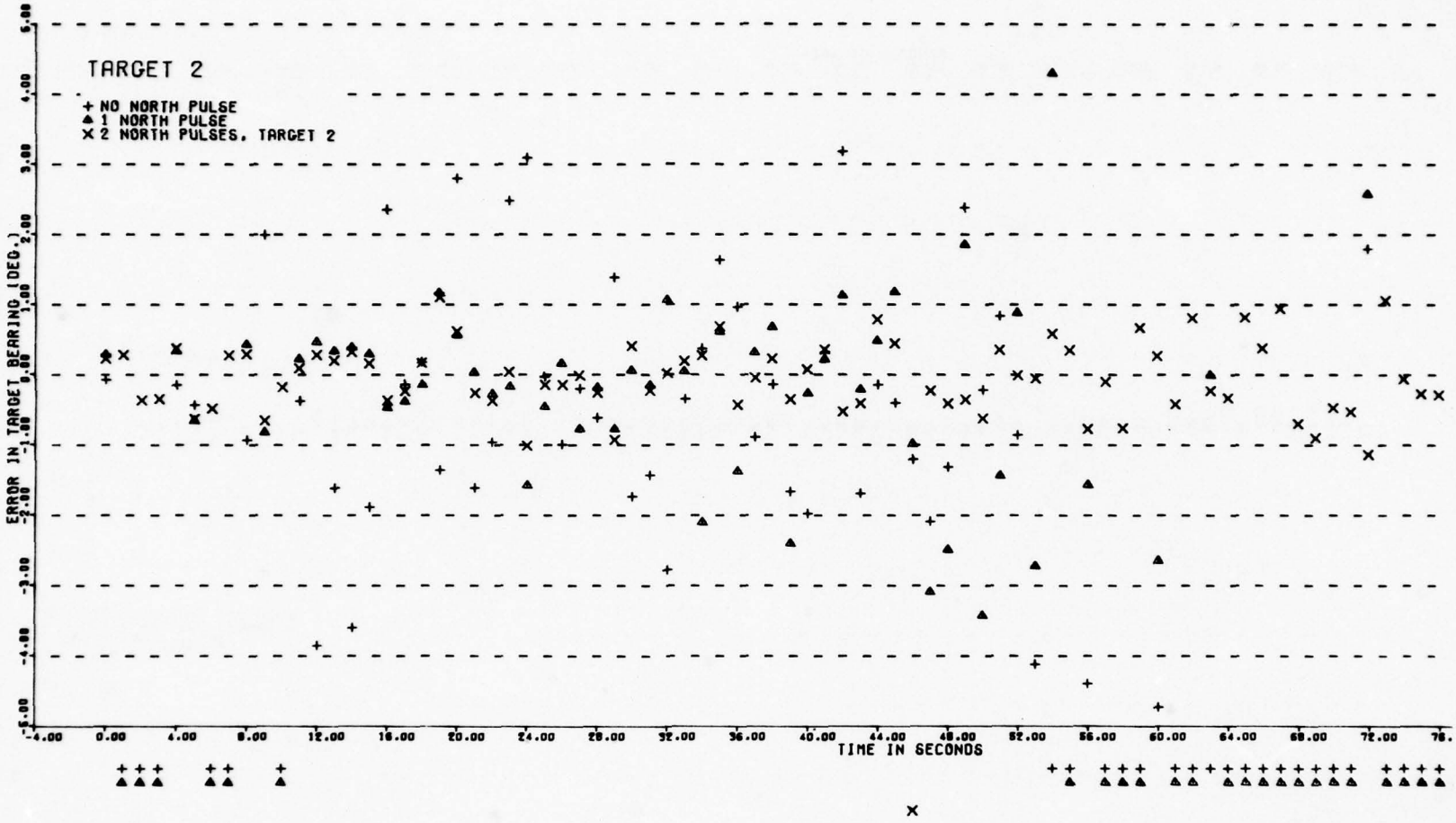
TARGET 2
+ NO NORTH PULSE
▲ 1 NORTH PULSE
× 2 NORTH PULSES, TARGET 2
ERROR IN TARGET BEARING (DEG.)
TIME IN SECONDS

FIGURE 6.3-12.

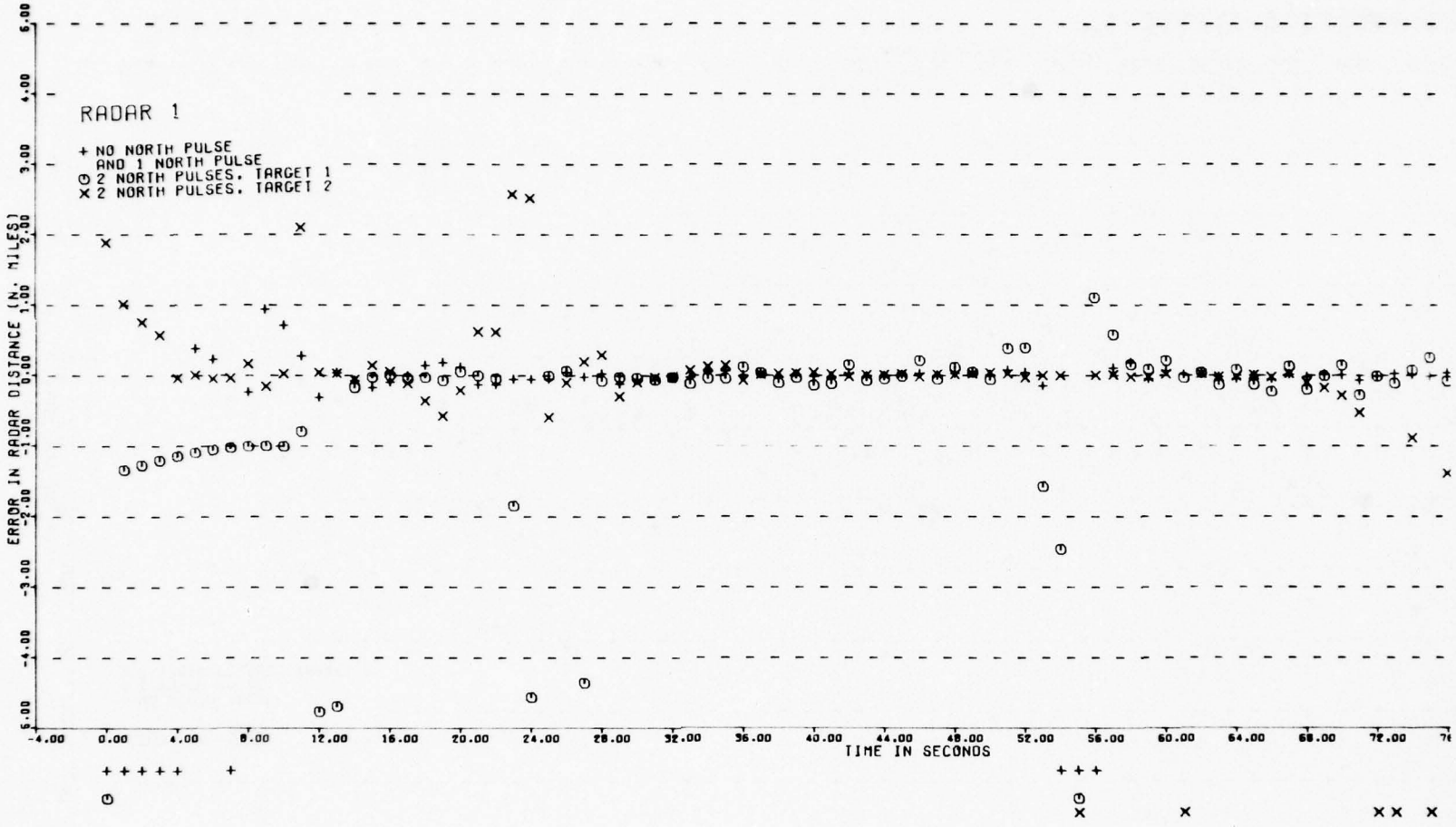
RADAR 1
+ NO NORTH PULSE
AND 1 NORTH PULSE
⊙ 2 NORTH PULSES. TARGET 1
× 2 NORTH PULSES. TARGET 2
ERROR IN RADAR DISTANCE (N. MILES)
TIME IN SECONDS

FIGURE 6.3-13.

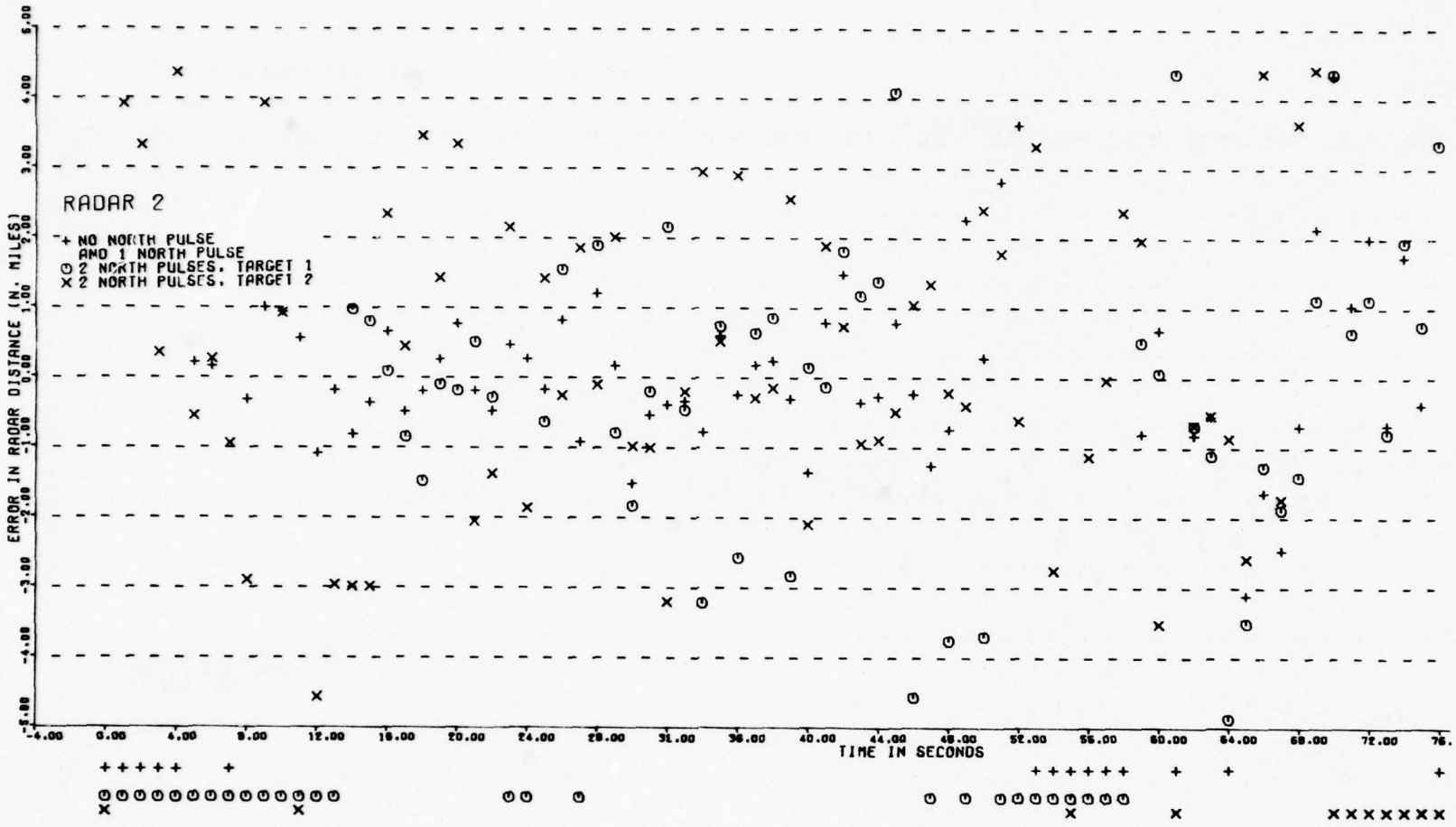
RADAR 2
+ NO NORTH PULSE
AND 1 NORTH PULSE
⊙ 2 NORTH PULSES, TARGET 1
× 2 NORTH PULSES, TARGET 2
ERROR IN RADAR DISTANCE (N. MILES)
TIME IN SECONDS

FIGURE 6.3-14.

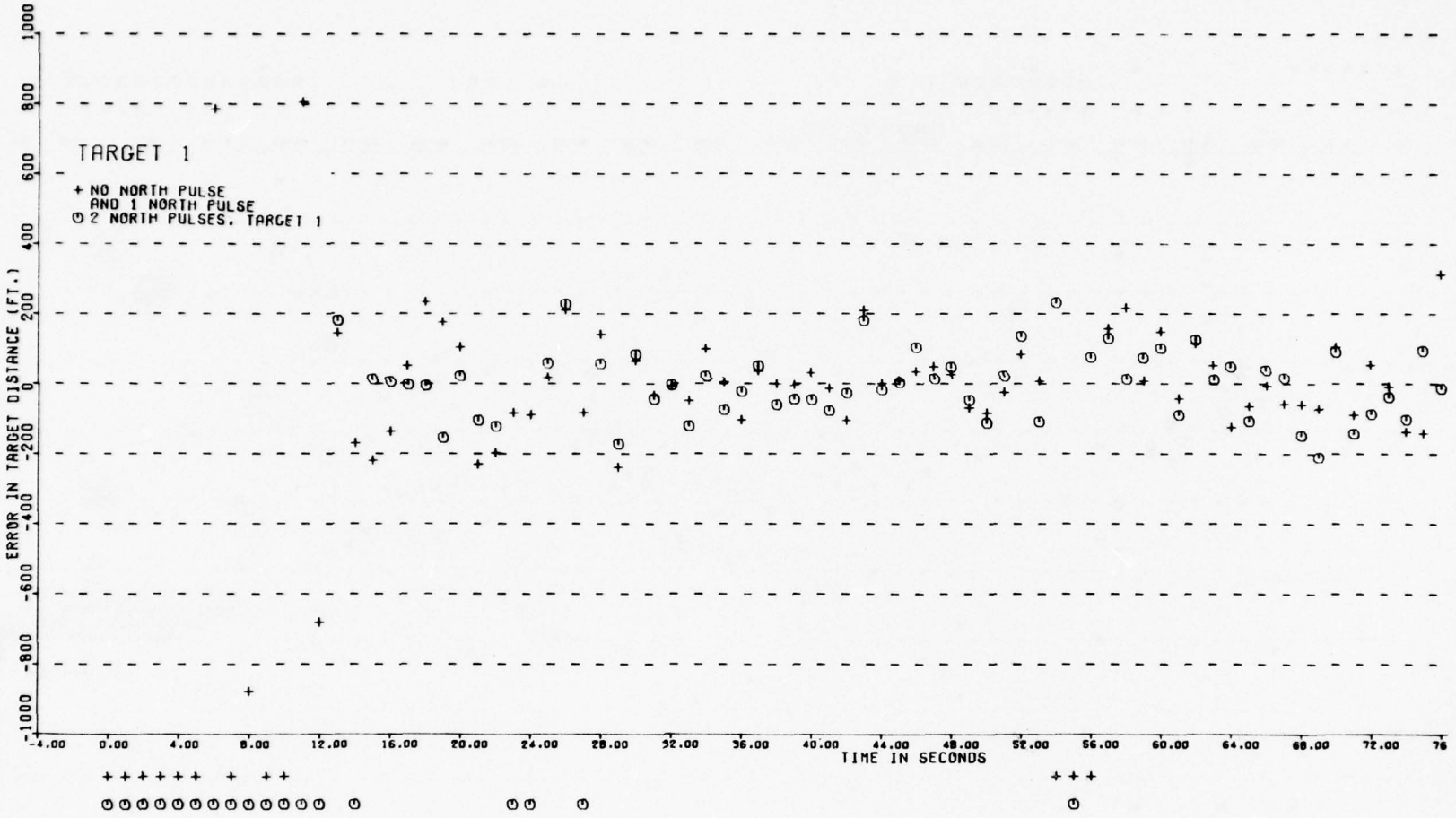
TARGET 1
+ NO NORTH PULSE
AND 1 NORTH PULSE
⊙ 2 NORTH PULSES. TARGET 1
ERROR IN TARGET DISTANCE (FT.)
1000
800
600
400
200
0
-200
-400
-600
-800
-1000
-4.00
0.00
4.00
8.00
12.00
16.00
20.00
24.00
28.00
32.00
36.00
40.00
44.00
48.00
52.00
56.00
60.00
64.00
68.00
72.00
76
TIME IN SECONDS

FIGURE 6.3-15.

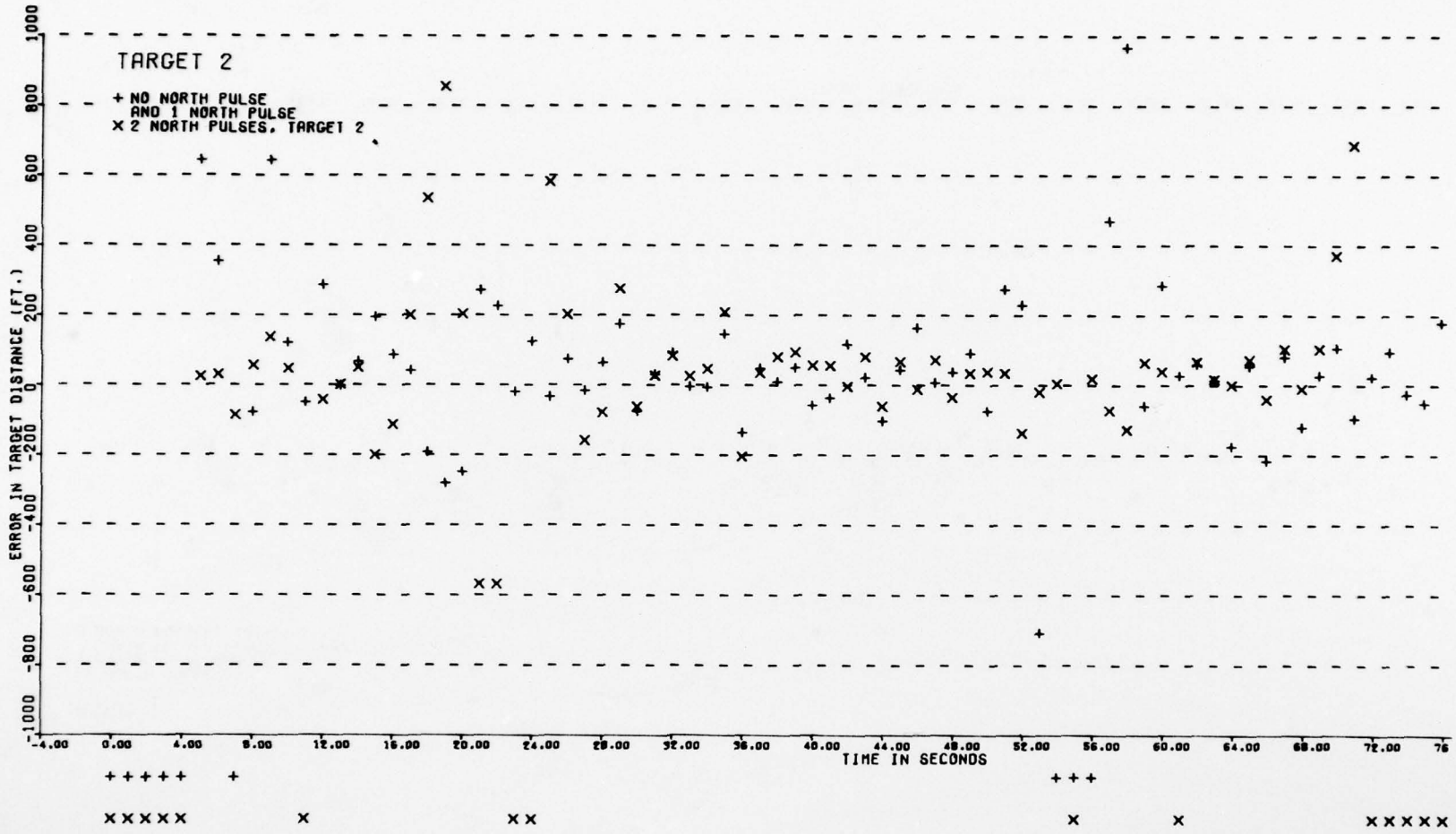
TARGET 2
+ NO NORTH PULSE
AND 1 NORTH PULSE
× 2 NORTH PULSES, TARGET 2
ERROR IN TARGET DISTANCE (FT.)
1000
800
600
400
200
0
-200
-400
-600
-800
-1000
-4.00
0.00
4.00
8.00
12.00
16.00
20.00
24.00
28.00
32.00
36.00
40.00
44.00
48.00
52.00
56.00
60.00
64.00
68.00
72.00
76
TIME IN SECONDS

FIGURE 6.3-16.

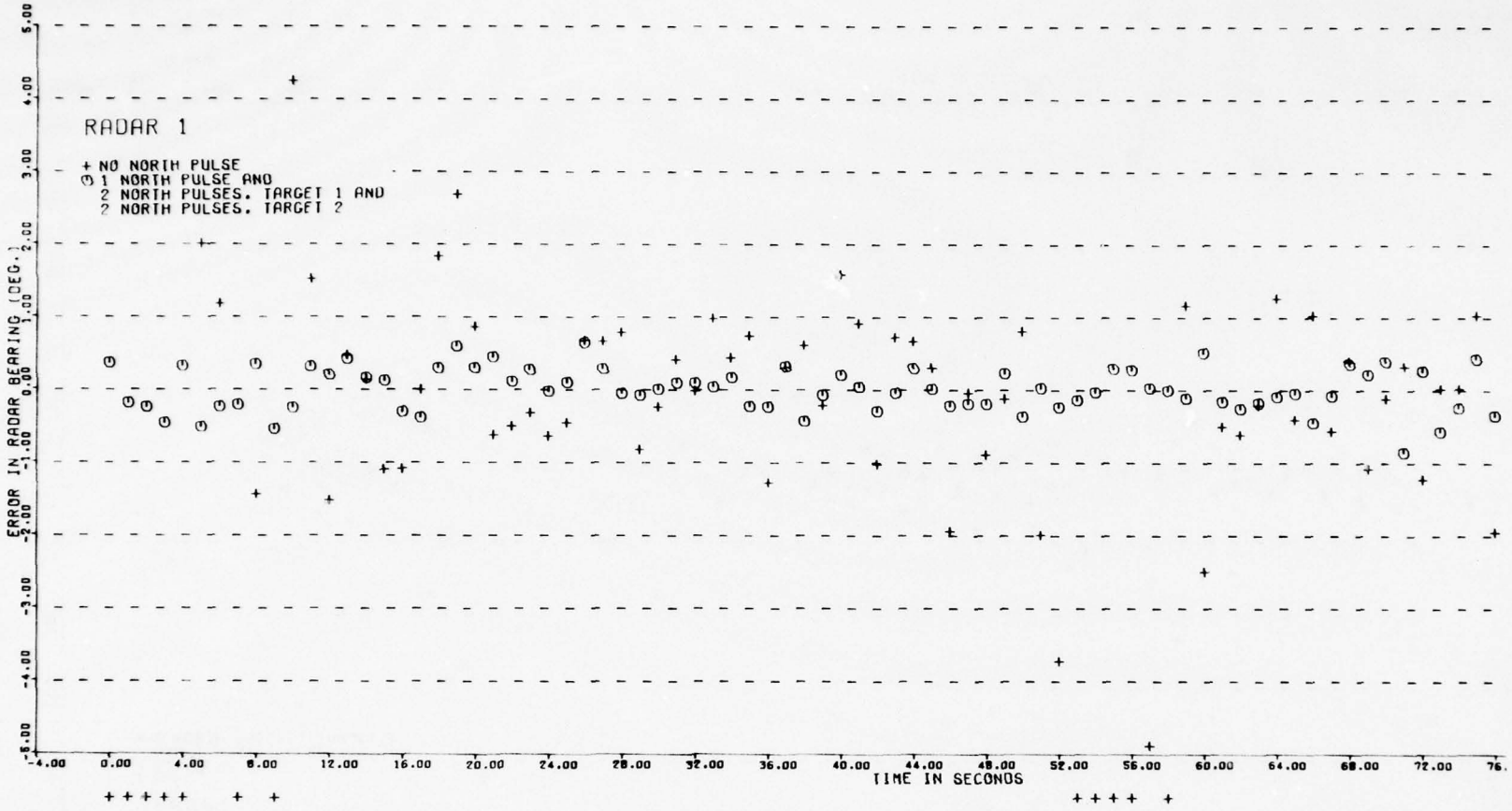
RADAR 1
+ NO NORTH PULSE
1 NORTH PULSE AND
2 NORTH PULSES. TARGET 1 AND
2 NORTH PULSES. TARGET 2
ERROR IN RADAR BEARING (DEG.)
TIME IN SECONDS
5.00
4.00
3.00
2.00
1.00
0.00
-1.00
-2.00
-3.00
-4.00
-5.00
-4.00
0.00
4.00
8.00
12.00
16.00
20.00
24.00
28.00
32.00
36.00
40.00
44.00
48.00
52.00
56.00
60.00
64.00
68.00
72.00
76.

FIGURE 6.3-17.

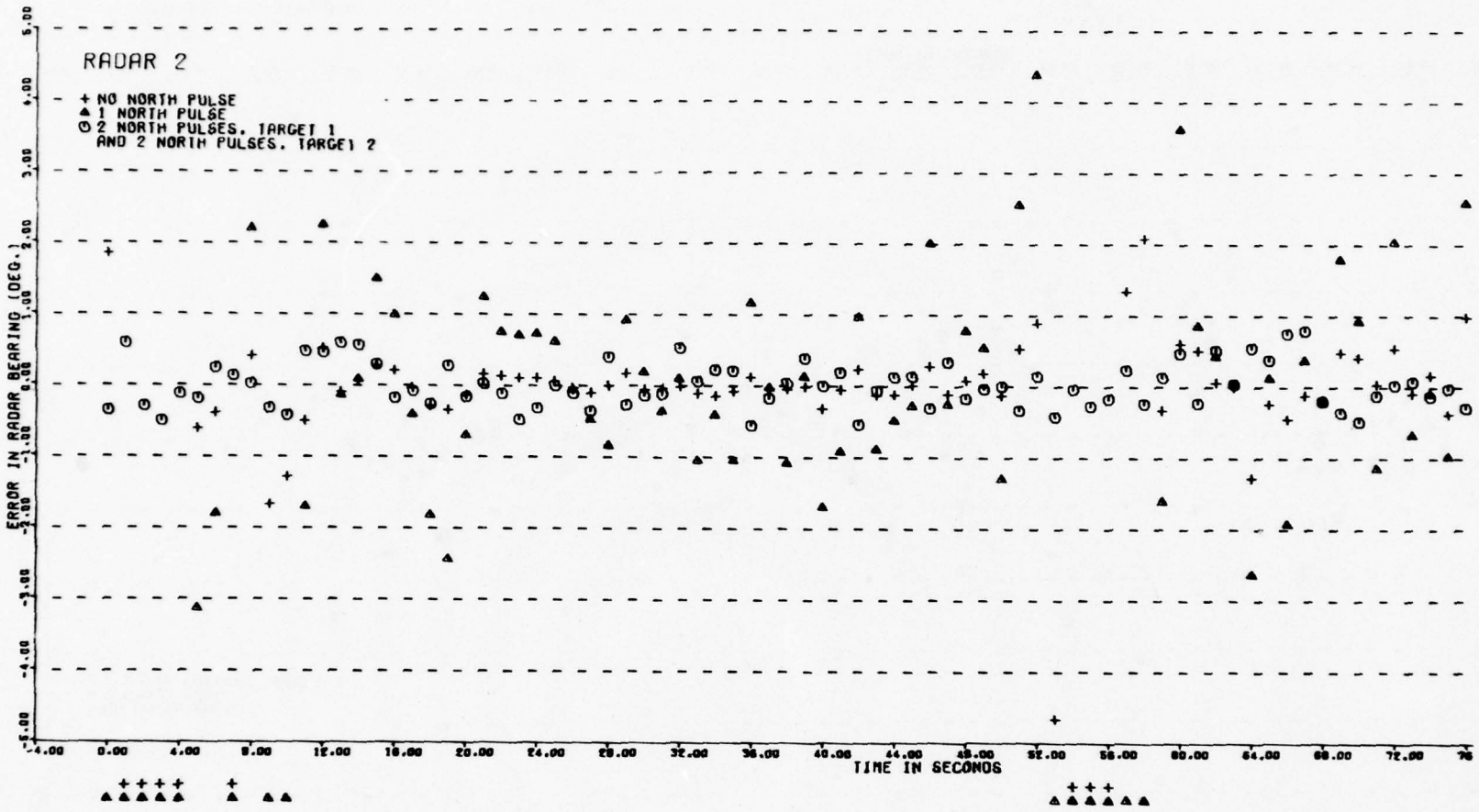
RADAR 2
+ NO NORTH PULSE
▲ 1 NORTH PULSE
⊙ 2 NORTH PULSES, TARGET 1
AND 2 NORTH PULSES, TARGET 2
ERROR IN RADAR BEARING (DEG.)
TIME IN SECONDS

FIGURE 6.3-18.

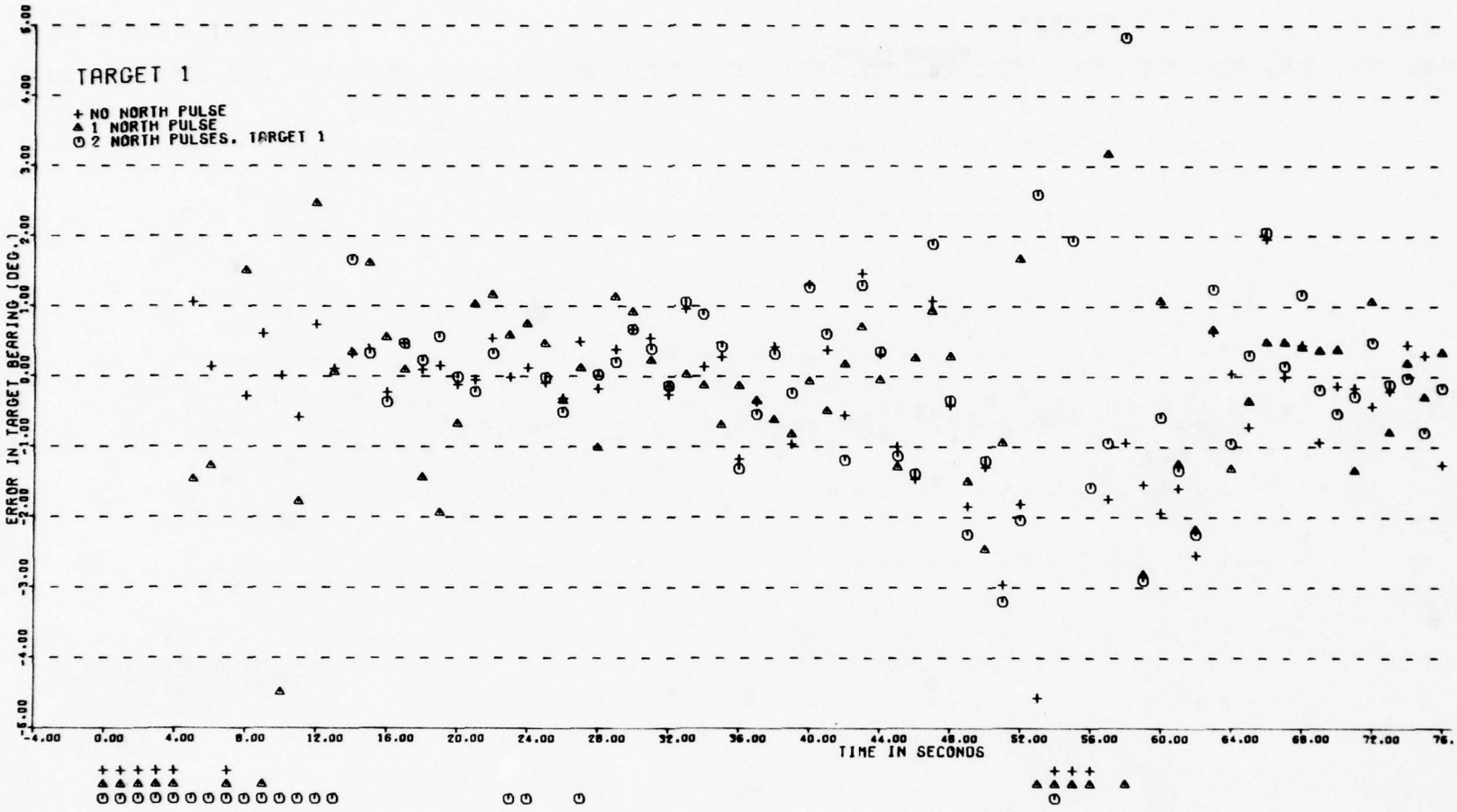
TARGET 1
+ NO NORTH PULSE
▲ 1 NORTH PULSE
ʘ 2 NORTH PULSES. TARGET 1
ERROR IN TARGET BEARING (DEG.)
TIME IN SECONDS

FIGURE 6.3-19.

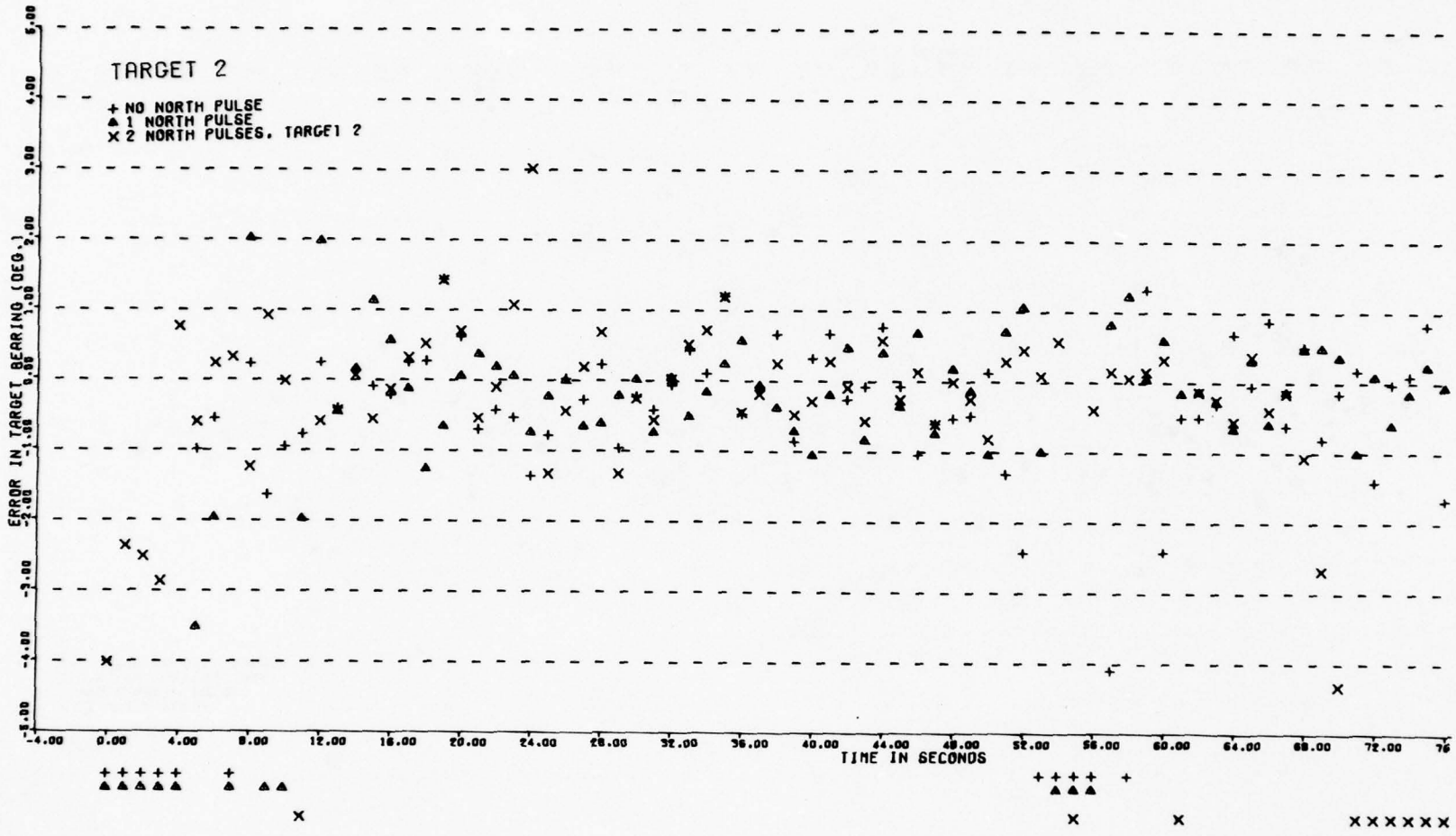
TARGET 2
+ NO NORTH PULSE
▲ 1 NORTH PULSE
× 2 NORTH PULSES. TARGET 2
ERROR IN TARGET BEARING (DEG.)
TIME IN SECONDS

FIGURE 6.3-20.

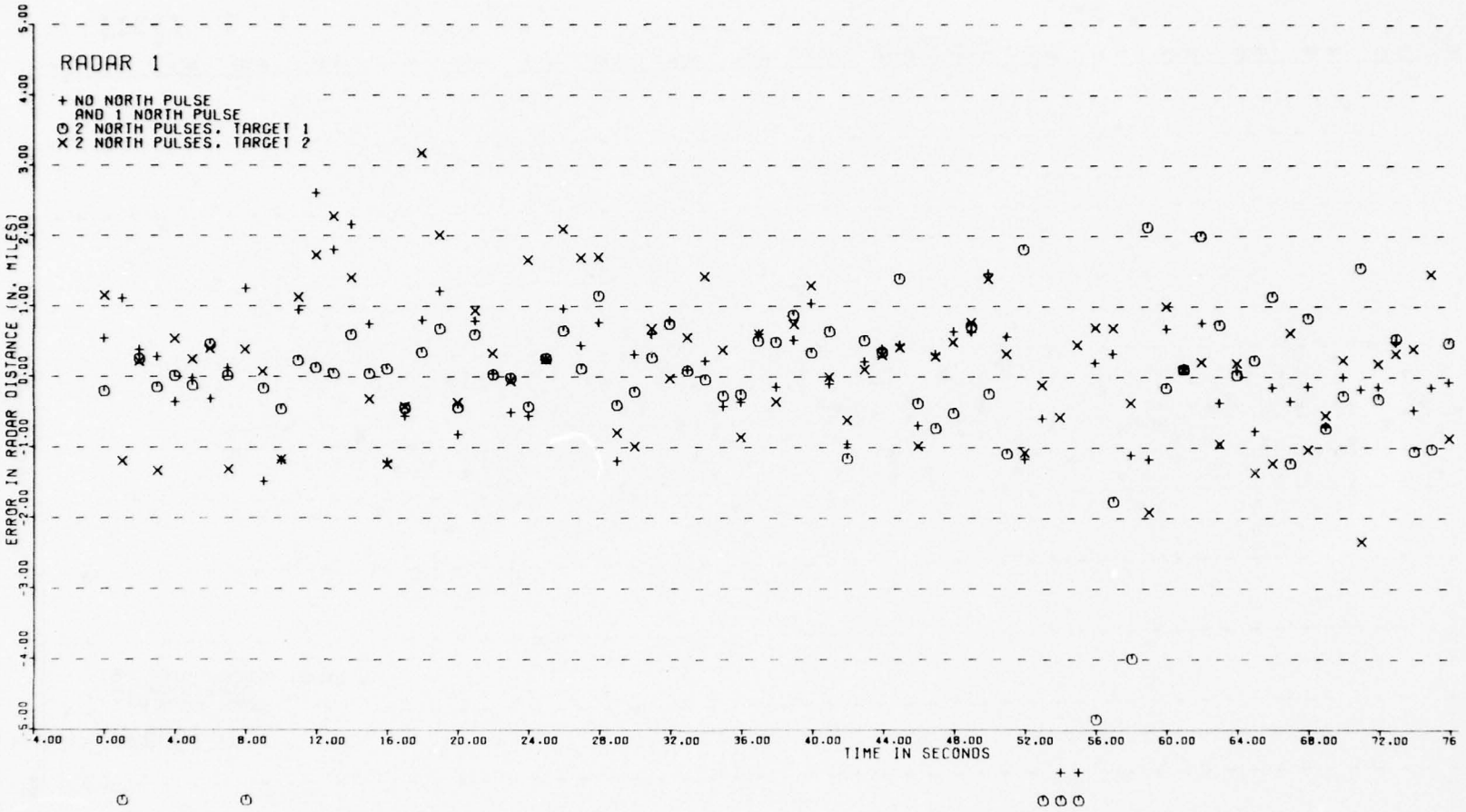
RADAR 1
+ NO NORTH PULSE
AND 1 NORTH PULSE
⊙ 2 NORTH PULSES. TARGET 1
× 2 NORTH PULSES. TARGET 2
ERROR IN RADAR DISTANCE (N. MILES)
5.00
4.00
3.00
2.00
1.00
0.00
-1.00
-2.00
-3.00
-4.00
-5.00
4.00
0.00
4.00
8.00
12.00
16.00
20.00
24.00
28.00
32.00
36.00
40.00
44.00
48.00
52.00
56.00
60.00
64.00
68.00
72.00
76
TIME IN SECONDS

FIGURE 6.3-21.

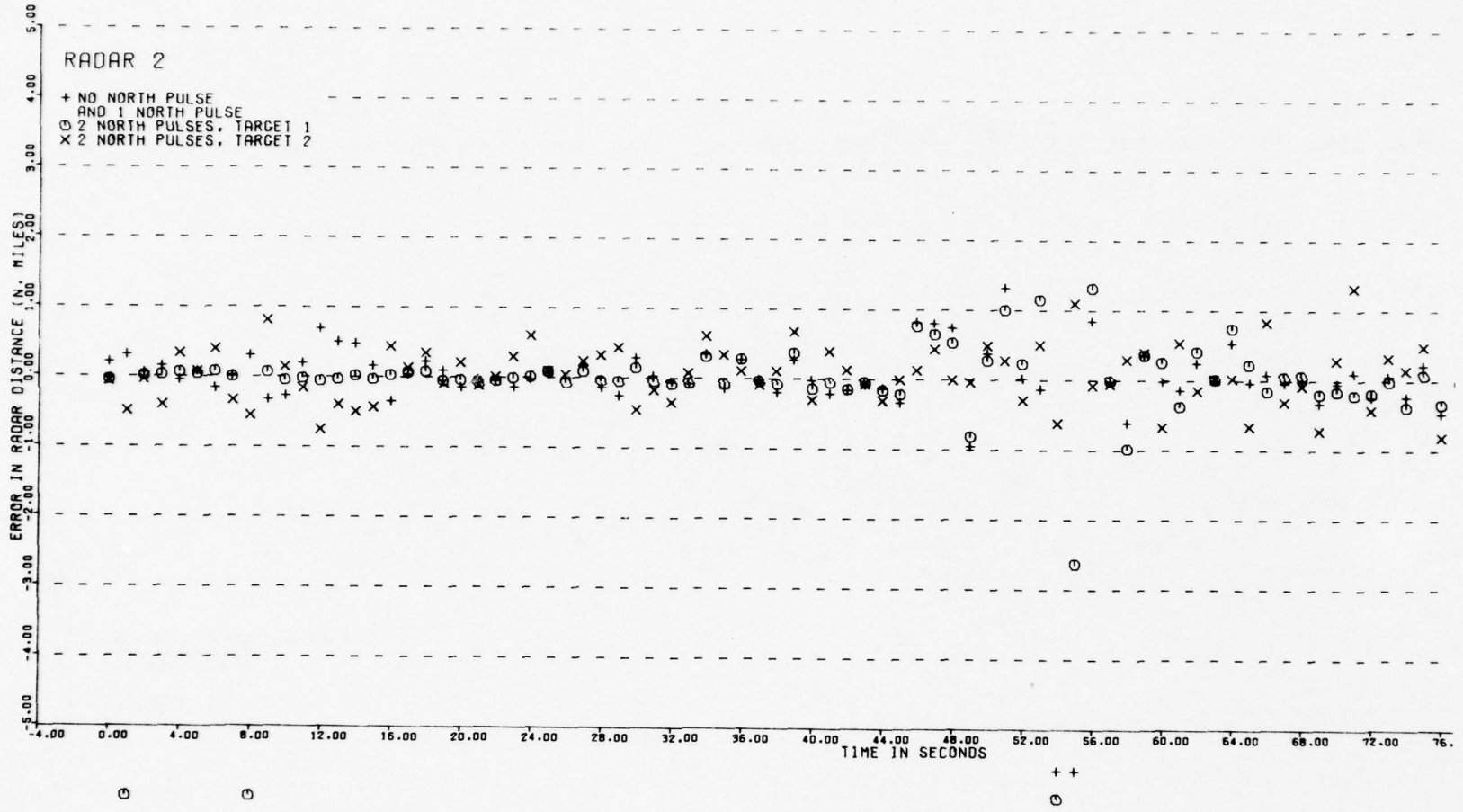
RADAR 2
+ NO NORTH PULSE AND 1 NORTH PULSE
⊙ 2 NORTH PULSES, TARGET 1
× 2 NORTH PULSES, TARGET 2
ERROR IN RADAR DISTANCE (N. MILES)
5.00
4.00
3.00
2.00
1.00
0.00
-1.00
-2.00
-3.00
-4.00
-5.00
-4.00
0.00
4.00
8.00
12.00
16.00
20.00
24.00
28.00
32.00
36.00
40.00
44.00
48.00
52.00
56.00
60.00
64.00
68.00
72.00
76.
TIME IN SECONDS

FIGURE 6.3-22.

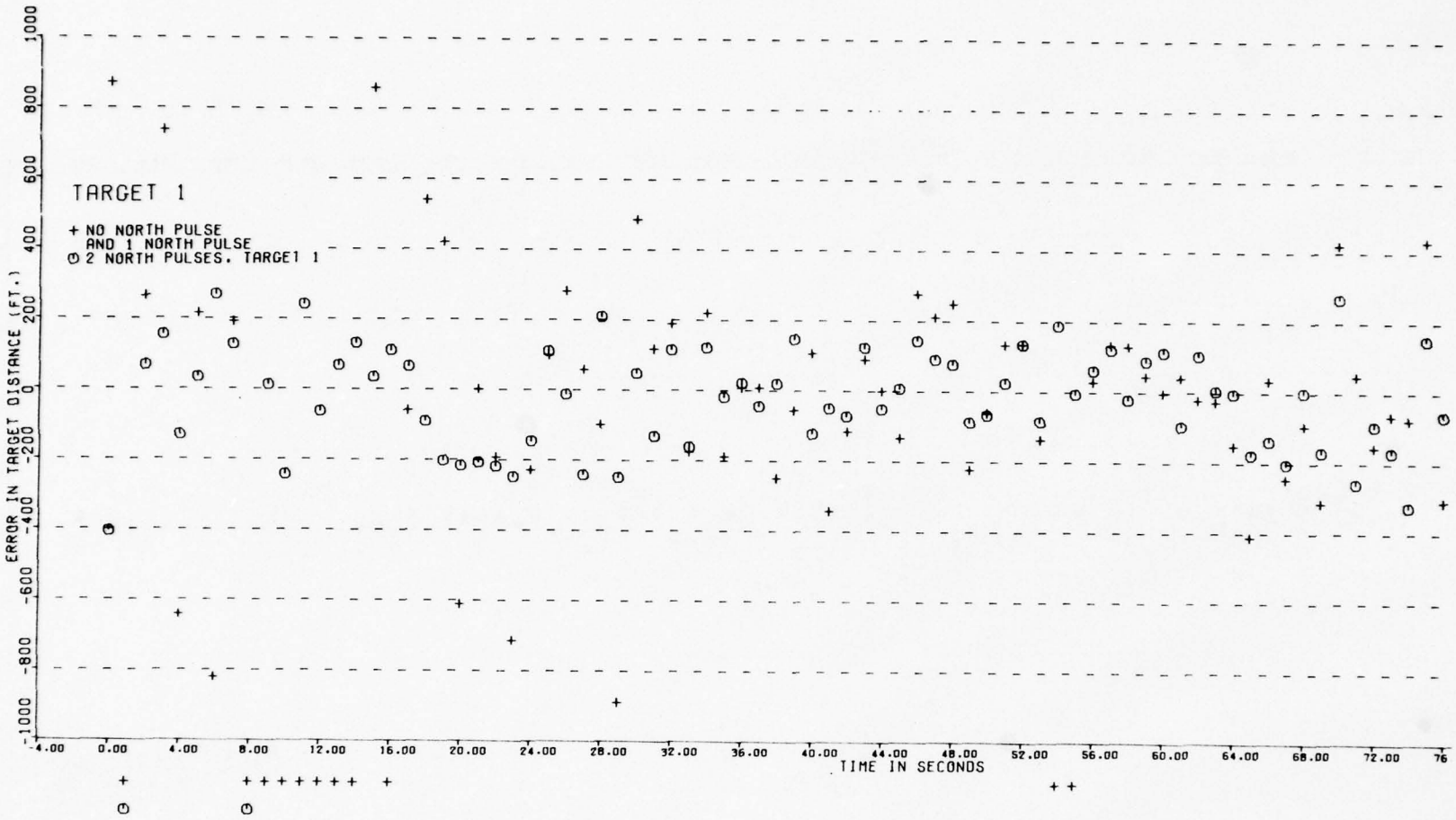
TARGET 1
+ NO NORTH PULSE
AND 1 NORTH PULSE
⊙ 2 NORTH PULSES. TARGET 1
ERROR IN TARGET DISTANCE (FT.)
1000
800
600
400
200
0
-200
-400
-600
-800
-1000
-4.00
0.00
4.00
8.00
12.00
16.00
20.00
24.00
28.00
32.00
36.00
40.00
44.00
48.00
52.00
56.00
60.00
64.00
68.00
72.00
76
TIME IN SECONDS

FIGURE 6.3-23.

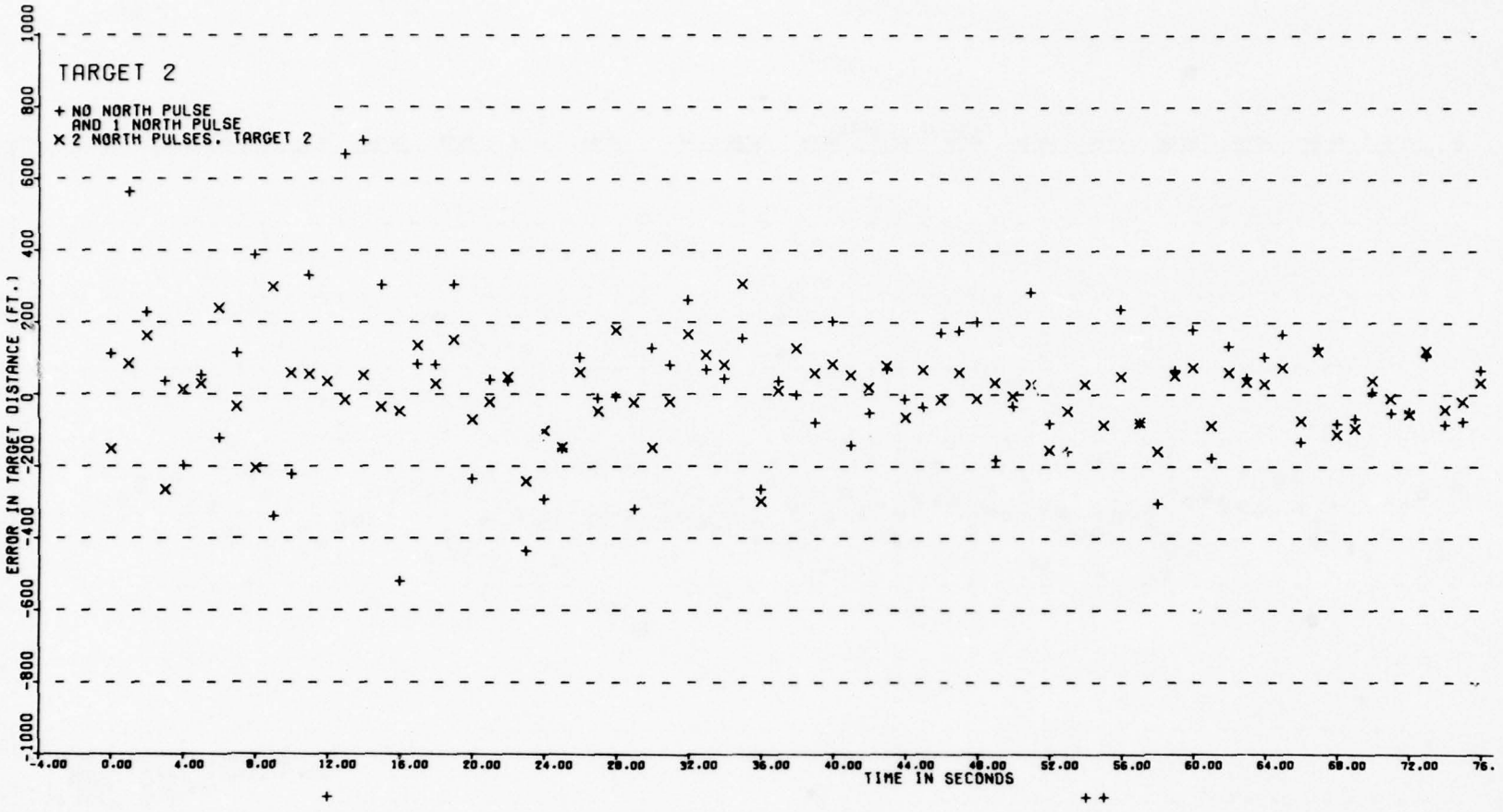
TARGET 2
+ NO NORTH PULSE
AND 1 NORTH PULSE
× 2 NORTH PULSES. TARGET 2
ERROR IN TARGET DISTANCE (FT.)
1000
800
600
400
200
0
-200
-400
-600
-800
-1000
-4.00
0.00
4.00
8.00
12.00
16.00
20.00
24.00
28.00
32.00
36.00
40.00
44.00
48.00
52.00
56.00
60.00
64.00
68.00
72.00
76.
TIME IN SECONDS

FIGURE 6.3-24.

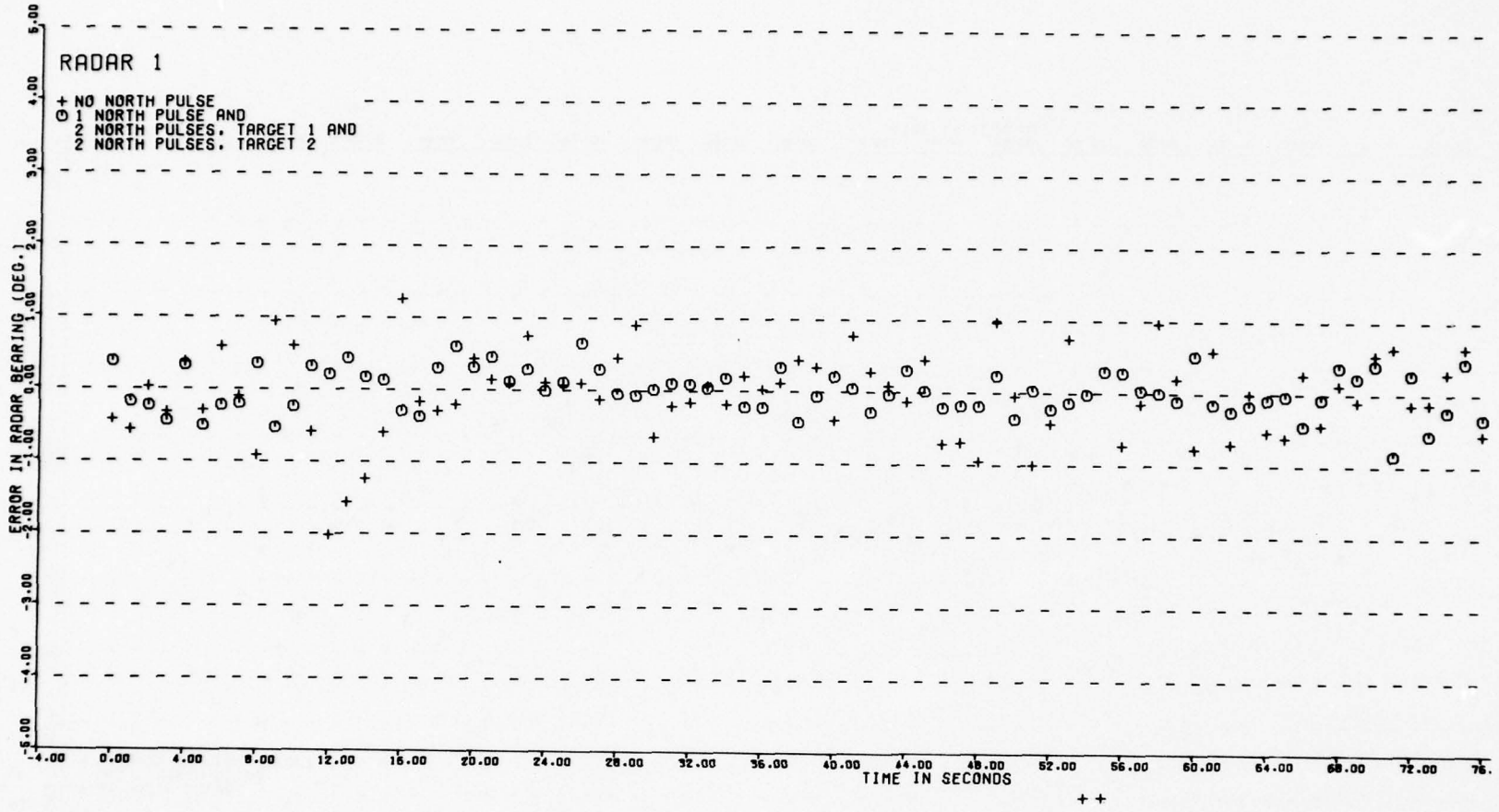
RADAR 1
+ NO NORTH PULSE
⊙ 1 NORTH PULSE AND
2 NORTH PULSES. TARGET 1 AND
2 NORTH PULSES. TARGET 2
ERROR IN RADAR BEARING (DEG.)
5.00
4.00
3.00
2.00
1.00
0.00
-1.00
-2.00
-3.00
-4.00
-5.00
-4.00
0.00
4.00
8.00
12.00
16.00
20.00
24.00
28.00
32.00
36.00
40.00
44.00
48.00
52.00
56.00
60.00
64.00
68.00
72.00
76.
TIME IN SECONDS

FIGURE 6.3-25.

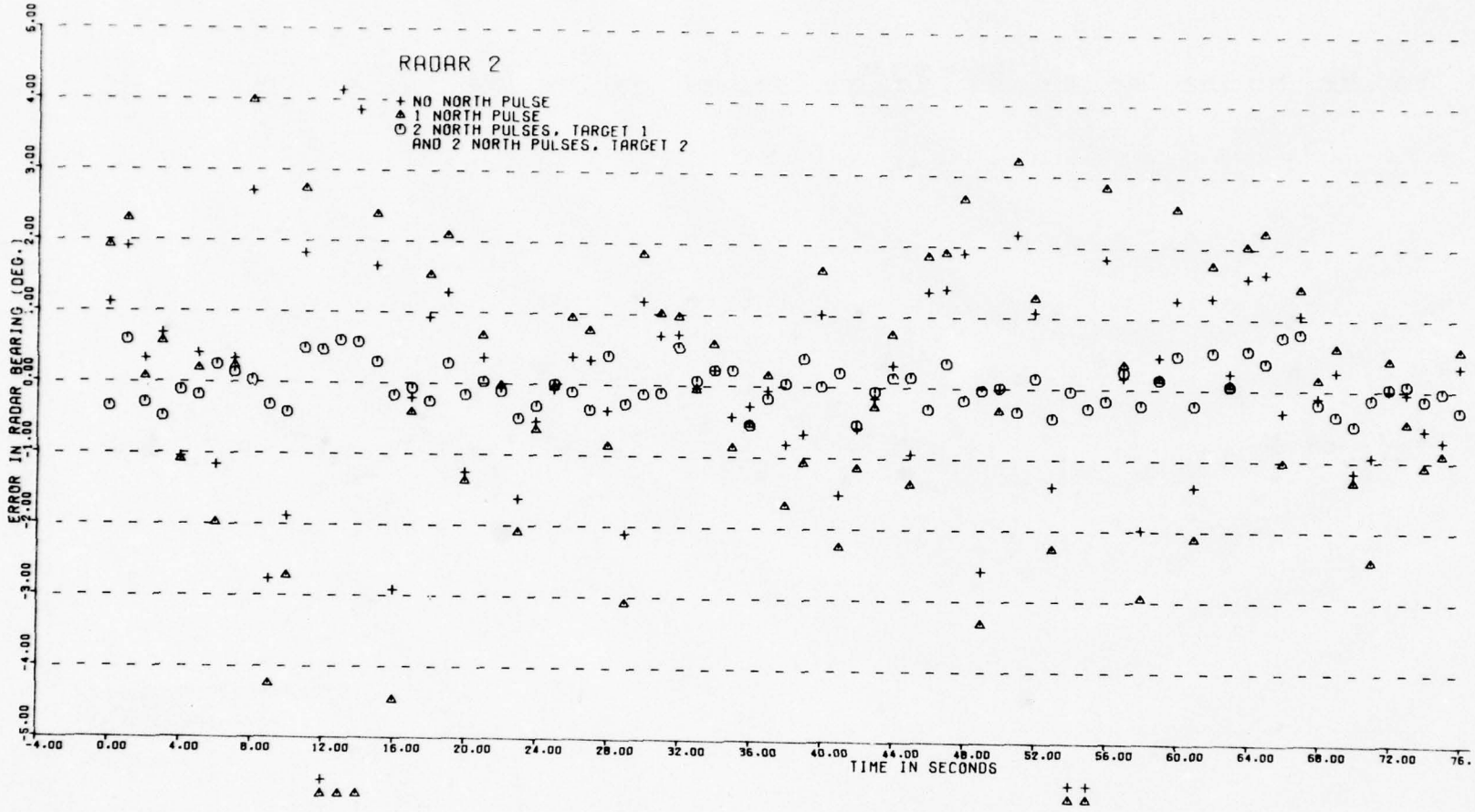
RADAR 2
+ NO NORTH PULSE
△ 1 NORTH PULSE
⊙ 2 NORTH PULSES, TARGET 1
AND 2 NORTH PULSES, TARGET 2
ERROR IN RADAR BEARING (DEG.)
6.00
4.00
3.00
2.00
1.00
0.00
-1.00
-2.00
-3.00
-4.00
-5.00
-4.00
0.00
4.00
8.00
12.00
16.00
20.00
24.00
28.00
32.00
36.00
40.00
44.00
48.00
52.00
56.00
60.00
64.00
68.00
72.00
76.
TIME IN SECONDS

FIGURE 6.3-26.

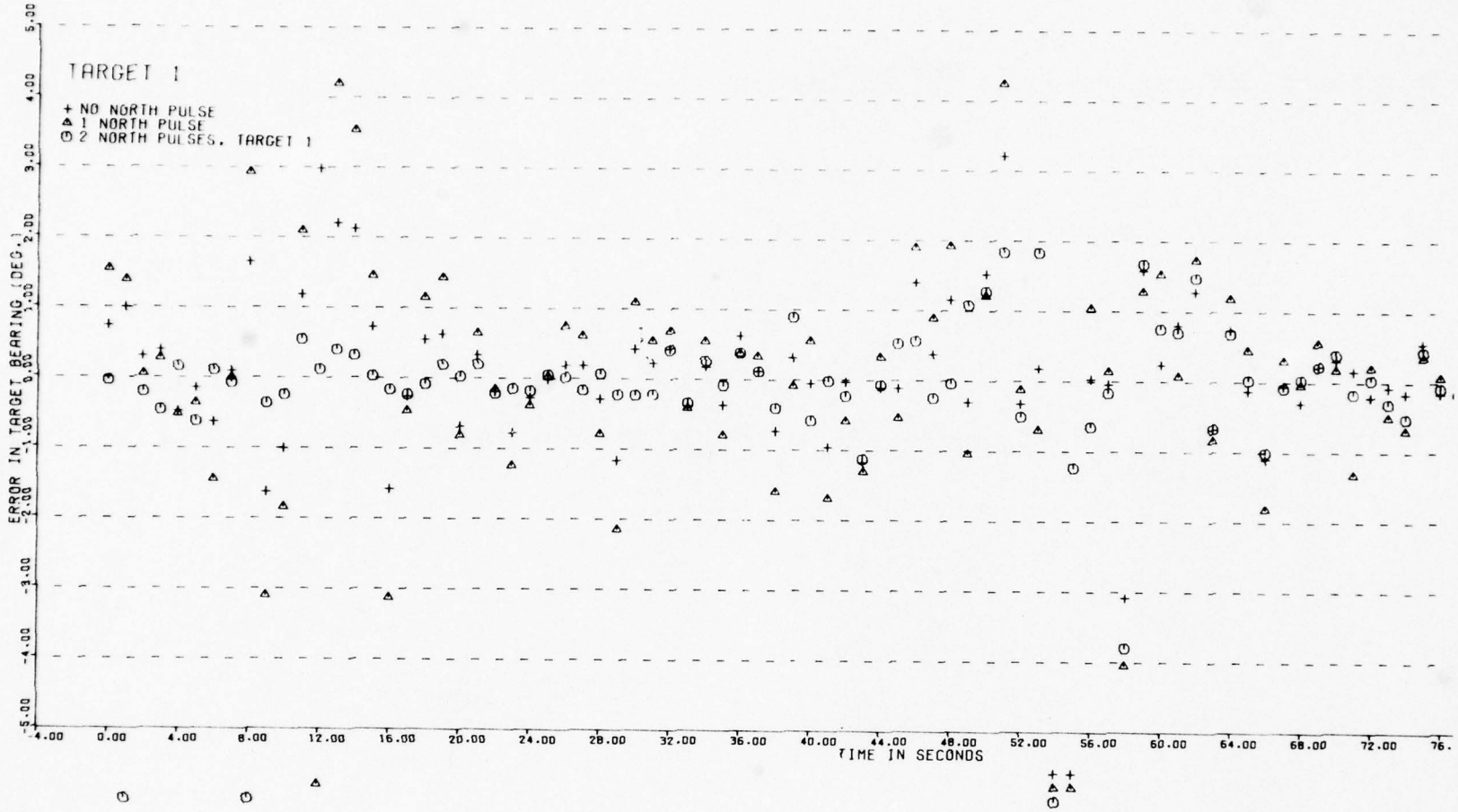
TARGET 1
+ NO NORTH PULSE
△ 1 NORTH PULSE
ⓘ 2 NORTH PULSES. TARGET 1
ERROR IN TARGET BEARING (DEG.)
5.00
4.00
3.00
2.00
1.00
0.00
-1.00
-2.00
-3.00
-4.00
-5.00
-4.00
0.00
4.00
8.00
12.00
16.00
20.00
24.00
28.00
32.00
36.00
40.00
44.00
48.00
52.00
56.00
60.00
64.00
68.00
72.00
76.
TIME IN SECONDS

FIGURE 6.3-27.

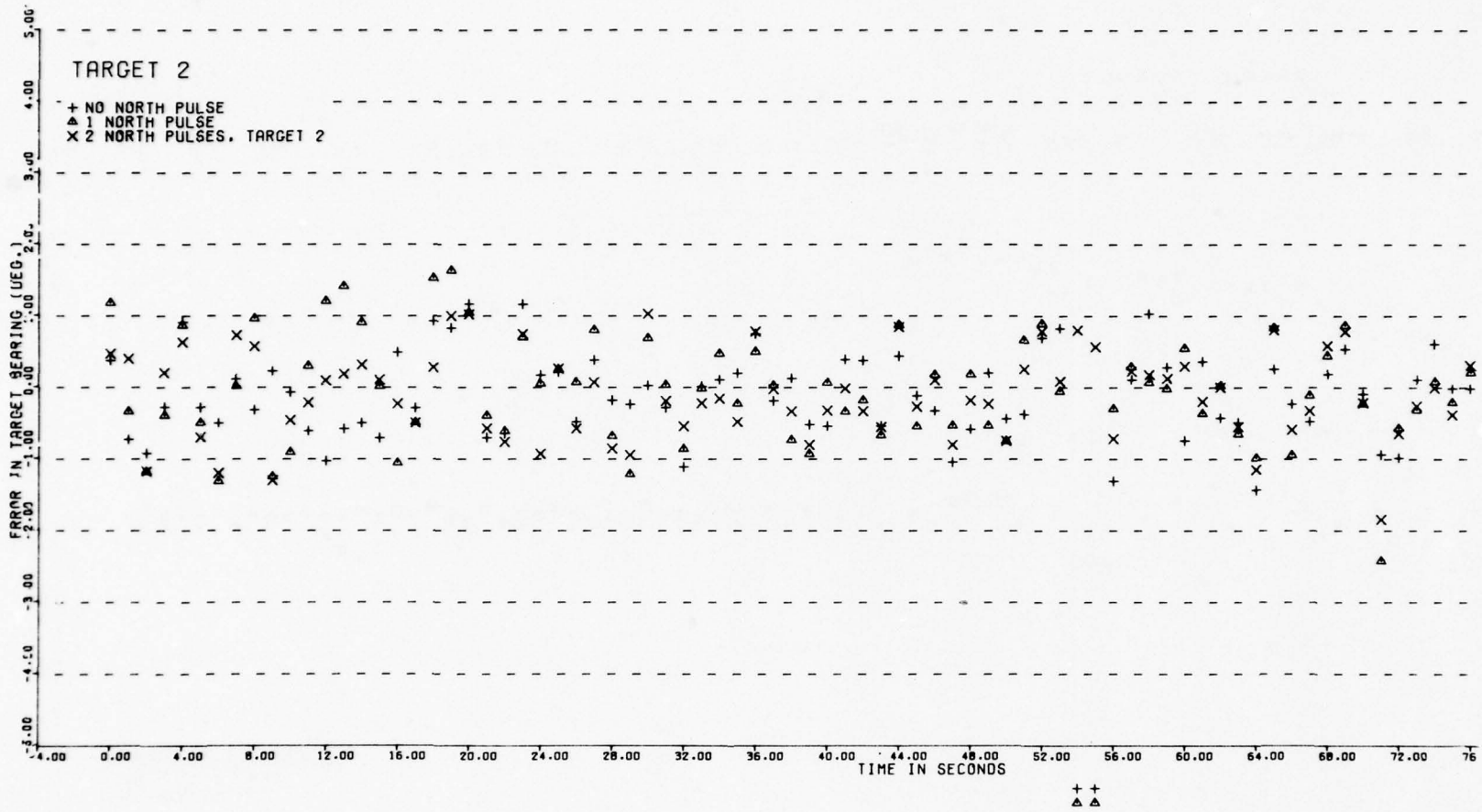
TARGET 2
+ NO NORTH PULSE
△ 1 NORTH PULSE
× 2 NORTH PULSES. TARGET 2
ERROR IN TARGET BEARING (DEG.)
5.00
4.00
3.00
2.00
1.00
0.00
-1.00
-2.00
-3.00
-4.00
-5.00
-4.00
0.00
4.00
8.00
12.00
16.00
20.00
24.00
28.00
32.00
36.00
40.00
44.00
48.00
52.00
56.00
60.00
64.00
68.00
72.00
76
TIME IN SECONDS

FIGURE 6.3-28.

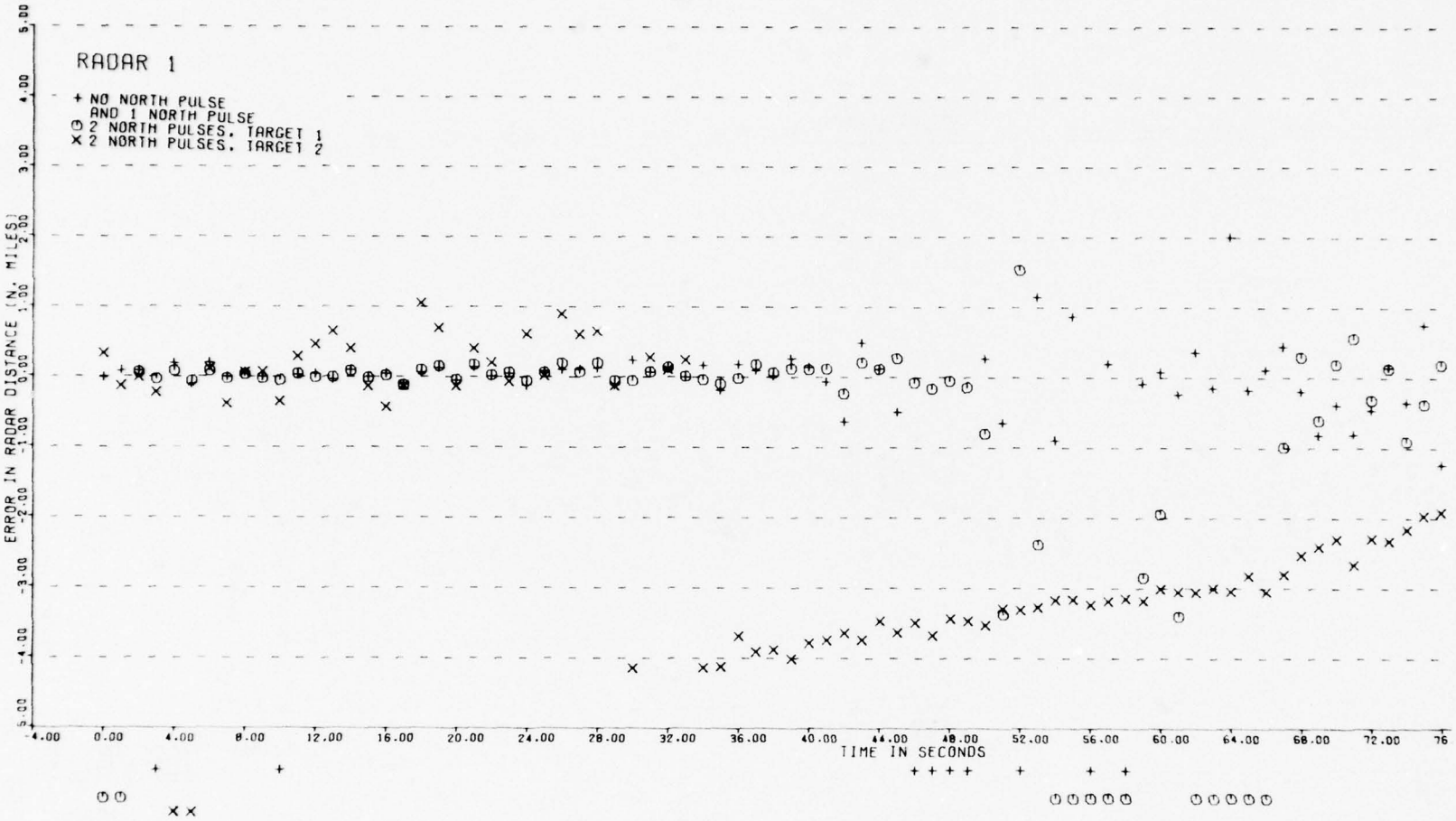
RADAR 1
+ NO NORTH PULSE
AND 1 NORTH PULSE
⊙ 2 NORTH PULSES. TARGET 1
× 2 NORTH PULSES. TARGET 2
ERROR IN RADAR DISTANCE (N. MILES)
5.00
4.00
3.00
2.00
1.00
0.00
-1.00
-2.00
-3.00
-4.00
-5.00
-4.00
0.00
4.00
8.00
12.00
16.00
20.00
24.00
28.00
32.00
36.00
40.00
44.00
48.00
52.00
56.00
60.00
64.00
68.00
72.00
76
TIME IN SECONDS

FIGURE 6.3-29.

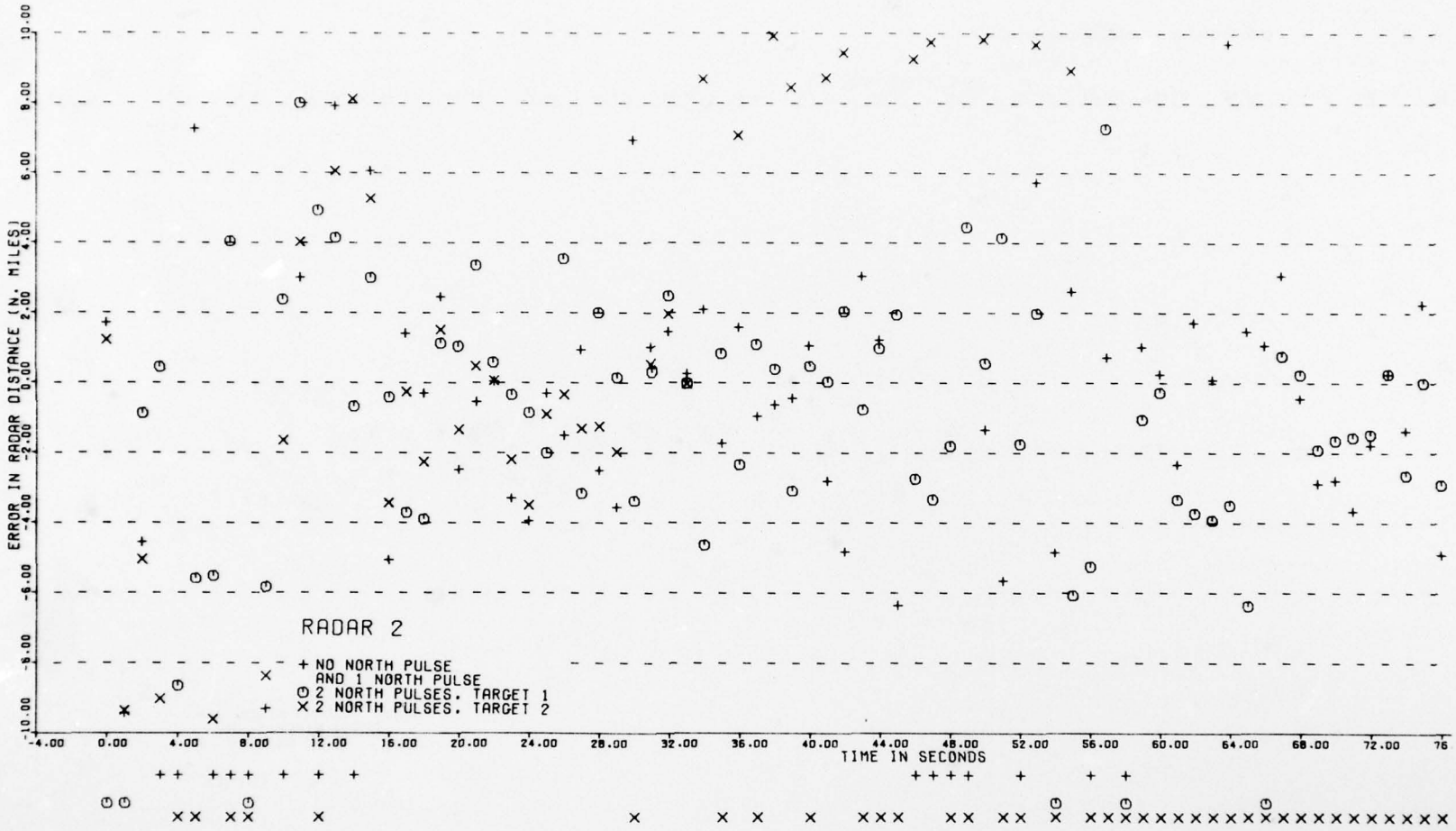
ERROR IN RADAR DISTANCE (N. MILES)
10.00
8.00
6.00
4.00
2.00
0.00
-2.00
-4.00
-6.00
-8.00
-10.00
-4.00
0.00
4.00
8.00
12.00
16.00
20.00
24.00
28.00
32.00
36.00
40.00
44.00
48.00
52.00
56.00
60.00
64.00
68.00
72.00
76
TIME IN SECONDS
RADAR 2
+ NO NORTH PULSE
AND 1 NORTH PULSE
⊙ 2 NORTH PULSES. TARGET 1
× 2 NORTH PULSES. TARGET 2

FIGURE 6.3-30.

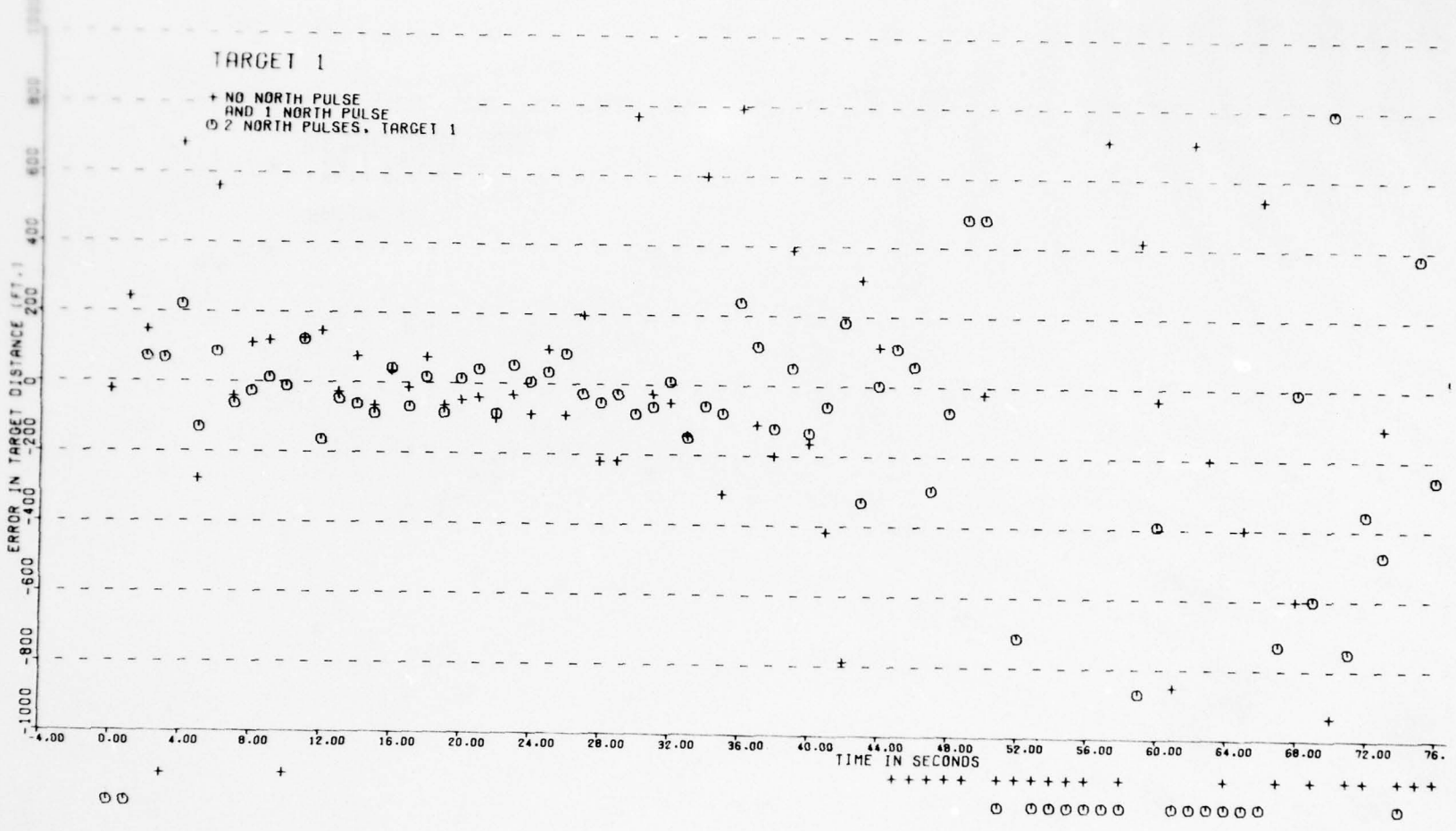
TARGET 1
+ NO NORTH PULSE
AND 1 NORTH PULSE
⊙ 2 NORTH PULSES, TARGET 1
ERROR IN TARGET DISTANCE (FT.)
-1000
-800
-600
-400
-200
0
200
400
600
800
-4.00
0.00
4.00
8.00
12.00
16.00
20.00
24.00
28.00
32.00
36.00
40.00
44.00
48.00
52.00
56.00
60.00
64.00
68.00
72.00
76.
TIME IN SECONDS

FIGURE 6.3-31.

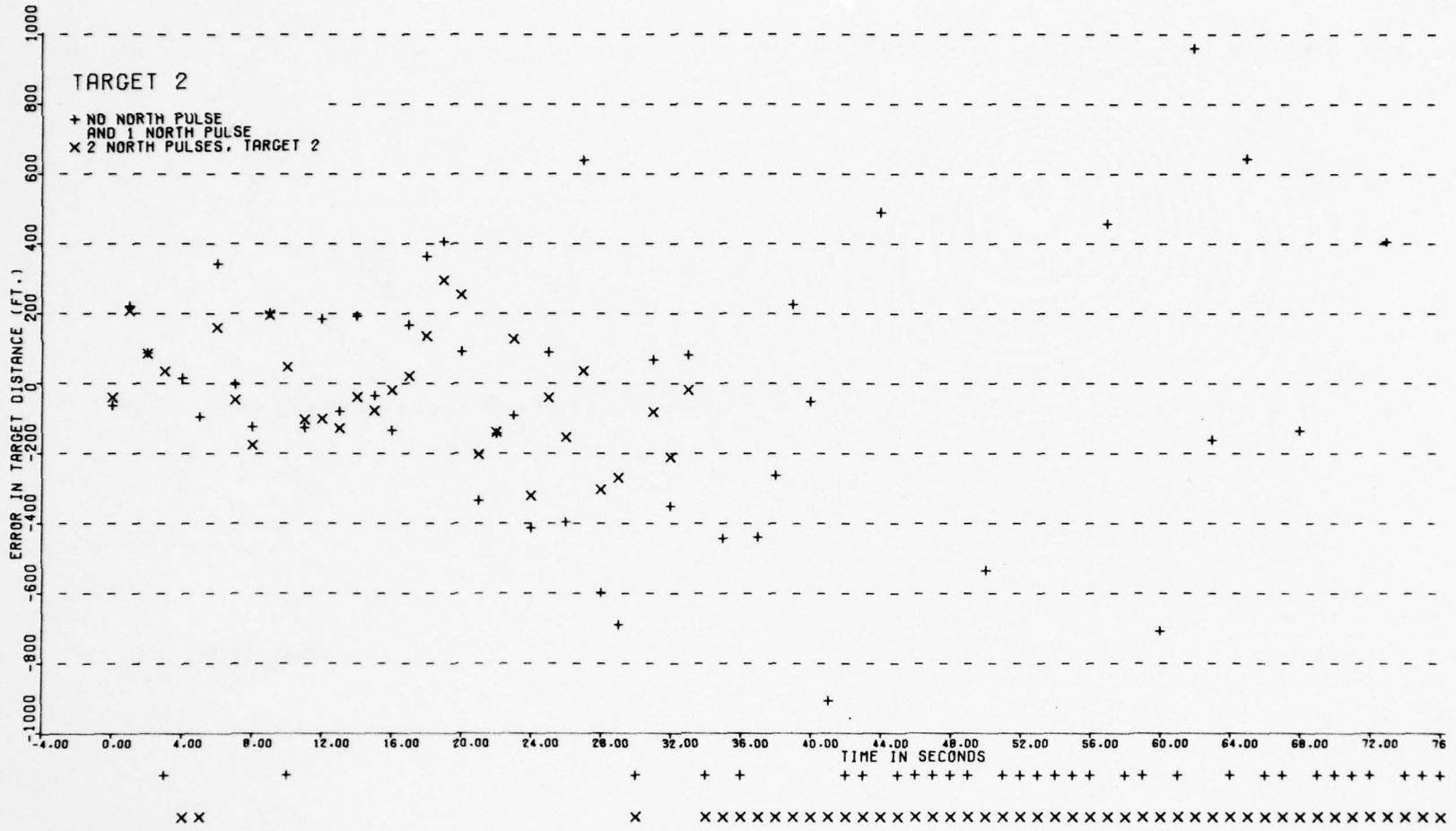
TARGET 2
+ NO NORTH PULSE
AND 1 NORTH PULSE
× 2 NORTH PULSES, TARGET 2
ERROR IN TARGET DISTANCE (FT.)
1000
800
600
400
200
0
-200
-400
-600
-800
-1000
-4.00
0.00
4.00
8.00
12.00
16.00
20.00
24.00
28.00
32.00
36.00
40.00
44.00
48.00
52.00
56.00
60.00
64.00
68.00
72.00
76
TIME IN SECONDS

FIGURE 6.3-32.

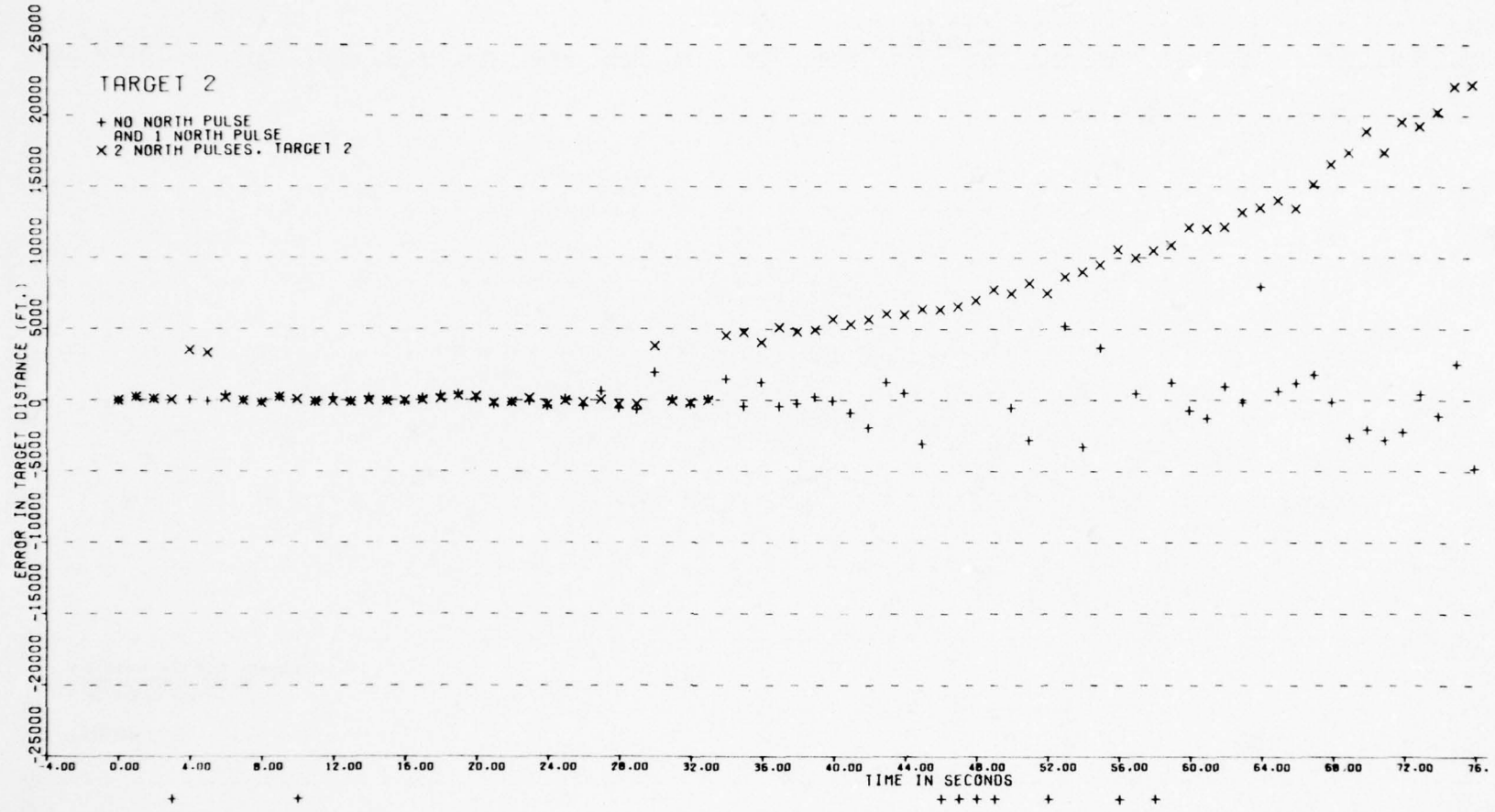
TARGET 2
+ NO NORTH PULSE
AND 1 NORTH PULSE
× 2 NORTH PULSES. TARGET 2
ERROR IN TARGET DISTANCE (FT.)
25000
20000
15000
10000
5000
0
-5000
-10000
-15000
-20000
-25000
-4.00
0.00
4.00
8.00
12.00
16.00
20.00
24.00
28.00
32.00
36.00
40.00
44.00
48.00
52.00
56.00
60.00
64.00
68.00
72.00
76.
TIME IN SECONDS

FIGURE 6.3-33.

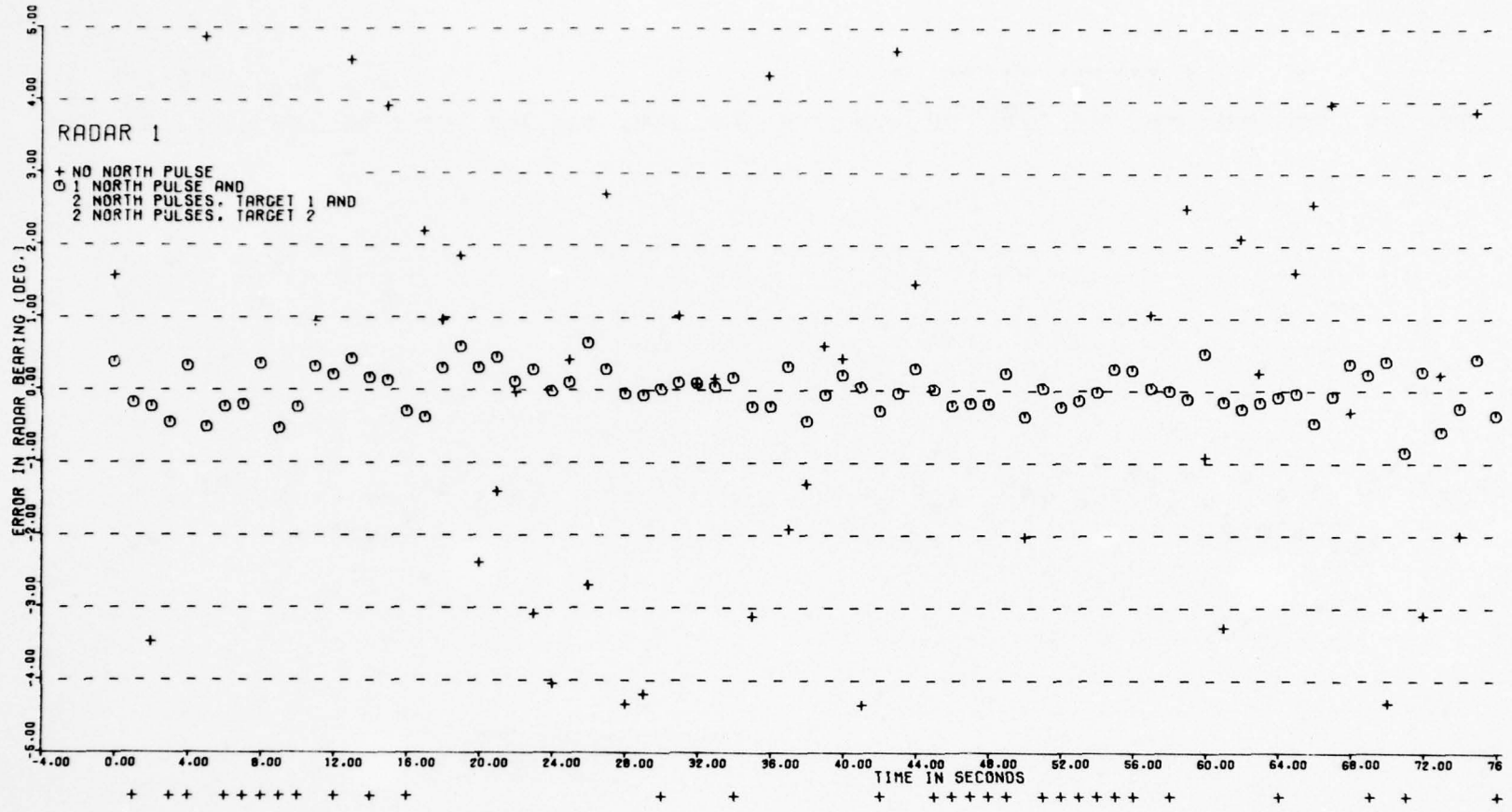
RADAR 1
+ NO NORTH PULSE
⊙ 1 NORTH PULSE AND
2 NORTH PULSES, TARGET 1 AND
2 NORTH PULSES, TARGET 2
ERROR IN RADAR BEARING (DEG.)
5.00
4.00
3.00
2.00
1.00
0.00
-1.00
-2.00
-3.00
-4.00
-5.00
-4.00
0.00
4.00
8.00
12.00
16.00
20.00
24.00
28.00
32.00
36.00
40.00
44.00
48.00
52.00
56.00
60.00
64.00
68.00
72.00
76
TIME IN SECONDS

FIGURE 6.3-34.

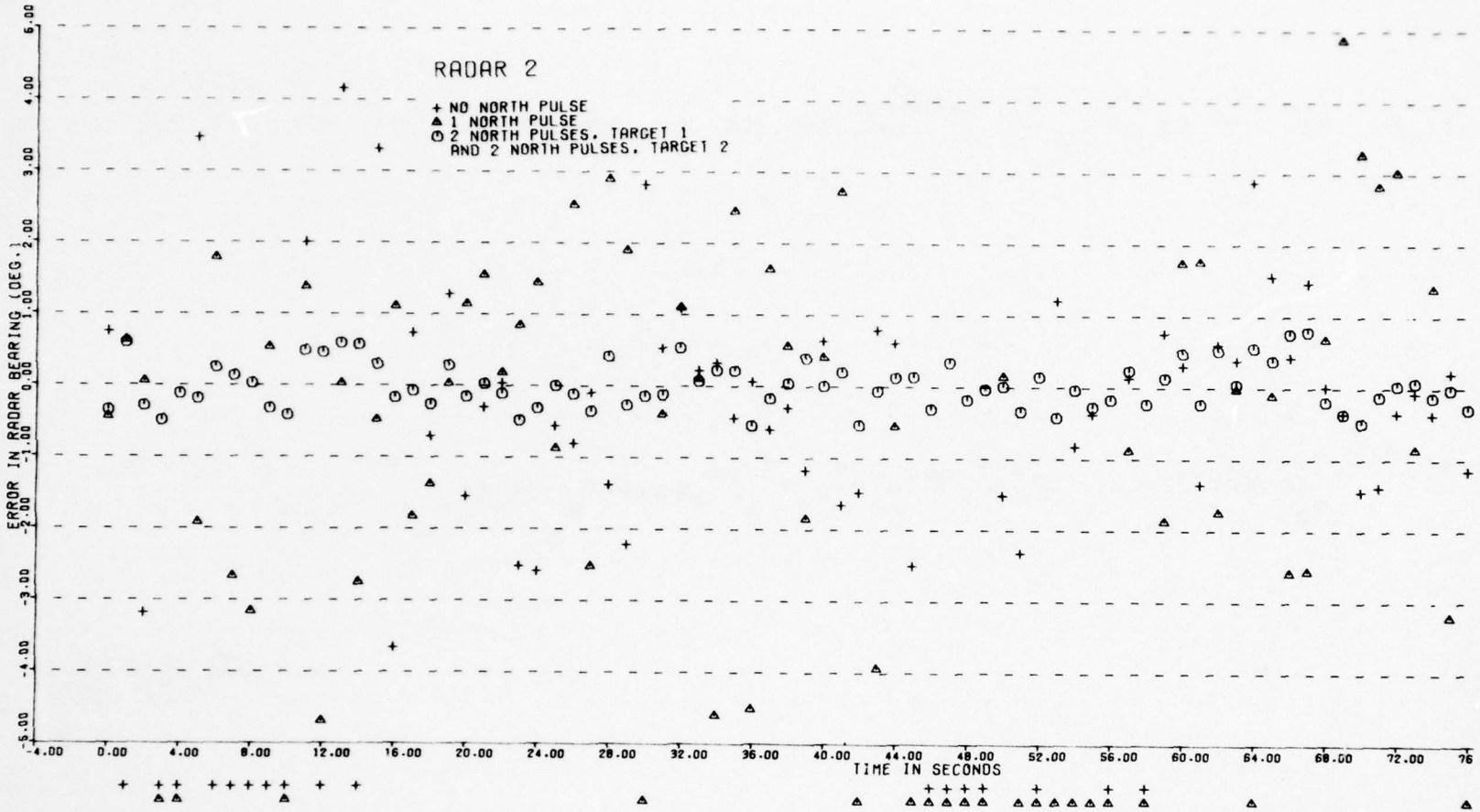
RADAR 2
+ NO NORTH PULSE
▲ 1 NORTH PULSE
Ⓣ 2 NORTH PULSES. TARGET 1
AND 2 NORTH PULSES. TARGET 2
ERROR IN RADAR BEARING (DEG.)
6.00
4.00
3.00
2.00
1.00
0.00
-1.00
-2.00
-3.00
-4.00
-5.00
-4.00
0.00
4.00
8.00
12.00
16.00
20.00
24.00
28.00
32.00
36.00
40.00
44.00
48.00
52.00
56.00
60.00
64.00
68.00
72.00
76
TIME IN SECONDS

FIGURE 6.3-35.

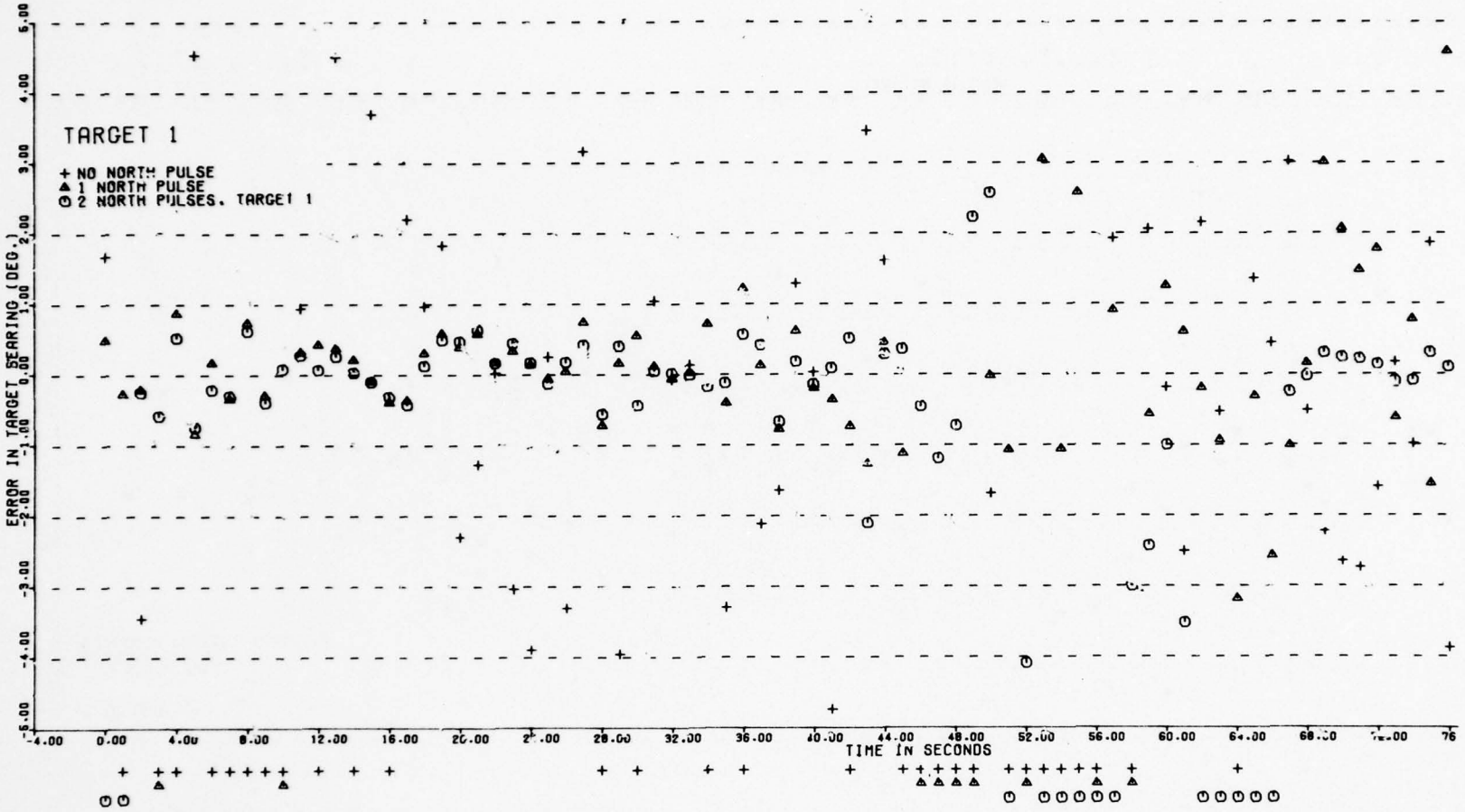
TARGET 1
+ NO NORTH PULSE
▲ 1 NORTH PULSE
⊙ 2 NORTH PULSES. TARGET 1
ERROR IN TARGET BEARING (DEG.)
TIME IN SECONDS

FIGURE 6.3-36.

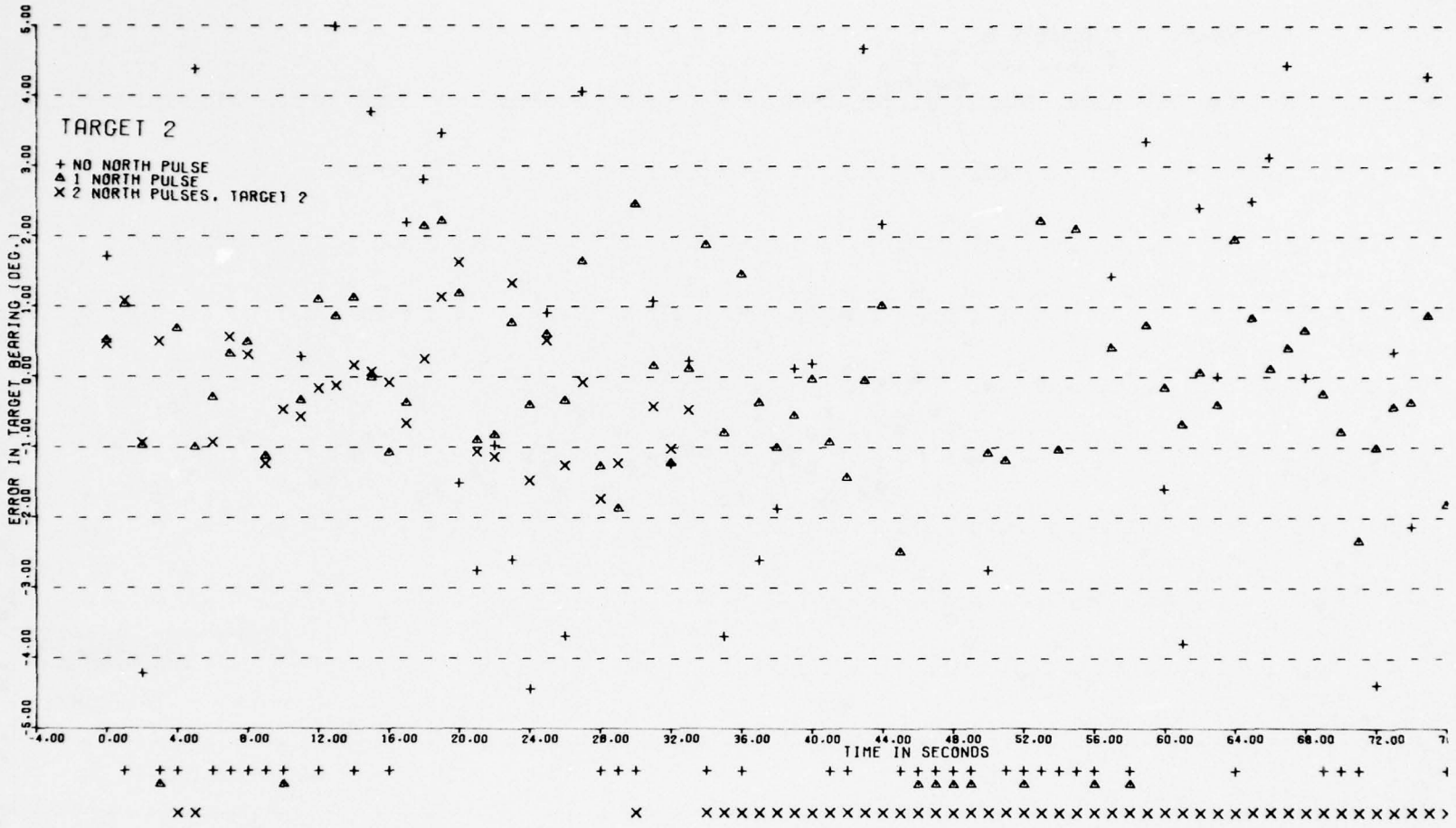
TARGET 2
+ NO NORTH PULSE
△ 1 NORTH PULSE
× 2 NORTH PULSES, TARGET 2
ERROR IN TARGET BEARING (DEG.)
5.00
4.00
3.00
2.00
1.00
0.00
-1.00
-2.00
-3.00
-4.00
-5.00
-4.00
0.00
4.00
8.00
12.00
16.00
20.00
24.00
28.00
32.00
36.00
40.00
44.00
48.00
52.00
56.00
60.00
64.00
68.00
72.00
TIME IN SECONDS

FIGURE 6.3-37.

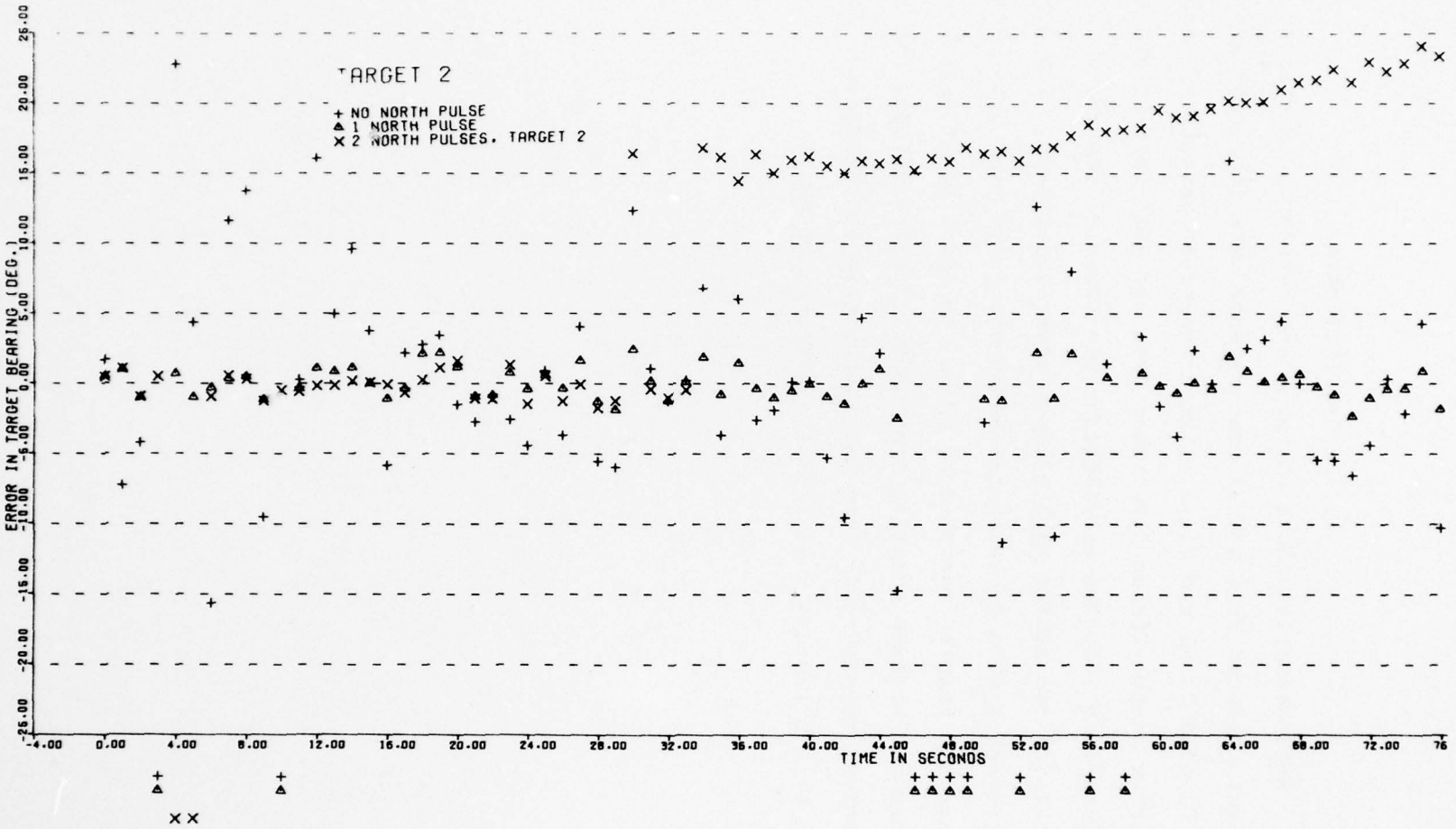
TARGET 2
+ NO NORTH PULSE
△ 1 NORTH PULSE
× 2 NORTH PULSES, TARGET 2
ERROR IN TARGET BEARING (DEG.)
25.00
20.00
15.00
10.00
5.00
0.00
-5.00
-10.00
-15.00
-20.00
-25.00
-4.00
0.00
4.00
8.00
12.00
16.00
20.00
24.00
28.00
32.00
36.00
40.00
44.00
48.00
52.00
56.00
60.00
64.00
68.00
72.00
76
TIME IN SECONDS

FIGURE 6.3-38.

7. FLIGHT TEST DATA

Representative plots of range and bearing to a stationary target computed from actual measurements made in flight are shown in Figures 7.1-1 and 7.1-2. These represent calculated range and bearing to the Mizpah fire tower from the BCAS test aircraft flying over it. The calculations are based on measurements utilizing two radars with azimuth reference pulses. The circles represent active interrogator measurements of range, the x's the range and bearing computed by BCAS, the short horizontal bars the range and bearing computed from ARTS III observations, and the vertical bars through them the approximate 90% confidence limits for the values computed from the ARTS measurements.

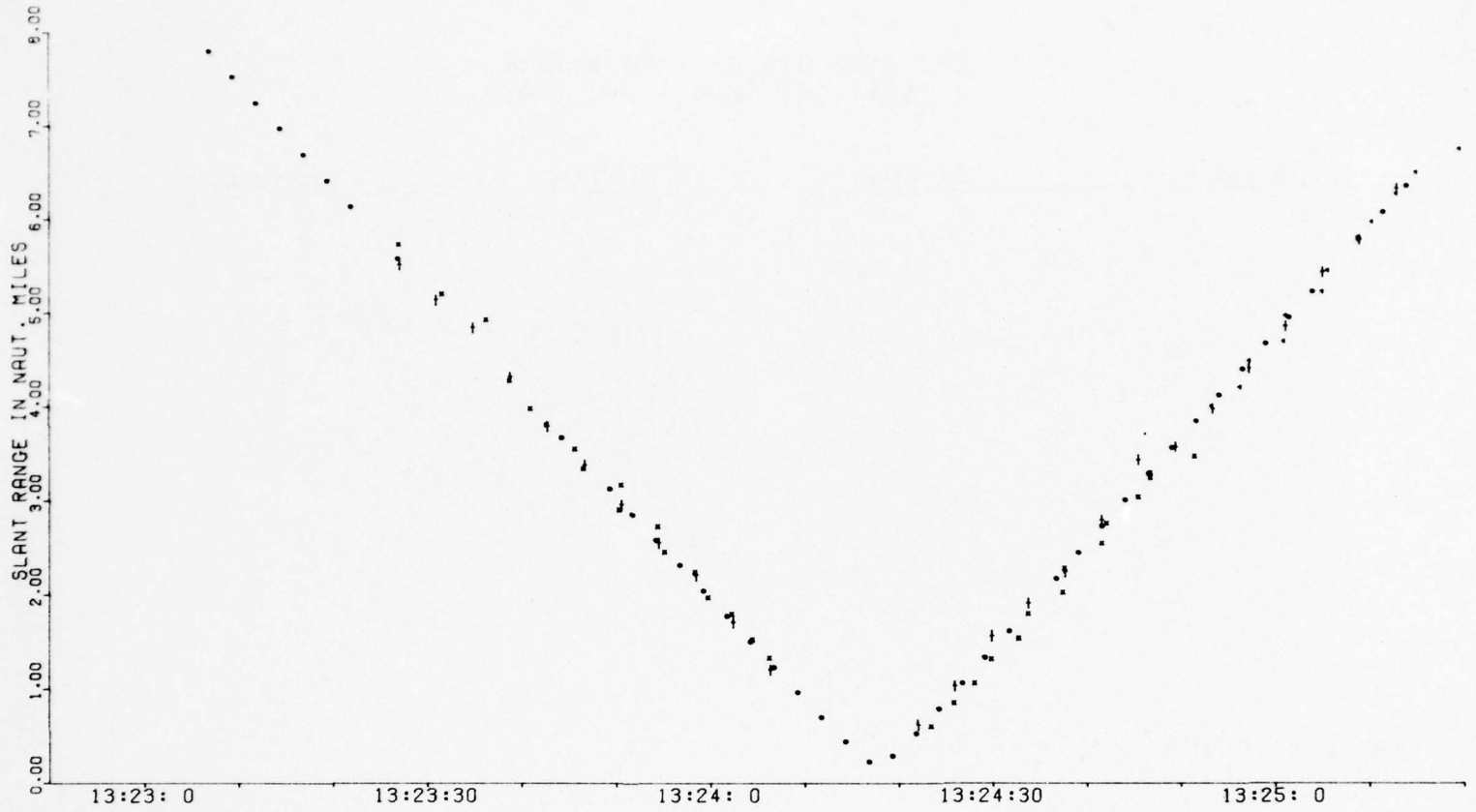

TEST DATE: OCT. 15, 1975
RUN #1 PATTERN #10 MODE I33

FIGURE 7.1-1. COMPUTED RANGE TO TARGET.

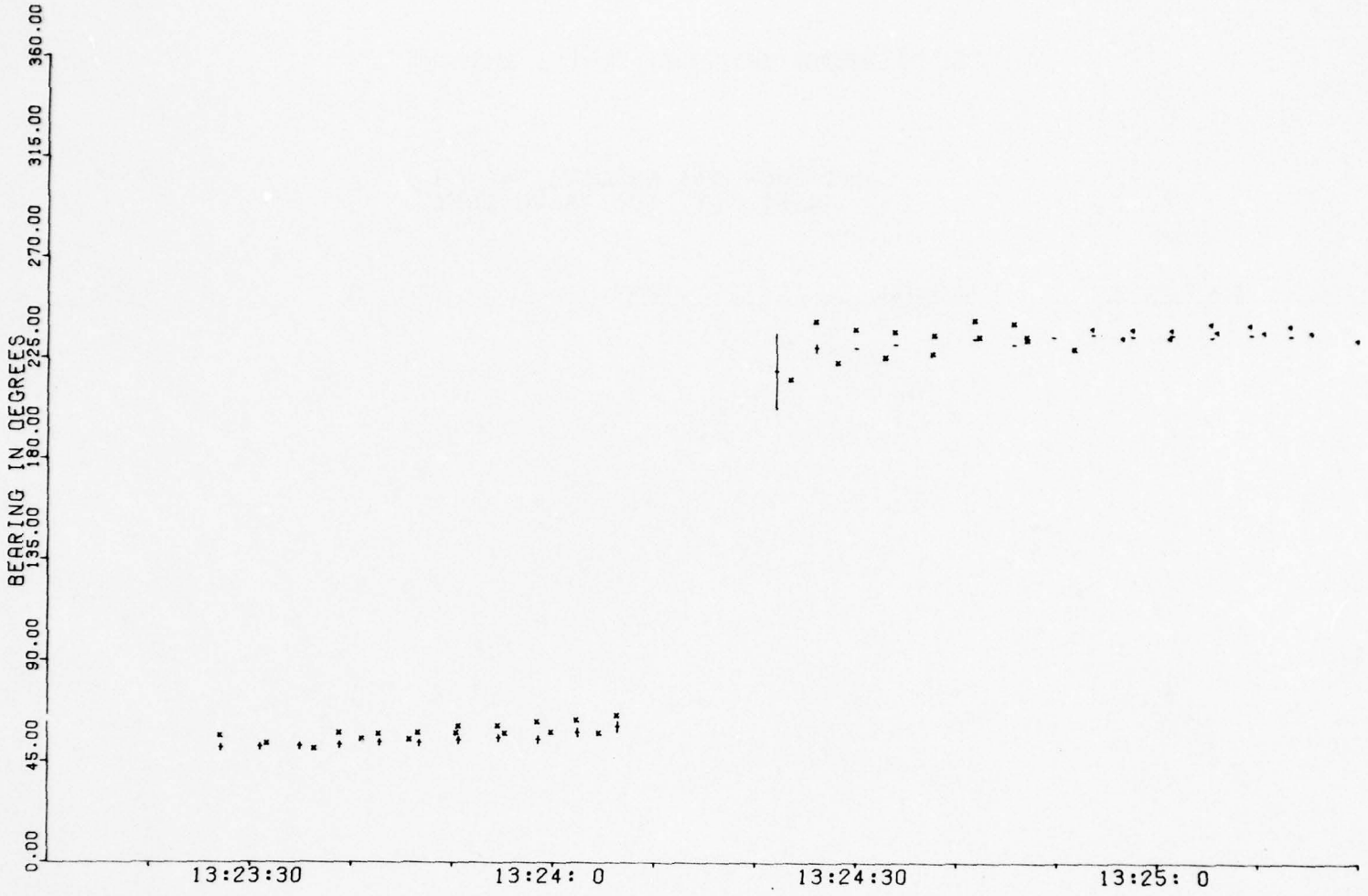

TEST DATE: OCT. 15, 1975
RUN #1 PATTERN #10 MODE I33

FIGURE 7.1-2. COMPUTED BEARING TO TARGET.

SUMMARY

Analyses have been performed for the static case and algorithms have been developed for computing range and bearing to potential threat aircraft and to ground radars, using passive-mode BCAS measurements as well as a combination of active and passive mode measurements for the single ground site geometry. Only the static solutions are presented. These are solutions based on the differential time of arrival (TOA), differential azimuth (DAZ) and, where appropriate, own azimuth (OAZ) measurements taken at one instant for the configuration as it exists at that time.

The algorithms compute range and bearing to intruder aircraft and radars on the basis of only the current measurements, making use of no a priori knowledge of either the positions of the aircraft or radars or of any previous measurements. For this reason, the accuracies of the computed positions are likely to be worse than those that would be obtained by dynamic tracking algorithms which would smooth out the effects of measurement errors over time.

The solutions obtained are the solutions that best fit the measurement data. Thus, their accuracy is the intrinsic accuracy to within which the relative positions of intruder aircraft and locked radars can be determined from the measurements made with the given accuracy at one point in time. Dynamic tracking algorithms, when they are developed, may be expected to have better overall performance because they will have available sequences of positions over a period of time and will be able to smooth out measurement errors by effectively averaging over time. The statically computed

accuracies should be suggestive of the accuracies that the tracking algorithms should be able to achieve.

Algorithms to determine target range and bearing from the BCAS measurements were developed and tested in simulations. In addition, an approach to the problem using target locus curves has been developed both as an aid to assessing the nature of the solutions qualitatively and as a potential basis for improved solution algorithms.

Three different modes of purely passive operation have been simulated. These assume all radars equipped with azimuth reference signals, none so equipped, and only one radar so equipped available at a given time.

It appears that when no radars are equipped with azimuth references, the target bearing cannot be derived sufficiently accurately to give good target tracks. This conclusion should be verified by dynamic simulation.

When all radars are equipped with azimuth reference signals, the positions of single targets can be determined. The range of configurations in which the solution is excessively error-sensitive is smaller than for the other cases, but under some circumstances the measurements lead to ambiguities in that several distinct configurations can give rise to the same measurements.

When only one radar has azimuth reference signals, two target aircraft must be observed to make calculations of position based on passive measurements possible. The range of configurations in which the solution is excessively sensitive to measurement error

is larger than when all radars have azimuth reference signals; multiple solutions do not occur.

In the good configurations of radars and aircraft, target aircraft positions can be determined to within an RMS error of less than 300 feet, assuming measurement accuracies like those obtained by the experimental BCAS system. Radar positions can be determined only to within a few miles using the system of two radars with azimuth reference and one target; radar position error is under one mile when the system with two target aircraft is used.

It is judged that either system - assuming all radars equipped with azimuth reference signals or only one radar within BCAS range so equipped - is technically feasible.

The results for the individual cases are summarized below:

1. All radars are assumed equipped with azimuth reference signals.

In this situation, the range and bearing from BCAS of a single intruder aircraft can be determined if it is being tracked by BCAS using two or more ground radars. The range to each radar can also be calculated.

Both simulated and flight test data verify that this mode of operation is possible in all but a set of unfavorable configurations. The unfavorable configurations are the following:

a) BCAS on an extension of the line connecting the two radars.

b) The intruder aircraft between BCAS and either of the radars.

c) The BCAS aircraft between one of the radars and the intruder.

AD-A062 912 TRANSPORTATION SYSTEMS CENTER CAMBRIDGE MASS F/G 1/2
BEACON COLLISION AVOIDANCE SYSTEM (BCAS) ALTERNATIVE CONCEPTS F--ETC(U)
SEP 78 J G RAUDSEPS, M D MENN, J VILCANS

UNCLASSIFIED TSC-FAA-78-19 FAA/RD-78/34 NL

3 OF 3
AD
A062912

END
DATE
FILMED
3-79
DDC

The width of the bad ranges depends on the characteristics of the configuration as a whole. In the worst part of each, the iterative solution algorithm fails to converge to any solution. Near the edges of the bad region, the configuration computed from the measurements is highly sensitive to measurement errors. This error sensitivity is intrinsic in that the configurations are such that large changes in the relative positions of the aircraft (and radars) cause small changes in the observed measurements. Then, inversely, small changes in the measurements, such as those arising from measurement noise, cause large changes in the configuration that can be deduced from the measurements.

Outside the bad ranges, the relative position of the intruder aircraft can be calculated with an RMS error in position of generally less than 300 feet, depending on the configuration.

The ranges to the radars can also be calculated, but the values obtained are quite sensitive to errors in the measurement of differential azimuth and may have errors of several miles.

It is important to notice that, under some circumstances, several distinct configurations of radars and aircraft will produce the same set of values for all the measurements obtained by the BCAS. In such a case, it is theoretically impossible to determine from the set of static measurements obtained at one time which of the possible configurations actually gave rise to the measurements. The ambiguity can be resolved by making other measurements, e.g., an active measurement of target range. In addition, although the possibility of the false solution may

persist for a period of time, so that a false track for the intruder may be established instead of the true one, the radar positions computed in conjunction with the false track will in time be seen to be inconsistent in that the radars will appear to move relative to each other.

2. No radars are assumed equipped with azimuth reference signals.

In this situation, BCAS can determine the shape of the configuration of radars and aircraft if there are two radars and two or more target aircraft. The measurements contain no absolute azimuth reference signal. Hence, the orientation of the configuration cannot be determined directly, but only the bearing of each radar and aircraft relative to some arbitrary reference within the configuration.

It has been suggested that the BCAS-equipped aircraft might be able to compute its own position relative to the radars at a number of consecutive times. Then it could relate its own flight direction to the fixed direction of the line connecting the two radars and use that as the known reference direction in determining the bearing angles toward the intruder aircraft.

It was found in the course of the simulations that the range of configurations in which the computed results are intrinsically highly sensitive to measurement error is more extensive in this case than in the case where both radars are equipped with azimuth reference signals. The bad configurations include the following:

a) BCAS on extension of line connecting the two radars.

b) Either intruder aircraft between BCAS and either of the radars.

c) Both intruder aircraft in the same direction as viewed from BCAS.

In addition, the current heuristic algorithm used to obtain an initial approximation tends to fail when an intruder aircraft is in the direction directly opposite that of a radar, when viewed from BCAS, or when BCAS is directly between the intruder aircraft. The difficulty in these regions can be eliminated, since it arises from the algorithm used and not from the nature of the dependence between the configuration and the measurements.

For those configurations in which the aircraft and radar positions can be reliably computed, (i.e., in the good ranges), the errors in range to the target aircraft are comparable to the errors obtained using radars that are all equipped with azimuth reference signals. The computed radar distances are considerably more accurate. However, the bearing angles computed relative to the line connecting the radars have errors on the order of several degrees. This suggests that the proposed scheme of operation with no azimuth reference signals at all may have difficulties. A definitive judgment must rest on an analysis of a tracking scheme in the dynamic situation.

3. Some radars, but not all, are equipped with azimuth reference signals.

It is assumed that the BCAS at any one time would be in range of only one radar with azimuth reference signals. Other radars would be available for locking and for tracking targets, but these would not have azimuth reference signals.

In such a situation, the problem of computing the configuration of radars and aircraft at any one instant is essentially the same as in the case of no azimuth reference signals. Two radars and two aircraft are required. The only difference is that, once the shape of the configuration has been determined, it can be properly oriented on the basis of the azimuth measurement.

The extent of the bad range for this case is identically the same as in the case of the system with no azimuth references, as is the error sensitivity of the computed ranges to the intruder aircraft and the radars. The bearing errors to the radars and the aircraft are comparable to those achieved when all radars are equipped with azimuth reference signals.

4. Limited simulations were also performed for the case of a single-site geometry, where active interrogation is used to establish target range. It was found that the accuracy to be obtained is comparable to that for the purely passive cases. The worst accuracies occur when the radar, the BCAS, and the target are approximately colinear. Two distinct solutions can occur if the target is at a sufficiently high altitude.

APPENDIX

ALGEBRAIC CONDITIONS FOR PROPERTIES OF LOCUS CURVE

A.1 GEOMETRIC ARGUMENTS

The properties of the target locus curves described in Section 2 largely depend on the relative values of T, H and H_o. The single most important determinant of the nature of the locus curves, in terms of the geometric construction carried out previously, is whether the vertical projection of the radar position is inside or outside the ellipse in the target altitude plane.

Figure A-1 shows a side view of the ellipsoid of revolution, cut along the LOP. The critical question is whether x is positive (as shown) or negative. For positive x, the radar projection is inside the ellipse; for x negative, it is outside.

The quantities in the figure are defined by

$$D = \sqrt{d^2 + H_o^2} \qquad \text{A1.1}$$

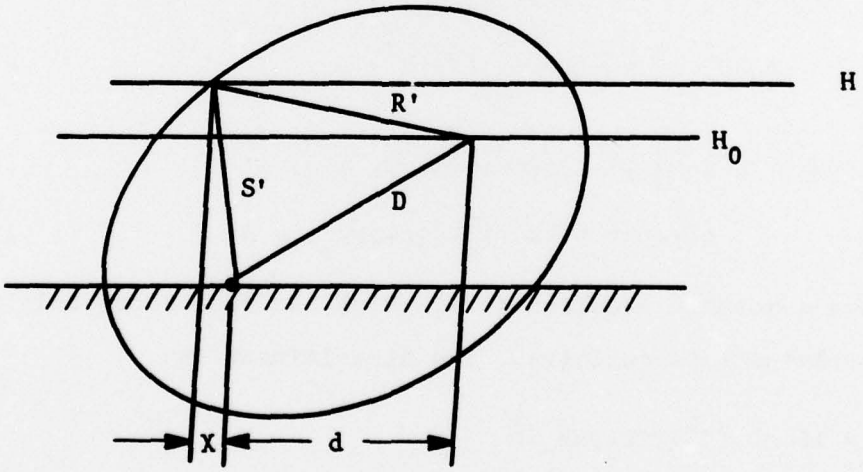

FIGURE A-1. SIDE VIEW OF ELLIPSOID OF REVOLUTION USED TO CONSTRUCT TARGET LOCUS CURVES.

$$S^1 = \sqrt{x^2 + H^2} \qquad \text{A1.2}$$

$$R^1 = \sqrt{(d+x)^2 + (H-H_o)^2} \qquad \text{A1.3}$$

By definition

$$T = S^1 + R^1 - D \qquad \text{A1.4}$$

Hence

$$(T+D-S^1)^2 = (R^1)^2 \qquad \text{A1.5}$$

or

$$(T+D)^2 - 2(T+D)\sqrt{x^2 + H^2} + x^2 + H^2$$

$$= d^2 + 2dx + x^2 + H^2 - 2HH_o + H_o^2 \qquad \text{A1.6}$$

Hence

$$T^2 + 2TD + 2HH_o - 2dx = 2(T+D)\sqrt{x^2 + H^2} \qquad \text{A1.7}$$

and, after squaring

$$(T^2+2TD+2HH_o)^2 - 4(T^2+2TD+2HH_o)\,dx$$

$$+ 4d^2 x^2 = 4(T+D)^2 (x^2+H^2) \qquad \text{A1.8}$$

or

$$\left[4(T+D)^2 - 4d^2\right] x^2 + 4(T^2+2TD+2HH_o)\,dx$$

$$+ 4(T+D)^2 H^2 - (T^2+2TD+2HH_o) = 0 \qquad \text{A1.9}$$

This is a quadratic equation in x, which has real roots only if its discriminant is positive. The discriminant is

$$\Delta = 16\, d^2\, (T^2+2TD+2HH_o)^2$$

$$- 16\left[(T+D)^2 - d^2\right]\left[4\,(T+D)^2\, H^2 - (T^2+2TD+2HH_o)^2\right] \qquad \text{A1.10}$$

or

$$\Delta = 16\ (T+D)^2 \left[4T^2D^2+4(T^3+2THH_o-2TH^2)\ D + T^4 + 4T^2\ HH_o - 4T^2\ H^2\right] \qquad \text{A1.11}$$

It is evident that Δ is always positive for D sufficiently large. To a first-order approximation, for D large

$$\Delta \approx 64\ (T+D)^2\ T^2\ D^2 \left(1 + \frac{T^2 + 2HH_o - 2H^2}{TD}\right) \qquad \text{A1.12}$$

Then show

$$\sqrt{\Delta} \approx 8\ (T+D)\ TD \left(1 + \frac{T^2 + 2HH_o - 2H^2}{2TD}\right)$$

$$= 8\ TD^2 + 12\ T^2D + 8\ HH_oD - 8\ H^2D \qquad \text{A1.13}$$

With this approximation and the approximation $D \approx d$ for large D, Equation 5 may be solved to yield, for large D

$$x \approx \frac{-4(T^2+2TD+2HH_o)\ D \pm (8TD^2+12T^2D+8HH_oD-8H^2D)}{16\ TD} \qquad \text{A1.14}$$

This gives

$$x_1 \approx \frac{T^2 - H^2}{2T} \qquad \text{A1.15}$$

and

$$x_2 \approx -D. \qquad \text{A1.16}$$

The second solution x_2 is always negative. It corresponds to the end of the ellipsoid nearer the radar cutting the target altitude plane and is of no interest. The solution x_1 is seen to be positive for $T > H$ and negative for $T < H$. This is the important result:

When T > H, for any D sufficiently large, the radar position will project inside the TOA ellipse in the target altitude plane. Hence there will be exactly one branch of the target locus curve compatible with large radar distances.

When T < H, for any D sufficiently large, the radar position will project outside the TOA ellipse in the target altitude plane. Hence, if the target locus curve exists at all for large radar distances, it has two branches. Furthermore, it is seen that as D becomes large, the distance along the LOP from the radar position to the TOA ellipse approaches a constant value (Equation A1.15). Also, as D becomes large, the ellipse locally near the LOP becomes more and more nearly a straight line perpendicular to the LOP (cf. Figure A-2). Then for the radar approximately

$$x \approx \frac{H^2 - T^2}{2T} \qquad \text{A1.17}$$

from the elipse along the LOP and α sufficiently small, the line determined by the DAZ will intersect the ellipse at a distance

$$y \approx \frac{H^2 - T^2}{2T} \tan \alpha \qquad \text{A1.18}$$

from the LOP; y is approximately constant for large D. Hence the "inner branch" of the target locus curve is seen to approach asymptotically a line parallel to the LOP a distance y from the LOP.

The next section gives in a concise form a more formal and complex algebraic proof of the properties of the locus lines far from OWN.

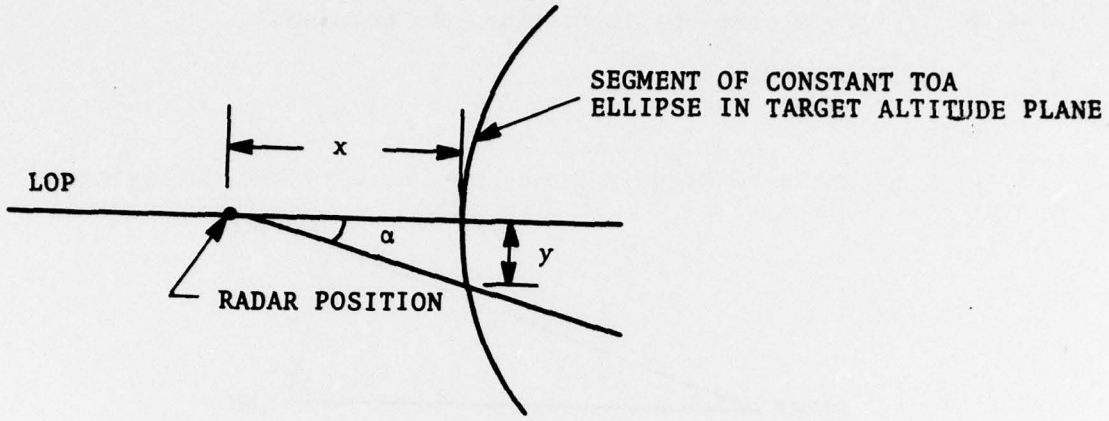

FIGURE A-2. DETAIL OF DIAGRAM FOR CONSTRUCTING TARGET LOCUS CURVE.

CONCLUSIONS

Let

H = height of TARGET

α = differential azimuth, assumed to be positive

T = TOA

The line parallel to the line joining OWN to RADAR and height H above it will be called the base line.

Then

1) If T > H the locus curve has a single asymptote. It is parallel to the base line at a distance of

$$\frac{T\cos\alpha + \sqrt{T^2 - H^2\sin^2\alpha}}{\sin\alpha}.$$

2) If H $\sin\alpha$ < T < H the locus curve has two asymptotes parallel to the base line at distances of

$$\frac{T\cos\alpha \pm \sqrt{T^2 - H^2\sin^2\alpha}}{\sin\alpha}.$$

3) If $T < H\sin\alpha$ the locus curve is bounded.

A.2 JUSTIFICATION

Let

H_o = height of OWN and define θ, r, s, d by the following

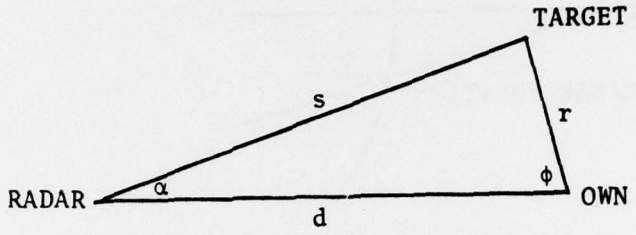

Here the points labeled TARGET and OWN actually represent the horizontal projections of TARGET and OWN.

Let $x = \frac{1}{r}$.

By the law of sines

$$d = \frac{\sin(\Phi+\alpha)}{x\sin\alpha}$$

and

$$s = \frac{\sin\Phi}{x\sin\alpha}$$

Now $T = \sqrt{s^2 + H^2} + \sqrt{\frac{1}{x^2} + (H-H_o)^2} - \sqrt{d^2 + H_o^2}$

Substitution and multiplication by $T\sin\alpha$ results in

$$\sin\alpha\left(Tx - \sqrt{1 + (H-H_o)^2 x^2}\right) = \sqrt{\sin^2\Phi + H^2x^2\sin^2\alpha}$$

$$- \sqrt{\sin^2(\Phi+\alpha) + H_o^2x^2\sin^2\alpha} \qquad \text{A2.1}$$

Suppose there is a not necessarily continuous or unique function Φ, defined for small non-negative values of x, and taking

values between 0 and $\pi - \alpha$ (the only physically realizable bearings) such that

$$\sin\alpha\left(Tx - \sqrt{1 + (H-H_o)^2\, x^2}\right) = \sqrt{\sin^2\Phi(x) + H^2x^2\,\sin^2\alpha}$$

$$- \sqrt{\sin^2\left(\Phi(x) + \alpha\right) + H_o^2\,\sin^2\alpha\, x^2} \qquad \text{A2.2}$$

$$0 \leq \Phi(x) \leq \pi - \alpha$$

If x is close to 0

$$-\sin\alpha \approx \sin\Phi(x) - \sin\left(\Phi(x) + \alpha\right) = -2\cos\left(\Phi(x) + \frac{\alpha}{2}\right)\sin\frac{\alpha}{2}$$

so

$$\cos\frac{\alpha}{2} \approx \cos\left(\Phi(x) + \frac{\alpha}{2}\right)$$

Since $\Phi(x) \approx -\alpha$ is not possible

$$\Phi(x) \approx 0.$$

It follows that $\Phi(0) = 0$ and that Φ is continuous at 0. By Taylor's Theorem applied to the sine function A2.2 may be written in the form

$$\sin\alpha\left(Tx - \sqrt{1 + (H-H_o)^2\, x^2}\right) = \sqrt{\Phi(x)^2 + H^2x^2\,\sin^2\alpha + \Phi(x)^3 g\left(\Phi(x)\right)}$$

$$- \sqrt{(1+H_o^2x^2)\,\sin^2\alpha + 2\sin\alpha\cos\alpha\,\Phi(x) + \Phi(x)^2\, h\left(\Phi(x)\right)} \qquad \text{A2.3}$$

where g and h are smooth functions

Let $u(x) = H_o^2\, x^2\,\sin^2\alpha + 2\sin\alpha\cos\alpha\,\Phi(x) + \Phi(x)^2\, h\left(\Phi(x)\right.$,

$$\sqrt{(1 + H_o^2\, x^2)\sin^2\alpha + 2\sin\alpha\cos\alpha\,\Phi(x) + \Phi(x)^2\, h\left(\Phi(x)\right.},$$

$$= \sqrt{\sin^2\alpha + u(x)}$$

Use the fact that the square root function is differentiable at positive arguments to write

$$\sqrt{\sin^2\alpha + u(x)} = \sin\alpha + \frac{1}{2\sin\alpha}\, u(x) + R\big(u(x)\big) \qquad \text{A2.4}$$

where R is a function with the properties

$$\lim_{v\to 0} \frac{R(v)}{v} = 0 \quad \text{and } R(0) = 0.$$

$$\frac{R\big(u(x)\big)}{x} = \frac{R\big(u(x)\big)}{u(x)} \cdot \frac{u(x)}{x}\ .$$

Since $\lim_{x\to 0} \Phi(x) = 0$, $\lim_{x\to 0} u(x) = 0$ from which it follows that

$$\lim_{x\to 0} \frac{R\big(u(x)\big)}{u(x)} = 0$$

Note that $\frac{u(x)}{x} = \frac{\Phi(x)}{x}\,(2\sin\alpha\cos\alpha + \varepsilon(x))$ where $\lim_{x\to 0} \varepsilon(x) = 0$

It follows that

$$\frac{\sqrt{\sin^2\alpha + u(x)} - \sin\alpha}{x} = \frac{\Phi(x)}{x}\left(\cos\alpha + \frac{1}{2\sin\alpha}\,\varepsilon(x)\right)$$

$$+ \frac{R\big(u(x)\big)}{u(x)} \cdot \left(2\sin\alpha\cos\alpha + \varepsilon(x)\right)\frac{\Phi(x)}{x}$$

$$= \frac{\Phi(x)}{x}\left(\cos\alpha + \delta(x)\right) \text{ where}$$

$$\lim_{x\to 0} \delta(x) = 0.$$

Then, taking difference quotients of both sides of A2.3,

$$T\sin\alpha \approx \sqrt{\left(\frac{\Phi(x)}{x}\right)^2 + H^2\sin^2\alpha + \left(\frac{\Phi(x)}{x}\right)^2 \Phi(x)\, g\big(\Phi(x)\big)}$$

$$- \frac{\Phi(x)}{x} \cdot \left(\cos\alpha + \delta(x)\right) \qquad \text{A2.5}$$

It is easy to see that if $\frac{\Phi(x)}{x}$ is very large, the right hand side of A2.5 will be much larger than the left hand side when x is

small. It follows that $\frac{\Phi(x)}{x}$ is bounded and A2.5 may be rewritten

$$T \sin\alpha \approx \sqrt{\left(\frac{\Phi(x)}{x}\right)^2 + H^2 \sin^2\alpha} - \frac{\Phi(x)}{x} \cos\alpha \qquad \text{A2.6}$$

Manipulation of A2.6 results in

$$\left(\frac{\Phi(x)}{x}\right)^2 \sin\alpha - \left(\frac{\Phi(x)}{x}\right) 2T \cos\alpha + \left(H^2 - T^2\right) \sin\alpha \approx 0$$

from which

$$\frac{\Phi(x)}{x} \approx \frac{T \cos\alpha + \sqrt{T^2 - H^2 \sin^2\alpha}}{\sin\alpha} \qquad \text{A2.7}$$

If $T < H \sin\alpha$ a contradiction results and result 3 follows immediately.

$\frac{\Phi(x)}{x}$ must be positive. A2.7 gives two positive expressions if and only if $T^2 \cos^2\alpha > T^2 - H^2 \sin^2\alpha$ or $T < H$. Note also that the limiting distance from the base line is $\lim_{x \to 0} \frac{\sin\Phi(x)}{x} = \lim_{x \to 0} \frac{\Phi(x)}{x}$.

It suffices to show that for small x

1) if $T > H$ there is a value of Φ satisfying A2.1

2) if $H \sin\alpha < T < H$ there is a value of Φ satsifying A2.1 and

$$\Phi/x \leq \frac{T \cos\alpha + \frac{1}{2}\sqrt{T^2 - H^2 \sin^2\alpha}}{\sin\alpha}$$

and one satisfying

$$\Phi/x \geq \frac{T \cos\alpha - \frac{1}{2}\sqrt{T^2 - H^2 \sin^2\alpha}}{\sin\alpha}$$

Define F by

$$F(x,\Phi) = \sin\alpha\left(Tx - \sqrt{1 + (H-H_o)^2 x^2}\right) - \sqrt{\sin^2\Phi + H^2 x^2 \sin^2\alpha} + \sqrt{\sin^2(\Phi+\alpha) + H_o^2 x^2 \sin^2\alpha}$$

$$F(x,0) = \sin\alpha\left(Tx - \sqrt{1 + (H-H_o)^2 x^2}\right) - Hx \sin\alpha + \sin\alpha \sqrt{1 + H_o^2 x^2}$$
$$\approx (T-H)x \sin\alpha$$

Therefore, $F(x,0) < 0$ if $T < H$ and $F(x,0) > 0$ if $T > H$.

$$F(x,\tfrac{\pi}{2}) = \sin\alpha\ (Tx - \sqrt{1 + (H-H_o)^2x^2})$$

$$- \sqrt{1 + H^2x^2\ \sin^2\alpha} + \sqrt{\cos^2\alpha + H_o^2x^2\ \sin^2\alpha}$$

$$\approx -1 - \sin\alpha + \cos\alpha < 0$$

Thus if $T > H$ there must be a Φ with $0 < \Phi < \frac{\pi}{2}$ and $F(x,\Phi) = 0$. Claim i) has been established.

Now suppose $H \sin\alpha < T < H$.

Let $\gamma = \frac{T\cos\alpha}{\sin\alpha}\ x$

The second claim will be established if it can be shown that, for small x, $F(x,\gamma) > 0$.

To a close enough approximation, $\sin\gamma = \gamma$ and $\sin^2(\gamma+\alpha) = \sin^2\alpha + 2\sin\alpha\cos\alpha\cdot\gamma$ (by differential approximation

Therefore

$$F(x,\gamma) \approx \sin\alpha\left(Tx - \sqrt{1 + (H-H_o)^2x^2}\right) - \sqrt{T^2\ \frac{\cos^2\alpha}{\sin^2\alpha}\ x^2 + H^2x^2\ \sin^2\alpha}$$

$$+ \sqrt{\sin^2\alpha + 2\ \sin\alpha\ \cos\alpha\ \frac{T\ \cos\alpha\ x}{\sin\alpha} + H_o^2x^2\ \sin^2\alpha}$$

$$F(x,\gamma) \approx \sin\alpha\left(Tx - \sqrt{1 + (H-H_o)^2x^2}\right)$$

$$- x\sqrt{\frac{T^2\ \cos^2\alpha}{\sin^2\alpha} + H^2\ \sin^2\alpha} + \sqrt{\sin^2\alpha + 2Tx\ \cos^2\alpha + H_o^2x^2\ \sin^2\alpha}$$

$$F(x,\gamma) \approx -\sin\alpha + Tx\sin\alpha - x\sqrt{T^2\frac{\cos^2\alpha}{\sin^2\alpha} + H^2\sin^2\alpha}$$

$$+ \sin\alpha + Tx\frac{\cos^2\alpha}{\sin\alpha}$$

$$F(x,\gamma) \approx x\left(\frac{T}{\sin\alpha} - \sqrt{T^2\frac{\cos^2\alpha}{\sin^2\alpha} + H^2\sin^2\alpha}\right)$$

$F(x,\gamma)$ will be positive if and only if

$$\frac{T^2}{\sin^2\alpha} > T^2\frac{\cos^2\alpha}{\sin^2\alpha} + H^2\sin^2\alpha$$

if and only if

$$T > H\sin\alpha$$

*U.S. GOVERNMENT PRINTING OFFICE: 1978—600-344/230